ISSN: 2067-3809

Universitatea Politehnica Timișoara

ACTA TECHNICA CORVINIENSIS – Bulletin of Engineering

Fascicule 2

[April–June]
Tome XVII [2024]

Editura POLITEHNICA

ACTA TECHNICA CORVINIENSIS
Bulletin of Engineering

Edited by:

UNIVERSITY POLITEHNICA TIMISOARA

Editor / Technical preparation / Cover design:

Assoc. Prof. Eng. KISS Imre, PhD.
UNIVERSITY POLITEHNICA TIMISOARA,
FACULTY OF ENGINEERING HUNEDOARA

Commenced publication year:
2008

ACTA TECHNICA CORVINIENSIS
Bulletin of Engineering

ASSOCIATE EDITORS and REGIONAL COLLABORATORS

The Editor and editorial board members do not receive any remuneration. These positions are voluntary. The members of the Editorial Board may serve as scientific reviewers.

We are very pleased to inform that our journal ACTA TECHNICA CORVINIENSIS – Bulletin of Engineering is going to complete its ten years of publication successfully. In a very short period it has acquired global presence and scholars from all over the world have taken it with great enthusiasm. We are extremely grateful and heartily acknowledge the kind of support and encouragement from you.

ACTA TECHNICA CORVINIENSIS – Bulletin of Engineering seeking qualified researchers as members of the editorial team. Like our other journals, ACTA TECHNICA CORVINIENSIS – Bulletin of Engineering will serve as a great resource for researchers and students across the globe. We ask you to support this initiative by joining our editorial team. If you are interested in serving as a member of the editorial team, kindly send us your resume to redactie@fih.upt.ro.

ISSN: 2067–3809

Fascicule 1
[January – March]

t o m e [2024] XVII

ACTA Technica CORVINIENSIS
BULLETIN OF ENGINEERING

ISSN: 2067-3809

INTERNATIONAL SCIENTIFIC COMMITTEE MEMBERS and SCIENTIFIC REVIEWERS

MANAGER & CHAIRMAN

ROMANIA 

Imre KISS, University Politehnica TIMISOARA, Faculty of Engineering HUNEDOARA

INTERNATIONAL SCIENTIFIC COMMITTEE MEMBERS & SCIENTIFIC REVIEWERS from:

ROMANIA 

Viorel-Aurel ȘERBAN, University Politehnica TIMIŞOARA – TIMIŞOARA
Teodor HEPUŢ, University Politehnica TIMIŞOARA – HUNEDOARA
Ilare BORDEAȘU, University Politehnica TIMIŞOARA – TIMIŞOARA
Liviu MARȘAVIA, University Politehnica TIMIŞOARA – TIMIŞOARA
Ioan VIDA-SIMITI, Technical University of CLUJ-NAPOCA – CLUJ-NAPOCA
Sorin VLASE, "Transilvania" University of BRAŞOV – BRAŞOV
Horatiu TEODORESCU DRĂGHICESCU, "Transilvania" University of BRAŞOV – BRAŞOV
Maria Luminița SCUTARU, "Transilvania" University of BRASOV – BRASOV
Carmen ALIC, University Politehnica TIMIŞOARA – HUNEDOARA
Sorin DEACONU, University Politehnica TIMIŞOARA – HUNEDOARA
Liviu MIHON, University Politehnica TIMIŞOARA – TIMIŞOARA
Valeriu RUCAI, University Politehnica BUCUREŞTI – BUCUREŞTI

SLOVAKIA 

Ervin LUMNITZER, Technical University of KOŠICE – KOŠICE
Miroslav BADIDA, Technical University of KOŠICE – KOŠICE
Karol VELIŠEK, Slovak University of Technology BRATISLAVA – TRNAVA
Imrich KISS, Institute of Economic & Environmental Security – KOŠICE
Vladimir MODRAK, Technical University of KOSICE – PRESOV

CROATIA 

Drazan KOZAK, Josip Juraj Strossmayer University of OSIJEK – SLAVONKI BROD
Predrag COSIC, University of ZAGREB – ZAGREB
Milan KLJAJIN, Josip Juraj Strossmayer University of OSIJEK – SLAVONKI BROD
Antun STOIĆ, Josip Juraj Strossmayer University of OSIJEK – SLAVONKI BROD
Ivo ALFIREVIĆ, University of ZAGREB – ZAGREB

HUNGARY 

Imre DEKÁNY, University of SZEGED – SZEGED
Cecilia HODÚR, University of SZEGED – SZEGED
Béla ILLÉS, University of MISKOLC – MISKOLC
Imre RUDAS, Óbuda University of BUDAPEST – BUDAPEST
István BIRÓ, University of SZEGED – SZEGED
Tamás KISS, University of SZEGED – SZEGED
Imre TIMÁR, University of Pannonia – VESZPRÉM
Károly JÁRMAI, University of MISKOLC – MISKOLC
Ádám DÖBRÖCZÖNI, University of MISKOLC – MISKOLC
György SZEIDL, University of MISKOLC – MISKOLC
Miklós TISZA, University of MISKOLC – MISKOLC
József GÁL, University of SZEGED – SZEGED
Ferenc FARKAS, University of SZEGED – SZEGED
Géza HUSI, **University of DEBRECEN** – DEBRECEN

SERBIA 

Sinisa KUZMANOVIC, University of NOVI SAD – NOVI SAD
Miroslav PLANČAK, University of NOVI SAD – NOVI SAD

The Scientific Committee members and Reviewers do not receive any remuneration. These positions are voluntary.
We are extremely grateful and heartily acknowledge the kind of support and encouragement from all contributors and all collaborators!

ACTA TECHNICA CORVINIENSIS – Bulletin of Engineering is dedicated to publishing material of the highest engineering interest, and to this end we have assembled a distinguished Editorial Board and Scientific Committee of academics, professors and researchers.
ACTA TECHNICA CORVINIENSIS – Bulletin of Engineering publishes invited review papers covering the full spectrum of engineering. The reviews, both experimental and theoretical, provide general background information as well as a critical assessment on topics in a state of flux. We are primarily interested in those contributions which bring new insights, and papers will be selected on the basis of the importance of the new knowledge they provide.

ACTA TECHNICA CORVINIENSIS – Bulletin of Engineering encourages the submission of comments on papers published particularly in our journal. The journal publishes articles focused on topics of current interest within the scope of the journal and coordinated by invited guest editors. Interested authors are invited to contact one of the Editors for further details.
ACTA TECHNICA CORVINIENSIS – Bulletin of Engineering accept for publication unpublished manuscripts on the understanding that the same manuscript is not under simultaneous consideration of other journals. Publication of a part of the data as the abstract of conference proceedings is exempted.

Manuscripts submitted (original articles, technical notes, brief communications and case studies) will be subject to peer review by the members of the Editorial Board or by qualified outside reviewers. Only papers of high scientific quality will be accepted for publication. Manuscripts are accepted for review only when they report unpublished work that is not being considered for publication elsewhere.

The evaluated paper may be recommended for:

- **Acceptance without any changes** – in that case the authors will be asked to send the paper electronically in the required .doc format according to authors' instructions;
- **Acceptance with minor changes** – if the authors follow the conditions imposed by referees the paper will be sent in the required .doc format;
- **Acceptance with major changes** – if the authors follow completely the conditions imposed by referees the paper will be sent in the required .doc format;
- **Rejection** – in that case the reasons for rejection will be transmitted to authors along with some suggestions for future improvements (if that will be considered necessary).

The manuscript accepted for publication will be published in the next issue of ACTA TECHNICA CORVINIENSIS – Bulletin of Engineering after the acceptance date.

All the authors and the corresponding author in particular take the responsibility to ensure that the text of the article does not contain portions copied from any other published material which amounts to plagiarism. We also request the authors to familiarize themselves with the good publication ethics principles before finalizing their manuscripts.

ISSN: 2067–3809

TABLE of CONTENTS

ACTA TECHNICA CORVINIENSIS – Bulletin of Engineering

Tome XVII [2024],

Fascicule 2 [April – June]

The ACTA TECHNICA CORVINIENSIS – Bulletin of Engineering, Tome XVII [2024], Fascicule 2 [April – June] includes original papers submitted to the Editorial Board, directly by authors or by the regional collaborators of the Journal.

Also, the ACTA TECHNICA CORVINIENSIS – Bulletin of Engineering, Tome XVII [2024], Fascicule 2 [April – June], includes scientific papers presented in the sections of:

- ISB–INMA TEH' 2023 – International Symposium (Agricultural and Mechanical Engineering), organized by Politehnica University of Bucharest – Faculty of Biotechnical Systems Engineering (ISB), National Institute of Research–Development for Machines and Installations Designed to Agriculture and Food Industry (INMA Bucharest), Romanian Agricultural Mechanical Engineers Society (SIMAR), National Research & Development Institute for Food Bioresources (IBA Bucharest), National Institute for Research and Development in Environmental Protection (INCDPM), Research–Development Institute for Plant Protection (ICDPP), Research and Development Institute for Processing and Marketing of the Horticultural Products (HORTING), Hydraulics and Pneumatics Research Institute (INOE 2000 IHP) and "Food for Life Technological Platform", in Bucharest, ROMANIA, between 05–06 October, 2023. The current identification numbers of the selected papers are the **#1–2**, **#11–12** and **#20**, according to the present contents list.
- IIZS 2023 – The XIII International Conference on Industrial Engineering and Environmental Protection, organized by Department of Mechanical Engineering, Department of Environmental Protection and Department of Industrial Engineering in Exploitation of Oil and Gas, Technical Faculty Mihajlo Pupin Zrenjanin, University of Novi Sad (SERBIA), in cooperation with partners University Politehnica Timisoara, Faculty of Engineering, Hunedoara (ROMANIA), University St. Kliment Ohridski, Technical Faculty, Bitola

(MACEDONIA), Aurel Vlaicu University of Arad, Faculty of Engineering, Arad (ROMANIA), University of East Sarajevo, Faculty of Mechanical Engineering East Sarajevo (BOSNIA & HERZEGOVINA) and University of Giresun, Faculty of Engineering, Giresun (TURKEY), in Zrenjanin, SERBIA, in 05–06 October, 2023. The current identification numbers of the selected papers are the **#6–8 and #18**, according to the present contents list.

ACTA TECHNICA CORVINIENSIS – Bulletin of Engineering is a good opportunity for the researchers to exchange information and to present the results of their research activity. Scientists and engineers with an interest in the respective interfaces of engineering fields, technology and materials, information processes, research in various industrial applications are the target and audience of ACTA TECHNICA CORVINIENSIS – Bulletin of Engineering. It publishes articles of interest to researchers and engineers and to other scientists involved with materials phenomena and computational modeling.

The journal's coverage will reflect the increasingly interdisciplinary nature of engineering, recognizing wide-ranging contributions to the development of methods, tools and evaluation strategies relevant to the field. Numerical modeling or simulation, as well as theoretical and experimental approaches to engineering will form the core of ACTA TECHNICA CORVINIENSIS – Bulletin of Engineering's content, however approaches from a range of environmental science and economics are strongly encouraged.

Publishing in ACTA TECHNICA CORVINIENSIS – Bulletin of Engineering is free of charge. There are no author fees. All services including peer review, copy editing, typesetting, production of web pages and reproduction of color images are included. The journal is free of charge to access, read and download. All costs associated with publishing and hosting this journal are funded by ACTA TECHNICA CORVINIENSIS – Bulletin of Engineering as part of its investment in global research and development.

ISSN: 2067–3809

Fascicule 2
[April – June]
tome XVII
[2024]

ACTA Technica CORVINIENSIS
BULLETIN OF ENGINEERING

ISSN: 2067-3809

ACTA TECHNICA CORVINIENSIS – Bulletin of Engineering | e–ISSN: 2067 – 3809
Tome XVII [2024] | Fascicule 2 [April – June]

[1.]Teodor Gabriel FODOREAN, [1.]Elena Mihaela NAGY, [1.]Nicolae CIOICA, [2.]Lucian FECHETE, [1.]Valentin VLADUT

RESEARCH REGARDING THE POSIBILIETIES OF USING NATURAL FIBERS AND WOOL FOR FABRICATION OF BIOCOMPOSITE MATERIALS

[1.]INMA Bucharest, ROMANIA
[2.]UT Cluj Napoca, Facultatea de Autovehicole, Mecatronica si Inginerie Mecanica, ROMANIA

Abstract: Biocomposite materials are a family of new materials that differentiate from the classic composite materials by the fact that are partially or completely obtained from biogenic raw materials and are biodegradable in natural environments. Products from plastic and composite materials became important components of the human's life in the last 60 – 70 years. Their main disadvantage consists is that they are not biodegradable, creating big environment issues. Biocomposite materials start to be recognized as a positive investment for the chemical industry, offering various opportunities and presenting a real interest for all industrial and social sectors. In present it exists the trend of continuing the research on the already known directions, but in the same time we have the horizon of some new researches in other domains of possible applications, that were not touched till now. The evolution of researches in the field of biocomposite materials conduct to the development of new bio materials and bio fabrication technologies, with applicability in agriculture, agriculture equipment's manufacturing, packaging industry, biomedicine, passengers and public transportation vehicles industry, civil construction industry etc. The researchers performed in this paper were orientated on the study of the possibilities of fabrication by extrusion of a few blends using biopolymers, natural fibers or wool. As raw materials have been used starch, PBAT biopolymer (ecoflex F BX 7011 is an oil–based, biodegradable polymer designed for film extrusion and extrusion coating, produced by BASF) and natural fibers as miscanthus, hemp or sheep wool. The mechanical properties of the new obtained biocomposite materials were also evaluated.

Keywords: biocomposite materials, sustainability, starch, natural fibres, wool

INTRODUCTION

Biocomposite materials are biodegradable materials obtained from biogenic raw materials originating from agricultural/natural resources.

Natural fibers are biogenic raw materials that are more and more introduced in many industries during the last two decades. Through the most used natural fibers in industry are hemp, curacao, mischantus, cocos etc. The most viable renewable resources used in the development and fabrication of biocomposite materials are: starch, cellulose, sugar or sucrose, casein, chitin and chitosan, gelatine, vegetable oils, protein from cereals, seaweeds, wool, hemp fibers, miscanthus fibers etc.

In Figure 1 is presented the ideal life cycle of renewable row materials that can be used at the biocombisite materials production.

As evolution of appearance of bioplastic and biocomposite materials we point that in 1869 Hyatt brothers opened the first cellulose factory, in 1923 was started the mass production of cellophane, in 1941 Henry Ford was uncover the fist car with plastic body made from biogenic row materials, in 1988 was discovered termoplastic starch (being after one of the most commune used raw material for obtaining the new bioplastic and biocomposite materials).

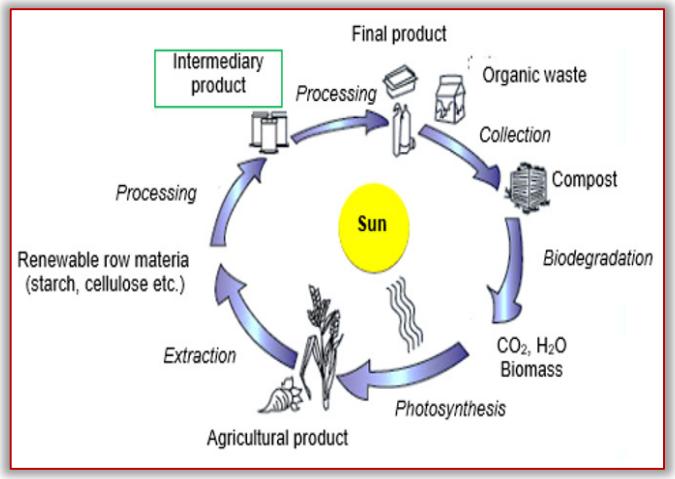

Figure 1 – Loop of the ideal life cycle of renewable raw materials in the case of their use for biocomposite materials production.

The global volume of plastic materials production is 390.7 million tones. From this 98.5% are fossil–bases, recyclable 8.3%, non–recyclable 91.7%. From this only 5.86 million tones (1.5%) are fabricated based on renewable resources.

The ideal solution to follow will be, to increase the percentage of biodegradable plastic and composite materials in correlation with creation of new muti–component completely biodegradable composites, with dedicated performance characteristics.

In the same time are regions worldwide with big production of sheeps. One of the resulting raw

materials of this business is the sheep wool. The climatic conditions and the industry was passing to some changes in the past 30 – 40 years. Based on this are regions as Transylvania, in Romania, where is produced a lot of wool and is not used in a big proportion in textile industry resulting many wool residues. Our goal is to use this wool residues fabrication of biocomposite materials from one side. From other side, we are also looking to other opportunities where is possible to use this wool residues.

In the context described above we was developing and testing two recipes:

— Starch – PBAT – miscanthus fibers,

— Starch – PBAT – sheep wool.

For the above two bleeds we was trying to establish the influence of blending conditions (thermal regime, rotation speed, residence time) to the mechanical properties of the new obtained composite material. In the same time we establish will be optimized and established the best processing conditions in order to obtain the expected mechanical proprieties of the new obtained blank biobased composite material.

MATERIALS AND METHODS

The materials used in this experiment was alimentary starch, PBAT (ecoflex F BX 7011) produced by BASF and PA (platamid) produced by ARKEMA.

The starch used was having a density of 1.78 g/cm^3.

Table 1. Chemical composition of starch depending of the source of provenience

Chemical composition	Wheat	Potato	Rice	Corn
Lipids (% dry substance)	0.8	0.05	0.8	0.77
Protein (% dry substance)	0.4	0.06	0.45	0.38
Ash (% of dry substance)	0.15	0.4	0.5	0.06
Phosphorus (% dry substance)	0.06	0.08	0.1	0.02
Amylose %	26–31	23	14–32	28
Amylopectin %	72	79	83	67–69

Souce: Banks and Greenwood 1975:263; Blanshard 1987:17; Swinkels 1985:25,27

Ecoflex F BX 7011 comes closer than any other biodegradable plastic to the processing properties of a classic polymer. A flexible plastic designed for film extrusion and extrusion coating. Blown film extrusion is a particular area where PBAT shows well–balanced processing properties and the resin can be used in extrusion coating applications.

The characteristics of PBAT (ecoflex F BX 7011) used, supplied by BASF are shown in table 2. In Figure 2 are presented some row granules of PBAT.

Table 1. PBAT (ecoflex F BX 7011) material proprieties

Property	Value	Test Method
Density (g/cc)	1.25 to 1.27	ASTM D792
Melt Index, g/10min (190°C/2.16Kg)	2.7 to 4.9	ASTM D1238
Melting Point, °C	110 to 120	DSC
Tensile Strength, (MPa)	34	ASTM D638
Elongation, %	700	ISO 527
Water Permeation Rate, g/(m^2*d)	140	DIN 53122

Figure 2 – PBAT raw granules.

In our bled we was using also natural fibers – miscanthus and sheep wool.

The miscanthus fibers (figure 3) was imported from South America and the sheep wool (figure 4) was obtained from sheep farms located in Fagaras, Transylvania region, Romania. The density of miscanthus fibers was 0.7–1 g/cm^3. The sheep wool was having a density of 3.45 g/cm^3.

Figure 3 – Miscanthus fibers

Figure 4 – Sheep wool

Processing was carried out using a Brabender mixer (figure 5) equipped with a 30 cm^3 mixing chamber and two counter–rotating rotors. The mixing took place for 10 minutes, at a

temperature of 140°C and having a rotors speed of 60 rpm. The amount of biopolymer used in the starch matrix (60%) was 30% PBAT in (mass/volumetric) percentage, miscanthus fibers and wool being incorporated in 10%. The materials were dried before processing at 75°C for 5 hours.

Two experiments/recipes were conducted:

— **Experiment 1** – Starch 60% – PBAT 40% – Wool 10% – temperature 140°C, mixing time 10 min, rotation speed 60 rpm,

Figure 5 – Brabender internal mixer 30 cm^3

— **Experiment 2** – Starch 60% – PBAT 40% – Miscanthus 10% – temperature 140°C, mixing time 10 min, rotation speed 60 rpm.

RESULTS

After the evacuation of the materials from the mixing chamber, they were inserted inside a Carver 4394 press, heated to 140°C, pre–melted for 2 minutes and then pressed in the form of plates for 2 minutes, the pressure used being 200 bars. After pressing, cooling the mold and obtaining plates with a thickness of 1 mm (± 0.05 mm) for tensile testing and bars with dimensions 1 mm x 4 mm x 80 mm for shock tests. The material was inspected to observe the dispersion of the fibers and subsequently prepared for mechanical tests. Good dispersion was observed in all cases.

Tensile test – the characteristics evaluated in the tensile tests (Young's modulus, tensile strength, elongation at break) were recorded according to the SR EN ISO 527–2/2012 standard, using an Instron 3345 machine, with a test speed of 10 mm/min, the distance between the clamps being 40 mm. All samples were initially conditioned at 23°C and 50% relative humidity.

In figure 6 we have presented the tensile strength curve for the three different processed mixtures made following the biocomposite material recipe with miscanthus (starch 60% – PBAT 30% – 10% miscanthus, extrusion at 140°C, 60 rpm, time 10 min.).

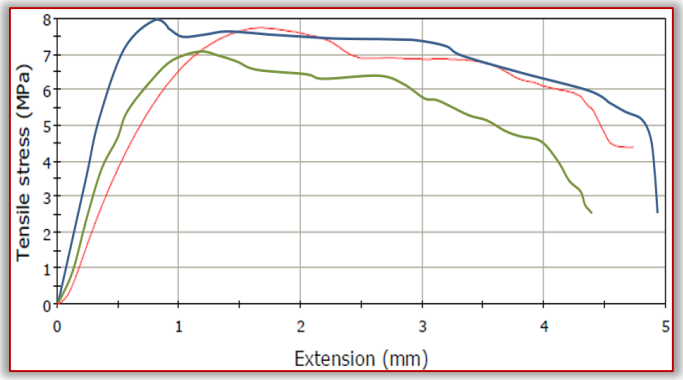

Figure 6 – Tensile strength curve for starch mixture 60%–PBAT30%–10%miscanthus, extrusion at 140°C, 60 rpm, time 10 min. Red curve – mix 1, blue curve – mix 2, green curve – mix 3.

In figure 7 are presented the tensile strength curve for the three different processed mixtures made following the biocomposite material recipe with sheep wool (starch 60% – PBAT 30% – 10% wool, extrusion at 140°C, 60 rpm, time 10 min.).

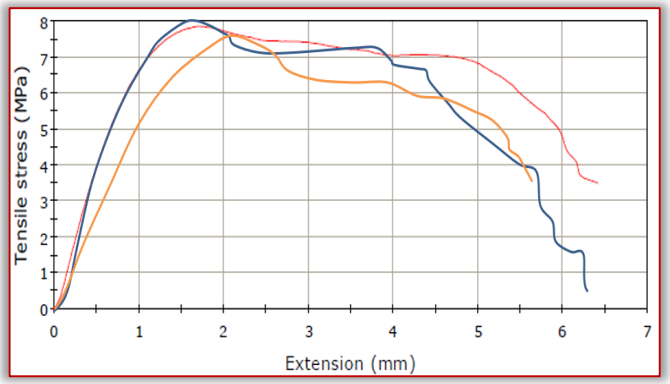

Figure 7. Tensile strength curve for starch mixture 60%–PBAT30%–10%sheep wool, extrusion at 140 °C, 60 rpm, time 10 min. Red curve – mix 1, blue curve – mix 2, orange curve – mix 3.

CONCLUSIONS

Plastic and composite products have become, in the last 70–80 years, important components of everyday life, characterized by good resistance, easy to be processed into different shapes, being much lighter and cheaper than other materials. Their big disadvantage is that they are not biodegradable, creating big environmental problems. An alternative to conventional plastic materials are bioplastic and biocomposite materials. The current research was focused on the development of optimal processes for production of biocomposite materials that meet the functional requirements of users as well as environmental ones. The applied research carried out within the work sought to highlight the connection between the parameters of the biocomposite materials production process (temperature, rpm, extrusion time), from one side, and the mechanical properties of the new material obtained, on the other side.

New biocomposite material recipes have been established, based on starch, biopolymers (PBAT) and natural fibres – miscanthus and sheep wool waste. In this work we analysed the mechanical properties (tensile strength) of the new obtained material. Following the obtained results for tensile strength we can conclude that the new obtained biocomposite materials can be used forward for new applications for agriculture, for agriculture equipments, for automotive industry etc.

In regards to the future research directions we are planning to follow the next steps:

- Production by extrusion of other recipes of starch–based biocomposites, containing natural fibers;
- Realization by injection or thermoforming of some elements for agriculture, agriculture equipments, interior of vehicles;
- Carrying out other tests to evaluate the mechanical properties of the new obtained materials.
- Carrying out tests to evaluate the behaviour in time and the biodegradability of new materials.

Acknowledgement

This work is financed by Ministry of Research, Innovation and Digitalization through Program 1 – Development of the national research–development system, Subprogram 1.2 – Institutional performance – Projects for financing excellence in RDI, Contract no. 1PFE/30.12.2021„ and by NUCLEU program contr. 9N/01.01.2023, project PN 23 04 02 02.

References

[1] Agassant J.–F., Coupez T., Demay Y., Vergnes B., Vincent M., Thermomechanical modelling of polymer processing, in: Advances in the Flow and Rheology of Non–Newtonian Fluids, D. A. Siginer, R. P. Chhabra, D. De Kee Eds., Elsevier (1999).

[2] Bastioli, C. Global status of the production of biobased packaging materials. Conference Proceedings: The Food Biopack Conference, Denmark, 2000, Copenhagen.

[3] Cai Z, Al Faruque MA, Kiziltas A, Mielewski D, Naebe M.(2021), Sustainable lightweight insulation materials from textile–based waste for the automobile industry, Materials, 14(5):1241.

[4] Fu Y., Fodorean G., Navard P., Peuvel–Disdier E. – Study of the partial wetting morphology in polylactide/poly[(butylene adipate)-co-terephthalate]/polyamide ternary blends: case of composite droplets, Polymer International (impact score 3.44), pp. 1378–1385, 2018, https://mc.manuscriptcentral.com/pi–wiley

[5] G. Della Valle, B. Vergnes, D. Lourdin, Viscous properties of thermoplastic starches from different botanical origin, Intern. Polym. Proc., 22, 471–479, 2007.

[6] J.F. Agassant, P. Avenas, J. Ph. Sergent, P.J. Carreau, Polymer Processing. Principles and Modeling, Oxford University Press, 1991.

[7] James E. R.Couper, Richard Erdlac, Handbook of bioplastics and biocomposites engineering applications, Srikanth Pilla, 2011.

[8] McGlashan, S. A., and Halley, P. J., Preparation and characterization of biodegradable starch–based nanocomposite materials. PolymerInternational, 2003.

[9] Mohanty A K, Misra M, Hinrichsen G, "Biofibres, biodegradable polymers and biocomposites: An overview", Macromolecular Materials and Engineering, 2000.

[10] Parra D.F., Tadini C.C., Ponce P. and Lugão A.B., Mechanical properties and water vapor transmission in some blends of cassava starch edible films, Carbohydrate Polymers, 2004.

[11] Remadevi R., Md Abdullah Al Faruque, Jizhen Zhang, Maryam Naebe,(2020), Electrically conductive honeycomb structured graphene composites from natural protein fibre waste, Materials Letters, 264:127311.

[12] *** Bioplastics: Plants, Raw Materials, Products, Fachagentur Nachwachsende Rohstoffe, Gülzov, Germany, 2005.

[13] *** Rosato, D. Global Bioplastics Legislative Drivers Recap, www.omnexus.com

Note: This paper was presented at ISB–INMA TEH' 2023 – International Symposium on Technologies and Technical Systems in Agriculture, Food Industry and Environment, organized by University "POLITEHNICA" of Bucuresti, Faculty of Biotechnical Systems Engineering, National Institute for Research–Development of Machines and Installations designed for Agriculture and Food Industry (INMA Bucuresti), National Research & Development Institute for Food Bioresources (IBA Bucuresti), University of Agronomic Sciences and Veterinary Medicine of Bucuresti (UASVMB), Research–Development Institute for Plant Protection – (ICDPP Bucuresti), Research and Development Institute for Processing and Marketing of the Horticultural Products (HORTING), Hydraulics and Pneumatics Research Institute (INOE 2000 IHP) and Romanian Agricultural Mechanical Engineers Society (SIMAR), in Bucuresti, ROMANIA, in 5–6 October, 2023.

ISSN: 2067-3809

ACTA TECHNICA CORVINIENSIS – Bulletin of Engineering | e–ISSN: 2067 – 3809
Tome XVII [2024] | Fascicule 2 [April – June]

[1.]Iuliana GĂGEANU, [1.]Ana–Maria TĂBĂRAȘU, [2.]Oana–Elena MILEA, [1.]Gabriel GHEORGHE,
[1.]Mihaela NIȚU, [2.]Carmen–Otilia RUSĂNESCU

SIMULATION OF PLANT GROWTH IN DIFFERENT CONDITIONS

[1.] National Institute of Research – Development for Machines and Installations Designed to Agriculture and Food Industry, ROMANIA;
[2.] National University of Science and Technology POLITEHNICA Bucharest – Faculty of Biotechnical Systems Engineering, ROMANIA

Abstract: As the global population is continuously increasing, the supply of food with equal accessibility has become a major issue and future challenge. To meet both the worldwide demand for food security and new environmental needs, agriculture must increase food production and quality while decreasing its detrimental impacts on ecosystems and the environment). However, new agricultural land is limited, so sustainable production and increasing productivity of existing agricultural land is an important aspect to address global food security. Climate change affects precipitations, water flows, humidity and temperature. These changes will influence crop growth, phenology and yields, in the end leading to drastic changes in areas that are suitable for specific plant cultivation and land use changes. The paper presents considerations for the simulation of plant growth, taking into account temperature, lighting, water availability and fertilization.
Keywords: climate change; growth simulation; plant monitoring; food safety

INTRODUCTION

As the global population is continuously increasing, the supply of food with equal accessibility has become a major issue and future challenge. To meet both the worldwide demand for food security and new environmental needs, agriculture must increase food production and quality while decreasing its detrimental impacts on ecosystems and the environment (*USDA, 2015; Grusson et al., 2021*). However, new agricultural land is limited, so sustainable production and increasing productivity of existing agricultural land is an important aspect to address global food security.

Soil moisture has significantly decreased in the Southern region and increased in parts of northern Europe since the 1950s (*Destouni & Verrot, 2014; European Environment Agency Report No 1/2017*). Similar effects are expected for the coming decades, as the rise in average temperatures continues and rainfall patterns change (*European Environment Agency, 2021; Arvis et al., 2020*).

Climate change affects precipitations, water flows, humidity and temperature. The frequency and magnitude of extreme weather and climate events will increase, and the distribution and abundance of pest species and pollinators may change, Figure 1 (*Bocci & Smanis T., 2019; European Environment Agency, 2021*). These changes will influence crop growth, phenology and yields, in the end leading to drastic changes in areas that are suitable for specific plant cultivation and land use changes (*Ceglar et al., 2019; Ahsan et al., 2021*).

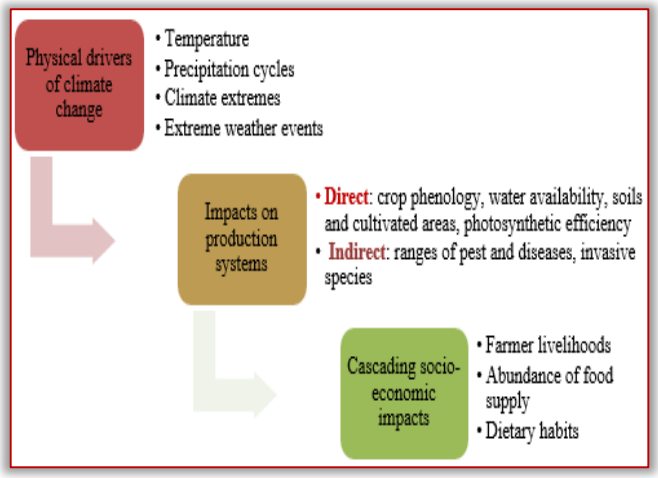

Figure 1 – Impacts of climate change on agriculture
(European Environment Agency, 2021, Arvis et al., 2020)

Also, fertilizers–pesticides–herbicides (FPH) play a sensitive role in food systems: they are applied in order to fertilize, protect crops from pests and diseases and to reduce food losses, but on the other hand they can have negative impacts on the environment and human health (*Ahsan et al., 2021; Aktar et al., 2009)*. The improper application of chemicals on crops may also contribute to accumulation of residues in food materials, soils and water. Vegetable production is an excellent example of intensive cropping systems that are indeed on the rise (*Eyhorn et al., 2015*).

Vegetable cropping systems are high–input and generally require large quantities of fertilization, frequent irrigation, and pest control.

The concept of IoT is more and more present in agriculture, guiding it in the direction of automation and intellectualization. A WSN, as a part of IoT, can act as a distributed measurement instrument that can offer improved information compared with a single manually operated instrument, especially in large areas. Considering the differences in parameters that can occur in large areas, multiple points have to be monitored.

A suitable solution is a WSN with long–range data transmission (*Centenaro et al., 2016*). The representative technology that can be successfully implemented in WSN (*Wixted et al., 2016*) for this type of network is LoRa (*Mekki et al., 2019*) developed by Semtech. For research and final user applications, Libelium released a wireless sensor node based on Arduino programming language with implementations in large areas through specific expansions boards. Libelium implemented more than 150 case studies with WSN, proving the applicability of the system for various real–life applications (*www.libelium.com/*).

The paper provides insights into the implementation of intelligent systems for simulating the growth of plants in various conditions, as a method for combating and reducing the impact of climate changes on agricultural crops and on food availability.

MATERIALS AND METHODS

An essential component of simulating plant growth is different environmental conditions. Researchers can investigate how various environmental elements, genetic factors, and management techniques affect plant growth and development. The following key conditions (figure 2) should be considered:

Temperature

Plants can thrive at temperatures between 4.5 and 36 degrees Celsius. The best temperature for growth varies depending on the species and stage of development, and it typically varies from night to day. Temperature affects a number of development processes. Respiration, a step in the photosynthetic process, maturity, flowering, fruit ripening, and dormancy are a few of these (*Janick J., 2019*).

Several temperature ranges can influence the growth and development of plants. It should be investigated how temperature affects plant development and yield by simulating various temperature situations.

Light

Plants are sensitive to light with wavelengths between 300 and 800 nm. Plants grown in the lack of light become etiolated. Chlorophyll is absent from etiolated plants, which are tall and wiry with long internodes and small, ungrown leaves. Their morphological expression of etiolation is connected to how light affect auxin synthesis and distribution.

The tissues generated in the light or the dark have the same anatomical characteristics, although light promotes some phases of growth while suppressing others, such as internode elongation (*Noggle & Fritz, 1983; Hartman et al., 1981*).

Light is a crucial element in the growth and development of plants. It should be investigated how light intensity, duration, and quality affect plant growth and development by modeling various lighting scenarios.

Soil moisture

It is well recognized that stomata closure, drought signaling in roots, reduced leaf water potential, and cellular dehydration are the main characteristics of moisture shortage.

Reduced cell size and growth, decreased cellular and metabolic activity, suppression of photosynthetic activity, turgor loss, production of reactive oxygen species, and altered carbon partitioning are all secondary or long–term impacts of soil moisture stress (*Jaleel et al., 2009; Bosco de Oliviera et al., 2013*).

Particularly during the germination and seedling stages, soil moisture levels can have an impact on plant growth and development. The impact of soil moisture on plant growth and development by can be assessed simulating various humidity situations.

Soil type

Living things, minerals, and organic substances all make up the soil. Decomposing materials like rotting plants and dead animals are where the organic matter in the ground comes from.

Since minerals are created when rocks are broken, the kind and quantity of minerals in the soil are influenced by the types of rocks that can be found nearby. Bacteria and earthworms are examples of the living creatures that make up soil. Plant growth is influenced by everything, including organic substances and ground–dwelling creatures (*USDA, 2015).*

Varying soil types can have an impact on a plant's growth and development because of differences in their nutrient and water–holding capacities. How different soil types affect plant

development and yield can be investigated by testing growing the same plants on various soil types.

Nutrient availability

Proper management of nutrients is crucial for preserving soil production. In order to make fertilizer recommendations for field crops, soil analysis is typically employed as a criterion. Soil fertility is a phrase used to characterize the quantity of nutrients present in the soil.

In order to forecast how plants will respond and manage nutrients, observations and tests are utilized to assess the availability of nutrients. Because of other factors like soil moisture content and soil temperature, the availability of vital nutrients to growing plants cannot be guaranteed even when there are sufficient total amounts of these elements present in the soil (*Fageria & Baligar, 2005*).

Nutrient availability is a critical factor for plant growth and development. By simulating different nutrient availability conditions, the effects of nutrient deficiencies or excesses on plant growth and yield can be studied.

Genetic factors

Genetic factors can play a significant role in plant growth and development. By simulating different genetic factors, such as plant traits, heritability, and gene expression patterns, researchers can study the effects of genetic factors on plant growth and development.

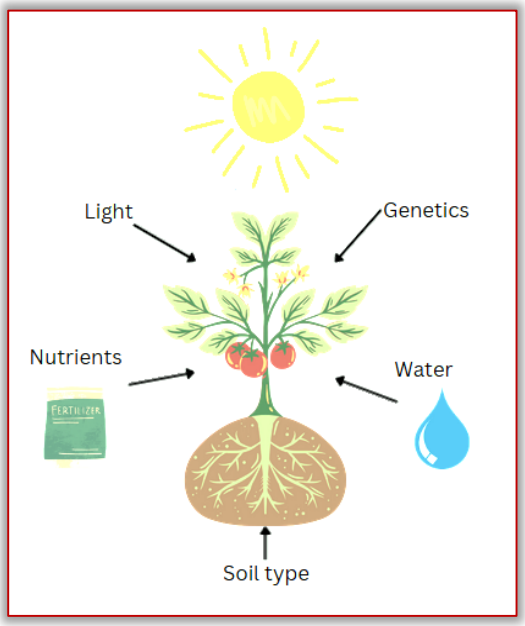

Figure 2 – Factors affecting plant growth

Overall, modeling different plant growth environments is crucial for comprehending the intricate interplay between many environmental, genetic, and management elements that influence plant growth and crop output. Simulated plant growth can assist scientists and growers in enhancing crop yields and minimizing the impact of agriculture on the environment.

RESULTS

There are numerous computer programs available that simulate plant growth, some of which include:

- **3D modelling models**: these programs simulate three–dimensional plant growth and development using mathematical models. They can be used to construct and test novel plant structures as well as to generate realistic virtual environments for studying plant behaviour.
- **Agent–based models**: these simulations depict how various components of a plant system—such as cells and organs—behave individually and in relation to one another to form emergent plant behaviour.
- **Physiological models**: the biochemical and physiological activities that take place inside a plant, such as photosynthesis, respiration, and nutrient intake, are simulated by these models. They can be applied to research how plants react to various environmental factors and to forecast agricultural output.
- **Machine learning models**: these models use algorithms predicting plant growth and development using information from actual plant growth studies. They can be used to forecast crop harvests, improve plant growth conditions, and create new plant varieties.

Apart from computer–based models, plant simulation modules can be used for simulating conditions that affect plant growth. A plant growth simulation module might include the following typical features:

- **Initial conditions**: The simulator allows the user to set the initial conditions for the simulation, such as the size and shape of the plant at the beginning of the simulation.
- **Environmental factors**: The simulator allows the user to adjust the environmental conditions in the module, such as the amount of light or water the plant receives, nutrients, weather conditions, etc.
- **Visualization**: The module may include tools for visualizing the growth of the plants over time, such as time–lapse videos.
- **Output data**: The module may provide output data on the growth of the plant, such as the size and shape of the plant at different points in time or the amount of biomass produced.
- **Validation**: The module may be validated using experimental data to ensure that it

accurately models the growth and development of real plants in the simulated conditions.

Plant simulation modules include:

- **Hydroponic systems**: Hydroponic systems are setups that allow plants to grow in nutrient–rich water solutions without soil. Hydroponic systems can be used to control the nutrient composition of the growing medium and to optimize the growth conditions for the plants.

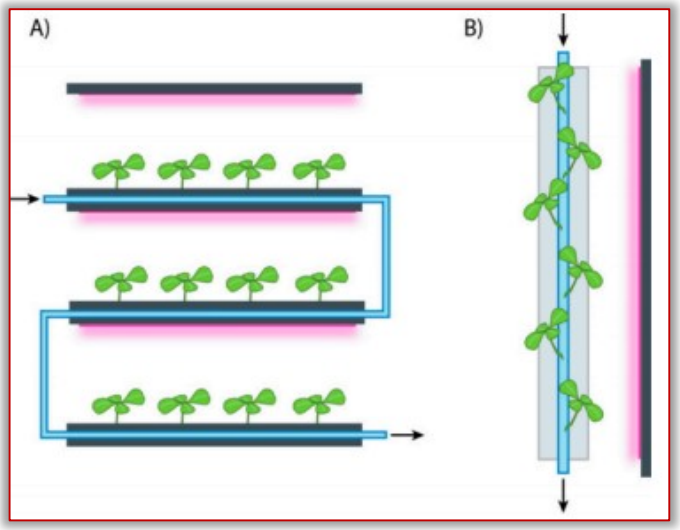

Figure 3 – Structure of the hydroponics vertical farm (Gentry M., 2019)
(A) Nutrient film technique. Each tray has LED lighting above it.
(B) Drip irrigation system. The column is dripped with nutrient water. This device can either allow for more natural daylight or be illuminated from the side by LEDs

- **Aeroponic systems**: in an Aeroponic system, plants are grown in an environment where air with very little water or mist and without soil are used. In this system, the plant roots are suspended in air. So, the roots are nourished by misting the root zones with a nutrient solution on a continual basis by using a fine sprayer to ensure that the roots get sufficient oxygen.

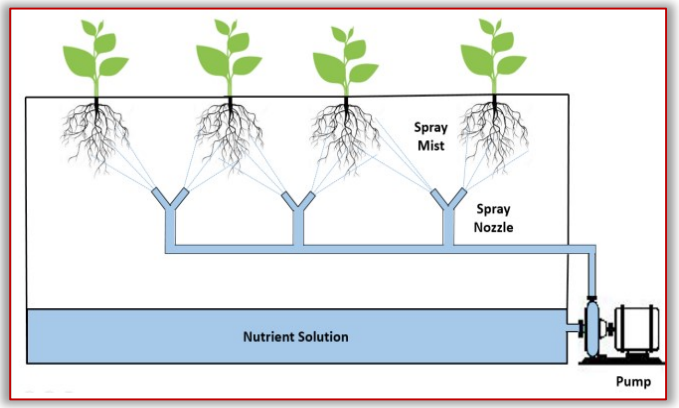

Figure 4 – Schematic diagram of an aeroponic system
(*Gupta & Ganapuram, 2019*)

- **Complete plant growth chambers**: Specialized environmental chambers known as "plant growth chambers" are created to replicate the conditions necessary for plant growth. In addition to other environmental elements, they can be used to regulate parameters like temperature, moisture, light intensity, and CO_2 levels. In these systems, the level of CO_2, moisture content and nutrition status within the chambers are monitored and controlled for maintaining simulated growing conditions with the help of a fully integrated computer management system.

CONCLUSIONS

- The use of plant growth simulation in agriculture has the potential to revolutionize the way in which crops are established, grown and managed.
- By providing more efficient and sustainable methods of monitoring and controlling the environment, plant simulation models and physical modules have the potential to improve the efficiency and profitability of agricultural operations, as well as to improve land use soil health.
- However, further research is needed to overcome the technical and financial challenges associated with computer aided and physical modules for plant simulation in this context, to allow more widespread adoption and use of these systems in agriculture.
- The employment of plant simulation can help farmers and researchers in the future to change both crop technologies and cultivated plants in accordance to current climate and soil factors that are found in particular areas and adapt their activity to foreseen changes in water availability, temperatures, light and nutrients.

Acknowledgement

This research was supported by the Romanian Ministry of Research Innovation and Digitalization, through the project "Intelligent plant growth systems under controlled environmental conditions" – PN 23 04 01 04– Ctr. 9N/01.01.2023 and through Program 1 – Development of the national research–development system, Subprogram 1.2 – Institutional performance – Projects for financing excellence in RDI, Contract no. 1PFE/30.12.2021.

References

[1] Ahsan D., Brandt U.S., Faruque H. (2021). Local agricultural practices to adapt with climate change. Is sustainability a priority?, Current Research in Environmental Sustainability, Volume 3, 100065

[2] Aktar MW, Sengupta D, Chowdhury A. (2009). Impact of pesticides use in agriculture: their benefits and hazards. Interdiscip Toxicol. 2(1):1–12

[3] Arvis, B., et al. (2020). Consequences of global climate change and their impacts on Europe – a view on agricultural commodities, report for the European Environment Agency, Ramboll France, Aix–en–Provence.

[4] Bocci, M. and Smanis, T. (2019). Assessment of the impacts of climate change on the agriculture sector in the southern Mediterranean: foreseen developments and policy measures, Union for the Mediterranean.
[5] Bosco de Oliveira A, Alencar NLM, Gomes–Filho E. (2013). Comparison between the water and salt stress effects on plant growth and development In: Akıncı S, editor. Responses of organisms to water stress: Agricultural and Biological Sciences. IntechOpen Publisher.
[6] Ceglar, A., et al. (2019). Observed northward migration of agro–climate zones in Europe will further accelerate under climate change, Earth's Future 7(9), p. 1088–1101.
[7] Centenaro M., Vangelista L., Zanella A., Zorzi M. (2016). Long–range communications in unlicensed bands: The rising stars in the IoT and smart city scenarios, IEEE Wireless Communications, vol. 23, no. pp. 60–67.
[8] Cook, B.I., Smerdon, J.E., Seager, R. et al. (2014). Global warming and 21st century drying. Clim Dyn 43, 2607–2627
[9] Destouni G., Verrot L. (2014). Screening long–term variability and change of soil moisture in a changing climate, Journal of Hydrology, Volume 516, p. 131–139
[10] European Environment Agency Report No 1/2017, Climate change, impacts and vulnerability in Europe 2016 – An indicator–based report.
[11] European Environment Agency. (2021). Global climate change impacts and the supply of agricultural commodities to Europe
[12] Eyhorn F, Roner T, Specking H. (2015): Reducing pesticide use and risks – What action is needed? https://pdfs.semanticscholar.org/
[13] Fageria N.K., Baligar V.C. Nutrient availability. (2005). Encyclopaedia of soils in the environment. Pp. 63–71
[14] Gentry M. (2019). Local heat, local food: Integrating vertical hydroponic farming with district heating in Sweden. Energy 2019, 174, pp. 191–197.
[15] Grusson Y., Wesstrom I., Joel A. (2019). Impact of climate change on Swedish agriculture: Growing season rain deficit and irrigation need, Agricultural Water Management, Volume 251, 106858.
[16] Gupta M. K., Ganapuram S. (2019) Vertical farming using information and communication technologies.
[17] Hartman, H.T., W.J. Flocker and A.M. Kofranck. (1981). Plant Science Growth, Development and Utilization of Cultivated Plants. Prentice–Hall, Inc. pp. 676.
[18] Jaleel CA, Manivannan P, Wahid A, Farooq M, Al–Juburi HJ, Somasundaram R, et al. (2009). Drought stress in plants: a review on morphological characteristics and pigments composition. Int J Agric Biol. 11(1): 100–105.
[19] Janick J. (1979). Horticulture Science. W.H. Freeman and Company, San Francisco. pp.608.
[20] Mekki K., Bajic E., Chaxel F., Meyer F. (2019). A comparative study of LPWAN technologies for large–scale IoT deployment, ICT express, vol. 5, no. 1, pp. 1–7.
[21] Noggle, G. R. and G. J. Fritz. (1983). Introductory Plant Physiology, 2nd Edition. Prentice–Hall Inc. Englewood Cliffs, New Jersey. pp. 625.
[22] Norris C.E., Congreves K.A. (2018). Alternative Management Practices Improve Soil Health Indices in Intensive Vegetable Cropping Systems: A Review. Front. Environ. Sci. 6:50
[23] USDA. (2015). World Agriculture Supply and Demand Estimates. U.S. Department of Agriculture.
[24] Wixted A. J., Kinnaird P., Larijani H. et.al. (2016). Evaluation of LoRa and LoRaWAN for wireless sensor networks, Sensors, 30 Oct.–3 Nov. 2016.
[25] Quan M., Liang J. (2017). The influences of four types of soil on the growth, physiological and biochemical characteristics of Lycoris aurea (L' Her.) Herb, Sci Rep. 7: 43284.
[26] *** www.libelium.com/ (accessed on April 25th, 2023).

Note: This paper was presented at ISB–INMA TEH' 2023 – International Symposium on Technologies and Technical Systems in Agriculture, Food Industry and Environment, organized by University "POLITEHNICA" of Bucuresti, Faculty of Biotechnical Systems Engineering, National Institute for Research–Development of Machines and Installations designed for Agriculture and Food Industry (INMA Bucuresti), National Research & Development Institute for Food Bioresources (IBA Bucuresti), University of Agronomic Sciences and Veterinary Medicine of Bucuresti (UASVMB), Research–Development Institute for Plant Protection – (ICDPP Bucuresti), Research and Development Institute for Processing and Marketing of the Horticultural Products (HORTING), Hydraulics and Pneumatics Research Institute (INOE 2000 IHP) and Romanian Agricultural Mechanical Engineers Society (SIMAR), in Bucuresti, ROMANIA, in 5–6 October, 2023.

ISSN: 2067–3809

Fascicule 2
[April – June]
tome XVII
[2024]

ACTA Technica CORVINIENSIS
BULLETIN OF ENGINEERING

ISSN: 2067-3809

ACTA TECHNICA CORVINIENSIS – Bulletin of Engineering | e–ISSN: 2067 – 3809
Tome XVII [2024] | Fascicule 2 [April – June]

[1.]Israa JAFAR, [2.]Jameel Al–NAFFAKH, [3.]Mohammed R. Al–QASSAB, [4.]Zaid Mohammed Al–MAKHZOOMI

COMPARATIVE ANALYSIS OF COMBUSTION PROPERTIES BETWEEN WASTE AUTOMOTIVE OIL AND LIGHT DIESEL OIL AS ALTERNATIVE FUELS

[1.] Basic Sciences Department, University of Kufa, College of Dentistry, Kufa, IRAQ
[2,3.] Mechanical power Department, Al–Furat Al–Awsat Technical University, Najaf Technical Engineering College, Najaf, IRAQ
[4.] Oil Product Distribution Company / Najaf Branch (OPDC), Najaf, IRAQ

Abstract: Given the extensive and widespread utilization of fossil fuels in various sectors, there is a pressing need to explore and develop novel alternative fuels in order to effectively address the increasing global energy demand. The finite nature of fossil fuel reserves has resulted in their rapid depletion, thus highlighting the need to explore sustainable alternatives. Additionally, the utilization of fossil fuels is associated with environmental issues such as the phenomenon of global warming, the release of detrimental emissions, and the instability of prices. Within this particular context, Waste Automotive Oil (WAO) presents itself as a potentially advantageous substitute fuel and additive, providing economically viable resolutions to the dual concerns of fuel requirements and waste management. This study aims to conduct a comparative analysis of the combustion characteristics of waste motor oil obtained from the wet air oxidation (WAO) process and conventional Light Diesel Oil (LDO). The utilization of waste motor oils as fuel was investigated in a cylindrical combustor equipped with a coil–over liquid oil burner under various operating conditions. The process of preheating waste automobile oil to a temperature of 90 °C inside the combustion chamber was found to be effective in reducing viscosity and improving compatibility with the properties of light diesel oil. In order to evaluate the fuel characteristics, a comprehensive examination of waste motor oils was carried out, following the guidelines set by the American Society for Testing and Materials (ASTM). This involved conducting both physical and chemical analyses. The study involved conducting an experimental assessment of the combustion characteristics of an oil burner, specifically focusing on the utilization of waste motor oils and light diesel oil. This evaluation encompassed the analysis of axial and radial flame temperatures, concentrations of exhaust gas emissions, and overall combustion efficiency. The results of the study indicated that raising the initial air pressure led to higher exhaust gas temperatures for both LDO and WAO. When comparing the indicated CO2 emission values, it was observed that LDO exhibited a higher level of emissions in comparison to WAO. Furthermore, it was observed that waste motor oils demonstrated elevated levels of hydrocarbon emissions when compared to low–density oil (LDO). Moreover, it was observed that the heat transfer proportion to the combustion wall was higher in the case of WAO compared to LDO. Variations in heat release at a higher parity ratio can explain the observed difference in radial flame temperature between the WAO and LDO. The presence of a greater carbon content within the chemical composition of waste motor oils was observed to result in a heightened flame intensity in comparison to diesel oil. In summary, this research offers valuable insights into the combustion properties of Waste Automotive Oil as a potential alternative fuel in comparison to conventional Light Diesel Oil. The results of this study make a valuable contribution to the ongoing endeavors aimed at identifying sustainable solutions to the challenges presented by conventional fossil fuels. These challenges include their limited availability and the negative environmental consequences they entail.

Keywords: Alternative fuels, Combustion characteristics, Environmental impacts, Environmental impacts, and Waste Automotive Oil (WAO)

INTRODUCTION

Global energy consumption has continued to increase in recent years, with total primary energy demand growing at an average annual rate of 2.3% between 2010 and 2018 [1]. Fossil fuels still dominate the energy mix, accounting for around 80% of total primary energy supply [2]. However, oil, natural gas and coal reserves are ultimately finite, geographically restricted and their continued use raises serious environmental issues [3–5].

Burning of fossil fuels remains the prime anthropogenic source of air pollutants and carbon emissions driving climate change [6–8]. Extreme weather events and changing weather patterns tied to global warming have intensified in recent years [9–11]. Energy security concerns also persist due to the uneven distribution and trade of fossil fuel resources [12,13]. Oil price volatility and supply disruptions continue to have macroeconomic consequences [14–16].

These factors have driven research and adoption of renewable energy sources. Considerable progress has been made in first generation biofuels from sugar, starch and oil crops [17,18]. However, their large–scale use competes with food production and requires significant land and water resources [19–21].

Hence, focus has shifted to advanced biofuels from non–food biomass including ligno–cellulosic materials, municipal waste, used cooking oil and algae [22–25]. Recent techno–economic assessments find waste cooking oil and algal oils to be attractive and relatively low–cost feedstocks for biodiesel production [26–28]. Additionally, direct combustion of waste vegetable oils in furnaces and boilers can displace fossil fuel use [29–31]. Detailed studies comparing key fuel properties and combustion characteristics of waste oils to petroleum fuels

remain vital [32–36].

This study aims to address these open questions by conducting a direct experimental comparison of WAO and light diesel oil (LDO) combustion in a test furnace under varying conditions. The key research objectives are to Measure and contrast flame temperatures, pollutant emissions, and thermal efficiencies. Also, Elucidate the impacts of fuel chemical composition and physical properties on observed combustion characteristics.

Determine the feasibility and potential of WAO as an alternative to replace or supplement diesel fuels. Fulfilling these aims will provide novel insights into WAO combustion properties and its viability as a sustainable fuel option. Findings will advance knowledge on substituting WAO in combustion systems previously designed for diesel fuels.

PROPERTIES OF WASTE AUTOMOTIVE OIL

Waste automotive oil, referring to contaminated lubricating oils previously used in internal combustion engines, possesses a number of properties that differ significantly from fresh engine oils or diesel fuels and present challenges for its use as a fuel substitute. In particular, waste automotive oils exhibit higher densities ranging from 0.87–0.95 g/cm3, substantially increased viscosities from 100–500 cSt due to accumulation of combustion byproducts compared to 10–20 cSt in fresh oils, lowered flash points below 100°C owing to fuel dilution and volatiles loss, variable chemical compositions containing oxidation products, metals, residues and additives dependent on engine types, reduced heating values around 35–40 MJ/kg versus approximately 45 MJ/kg for diesel fuels, heightened acidity with acid numbers of 3–7 mg KOH/g arising from hydrocarbon oxidation to carboxylic acids, and contamination from chlorinated compounds, paint, plastics, and heavy metals.

The elevated viscosity, corrosion from acidity, decreased energy density, and prevalence of impurities present significant challenges for waste oil combustion and emission performance that necessitate careful evaluation and treatment before these oils can serve as effective substitutes for conventional liquid fuels.

In summary, while waste automotive oils hold potential as alternative fuels, their specific properties must be analyzed in detail to determine viability as substitutes for typical diesel fuels as shown in table 1.

Table 1. Properties of waste automotive oil [5]

Property	Typical Value
Density	0.87 – 0.95 g/cm3
Viscosity	100 – 500 cSt
Flash Point	< 100°C
Heating Value	35 – 40 MJ/kg
Acid Number	3 – 7 mg KOH/g

Table 2 quantitatively compares the chemical and physical properties of waste automotive oil and light diesel oil. In comparison to diesel fuel, waste oil possesses inferior fuel properties such as increased density and viscosity. Specifically, the heating value of waste oil becomes reduced due to contaminants accumulated from previous use. Oxidation of the waste oil lowers the cetane number. Furthermore, waste oil exhibits heightened levels of sulfur, ash, carbon residue, and acidity relative to diesel fuel standards.

The flash point decreases as well in waste oil because of dilution by residual fuels. In summary, key fuel performance metrics like density, viscosity, heating value, cetane number, contaminants, acidity, and flash point are negatively impacted in waste oils compared to diesel fuels.

These inferior fuel properties present technical challenges for direct substitution of waste oils in diesel engines and would necessitate upgrading of waste oils to improve fuel quality before they could be utilized as effective diesel replacements.

Table 2. Chemical and Physical properties of waste Automotive oil and light diesel oil [13]

Properties	Light Diesel Oil	Waste Automotive Oil
Density at 15°C (kg/m3)	830–860	0.87–0.95
Viscosity at 40°C (cSt)	2–4.5	100–500
Lower heating value (MJ/kg)	43	35–40
Cetane number	40–55	15–30
Sulfur content (ppm)	<500	1000–5000
Carbon residue (%)	0.1	0.5–2.0
Ash content (%)	<0.01	0.1–0.4
Flash point (°C)	>55	<100
Acid number (mg KOH/g)	<0.6	3–7

Gas chromatography analysis reveals the fatty acid profile of waste automotive oils shifts significantly from fresh lubricants due to engine use. Saturated acids like palmitic and stearic increase through oxidation while unsaturated acids including oleic and linoleic decline as shown in table 3.

Contaminants from combustion, dilution, breakdown of oils, and environmental pollutants also accumulate, altering the composition away from original oil formulations. The complex

mixture presents technical challenges for direct use as fuel.

Table 3. Fatty Acid Composition for waste Automotive oil [13]

Fatty Acid Methyl Ester	Fatty Acid Composition (wt. %)
Palmitic acid (C16:0)	15–20
Stearic acid (C18:0)	5–10
Oleic acid (C18:1)	15–30
Linoleic acid (C18:2)	10–15
Linolenic acid (C18:3)	1–5
Erucic acid (C22:1)	<5
Lignoceric acid (C24:0)	<2
Other/unidentified	15–30

The automobile oils contain a complex mixture of fatty acids and other organic compounds that differ significantly from the composition of the original lubricating oil. Specifically, saturated fatty acids including palmitic and stearic acids are increased in waste oils as the base oil undergoes oxidation during engine operation.

In contrast, unsaturated fatty acids such as oleic and linoleic acids are reduced because the C=C double bonds are broken through oxidation reactions. Polyunsaturated linolenic acid is particularly susceptible to hydrolysis under oxidative conditions.

Longer chain fatty acids such as erucic and lignoseric acids may also be introduced from fuel residues and oil additives. In addition, oxidation processes generate other organic compounds not attributable to specific fatty acid peaks. Contaminants from combustion and contamination also contribute to compounds detected in chemical analysis. In summary, the fatty acid profile of waste motor oils shifts significantly away from the original lubricant formulations due to oxidation, fuel dilution, further breakdown, and environmental pollutants accumulating during use in engines.

EXPERIMENTAL TESTING FACILITIES

These experiments were conducted in the Continuous Combustion Laboratory, Department of Power Mechanics, College of Engineering Technology, Najaf. Al–Furat Al–Awsat University. Figure 1 shows the schematic diagram of the experimental setup. The system consists of a heavy oil burner with a heating load of 150 kW.

Three repeated tests were performed at each equivalence ratio for both diesel and waste oil to evaluate consistency. Fuel was supplied from separate tanks through a gravity feed system at a constant flow rate of 2 ml/min and monitored with a rotameter. Temperatures were recorded using a K–type thermocouple with an uncertainty of ±1°C.

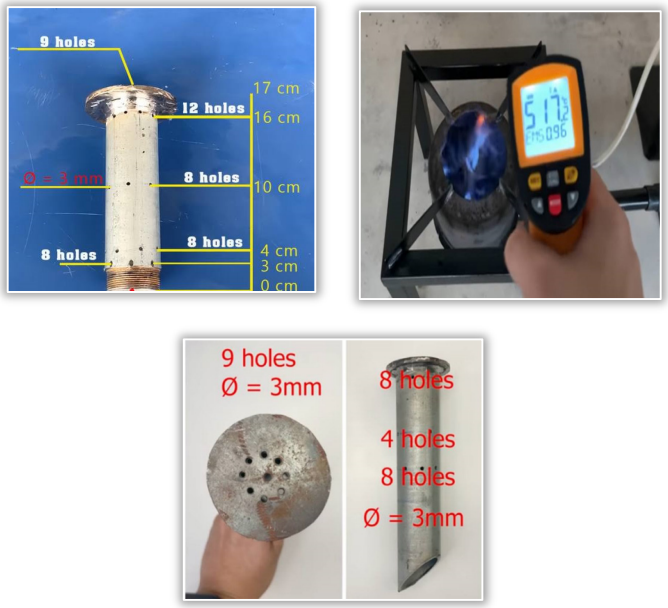

Figure 1. Experimental design of the burner

Exhaust emissions were measured using a portable gas analyzer with a ±2% uncertainty for CO_2, CO and NOx readings.

Uncertainty analysis was performed on the calculated combustion efficiency and heat transfer values based on standard error propagation methods. The measuring equipment was calibrated prior to testing and calibration curves were used to account for instrument uncertainties. The data in each condition of the replicate tests were averaged to improve consistency in the results. The standard deviations were less than 2.5% of the mean values, indicating good repeatability.

The burner is cylindrical with a diameter of 6 inches and contains a cylindrical head with a diameter of 2 inches and a length of 18 cm. It contains holes with a diameter of 3 mm and a number of 33. The burner is supplied with air using a fan. It is equipped with an automatic control system in the air mass flow rates.

Fuel is supplied by gravity using a separate fuel tank connected to the combustion chamber of the burner. Where the fuel is burned up to 90 degrees Celsius as an initial burn to heat it, and then the air is expelled through the holes in the burner head at certain flow rates, and a thermostat to adjust to the required temperature (depending on the type of fuel).

The burner is inserted vertically into the combustion chamber for use in various industrial applications.

RESULTS AND DISCUSSIONS

The exhaust emissions analysis reveals some key advantages of using waste automotive oil (WAO) as an alternative fuel compared to light

diesel oil (LDO) under different equivalence ratios. WAO demonstrated substantially lower carbon monoxide (CO) emissions, with a maximum reduction of 71.4% observed at an equivalence ratio of 0.94. The elevated oxygen content of WAO improves oxidation reactions, facilitating more complete combustion and conversion of CO to CO2. However, elevated WAO viscosity led to issues with improper fuel–air mixing, resulting in around 72% higher unburned hydrocarbon emissions relative to LDO. This indicates the need for enhanced injection systems and atomization methods optimized for WAO's higher viscosity. WAO did provide the benefit of reduced NOx emissions attributed to its lower combustion temperatures. For both fuels, exhaust gas temperatures increased with higher primary air pressures as greater fuel mass flow rates were achieved.

The thermal heat balance calculations revealed the percentage of heat transferred to the combustor walls was consistently higher for WAO fuel compared to LDO, with a maximum rise of 12% observed. This divergence suggests increased heat loss associated with WAO combustion, likely resulting from its higher fuel consumption and the impact of its elevated viscosity. Greater heat transfer to the walls may also relate to differences in flame geometry between the fuels. Optimizing the combustor insulation and cooling design could help reduce excessive WAO heat loss to improve thermal efficiency.

The inflame temperature analysis showed that for both WAO and LDO, increasing primary air pressure led to higher inflame temperatures attributed to greater heat release rates. However, peak inflame temperatures were generally greater for WAO, especially at higher equivalence ratios where its central inflame temperatures exceeded those of LDO. The improved oxygenation of WAO facilitates more energetic combustion reactions upon sufficient heating, despite its lower heating value relative to LDO. The study also found radial inflame temperatures declined moving outwards from the center for both fuels due to the cooling effect of the water–jacketed combustor walls.

Visual observation of the combustion flames revealed key distinctions between WAO and LDO. LDO exhibited wider, more luminous and soot–laden yellowish flames compared to dimmer blue flames for oxygenated WAO. The increased luminosity and sooting arise from LDO's higher carbon content. Superior fuel–air mixing in WAO flames due to intrinsic oxygen enables cleaner, more complete combustion. However, the narrowing of WAO flames suggests potential issues with flame stability that should be addressed through combustor design modifications. Swirl injection, chamber geometry and flow turbulence should be optimized for WAO's viscosity. While WAO has some technical challenges remaining, it demonstrates viability as an alternative fuel with the advantage of substantially lower emissions of pollutants like CO, NOx and soot compared to conventional diesel fuels. Further efforts to engineer improved combustors tailored to WAO's unique fuel properties are recommended to enhance performance as shown in figures (2–6).

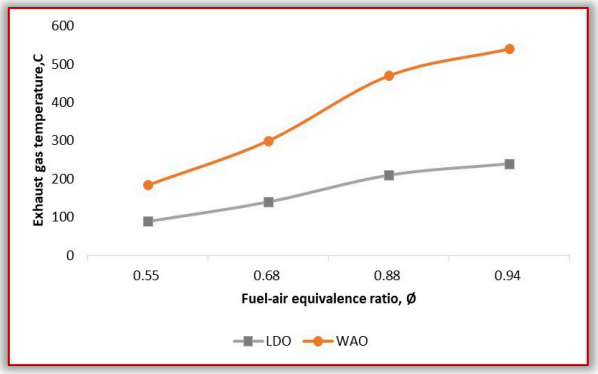

Figure 2. Effects of Air Pressure on Exhaust Gas Temperatures across Fuel–Air Equivalence Ratios

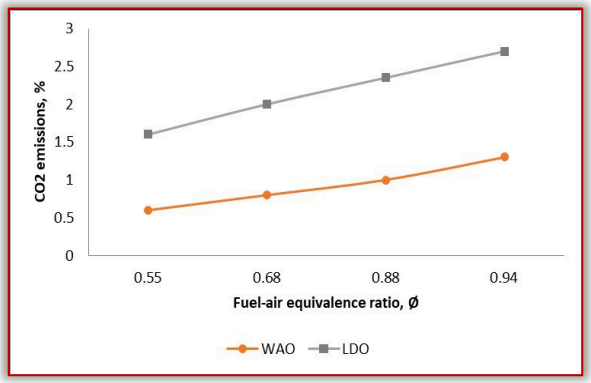

Figure 3. CO2 Emissions for Waste Cooking Oils and Diesel Fuels at Varying Fuel–Air Equivalence Ratios

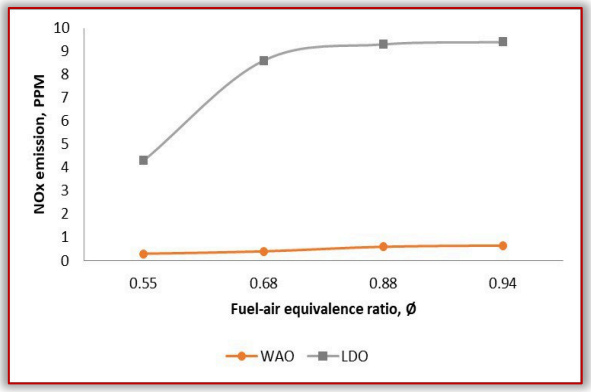

Figure 4. NOx emissions at different equivalence ratios

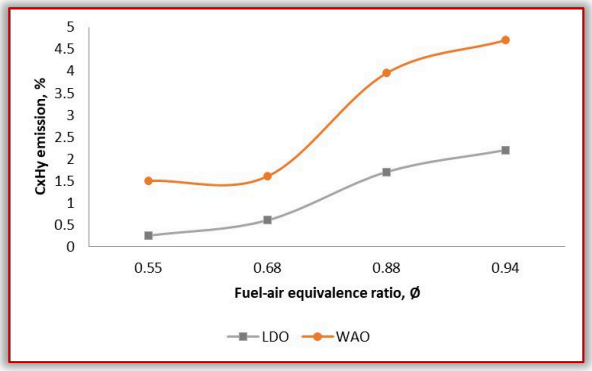

Figure 5. Hydrocarbon Emissions across Varying Fuel–Air Equivalence Ratios

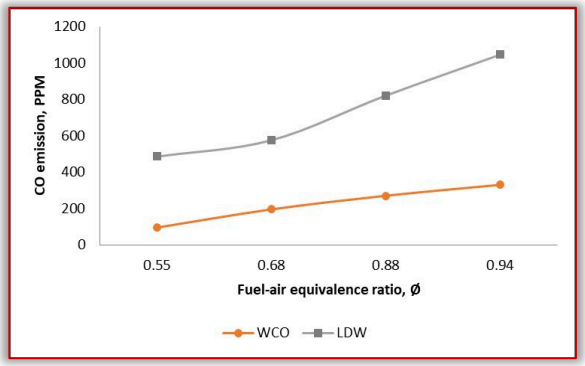

Figure 6. CO emissions at different equivalence ratios

Looking at thermal heat balance, the percentage of heat transferred to the combustor walls increased for WAO compared to LDO, with a maximum rise of 12% for WAO. This heat transfer difference can likely be explained by WAO's higher fuel consumption and subsequent increased heat loss. The study also analyzed inflame temperatures radially from the center to the cooled combustor walls. Here, inflame temperatures increased with primary air pressure for both LDO and WAO, but were higher for WAO due to greater heat release. At higher equivalence ratios, inflame temperatures were greater in the center for WAO compared to LDO.

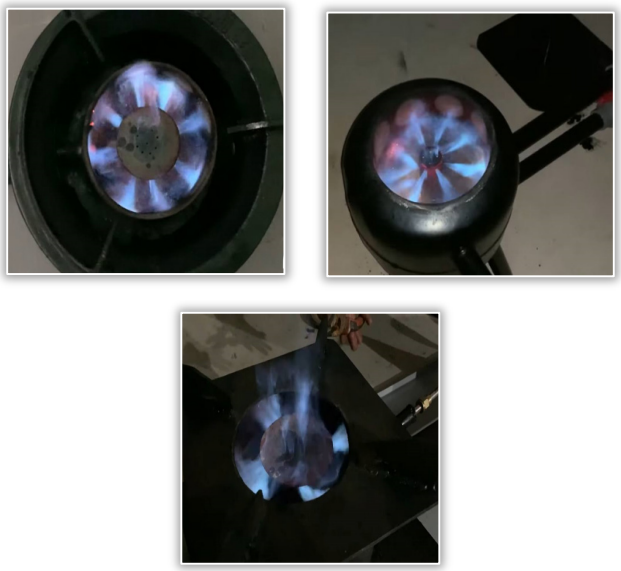

Figure 7. Effect of primary air pressure on flame visual observation of WCO

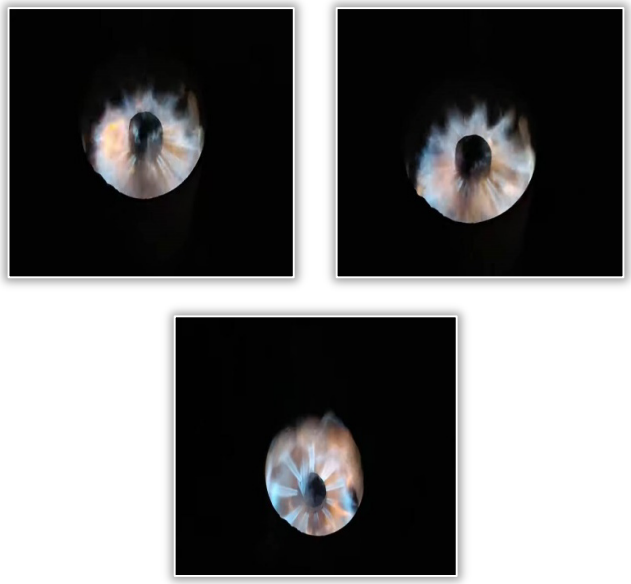

Figure 8. Effect of primary air pressure on flame visual observation of LDO

Finally, visual analysis of the flames revealed key differences between LDO and WAO. LDO flames were wider, more luminous, and yellow/orange in color – indicating more soot compared to the less luminous WAO flames. The authors attributed the cleaner, bluer WAO flames to improved fuel–air mixing from oxygen content, allowing more complete combustion as shown in figure (7–8).

CONCLUSION

In conclusion, this study provides valuable insights into the combustion properties and feasibility of using Waste Automotive Oil (WAO) as an alternative fuel compared to conventional Light Diesel Oil (LDO).

The key findings show that WAO demonstrated substantially lower carbon monoxide and nitrogen oxide emissions due to its higher oxygen content enabling more complete combustion. However, WAO did produce higher levels of unburned hydrocarbons resulting from its higher viscosity and improper fuel–air mixing. WAO also showed increased heat transfer to the combustor walls attributed to greater fuel consumption and heat loss.

Analysis of inflame temperatures and visual flame characteristics revealed additional differences between the fuels. WAO exhibited higher inflame temperatures at increased primary air pressures and equivalence ratios because of greater heat release. Flame imaging showed LDO had wider, more luminous and sooty flames compared to the cleaner, bluer flames of WAO.

In summary, while challenges remain regarding viscosity, atomization, and unburned hydrocarbons, WAO shows promise as an alternative fuel with comparable or improved performance over conventional diesel oil in key

aspects like lower emissions of pollutants. With further research to optimize fuel properties and design improved combustors tailored to WAO, waste automotive oils could prove to be an effective and more sustainable substitute for diesel fuels. The insights from this study make a valuable contribution to ongoing efforts assessing and developing alternative fuels to address the environmental and supply issues associated with continued fossil fuel dependence.

References

[1] BP Statistical Review of World Energy, 2019.
[2] REN21 Renewables 2018 Global Status Report
[3] Wang, J., Zhao, P., Niu, S., Dai, Y. and Zhang, Y., 2019. The forecast of coal consumption in China using a GM (1, 1) model. Energies, 12(4), p.751.
[4] Capellan–Perez, I., de Castro, C. and Miguel, L.J., 2019. Dynamics of primary energy consumption and decomposition analysis in South America. Energies, 12(6), p.1167.
[5] Karabulut, A., Bilgen, S., Keçebaş, A., Gedik, E. and Sarıtas, A., 2020. An assessment of distributed energy resource penetration impacts on power markets in the United States. Energy Sources, Part B: Economics, Planning, and Policy, 15(1), pp.52–67.
[6] Kuik, F., Kerssemeeckers, M., Lauer, A., Chakraborty, S., Liu, J., Elser, M., da Silva, T.F., Ginzburg, V., Hofmann, T. and Archibald, A.T., 2021. Amplifying the loss in fossil fuel emissions due to COVID–19 through enhanced monitoring of air quality. Remote Sensing of Environment, 252, p.112200.
[7] Zhang, Z., Wang, J., Chen, B. and Chen, G.Q., 2020. Reduced carbon emission from fossil fuel consumption of Beijing–Tianjin–Hebei region, China: An analysis based on production–pollution framework. Energy Policy, 140, p.111404.
[8] Tong, D., Zhang, Q., Zheng, Y., Caldeira, K., Shearer, C., Hong, C., Qin, Y. and Davis, S.J., 2019. Committed emissions from existing energy infrastructure jeopardize 1.5 C climate target. Nature, 572(7769), pp.373–377.
[9] Seneviratne, S.I., Nicholls, N., Easterling, D., Goodess, C.M., Kanae, S., Kossin, J., Luo, Y., Marengo, J., McInnes, K. and Rahimi, M., 2012. Changes in climate extremes and their impacts on the natural physical environment. Managing the risks of extreme events and disasters to advance climate change adaptation, pp.109–230.
[10] Zhang, W., Villarini, G., Vecchi, G.A. and Smith, J.A., 2018. Urbanization exacerbated the rainfall and flooding caused by hurricane Harvey in Houston. Nature, 563(7731), p.384.
[11] Mazdiyasni, O. and AghaKouchak, A., 2015. Substantial increase in concurrent droughts and heatwaves in the United States. Proceedings of the National Academy of Sciences, 112(37), pp.11484–11489.
[12] Aid, R. and Gruenwald, P., 2018. Germany's Green Energy Shift is More Fizzle than Sizzle. The Heritage Foundation.
[13] Jeon, S.M. and Shin, W.K., 2019. The dynamic relationship between oil and renewable energy consumption: Evidence from a panel VARX analysis. Energy Policy, 132, pp.240–248.
[14] Ji, Q. and Fan, Y., 2015. How does oil price volatility affect non–energy commodity markets? Applied Energy, 145, pp.273–283.
[15] Alquist, R., Bhattarai, S. and Coibion, O., 2020. Commodity–price comovement and global economic activity. Journal of Monetary Economics, p.102676.
[16] Chen, H., Liao, H. and Tang, B.J., 2019. Impacts of OPEC's political risk on the international crude oil prices: An empirical analysis based on the SVAR models. Energy Economics, 80, pp.895–910.
[17] Souza, S.P., Seabra, J.E. and Nogueira, L.A., 2020. Sustainable production of bioethanol from sugarcane, corn and lignocellulosic biomass. In Biomass, Biopolymer–Based Materials, and Bioenergy (Vol. 2, pp. 97–126). Elsevier.
[18] Yan, L., Yang, N., Piao, Z., Li, Z. and Sun, Y., 2019. Progress in researching Chinese dominant bioenergy plants. Renewable and Sustainable Energy Reviews, 101, pp.332–346.
[19] Searchinger, T., Heimlich, R., Houghton, R.A., Dong, F., Elobeid, A., Fabiosa, J., Tokgoz, S., Hayes, D. and Yu, T.H., 2008. Use of US croplands for biofuels increases greenhouse gases through emissions from land–use change. science, 319(5867), pp.1238–1240.
[20] Fargione, J., Hill, J., Tilman, D., Polasky, S. and Hawthorne, P., 2008. Land clearing and the biofuel carbon debt. science, 319(5867), pp.1235–1238.
[21] Gasparatos, A., Stromberg, P. and Takeuchi, K., 2013. Biofuels, ecosystem services and human wellbeing: Putting biofuels in the ecosystem services narrative. Agriculture, ecosystems & environment, 172, pp.111–128.
[22] Moutinho, D., Schwartz, C., Trabold, T.A. and Heimiller, D.M., 2020. Algae–based bioenergy and biofuels: Rate, economics and implications at scale. Applied Energy, 278, p.115634.
[23] Chongkhong, S., Tongurai, C. and Chetpattananondh, P., 2018. Biodiesel production from waste cooking oil using sulfated TiO2 nanocatalyst. Renewable Energy, 118, pp.635–642.
[24] Hossain, A.K., Davies, P.A., Plant, S., Loh, W.S., Nahil, M.A., Tahmasebim A., Rahman, P.K.S.M., Bafana, A., Xu, X. and Yan, D.Y.S., 2021. Biofuel production from microalgae cultivation: Progress and prospects. Journal of Cleaner Production, 288, p.125685.
[25] Gurung, S., Karmacharya, P., Pathak, S.R., Kabuye, V.K. and Kumar, A., 2020. Biodiesel production from microalgae and waste cooking oil: An integrated approach. 3 Biotech, 10, pp.1–23.
[26] Behzadi, H. and Farid, M.M., 2018. Yield of extracted biodiesel versus theoretical yield. Biofuel Research Journal, 5(1), pp.743–746.
[27] Olagunju, A., Olabanjo, O., Fagbiele, O., Adeniyi, O., Adeyinka, S. and Oguntoke, O., 2021. Waste cooking oil: A hindrance transformed into biodiesel using a supportive heterogeneous nanocatalyst. Energy Sources, Part A: Recovery, Utilization, and Environmental Effects, 43(12), pp.1448–1462.
[28] Nasution, M.A., Hamidi, N., Lennartsson, P.R., Taherzadeh, M.J. and Zamani, A., 2019. Biogas production from microalgae and macroalgae: A review. Renewable and Sustainable Energy Reviews, 105, pp.187–201.
[29] Arumugam, K. and Ponnusami, V., 2019. Biofuels production from waste eggshells and chicken bones catalyst and waste cooking oil an economical source for biodiesel: A review. Waste and Biomass Valorization, 10(3), pp.633–646.
[30] Dhar, A. and Kevin, R., 2016. Production of biodiesel from high free fatty acid content feedstock. Scientifica, 2016.
[31] Haik, Y., Selim, M.Y. and Abdulrehman, T., 2011. Combustion of algal oil methyl ester in an indirect injection diesel engine. Energy, 36(3), pp.1827–1835.
[32] Song, J., Wang, Y. and Lv, G., 2020. Engine combustion characteristics using aviation kerosene, biodiesel and swirl in high–altitude plateau regions. Energy, 190, p.116461.
[33] Attia, A.M.A. and Kulchitskiy, A., 2014. The blending of ethanol in diesel fuel as an alternative. Fuel, 116, pp.703–709.
[34] Moghaddas, A., Mehrpooya, M. and Salehi, M., 2022. A review on application of biodiesel–alcohol–diesel blends in diesel engines. Fuel, 307, p.121631.
[35] Xue, J., Grift, T.E. and Hansen, A.C., 2011. Effect of biodiesel on engine performances and emissions. Renewable and sustainable energy reviews, 15(2), pp.1098–1116.
[36] Di, Y., Cheung, C.S. and Huang, Z., 2009. Comparison of the effect of biodiesel–diesel and ethanol–diesel on the gaseous emission of a direct–injection diesel engine. Atmospheric Environment, 43(17), pp.2721–2730.

ISSN: 2067-3809

ACTA TECHNICA CORVINIENSIS – Bulletin of Engineering | e–ISSN: 2067 – 3809
Tome XVII [2024] | Fascicule 2 [April – June]

[1.]Benny JOSEPH , [2.]George MATHEW

STRENGTH LOSS CHARACTERISTICS OF FLY ASH BASED GEOPOLYMER CONCRETE EXPOSED TO ELEVATED TEMPERATURES

[1.] Department of Civil Engineering, V K C E T Thiruvananthapuram74, Kerala State, INDIA
[2.] Division of Safety and Fire Engineering, School of Engineering, Cochin University of Science and Technology, Cochin–22, Kerala State, INDIA

Abstract: Fly ash based geopolymer concrete, one of the environment friendly alternatives to conventional concrete, is expected to behave better at elevated temperatures. However limited information is available about its behaviour at elevated temperatures. This paper presents the engineering properties of fly ash based geopolymer concrete after exposure to elevated temperatures and compares the corresponding results with those of a conventional concrete having almost the same compressive strength of geopolymer concrete (at ambient temperature). The specimens were heated at a constant rate (5.5 °C /minute) to different set temperatures (200,400, 600 and 800 °C). They were cooled to ambient temperature by air cooling and water cooling and then tested for their strength properties. It could be observed that, the fly ash based geopolymer concrete undergoes a higher rate of strength loss during its early heating period (up to 200°C) compared to OPC concrete. However, the residual strength properties of both the concrete are almost the same at 400°C temperature exposure and beyond 600°C, while OPC concrete loses its strength properties rapidly; geopolymer concrete improves its strength. Hence, it could be concluded that the fly ash based geopolymer concrete could be considered as a better sustainable material than conventional concrete under the situations where it may be exposed to temperatures beyond 400 °C..

Keywords: Geopolymer, Fly ash, Concrete, High temperature, Engineering properties

INTRODUCTION

Construction industry needs materials and technologies that are environment friendly and sustainable. Most widely used construction material is cement. However, its manufacturing process leads to the production of greenhouse gas [1]. Fly ash, a waste product generated from thermal power stations causes environmental issues, unless disposed off properly [2]. Use of fly ash based geopolymer concrete as one of the construction materials will not only eliminate consumption of cement but also utilize industrial waste effectively. As a result, geopolymer (GP) concrete is emerging as one of the environment friendly alternatives to Ordinary Portland Cement (OPC) concrete

In GP concrete, a geopolymer binder is formed by alkali activation of amorphous alumina–silicate material under warm atmosphere. The result of geopolymerisation is the formation of a three dimensional structural framework which is formed after dissolution, hydrolysis and polycondensation reaction [3,4]. The effectiveness in the geopolymerisation process depends on type, particle size, and the degree of amorphous character and the chemical composition of alumino–silicate source materials [5–8]. Variables such as water to solid ratio, type and concentration of alkali, temperature of curing , period of curing, method of mixing etc. influence the properties of geopolymer mortar and concrete [9–11].

For normal applications, OPC concrete generally provides satisfactory thermal resistance up to a temperature exposure of about 400 °C. However, beyond this temperature, its strength properties decreases rapidly and wide spread cracking and subsequent spalling occurs [12–17]. Because of the low energy need for the production and expected better behaviour at elevated temperatures compared to OPC concrete, geopolymer compounds are being considered as sustainable fireproof building materials, heat insulators etc. However, most of the studies at elevated temperatures are on geopolymer paste and mortar [18–19]. Kong and Sanjayan [20], based on their study on fly ash based geopolymer concrete, have reported that the compressive strength of geopolymer concrete when exposed to elevated temperatures are influenced by the specimen size, size of coarse aggregate and type of aggregate. Kong et al. [19] observed a higher strength loss at elevated temperatures for metakaolin based geopolymer paste as against fly ash based geopolymer paste. At 800 °C, while metakaolin based geopolymer paste continued its strength loss, they observed a strength gain in fly ash based geopolymer.

Review of literature shows that, a systematic study on the engineering properties of geopolymer concrete exposed to elevated temperatures is still a gap area. Present paper focuses on an experimental investigation on the

engineering properties of geopolymer concrete exposed to elevated temperatures and compares the corresponding behavior of a comparable OPC concrete.

EXPERIMENTAL PROGRAM

Fly ash based geopolymer (GP) concrete specimens were made and were exposed to a constant rate of temperature increase (5.5 °C/ minutes). The specimens were then cooled to ambient temperature by air cooling and water cooling. Specimens were then tested at ambient temperature to determine their various engineering properties. OPC concrete was designed in such a way that the cube compressive strength of both GP and OPC concrete are almost the same at ambient temperature so that their test result could be compared.

Materials

Low calcium fly ash (ASTM Class F) obtained from a thermal power station (India) has been used for the present study. The chemical composition of fly ash is presented in Table1. The fly ash used had a specific gravity of 1.9. Partilce size distribution and XRD analysis are available in a publication [21].

A mixture of NaOH and Na_2SiO_3 solution (SiO_2 = 34.64%, Na_2O= 16.27%, water 49.09%) was used as alkali solution in the present investigation. NaOH pellets of 98% purity were used to make sodium hydroxide solution. The specific gravity of alkali liquid solution, having Na_2SiO_3/ NaOH (molarity 10) ratio 2.5 was 1.54.

Crushed granite aggregates of nominal size 20 mm was used as coarse aggregate. Natural river sand having fineness modulus of 2.36 was used as fine aggregate. The specific gravity of coarse and fine aggregate was 2.72 and 2.64 respectively. Ordinary Portland cement was used for making OPC concrete.

Table 1. Chemical composition of fly ash

Parameter	Content % by mass)
SiO_2	59.70
Al_2O_3	28.36
Fe_2O_3+Fe_2O_4	4.57
CaO	2.10
Na_2O	0.04
MgO	0.83
Mn_2O_3	0.04
TiO_2	1.82
SO_3	0.40
Loss of ignition	1.06

Mix proportioning

A preliminary study was carried out to arrive at the optimum proportion of the various constituents of GP concrete and it details are presented elsewhere [22]. Accordingly, the parameters that kept constant in the present investigation includes, aggregate content by volume (70%), the ratio of fine aggregate to total aggregate(0.35), ratio of alkali to fly ashy by mass (0.55), molarity of NaOH (10), ratio of Na_2SiO_3 to NaOH (2.5), ratio of water to geopolymer solid (0.25). The quantity of materials required to produce 1m^{3}of GP concrete based on the above proportions is given in Table 2.

Table 2. Quantity of materials required to produce 1m^{3}of GP and OPC concrete

Mix ID	Cemen (kg)	Flyash (kg)	Coarse aggregate (kg)	Fine Aggregate (kg)	NaOH Solution (kg)	Na2SO3 (kg)	Super Plasticizer (kg)
GP concr	––	310	1204	648	48.7	121	6.2
OPC concrete	475	–––	1204	648	–––	–––	1.9

Mixing

The prepared NaOH solution was first mixed with calculated amount of Na_2SiO_3 liquid and kept for 24 hours before use. Coarse and fine aggregates in saturated surface dry conditions were thoroughly mixed with fly ash in a pan mixture. The alkali liquid and Naphthalene based superplastisizer (2% by weight of fly ash) were mixed together and then added to the dry mix. The whole mixture was then mixed together for 5 minutes.

Casting of specimens

Steel moulds of size150 mm x 150 mm x 150 mm, 100 mm x 100 mm x 500 mm, and 150 mm diameter, 300mm height were used for mechanical properties of both GP and OPC concrete. The fresh GP and OPC concrete filled in 3 layers and compacted with the help of a table vibrator. The OPC concrete specimens were kept in the mould for 24 hours under laboratory conditions and then they were demoulded and immersed in water for curing. GP concrete specimens were kept under laboratory condition for 60 minutes and then, after covering with thin steel plate, they were subjected to heat curing in an electric oven at 100 °C for a period of 24 hours. The curing temperature and period of curing were arrived at based on a preliminary study [22]. After temperature curing, GP concrete specimens were kept at room temperature till they were tested. Geopolymer paste was prepared with the same GP concrete and specimens were prepared for different microstructural analysis.

Heating and testing of specimens

OPC concrete specimens were taken out of curing tank on the 27th day, their surfaces dried with cloth and kept in the laboratory for 24 hours. The specimens were then kept in an oven for 1 hour at 60°C to remove surface moisture so that exposure spalling could be avoided during heating.

GP and OPC concrete specimens were heated in an electric furnace to 200°C, 400°C, 600°C and 800°C. The rate of heating was kept at 5.5°C /minute. After attaining the target temperature, specimens were kept at the same temperature for 1 hour to ensure that the specimens attain a uniform temperature throughout. The heated specimens were then cooled by two different methods namely air cooling and water cooling. Both GP and OPC concrete specimens were tested after they were cooled down to ambient temperature.

RESULTS

Compressive strength

Table 3 gives the compressive strength of GP and OPC concrete after exposed to elevated temperature. From the Table 3, it could be observed that, for almost the same compressive strengths of both GP and OPC specimens at ambient temperature, there is a higher strength loss for GP concrete during the early stages of the temperature rise. In the present study, at 200°C , while air cooled and water cooled OPC concrete had a strength loss of about 0.4 % and 9% respectively, the corresponding loss of strength of GP concrete is about 26 % and 31% respectively.

Table 3. Cube compressive strength of GP and OPC specimens after exposed to elevated temperatures

Exposure Temperature (°C)	GP Concrete				OPC Concrete			
	Air cooled		Water cooled		Air cooled		Water cooled	
	Comp. strength (MPa)	SD*	Comp. strength (MPa)	SD*	Com. strength (MPa)	SD*	Comp strength (MPa)	SD*
Ambient (28)	57.30	0.45	–	–	59.85	0.68	–	–
200	42.52	0.68	39.40	0.68	59.60	1.17	54.37	0.88
400	37.33	0.45	35.85	0.44	42.66	0.44	39.85	1.14
600	30.82	0.67	28.00	0.94	32.44	0.84	31.48	0.54
800	32.88	0.38	31.30	0.31	21.00	0.31	19.55	0.62

* – SD – Standard deviation

The FTIR spectrum analysis of GP paste exposed to elevated temperatures is presented in figure 1[23], which shows a shift in the wave number and a substantial reduction of the peak in Si–O–Al (alumino silicate) and Si–O–Si regions (wave number 460cm^{-1} to 1088cm^{-1}) at a temperature exposure of 200°C, indicating a reduction in their bonding force and decrease in chain length [6]. Also, the bands representing water molecule (hydroxyl groups) in GP paste showed a marked decrease in their peak at a temperature exposure of 200°C and further increase in exposure temperature did not cause any further decrease in these peaks(wave number 3440 cm^{-1}). This means that, most of the weakly bound water molecules that were either adsorbed on the surface or trapped in the large cavities between the geopolymeric products get expelled at about 200°C. The combined result of the above may lead to a higher strength reduction in GP concrete compared to OPC concrete during the initial heating process.

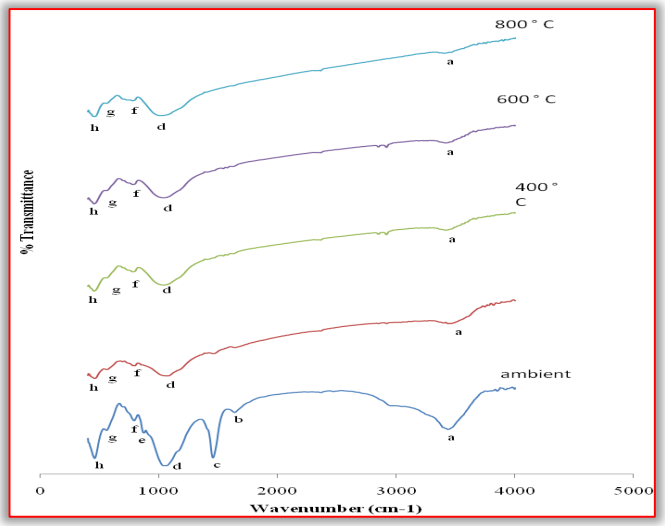

Figure 1. FTIR of Geopolymer paste exposed at different temperature (air cooled)
ambient : a= 3430 cm^{-1},b=1635 cm^{-1}, c=1453.13 cm^{-1}, d=1045 cm^{-1}, e=870.26 cm^{-1}
f=788 cm^{-1}, g=555 cm^{-1} and h=455 cm^{-1}
200 °C: a_1=3436 cm^{-1} d_1=1062 cm^{-1} f_1=795 cm^{-1} h_1=458 cm^{-1}
400 °C: a_2=3399 cm^{-1} d_2=1046 cm^{-1} f_2=788 cm^{-1} h_2=446 cm^{-1}
600 °C : a_3=3419 cm^{-1} d_3=1039 cm^{-1} f_3=776 cm^{-1} h_3=451 cm^{-1}
800 °C: a_4=3399 cm^{-1} d_4=1006 cm^{-1} f_4=775 cm^{-1} h_4=453 cm^{-1}

Even though the free water in concrete gets removed during the initial heating of OPC, the strength gained due to the hydration of unreacted cement particles compensates the strength loss due to other parameters in concrete when heated up to about 200 °C; a behaviour well accepted by many researchers [13,24].

Figure 2 shows the residual compressive strength of test specimen (in percentage of strength at ambient temperature) after the exposure to different temperatures and tested after cooling by air and water cooling methods. From Fig 2, it could be observed that, the air cooled OPC specimen does not experiences much strength reduction up to 200°C and beyond this, there is more or less a constant rate of strength reduction up to 800°C.

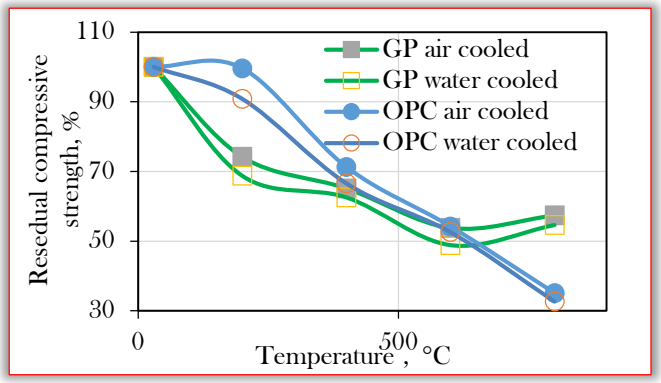

Figure 2. Residual cube compressive strength of GP and OPC concrete after exposure to elevated temperatures

Compared to air cooled OPC specimen, the rate of strength reduction between 200°C and 400°C is less for GP concrete and the percentage residual strength is almost same for both the types of concrete at 400°C. It may further be noted that, while the rate of strength loss between 400°C and 600°C is almost the same for both the types of concrete. However GP concrete shows a strength gain beyond 600°C, while OPC concrete continues to lose its strength.

From the XRD analysis (figure 3) of GP paste[23], an additional polymerization of GP concrete could be observed for a temperature exposure after 600°C, which is evident from the increased glass phase content above 600°C, as against the 90% glass phase content up to 600°C. Also, while the FTIR spectrum of GP paste showed only marginal reduction in the peak intensities over the Si–O–Al and Si–O–Si region for the temperature exposure between 200°C and 600°C, the peak intensity corresponding to Si–O–Si linkage increases slightly beyond 600°C, confirming the polymerization of initially unreacteted materials beyond 600°C.

It could be observed that, water cooled OPC specimens showed a lower strength at all exposure temperatures in the range between 3% and 9% compared to the strength of air cooled specimens primarily due to the thermal shock induced due to sudden cooling. Similar behaviour has been reported by other investigators also [25–27]. The water cooled GP concrete specimens also shows a lower strength compared to air cooled GP specimens (4% to 9% lower strength) and its behaviour is similar to that of OPC concrete when exposed to water cooling.

The strength reduction in OPC concrete when exposed to high temperatures is primarily due to the decomposition of the cement paste and the corresponding loss of adhesion [28].

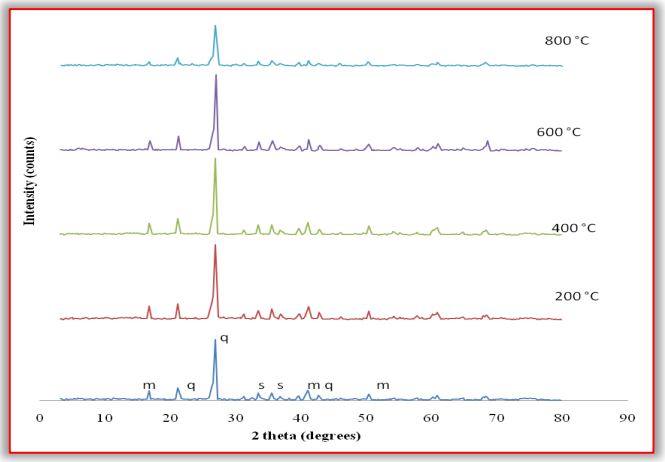

q=quartz, m=mullite s=siliminate

Figure 3. XRD of Fly ash and Geopolymer binder paste exposed to elevated temperatures (air cooled)

Further, the reason for a lower compressive strength of water cooled OPC specimen compared to air cooled specimen is due to the micro cracks developed subsequent to the induced thermal shock [17,21]. The free calcium hydroxide present in hydrated Portland cement decomposes into calcium oxide at high temperature. If this calcium oxide is wetted after being cooled, it transforms into calcium hydroxide again, causing a volume change (may be up to about 40%) and this may also result to the formation of micro cracks in concrete

Tensile strength

Tables 4 and 5 shows the split tensile strength and flexural strength of GP and OPC specimen respectively, tested after exposure to elevated temperatures. The plots of these residual strengths in terms of percentage initial strength are given in the fig 5 and 6 respectively.

From Tables 4 and 5 as well as from figs.4 and 5, it could be observed that, both split and tensile strength of GP concrete is slightly lower than the corresponding values of OPC concrete up to a temperature of 400°C. However, beyond this temperature, GP concrete behaves better. Further, similar to the compressive strength, beyond 600°C, there is a strength gain for GP concrete in both split and flexural strength. Similar behaviour has been observed by other investigators [29]. In the present investigation, the residual split tensile strength of air cooled GP concrete exposed to 600 °C is 32.3% and that in OPC concrete is 27.0%. However, the corresponding values at 800°C exposure temperature are respectively 35.6% and 19.3%.

Further, the rate of strength reduction of both OPC and GP concrete is more or less the same

up to 600°C in the case of split tensile strength as well as flexural strength.

Table 4. Split tensile strength of GP and OPC specimens after exposed to elevated temperatures

Exposure Temperature (°C)	GP Concrete				OPC Concrete			
	Air cooled		Water cooled		Air cooled		Water cooled	
	Split tensile strength (MPa)	SD*	Split tensile strength (MPa)	SD*	Split tensile strength (MPa)	SD*	Split tensile strength (MPa)	SD*
Ambient (27)	5.44	0.76	–	–	5.47	0.46	–	–
200	4.17	0.38	3.89	0.49	4.45	0.63	4.30	0.92
400	2.61	0.89	2.47	0.69	3.04	0.87	2.89	0.43
600	1.76	0.86	1.37	0.55	1.48	0.64	1.45	0.78
800	1.94	0.75	1.58	0.69	1.06	0.57	0.95	1.10
* SD – Standard deviation								

Table 5. Flexural strength of GP and OPC specimens after exposed to elevated temperatures

Exposure Temperature (°C)	GP Concrete				OPC Concrete			
	Air cooled		Water cooled		Air cooled		Water cooled	
	Flexural strength (MPa)	SD*	Flexural strength (MPa)	SD*	Flexural strength (MPa))	SD*	Flexural strength (MPa))	SD*
Ambient (28)	5.30	0.68	–	–	5.44	0.45	–	–
200	4.23	0.53	4.10	0.68	4.53	0.67	4.40	0.38
400	2.89	1.21	2.61	0.86	3.36	0.77	3.19	0.82
600	1.86	0.87	1.52	0.58	1.72	0.83	1.49	0.89
800	1.90	0.47	1.65	0.96	0.72	0.66	0.61	0.87
* SD – Standard deviation								

Modulus of elasticity

The slope of secant drawn at one third of the characteristic compressive strength of concrete has been considered as the modulus of elasticity of concrete. Standard cylinder specimens have been used to determine the modulus of elasticity.

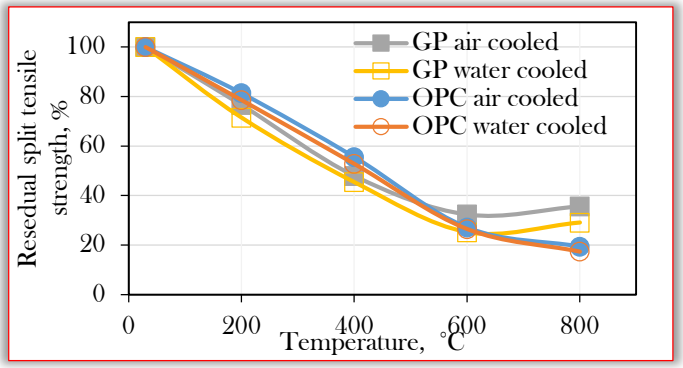

Figure 4. Residual split tensile strength of GP and OPC concrete after exposure to elevated temperatures

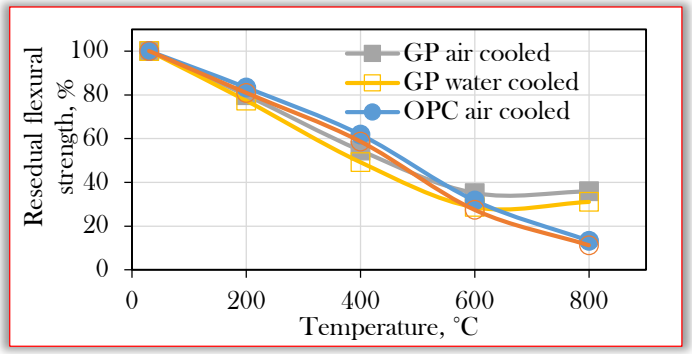

Figure 5. Residual flexural strength of GP and OPC concrete after exposure to elevated temperatures

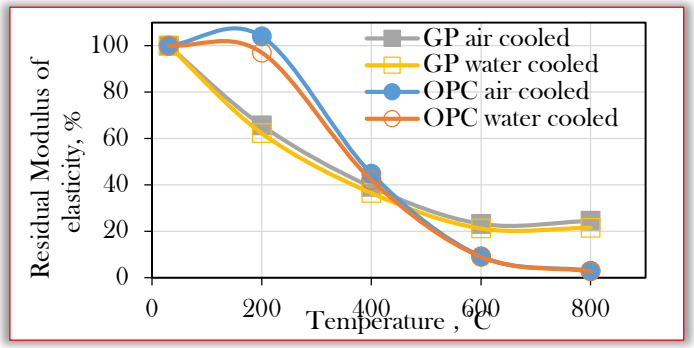

Figure 6. Modulus of elasticity of GP and OPC concrete after exposure to elevated temperatures

Figure 6 shows the variation of the modulus of elasticity (%) of GP and OPC concrete after exposure to elevated temperatures.

It could be observed that, compared to OPC concrete, while GP concrete shows a lower residual modulus of elasticity up to about 450°C, and higher values for exposure temperatures above 450°C. Also, unlike OPC concrete, GP concrete does not undergo further reduction in modulus of elasticity beyond 600°C, a behaviour similar to that of compressive strength of GP concrete. For the present study, at 600°C air cooled GP had a residual modulus of elasticity of 23.2% as against 9.2% in the case of OPC concrete. Further, at 800°C, air cooled GP concrete had a residual modulus of elasticity of 24.5% and the corresponding value of air cooled OPC concrete is only 2.9%.

CONCLUSIONS

Following conclusions could be derived from the study conducted on the fly ash based concrete.

- Fly ash based geopolymer (GP) concrete undergoes a high rate of strength loss (compressive strength, tensile strength and modulus of elasticity) during its early heating period (up to 200°C) compared to OPC concrete.
- The high rate of strength loss in GP concrete at its early heating period is contributed primarily due to the chemical restructuring of Si–O–Al (alumino silicate) and Si–O–Si compound and due to the formation of micro crack as a result of the removal of water (weakly bound and free water) from the geopolymer matrix.
- At a temperature exposure beyond 600°C, the unreacted crystalline materials in GP concrete get transformed into amorphous state and undergo polymerization. As a result, there is no further strength loss (compressive strength, tensile strength and modulus of elasticity) in GP concrete, whereas, OPC concrete continues to lose its strength properties at a

faster rate beyond a temperature exposure of 600°C.

- For the present study, after a temperature exposure of 600°C, both air cooled GP and OPC concrete had about 54% residual cube compressive strength (compared to the strength at ambient temperature, which is almost the same for both GP and OPC concrete). However, at 800°C, while GP concrete slightly gained its residual strength (to 57%), while OPC concrete continue to lose its strength (35% residual strength).
- Effect of thermal shock due to water cooling on GP and OPC concrete after exposed to elevated temperatures is more or less similar. For the present study, both GP and OPC concrete had a maximum strength loss of about 10% due to water cooling.

Hence, it could be concluded that the fly ash based geopolymer concrete could be considered as a better sustainable material than conventional concrete under the situations where it may be exposed to temperatures beyond 400 °C.

References

[1] V .M. Malhotra, Making Concrete 'Greener' With Fly Ash, ACI Concr. Int. 21 (1999) 61–66.
[2] B.Lokeshappa, Dikshit AK, Disposal and Management of Flyash, International Conference on Life Science and Technology. IPCBEE 3(2011) 11–14
[3] J.G.S Van Jaarsveld , J.S.J. Van Deventer, L. Lorenzen , The potential use of Geopolymeric materials to immobilise toxic metals: Part I. Theory and applications, Mineral Engineering. 10(1997) 659–669.
[4] J. Davidovit, Chemistry of geopolymer system–Terminology, Geopolymer International Conference, France (1999).
[5] E.I. Diaz , E.N. Allouche, S. Eklund , Factors affecting the suitability of fly ash as source material for geopolymers, Fuel 89(2003) 992–996.
[6] P.Duxson,J.L. Provis, G.C. Lukey, S.W. Mallicoat Understanding the relationship between geopolymer composition, microstructure and mechanical properties, Colloids and surf. 269 (2005) 47–58.
[7] H. Xu , J.S.J. Van Deventer ,Effect of Source Materials on Geopolymerization., Ind. Eng. Chem. Res.42(2003) 1698–1706.
[8] Temuujin, P.P. Williams, V.A. Riessen, Effect of mechanical activation of fly ash on the properties of geopolymer cured at ambient temperature, J. Mater. Proc. Tech 209(2009) 5276–5280.
[9] R.N. Thakur, S. Ghosh , Effect of mix composition on Compressive strength and Microstructure of Fly ash based Geopolymer composites, ARPN J.of Eng Appl.Sc.4(2009) 68–74
[10] D. Hardjito,S.E. Wallah, D.M.J. Sumajouw, B.V. Rangan, On the development of fly ash–based geopolymer concrete, ACI Mater. J. 101(2004), 467–472.
[11] A.M. Fernández–Jiménez, A. Palomo, C. Lopez–Hombrados , Engineering properties of alkali–activated fly ash concrete, ACI Mater. J. 103(2006) 106–112.
[12] L. T. Phan, Fire performance of high strength Concrete: A report of the State of the Art, National Institutes of Standards and Technology, Maryland (1996).
[13] W.M. Lin, T.D. Lin, C. L .J. Powers, Microstructures of Fire–Damaged Concrete, ACI Mater.J. 93(1996) 199–205.
[14] S. Y.N. Chan, G.F. Peng, M.Anson, Fire Behavior of High–Performance Concrete Made with Silica Fume at Various Moisture Contents, ACI Mater. J. 96,(1999)405–409.
[15] G. Chanvillard, L. Aloia, Concrete Strength Estimation at Early Ages: Modification of the Method of Equivalent Age, ACI Mater.J. 94(1997)520–530.
[16] G. J. Escalante, J. H. Sharp, Effect of temperature on the hydration of the main clinker phases in portland cements: Part 1. Neat cements, Cem. Concr. Res 28 (1998) 1259–1274.
[17] V. Kodur, W.Khali , Effect of Temperature on Thermal Properties of Different Types of High Strength Concrete, J. Mater. Civ. Eng. 23 (2003) 793–801.
[18] Z. Pan, J.G. Sanjayan, Stress–strain behavior and abrupt loss of stiffness of geopolymer at elevated temperatures, Cem and Concr. Comp 32(2010) 657–664.
[19] D.L.Y. Kong, J.G. Sanjayan, K.S.Crentsil, Comparative performance of geopolymers made with metakaolin and flyash after exposure to elevated temperatures, Cem. Concr. Res. 37(2007) 1583–1589
[20] D.L.Y. Kong, J.G. Sanjayan, Effect of elevated temperatures on geopolymer paste, mortar and concrete, Cem. Concr. Res 40(2010)334–339.
[21] George Mathew, Benny Joseph, Flexural behaviour of geopolymer concrete beams exposed to elevated temperatures, J Building Eng. 15 (2018) 311–318.
[22] B. Joseph , G. Mathew , Influence of Aggregate content on the Behavior of Fly ash based Geopolymer Concrete, Scientia Iranica19(2012)1188–1194.
[23] George Mathew, Benny Joseph, Microstructural analysis of fly ash based geopolymer exposed to elevated temperatures, Bull Eng. 10 (2017) 117–122.
[24] G.F. Peng, S.Y.N. Chan, M. Anson , Chemical kinetics of C–S–H decomposition in hardened cement paste subjected to elevated temperatures up to 800, Adv. in Cem. Res. 13(2001):47–52.
[25] G.F. Peng, S.H. Bian, Z .Q. Guo, J. Zhao, X.L. Peng, Y.C. Jiang, Effect of thermal shock due to rapid cooling on residual mechanical properties of fiber concrete exposed to high temperatures, Constr. and Build. Mater 22(2008) 948–955.
[26] O. Lanre, M. Asce The influence of weather on the performance of laterized concrete, J.Eng. and appl.Sc. 2, (2007) 129– 135.
[27] G. Mathew, M. Paul, Influence of Fly Ash and GGBFS in Laterised Concrete Exposed to Elevated temperatures, J.Mater.Civ.Engg.(2013)
[28] S.N. Shoukry, G.W. William, B. Downie, M.Y.Raid , Effect of moisture and temperature on the mechanical properties of concrete, Constr. and Build.Mater. 25(2011) 688–696
[29] Manvendra Verma , Kamal Upreti, Prashant Vats, Sandeep Singh, Prashant Singh, Experimental Analysis of Geopolymer Concrete: A Sustainable and Economic Concrete Using the Cost Estimation Model, Advances in Materials Science and Engineering, 2022 (2022), 1–16.

ISSN: 2067-3809

ACTA TECHNICA CORVINIENSIS – Bulletin of Engineering | e–ISSN: 2067 – 3809
Tome XVII [2024] | Fascicule 2 [April – June]

[1.]Muofunanya Francis UMUNNA, [2.]Kayode Joshua SIMONYAN

THIN LAYER DRYING KINETICS OF INDIGENOUS GINGER RHIZOM, FOR BLANCHED AND UNBLANCHED TREATMENTS, USING ACTIVE SOLAR ENERGY

[1.]Department of Agricultural Engineering, Delta State University of Science and Technology, Ozoro, Delta State, NIGERIA
[2.]Department of Agricultural and Bio–resources Engineering, Michael Okpara University of Agriculture, Umudike, Abia State, NIGERIA

Abstract: The thin layer drying kinetics of indigenous ginger rhizomes of two varieties which are Umudike Ginger I (UG I) and Umudike Ginger II (UG II) was investigated in an active solar dryer. The blanching experiment was conducted at temperature of 50∘C for 3mins, 6mins and 9mins for whole and split samples of peeled and unpeeled treatments before drying. There is a significant difference between the drying curves for whole and split samples which is due to the effect of blanching on the samples. For the unpeeled samples, gradual moisture removal was noted during the drying period. This shows that the thick skin of the unpeeled samples reduces moisture diffusion; it was observed that the drying rate decreased with sample treatments. The result for the effect of splitting on drying characteristics of UG I and UG II samples of peeled and unpeeled treatments under active solar dryer indicates that splitting increases the drying rate. The study indicates that the general objective concerning experimental and analytical studies of thin–layer drying process of ginger rhizomes for an active solar drying of the two ginger varieties were met.
Keywords: Ginger, Solar, drying, blanched and unblanched

INTRODUCTION

Nigeria is among the major producers and exporters of ginger globally, with an annual production of about 160,000 metric tons (MT) on 48,910 hectares, which is 7.9% of world production (FAO, 2013). Although, it is grown in some States of Nigeria, namely Kaduna, Nasarawa, Benue, Niger, and Gombe. Southern Kaduna in Kaduna State, is the main producing zone with over 95% of the country's total production (Okafor, 2002). According to Fumen *et al*. (2003) and Yiljep et al. (2005), the two popular ginger varieties produced in the country are the 'Tafin–Giwa,' a yellowish variety with plump rhizomes, and 'Yatsun–Biri,' which is black variety and has small compact rhizomes. Ginger has in abundant volatile and fixed oil, as well as pungent compounds, minerals, resins, starch and protein. (Ravindran and Nirmal, 2005). Drying is a useful food preservation method widely practiced globally. It is the act of extracting the moistness in a product up to a specific threshold value by evaporation. In this way, the product can be stored for an extended period to decrease the product's water activity, reduces microbiological activity, and minimizes physical and chemical changes encountered when stored (Darvishi and Hazbavi, 2012). As cooling is not a viable option to extend ginger's life shelf, an alternative is drying and operations of dryers and improving the existing drying systems. The goal of modern drying nowadays is to minimize the consumption of energy and providing a high quality of product with a minimal increase in economic inputs, which is attracting an increasing number of applications in the drying process (Darvishi *et al.,*2013).

The method of drying in a thin layer of sample particle is known as thin layer drying (Panchariya *et al.,* 2002). It is also a portion of sample that's fully exposed to air during drying; the layer's depth (thickness) should be consistent, without exceeding three layers of particles (ASAE, 1999). Most agricultural samples are dried by thin–layer drying because of its faster drying rate without losing much of nutrients (Kumar *et al.,* 2011). It is believed that the entire particles are exposed to the drying medium to understand the drying rate and time. The drying periods' knowledge enables us to establish the most economical and practical operating conditions for drying agricultural products. It is a form of carrying out drying tests on specific materials at various air temperatures, relative humidity, and air velocities (Kumar *et al*., 2011).

The aim is to minimize deterioration and microbial spoilage by reducing the water level to a certain threshold. Doungporn *et al.* (2012) reported that Fick's second law is usually used to explain liquid diffusion theory, which describes agricultural products' drying phenomenon when employing thin–layer drying equations.

The knowledge of the changes in agricultural products characteristics when subjected to drying process is of fundamental importance for correct storage, processing and the design,

fabrication, and operation of equipment applied during the post–harvest processing of these products (Bleoussi *et al.,* 2010). Thereby, it improves food productivity, reduces heavy post–harvest losses, and increases the farmers' income by recommending the best drying method for preserving ginger rhizomes. Thus, there is a great need to clearly understand the drying principles and estimate the energy needed to dry ginger rhizomes using the drying method of thin layer drying.

This work's general objective is to carry out thin layer drying kinetics of ginger rhizome using active solar energy and also Determine the effects of treatment, blanched and unblanched for [Split (peeled and unpeeled), Whole (peeled and unpeeled)] on the drying of ginger rhizomes. Justification of this research work can be based on Experimental and analytical studies of thin layer process of drying which are essential for performance improvements of drying systems (Alibas, 2012). Many countries dry vast amounts of food to extend their shelf–life, reduce packaging costs, reduce shipping weights, boost appearance, encapsulate original taste, and keep nutritional value (Gunhan *et al.,* 2010). Imagine what happens when the dryers are improperly produced, the objective of drying will not be achieved, and the product quantity and quality would be compromised.

MATERIALS AND METHODS

Material selection and preparation

A custard bowl (4 kg) for each of the two ginger varieties, that is Umudike Ginger I (UG I) and Umudike Ginger II (UG II), were purchased, from the National Root Crop Research Institute (NRCRI), Umudike, Abia State, Nigeria. The ginger varieties which were whole, were sorted by their appearance and size, It was kept in the laboratory to obtain a uniformed room atmosphere for about 24 hours of purchase. It was also noted that the ginger varieties were purchased after about five days to one week of harvest.

Experimental treatments

Four Kilograms each of UG I and UG II was cleaned and separated into samples. One of the samples (4kg) was peeled and splitted with a sharp stainless–steel knife. The UG I and UG II split and whole (peeled and unpeeled) were blanched with the aid of an Electric water bath (DK420 model, Techmel and Techmel, USA) in the Soil and Water Laboratory, Department of Agricultural and Bioresources Engineering, Michael Okpara University of Agriculture, Umudike, Abia State. The UG I and UG II, were blanched for 3, 6, and 9 minutes, at temperature of 50℃, respectively. Each sample with various treatments was subjected to active solar drying in sequence. Also, unblanched UG I and UG II split and whole (peeled and unpeeled) were subjected to active solar drying to determine the drying rate, drying time, drying efficiency.

Figure 1: UG I and UG II unblanched samples with various treatments (whole peeled, whole unpeeled, split peeled and split unpeeled) using solar dryer.

Figure 2: UG I and UG II blanched samples @ 50℃ for 3minutes, 6minutes, and 9minutes respectively for the various treatments (whole peeled, whole unpeeled, split peeled and split unpeeled) using solar dryer. Various treatments (whole peeled, whole unpeeled, split peeled and split unpeeled) using solar dryer.

Experimental set–up and procedures

— Active solar drying method

An existing active solar dryer in the Department of Agricultural and Bioresources Engineering, Michael Okpara University of Agriculture, Umudike, was used in the experiment. It consists of a solar collector, solar panel 180W, DC aspirator fan, drying chamber, heat storage unit, drying trays and a solar battery rated 200Ah. The dryer body was constructed using a transparent cover made of perplex material. The solar panel traps solar energy and uses it to charge the dc battery, which powers the control box; the control box was programmed to regulate the dc blower periodically to aid the moisture removal at the drying chamber. The drying chamber houses the dried products placed in perforated metal trays and has a door to allow for easy

loading and unloading of crops in the tray. The heat storage unit was incorporated with black pebbles that trap the sunlight that falls on it and stores it in the form of heat for further use when there is no solar radiation.

There was an aspirator on top of the dryer that forces air from the inlet opening through a solar collector section through the product bed in the drying chamber. Solar radiation falling on the dryer was utilized to heat the air passing through the samples. Heated air is blown through the drying chamber. At the top of the drying chamber, vents were provided through which moisture is removed.

During the experiment, solar radiation intensity, ambient air, drying chamber, collector temperature, relative humidity, wind speed, and material weight loss were measured and recorded at 2 hours intervals. The samples were spread in a thin layer on the metal trays and dried until equilibrium moisture content was achieved. This procedure was followed for blanched and unblanched treatments for Split–Peeled (SP), Split–Unpeeled (SU), Whole–Peeled (WP), and Whole–Unpeeled (WU), respectively. Drying started from 8.00 a.m to 6.00 p.m daily till equilibrium moisture content was reached. The experiment was replicated three times, and the average value was used for further calculations.

Figure 3: A pictorial view of an active solar dryer used for the experiment

— **General observations for active solar drying**

Ginger samples, UG I and UG II, were dried for both blanched and unblanched treatments, respectively.

For Blanched treatments, the initial weight of UG I and UG II samples were recorded as $w0_1$, $w0_2$ and $w0_3$, for the three replicates, respectively, and that of weight loss after blanching, was also recorded as $w1_1$, $w1_2$ and $w1_3$, while the weight loss after solar drying at two hours intervals was recorded as $w2_1$, $w2_2$ and $w2_3$.

For unblanched treatments, the initial weight of UG I and UG II samples was recorded as $w0_1$, $w0_2$ and $w0_3$, while the weight loss after solar drying at two hours intervals was recorded as $w1_1$, $w1_2$ and $w1_3$.

The solar dryer's temperature collector, the wind gauge, and the ambient wind gauge were also determined. The environmental factors (relative humidity, temperature, wind speed, and sun intensity) were determined with digital instruments, wind gauge meter, and thermometer aid during the solar drying period.

— **Moisture content determination**

UG I and UG II initial moisture contents were determined for about 300g sample quantity, using Mermet oven at 105°C for 24 hours until constant weight reached according to the method described by AOAC (1990). The experiment was replicated three times. The following equation was used to calculate the moisture content on a wet basis:

$$Mc\ (w.b)\ \% = \frac{W_w - W_d}{W_w} X \frac{100}{1} \quad (1)$$

where;

Mc = (W.b) moisture content wet basis

Ww = weight of the wet sample (g)

Wd = weight of the dried sample (g)

— **Determination of moisture ratio (MR)**

The moisture ratio (MR) of UG I and UG II was determined using equation [2] (Babalis et al., 2004).

$$MR = \frac{Mt - Me}{Mo - Me} \quad (2)$$

The moisture ratio is further simplified according to Goyal et al (2007) as:

$$MR = \frac{Mt}{Mo} \quad (3)$$

where;

MR = moisture ratio

Mt = the moisture content at any time t (g water/g dry matter)

Mo = the initial moisture content (g water/g dry matter)

Me = the equilibrium moisture contents, (g water/g dry matter), respectively

All values expressed as g water/g dry matter. Me's values were determined as the moisture content at the end of drying when the sample ceased to lose mass.

— **Drying rate calculation (DR)**

The drying rate was calculated as expressed by (Ceylan et al., 2007; Doymaz, 2007; Ozbek and Dadali, 2007)

$$D_r = \frac{M_{t+dt} - M_t}{dt} \quad (4)$$

where,

M_t = moisture content at a specific time (g water/g dry matter)

M_{t+dt} = moisture content t+dt (g water/g dry matter)

t = drying time (hr)

— **Determination of effective moisture diffusivity**

The effective moisture diffusivity (D_{eff}) for a lumped parameter approach considers all possible resistances to moisture transport. When interpreted for an infinite slab in one dimension, assuming negligible temperature gradient within the product, constant temperature, and diffusivity, and no significant external resistance, Moisture transfer during the falling rate drying period of the samples was determined using Fick's Second law as expressed in equation 5 (Aghbashlo et al., 2008).

$$MR = \frac{8}{\pi^2}\sum_{n=0}^{\infty}\left(\frac{1}{2n+1}\right)\exp\left(-\frac{(2n+1)^2\pi^2 D_{eff}t}{4L^2}\right) \quad (5)$$

where; MR is the moisture ratio

D_{eff} = effective diffusivity (m^2/s)

n=1,2,3, the number of terms taken into consideration

t = the time of drying in second

L=the thickness of the sample (m)

Equation (3.5) is further simplified as shown in equation (3.6) by (Lopez et al., 2000)

$$MR = \frac{8}{\pi^2}\exp[\frac{\pi^2 D_{eff}t}{4L^2}] \quad (6)$$

$$MR = \frac{8}{\pi^2}\exp(-kt) \quad (7)$$

The slope k was determined by plotting ln (MR) versus time (t)

$$k = \frac{\pi^2 D_{eff}}{4L^2} \quad (8)$$

RESULTS & DISCUSSION

EFFECT OF TREATMENTS ON DRYING CHARACTERISTICS OF UMUDIKE GINGER (I AND II) USING ACTIVE SOLAR DRYER

The solar drying was carried out from February to March 2019. During the drying experiment, the initial moisture content of 71.12 and 72.47% (wb) for UG I and UG II were reduced to a final moisture content of 6.09 and 6.94% (wb). The results of the experiment under different treatment and controlled conditions are presented and discussed.

— **Drying characteristics of Unblanched UG I and UG II varieties of ginger rhizomes**

Figure 4 to 7 show the drying curves of unblanched and blanched UG I and UG II ginger varieties for the whole peeled, whole unpeeled, split peeled, and split unpeeled treatments dried under solar drying process.

Unblanched treatment, there was an initial high moisture removal at the falling rate period, followed by slow moisture removal at the constant rate period of drying, as shown in Figure 4 to 7. At the continuation of drying, the rate of moisture released to the drying air tends to reduce.

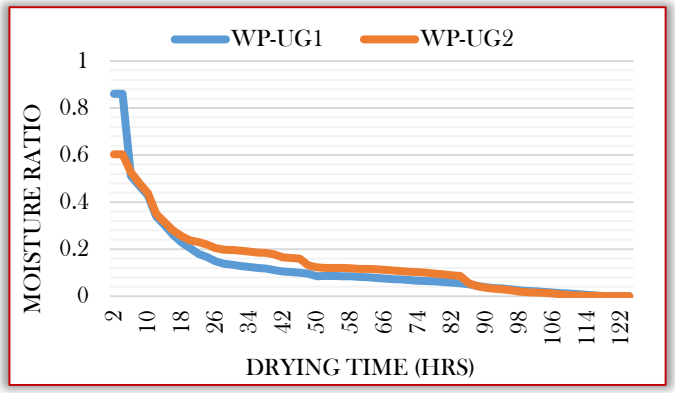

Figure 4. Effect of peeling on the drying characteristics of UG I and UG II (a) whole peeled

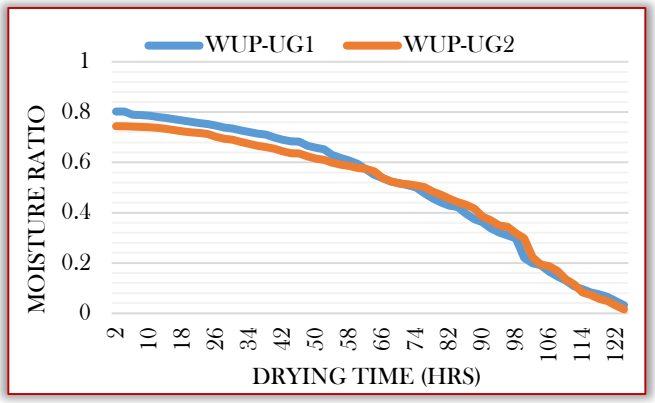

Figure 5. Effect of peeling on the drying characteristics of UG I and UG II (b) whole unpeeled

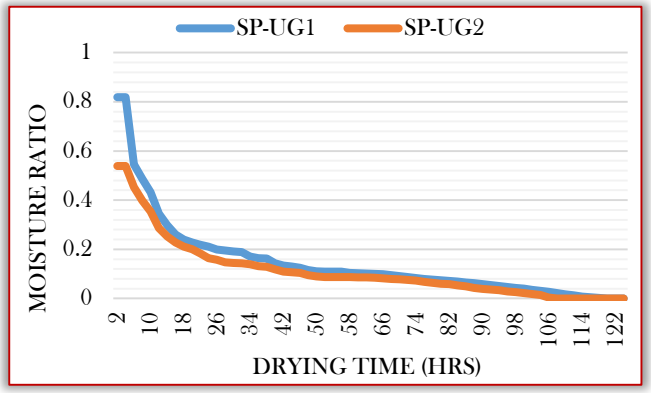

Figure 6. Effect of spliting on the drying characteristics of UG I and UG II (c) split peeled

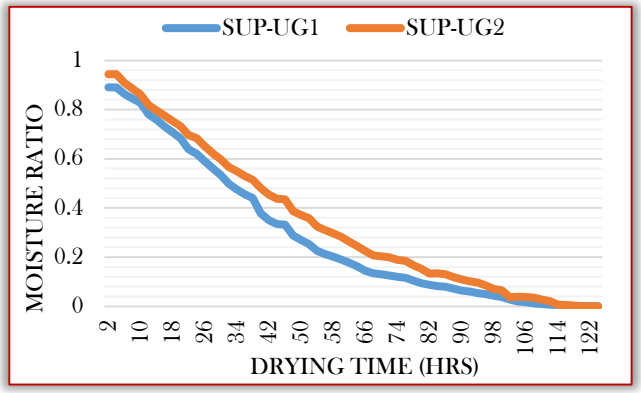

Figure 7. Effect of spliting on the drying characteristics of UG I and UG II (d) split unpeeled

The process of drying continues till equilibrium moisture content was attained. It can also be observed that moisture content decreased continuously with drying time. The drying process for the samples ended in the range of the falling rate period. This implies that diffusion is the most physical mechanism governing moisture movements in the materials, which are dependent on the moisture content of the samples (Akpinar *et al*., 2003; Doymaz, 2007b, Prachayawarakorn *et al*., 2008)

The curves of both drying rate periods agree with the results of other studies on basil, plantain, and banana (Rocha *et al*., 1993; Saeed *et al*., 2006).

— **Effect of Blanching time on the Drying characteristics of UG I and UG II**

The results of the effect of blanching time on the drying characteristics of UG I and UG II samples of whole peeled, whole unpeeled, split peeled, and split unpeeled treatments dried under active solar dryer are shown in Figures 8 to 15, respectively. Blanching increases the drying rate (Bala, 1997).

There is a significant difference between the drying curves for blanched and unblanched samples for whole and split UG I and UG II samples. This difference becomes minimal for whole peeled, split peeled and split unpeeled treatments. This might be because, during blanching, the samples were partially cooked, and some cells or tissues of split peeled, split unpeeled and whole peeled UG I and UG II samples might be disrupted or loosened. As a result, moisture diffusion was higher, and hence the drying rate was higher. Similar results have been reported by Hossain *et al*. (2007) for red chili.

The moisture content of the whole unpeeled UG I and UG II samples, gradual moisture removal are noted during the drying period, and this is true for either blanched whole unpeeled UG I and UG II samples and unblanched whole unpeeled UG I and UG II samples. This shows that the thick skin of the whole unpeeled UG I and UG II samples reduces moisture diffusion through the skin.

At Figure 8 and 15, it was observed that split peeled UG I and UG II, blanched at 50°C for 3mins, gained moisture from the environment over the night, which affected the slope of the Figure.

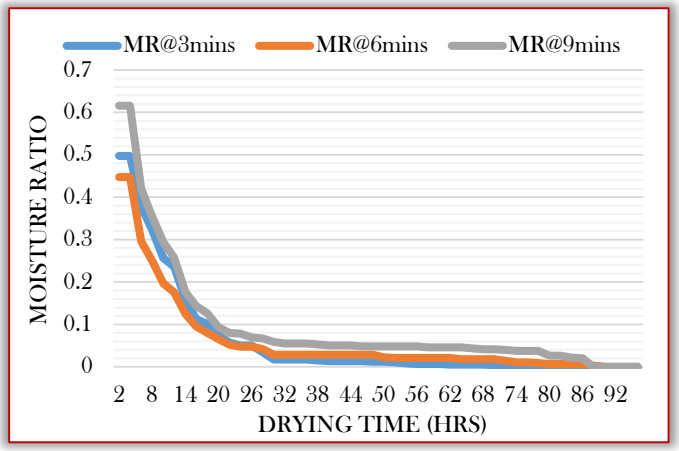

Figure 8. Effect of blanching time on the drying characteristics of Whole peeled UG I

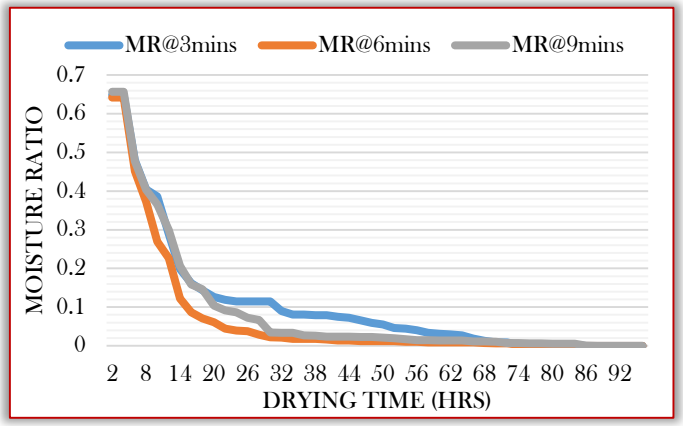

Figure 9. Effect of blanching time on the drying characteristics of Whole peeled UG II

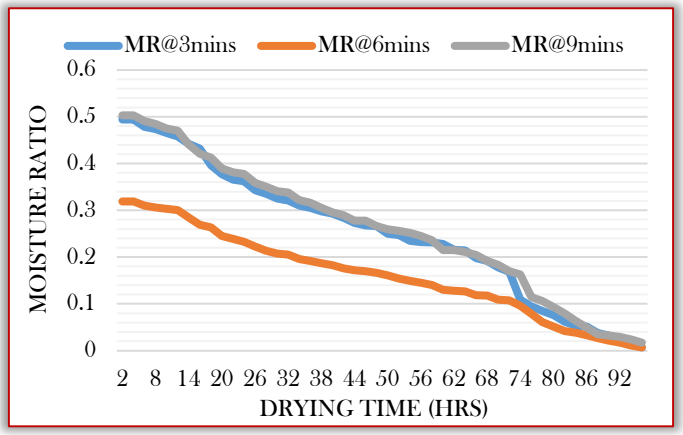

Figure 10. Effect of blanching time on the drying characteristics of Whole unpeeled UG I

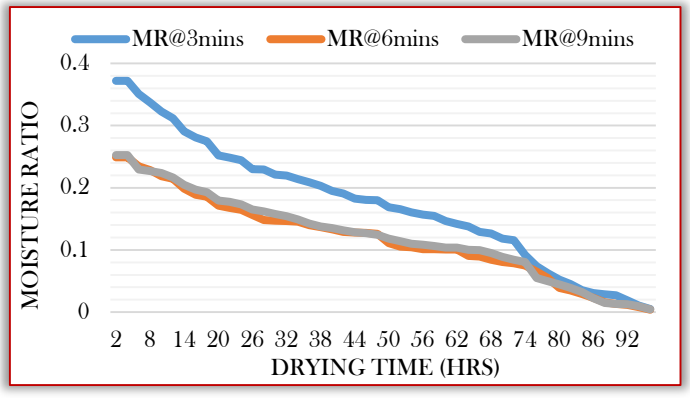

Figure 11. Effect of blanching time on the drying characteristics of Whole unpeeled UG II

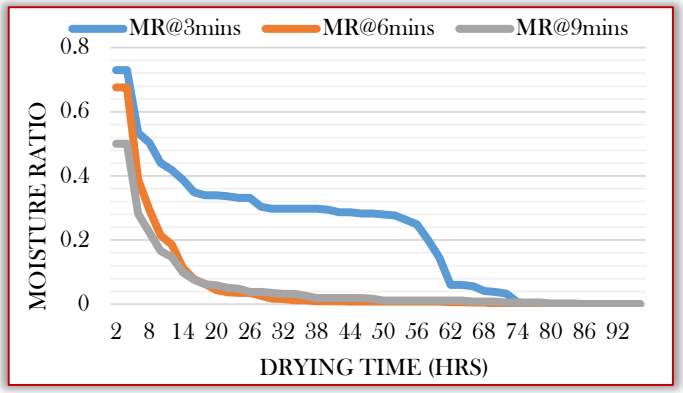

Figure 12. Effect of blanching time on the drying characteristics of Split peeled UG I

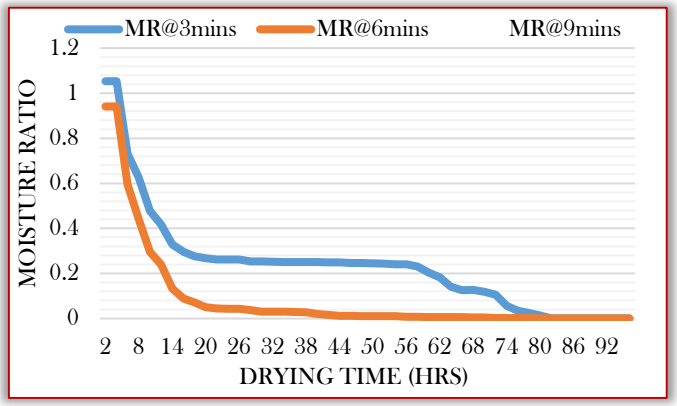

Figure 13. Effect of blanching time on the drying characteristics of Split peeled UG II

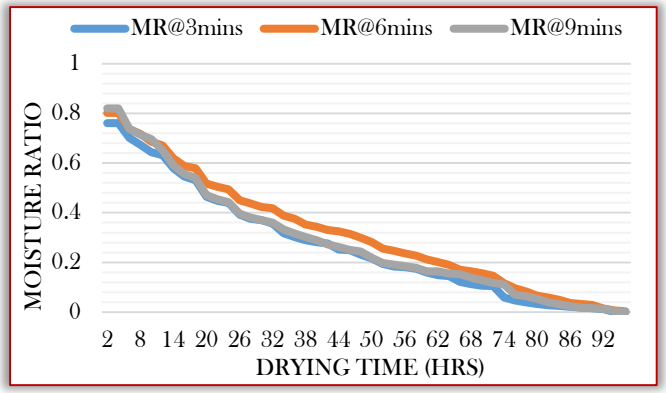

Figure 14. Effect of blanching time on drying characteristics of Split unpeeled UG I

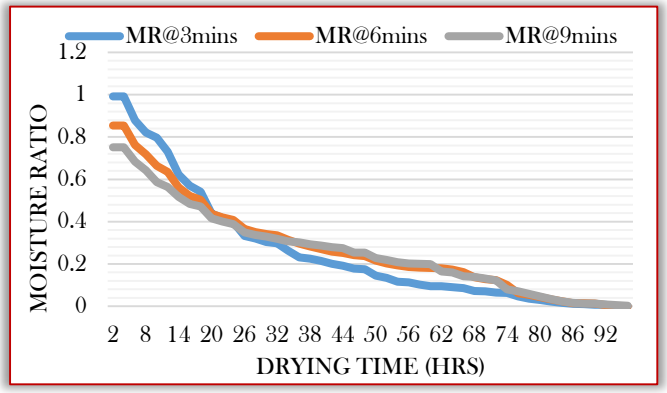

Figure 15. Effect of blanching time on drying characteristics of Split unpeeled UG II

— Drying rate of UG I and UG II unblanched

Figures 16 to 27 shows the drying rate curves of unblanched and blanched UG I and UG II samples with various treatments against drying time. It was observed that the drying rate decreased with sample treatments. It could also be observed that drying time increased for a split peeled samples treatment due to decreased drying rate. A similar observation was reported (Maskan *et al*., 2002; Agarry and Owabor, 2012).

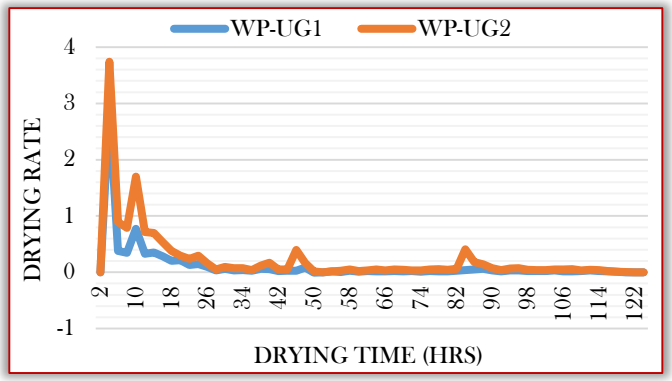

Figure 16. Effect of peeling on drying rate of Whole peeled UG I and UG II

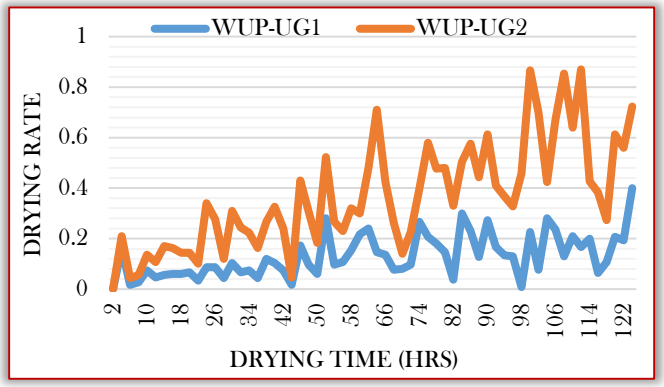

Figure 17. Effect of peeling on drying rate on drying time at whole unpeeled UG I and UG II

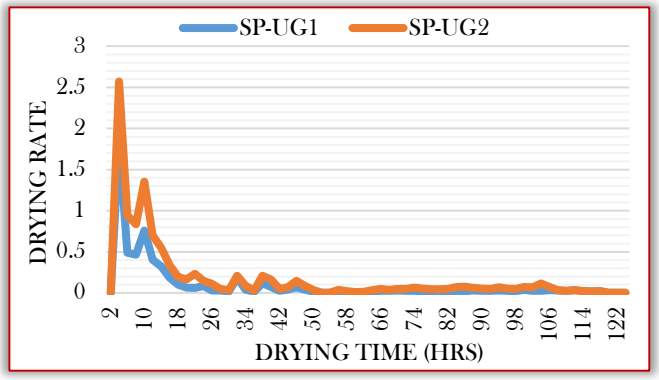

Figure 18. Effect of splitting on drying rate of Split peeled UG I and UG II

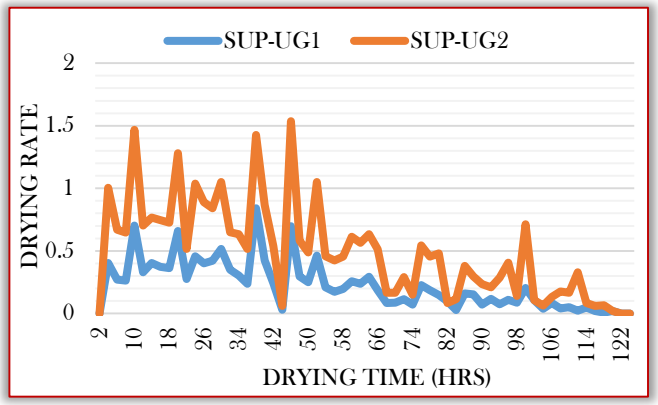

Figure 19. Effect of splitting on drying rate of Split unpeeled UG I and UG II

The highest drying rate was found for split peeled UG I and UG II samples, followed by unpeeled split samples and then whole peeled samples, while the whole unpeeled samples were the least drying rate.

The split peeled samples' highest drying rate might be due to higher diffusion for split peeled samples because of its one cut surface and the peeled back, which has a small diffusion length to travel towards the cut surface.

The diffusion rate of whole unpeeled samples was minimal, and the drying rate was also extremely low. This was also observed during the cabinet drying process.

— **Drying rate of blanched UG I and UG II**

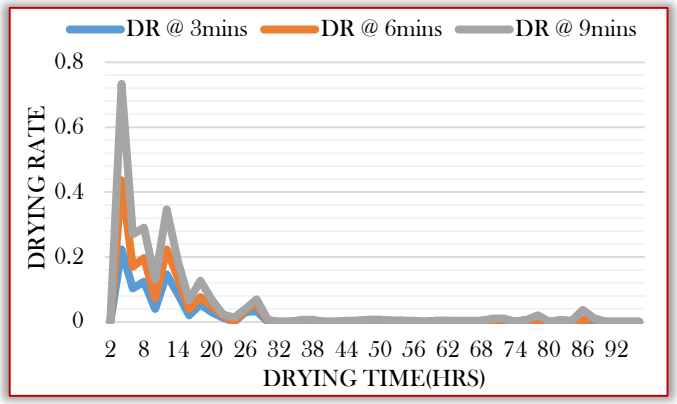

Figure 20. Effect of blanching on drying rate and drying time of whole peeled UG I

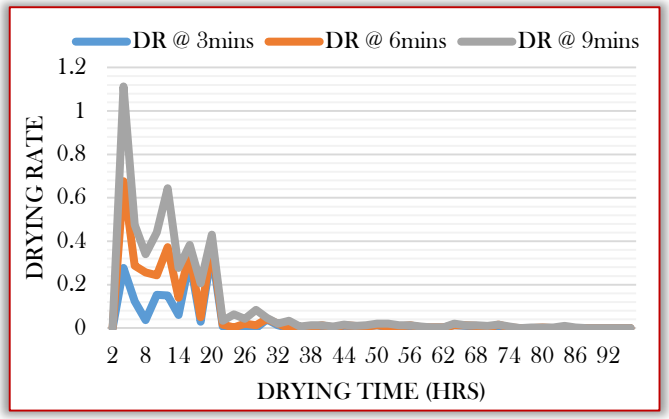

Figure 21. Effect of blanching on drying rate and drying time of whole peeled UG II

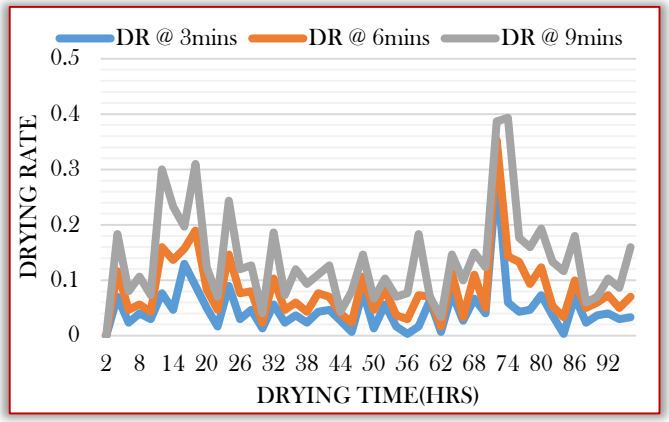

Figure 22. Effect of blanching on drying rate and drying time of whole unpeeled UG I

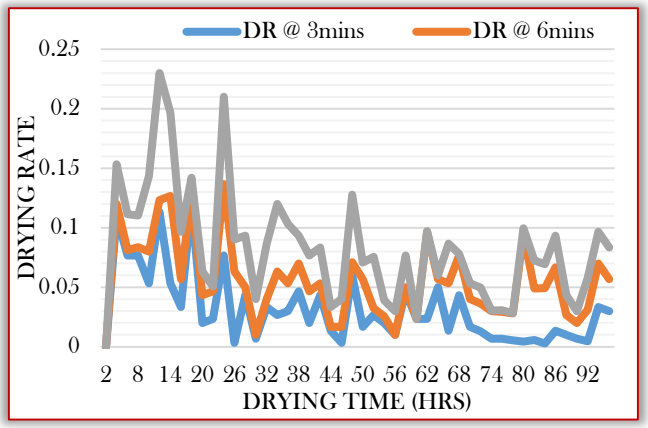

Figure 23. Effect of blanching on drying rate and drying time of whole unpeeled UG II

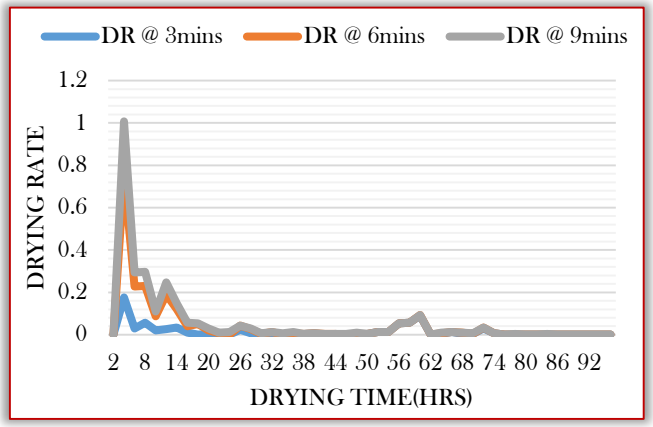

Figure 24. Effect of blanching on drying rate and drying time of Split peeled UG I

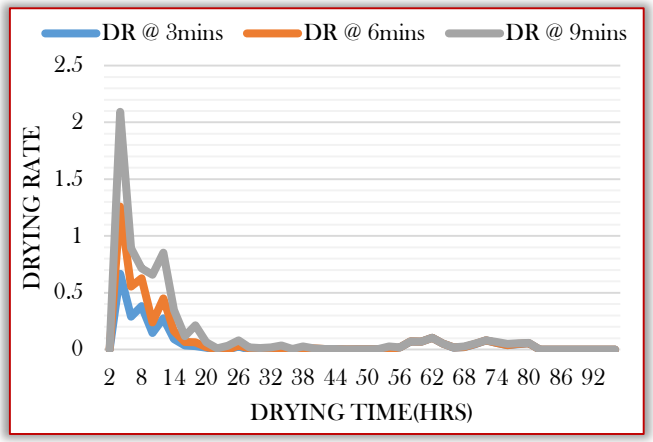

Figure 25. Effect of blanching on drying rate and drying time of Split peeled UG II

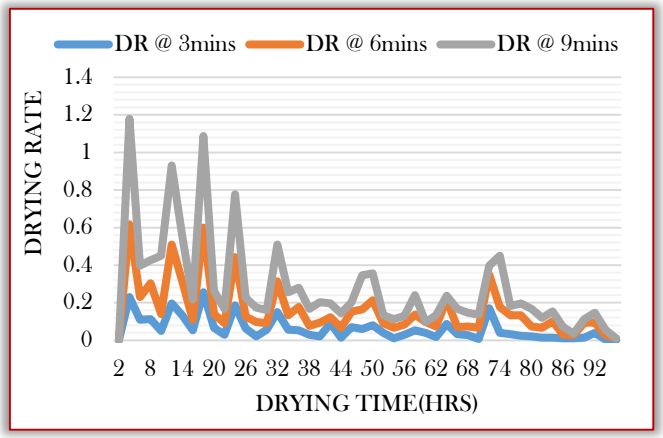

Figure 26. Effect of blanching on drying rate and drying time of Split unpeeled UG I

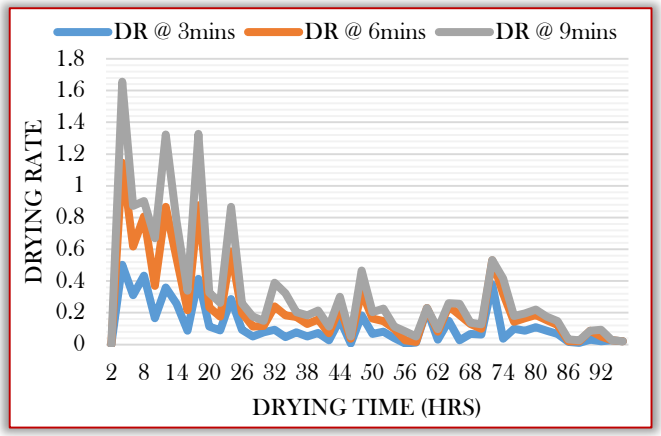

Figure 27. Effect of blanching on drying rate and drying time of Split unpeeled UG II

Figure 28 and 29 show the drying measurement and parameter recorded during the drying duration. The various sample treatments and varieties were loaded with a different tray at the various drying layers, inside the solar drying chamber at the same time intervals.

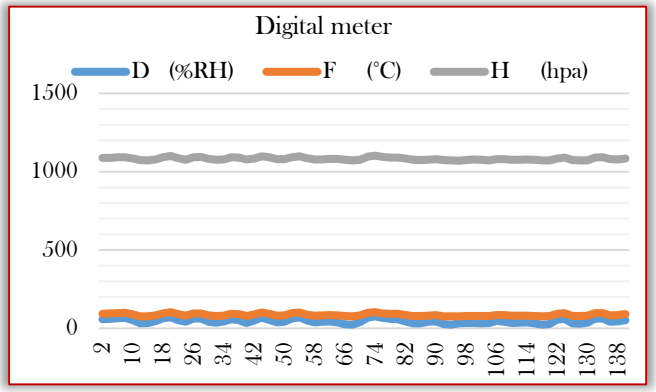

Figure 28. Drying parameter values for solar drying

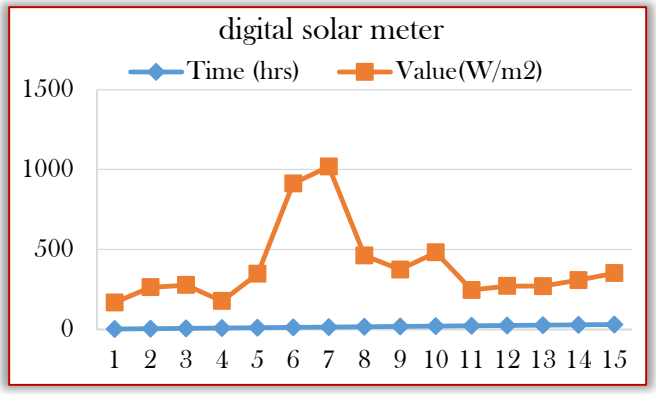

Figure 29. Solar meter reading for sun intensity for two weeks

The drying chamber temperature is shown to approach its peak during the midday at 12:00 pm, and it was always higher than ambient temperature. Solar intensity tends to be highest around 11:30 am to 2:00 pm, after which it starts going down. Relative humidity has a reverse trend of drying chamber and ambient temperature due to the heated air relative humidity decreased sharply towards the noon period. Wind speed was higher during the afternoon and evening periods compared to early morning time. An increase in drying rate coincided with an increase in solar intensity. It was observed that the maximum drying rate occurs between 12:00 pm and 2:00 pm. The drying was carried out from February to March 2019. A period of about a month, between 10 to 70 hours' duration.

— **Determination of Effective Moisture Diffusivity for Active Solar Dryer**

The results for effective moisture diffusivity for unblanched and blanched UG I and UG II treatments dried under Active solar dryer were computed and presented in Tables 1 and 2, using equations 7 and 8, after obtaining k value from plot of ln MR versus time.

Table 1. Unblanched and Blanched UG I and UG II

Sample type	UG I		UG II	
	K $(Hrs)^{-1}$	Deff (m^2/s)	K $(Hrs)^{-1}$	Deff (m^2/s)
	UNBLANCHED			
WP	–0.00368	9.082E–05	–0.00358	8.836E–05
WUP	–0.00664	1.639E–04	–0.00608	1.501E–04
SP	–0.00378	9.329E–05	0.00324	7.996E–05
SUP	–0.00763	1.883E–04	–0.00817	2.016E–04
	BLANCHED @ 3 Mins			
WP	–0.00344	8.490E–05	–0.00543	1.340E–04
WUP	–0.00511	1.261E–04	–0.00357	8.8E–05
SP	–0.00711	1.755E–04	–0.00742	1.83E–04
SUP	–0.0078	1.925E–04	–0.00923	2.278E–04
	BLANCHED @ 6 Mins			
WP	–0.00278	6.86E–05	–0.00454	1.120E–04
WUP	–0.00327	8.070E–05	–0.00246	6.07E–05
SP	–0.00511	1.261E–04	–0.00626	1.545E–04
SUP	–0.00811	2.00E–04	–0.00799	1.972E–04
	BLANCHED @ 9 Mins			
WP	–0.00385	9.50E–05	–0.0047	1.160E–04
WUP	–0.00512	1.264E–04	–0.00242	5.973E–05
SP	–0.00304	7.503E–05	–0.00555	1.370E–04
SUP	–0.00799	1.97E–04	–0.0071	1.752E–04

where, WP – Whole peeled; WUP – Whole unpeeled; SP – Split peeled; SUP – Split unpeeled; k – Slope; Deff – Effective moisture diffusivity

The effective moisture diffusivity values increased considerably with the increase in drying rate. This might be explained by the increased heating, which would increase the water molecules' activity, leading to higher moisture diffusivity. These values are consistent with those in literature, 1.26 to 3.32 $\times 10^{-9} m^2/s$ for hot –air drying of garlic (Senadeera et al., 2003), 9.3 $\times 10^{-9}$ to 1.06 $\times 10^{-11} m^2/s$ for convective drying of ginger (Da Silva et al., 2009) and 0.35 to 1.01 $\times 10^{-10} m^2/s$ for hot–air drying of bean slices (Rossello et al., 1997).

The slope (k) was derived from the moisture ratio log variation with drying time used to calculate moisture diffusivity. This implies that the drying

constant (k) was obtained from the slope of the plot of the log of moisture ratio against drying time. The higher k values confirm the elevated moisture removal rates and indicate an enhancement of drying potential (Evin, 2011; Darvishi et al., 2014).

The effective moisture diffusivity (Deff) of Unblanched UG I and UG II and slope (k) ranges from 1.501 $\times 10^{-4}$to 9.329 $\times 10^{-5}\mathrm{m}^2/\mathrm{s}$ and –0.00324 to –0.00817$(\mathrm{hrs})^{-1}$, respectively. This shows that the effective moisture diffusivity for unblanched treatment during solar drying was obtained at split peeled (UG I) higher than the whole unpeeled (UG II).

The effective moisture diffusivity (Deff) of Blanched UG I and UG II at 50℃ and slope (k) ranges from 1.120× 10^{-4} to 9.50 × $10^{-5}\mathrm{m}^2/\mathrm{s}$ and –0.00242 to –0.00923 $(\mathrm{hrs})^{-1}$ respectively. It shows that the effective moisture diffusivity (Deff) was higher at whole peeled (UG I) MR at 9mins and lower at whole peeled (UG II) MR at 6mins.

Table 2. Unblanched and Blanched UG I and UG II

Sample type	UG I	UG II
	K $(\mathrm{Hrs})^{-1}$	K $(\mathrm{Hrs})^{-1}$
	UNBLANCHED	
WP	–0.00434	–0.00273
WUP	–0.001727	–0.003761
SP	–0.00343	–0.00243
SUP	–0.00371	–0.00346
	BLANCHED @ 3 Mins	
WP	–0.00104	–0.00109
WUP	3.48278E–05	–0.00019
SP	–0.00031	–0.00214
SUP	–0.00119	–0.00228
	BLANCHED @ 6 Mins	
WP	–0.0007	–0.00186
WUP	–4.07982E–05	–0.00037
SP	–0.00245	–0.00238
SUP	–0.00134	–0.00291
	BLANCHED @ 9 Mins	
WP	–0.00099	–0.00201
WUP	7.22789E–05	–0.00014
SP	–0.00073	–0.00367
SUP	–00244	–0.00282

The differences between the results in the literature and present investigation can be explained by the effect of drying methods, unblanched and blanched treatments, and tissue characteristics of the UG I and UG II varieties of the samples, composition, and the proposed model used for calculations.

CONCLUSION AND RECOMENDATIONS

The following conclusions can be drawn from this study:

The result for the effect of blanching on drying characteristics of UG I and UG II samples of whole peeled, whole unpeeled, split peeled, and split unpeeled treatments under active solar dryers, indicates that splitting increases the drying rate. The above indicates that this work's general objective concerning experimental and analytical studies of thin–layer drying process of ginger rhizomes for an active solar drying of two varieties of ginger, UG I and UG II were met.

Further research concerning the effect of initial moisture content, relative humidity, and airflow rate on drying characteristics of UG I and UG II, Whole and Split treatments, for the optimization of the drying process.

These drying methods on thermal properties such as thermal conductivity, specific heat capacity, and thermal diffusivity should also be investigated.

References

[1] Agarry S.E., and Owabor O. (2012). Modelling the Drying characteristics and Kinetics of Hot Air drying of Unblanched Whole Red pepper and Blanched Bitter leaf slice. Turkish Journal of Agriculture Food science and Technology 5(1):24

[2] Akpinar, E., Midilli, A. and Bicer, Y. (2003). Single–layer drying behaviour of potato slices in a convective cyclone and mathematical modeling, Journal of Energy Conversion and Management, 44(1):1689–1705.

[3] Alibas, I. (2012). Selection of the Best Suitable Thin–Layer Drying Mathematical Model for Vacuum Dried Red Chili Pepper. Journal of Biological and Environmental Science, 6(17):161–170.

[4] AOAC(1990) Official Methods of Analysis. 15th Edition, Association of Official Analytical Chemist, Washington DC.

[5] ASAE 1999 Standards Engineering Practices, data. 46th Edition, American Society of Agricultural Engineers.

[6] Babalis, S.J. and Belessiotis, V.G. (2004). Influence of the drying conditions on the drying constants and moisture diffusivity during the thin layer drying of Figures, Journal of Food Engineering, 65(1):449–458.

[7] Bala, B.K. 1997. Drying and Storage of Cereal Grains. Oxford and IBH publishing co. Pvt. Ltd. India.

[8] Bleoussi, T. M. R., Fofana, M., Bokossa, I. and Futakuchi, K. (2010). Effect of parboiling and storage on grain physical and cooking characteristics of some NERICA rice varieties. Second Africa Rice Congress. Innovation and Partnerships to Realize Africa's Rice Potential. 3(3):1–7.

[9] Ceylan .I., M. Aktas, H. Dogan (2007) Mathematical Modelling of drying Characteristics of tropical Fruits. Applied thermal Engineering 2007 – Elsevier

[10] Da Silva, W.P., Precker, J.W. and De Lima, A.G.B. (2009): Drying kinetics of Lima bean (Phaseolus lunatis L.) experimental determination and prediction by diffusion models. International Journal of Food Engineering, 5(3):1– 9.

[11] Darvishi H., Azadbakht M., Rezaeias, IA., Farhang A. (2014): Drying characteristics of sardine fish dried with microwave heating. Journal of the Saudi Society of Agricultural Sciences, 12(1): 121–127.

[12] Darvishi, H. and Hazbavi, E. (2012). Mathematical modeling of thin–layer drying behaviour of date palm. Glob J Sci Front Res Math Dec Sci, 12(10):9–17.

[13] Doungporn, S., Poomsa–ad, N. and Wiset, L. (2012). Drying Thai Hom Mali paddy equations using hot air, carbon dioxide, and nitrogen gases as drying media. Food Bioproduction Processing, 90(1):187–198.

[14] Doymaz, I. (2007b). Air–drying characteristics of tomatoes. Journal of Food Engineering, 78(4): 1291–1297.

[15] Evin, D. (2011). Thin layer drying kinetics of Gundelia tournefortii. Journal of Food Bioproduction Process, 2(1):12–15
[16] FAO (2013). Export product profile: Ginger. Retrieved from http;//exportNigeriablogspot.com/2009/12/export–product–profile–ginger.html
[17] Fumen, G.A., Y.D. Yiljep and E.S.A Ajisegiri (2003). Survey of ginger processing and drying Methods in Nigeria: A case of Southern Kaduna of Kaduna State. Fourth International Conference and 25th AGM of the Nigeria Institution of Agricultural Engineers, Damaturu, Nigeria, September 8th–12th.
[18] Goyal G., Fell B., Sarin A., Youle R.J., Sriram V. (2007) Role of Mitochondrial remodelling in programmed cell death in Drosophila melanogaster. Dev. Cell 12(5) : 807 – 816
[19] Gunhan Tuncay, Vedat Demir, Ebru Hancioglu Kuzgunkaya and Arif Hepbasli (2010) Mathematical Modelling of drying bay leaves. Research Gate, Energy Conversion and Management 46(11–12) : 1667 – 1679
[20] Hossain, M.A., Woods, J.L. and Bala, B.K. (2007). Single–layer drying characteristics and color kinetics of red chili. Int J Food Sci Technol, 42(11):1367–75.
[21] Kumar, N., Sarkar, B. C. and Sharmar, H. K. (2011). Mathematical modeling of thin layer hot air drying of carrot pomace. Journal of Food Science and Technology, 49(1):33–41.
[22] Lopez, A., Iguaz, A., Esnoz, A., and Virseda, P. (2000). Modeling of sorption isotherms of dried vegetable wastes from the wholesale market. Drying Technology, 18(5):985– 994
[23] Maskan, A., Kaya, S., and M. Maskan. (2002). Hot air and sun drying of grape leather (pestil). Journal of Food Engineering, 54(1): 81–88.
[24] Mortaza Aghbashlo, Mohammad Hossein Kianmehr and Seyed Reza Hassan–Beygi (2008). Specific Heat and Thermal Conductivity of Berberis Fruit (Berberis Vulgaris). American Journal of Agricultural and Biological Sciences 3(1) : 330 – 336, 2008.
[25] Okafor, G.I. (2002). Effects of pricking, sun–drying, and sieving on Ginger (zingiber Officinale Roscoe) Colour and powder. Nigerian Food. Journal 2(1): 155–160
[26] Ozbek, B. And Dadali, G. (2007). Thin–layer Drying Characteristics and Modelling of Mint leaves Undergoing Microwave Treatment. Journal of Food Engineering, 83, 541–549
[27] Panchariya, P. C., Popovic, D. and Sharma, A. L. (2002). Thin–layer modeling of the black tea drying process. Journal of Food Engineering, 52(4):349–357.
[28] Prachayawarakorn, S., Tia, W.N., Plyto, S. and Soponronnarit, S. (2008). Drying kinetics and quality attributes of low–fat banana slices dried at high temperature. Journal of Food Engineering, 85(4):509–517
[29] Ravindran, P.N. and Nirmal, B.K. (2005). Ginger: The Genus Zingiber. CRC Press, Florida, U.S.A, pp 105–114
[30] Rocha Benedita, Corinne Tanchot, Harald Von Boehmer (1993). Clonal anergy blocks in vivo growth of mature T cells and can be reversed in the absence of antigen. The Journal of experimental medicine 177(5), 1517–1521
[31] Rossello, C., Simal, S., Sanjuan, N. and Mulet, A. (1997): Nonisotropic mass transfer model for green bean drying. Journal of Agricultural and Food Chemistry, 45(1):337–342.
[32] Saeed, I. E., Sopian, K. and Zainol Abidin, Z. (2006). Drying kinetics of Roselle (Hibiscus sabdariffa L.): dried in constant temperature and humidity chamber. Proc. SPS 2006. Edited by Muchtar. 29th–30th August. Permata, Bangi, S.D.E., Malaysia: 143–148.
[33] Senadeera Wijitha, Bhesh R. Bhandari, Gordon Young, Bandu Wijesinghe (2003). Influence of Shapes of Selected Vegetable materials on drying Kinetics during fluidized bed drying. Journal of Engineering 58(3) 277–283
[34] Senadeera, W., Bhandari B., Young G. and Wijesinghe, B. (2000). Physical properties and fluidization behaviour of fresh green bean particulates during fluidized bed drying. Food and Bioproducts Processing, 78(1): 43–47.
[35] Yiljep, Y.; Fumen, G. and Ajisegiri, E. (2005). The Effects of Peeling, Splitting, and Drying on Ginger Quality. Agricultural Engineering International: the CIGRE journal. Vol.7. pp 203–211

ISSN: 2067–3809

ACTA TECHNICA CORVINIENSIS – Bulletin of Engineering | e–ISSN: 2067 – 3809
Tome XVII [2024] | Fascicule 2 [April – June]

[1.]Rade DRAGOVIĆ, [2.]Sanja STANISAVLJEV, [2.]Dalibor DOBRILOVIĆ, [3.]Dragan DRAGOVIĆ, [2.]Vladimir MILOŠEV

SOFTWARE INFORMATION SECURITY MANAGEMENT FOR GOVERNMENT AUTHORITIES

[1.]Institute for standards and technologies, Belgrade, SERBIA
[2.]University of Novi Sad, Technical Faculty "Mihajlo Pupin", Zrenjanin, SERBIA
[3.]Serbian Business Registers Agency, Belgrade, SERBIA

Abstract: This article treats two very important items in the functional matrix of the state bodies work: information security and software development. Information security is not only a recommendation with content in the domain of organization, technology, and procedure but is also defined by legal and by–laws. Lately, software development has been increasingly outsourced, so it is important for state authorities to know that software development is no longer a free assessment of the client and programmer, how and what will be developed, and to what extent the software will be delivered.
Keywords: software development, standards, information security, state authority, cyber security

INTRODUCTION

Digitalization of the state bodies through information systems implies the application of appropriate laws and standards in the management of ICT systems. The increased number of existing information systems is a consequence of legislative changes and digitization of work of the state bodies so that they can respond to the specifics of work tasks related to the maintenance of the existing state and the improvement of their information systems both to other state bodies and to legal and natural persons. The initial requirements refer to the requirements by the law, prevention of security incidents, system control and management of access to information systems, and the prevention of data leaks, but also the technological monitoring of adopted security acts, the introduction of technological measures for monitoring and preserving data security and documenting the application of security solutions within the implemented ICT systems. Considering the number and complexity of these systems, as well as the fact that their operator is the state as well as relevant ministries (which establish and maintain them), it is necessary to manage software development organizational, technological, and procedural according to the requirements of the Information Security Act and the ISO/IEC 27001 – Security standard information, cyber security and privacy protection – Information security management systems – Requirements.

INFORMATION SECURITY

Frequent incidents in the immediate and wider environment impose the need to strength the field of information security in state bodies and to establish a strengthened framework for information security management called ISMS (Information security management systems). ISMS should represent a systematic approach for establishing, implementing, functioning, monitoring, reviewing, maintaining and improving the information security of the state body, in order to achieve business goals, but the risk matrix must not be ignored. ISMS must be based on an assessment of information security risks and the level of acceptability of such risks by the state authority in such way that effectively and efficiently treats the risks and manage the risks in an appropriate manner. Requirements for the protection of information assets, whether they are legal, regulatory, contractual or as a consequence of risk management and the application of appropriate controls, when necessary, contribute to the successful implementation of ISMS. The requirements of the standard mean all the obligations that the standard stipulates that the state body must fulfill [1].

The Cyber Security Program should be developed for the entire organization of the state body, including all software through business and IT–related functions, considering the fact that attacks and threats to information security can occur anywhere within the state body. It is necessary to implement the requirements of the standards ISO/IEC 27001, ISO/IEC 27701, ISO/IEC 27032, ISO/IEC 22301, in areas that include security in the intranet/internet space, i.e. intranet/internet security issues that focus on bridging results risk

analysis between different domains of information security in intranet/internet space. According to the stated standards, it is necessary to implement technical guidelines for solving intranet/internet security risks, including social engineering attacks, hacking, spyware and attacks using other potentially malicious malware software. These technical guidelines should provide controls for the treatment of these risks, including controls for preparing responses to attacks from malicious software (malware), malware organizations for detecting and monitoring attacks [2].

It is necessary to generate a framework for efficient and effective information exchange, coordination and incident management among interested parties in the Internet space. Stakeholders that may be involved are employees, clients and third parties, which may be different types of organizations or individuals, as well as providers, which include service providers as well as all those identified by the risk matrix.

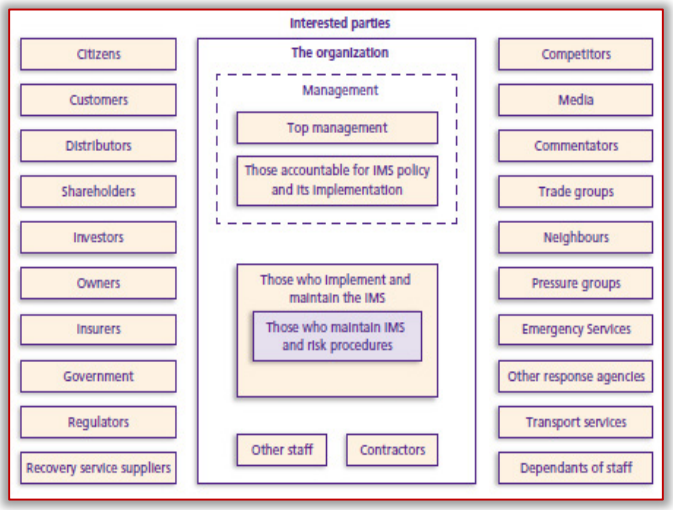

Figure 1. Stakeholders by ISO 22301 [2]

The implementation of the requirements of the standard through the delivery of the Cyber Security Program according to the requirements of the ISO/IEC 27032 standard should include at least the following units: Stakeholders, Information means (information carriers), Threats against intranet/internet space security, Roles of interested parties in information security, Guidelines for interested parties, Information security controls [4].

Requirements of the information security standard ISO 27001 in the domains [5]:

— A.5 Organizational controls, 37 control requirements
— A.6 Human controls, 8 control requirements
— A.7 Physical controls, 14 control requirements
— A.8 Technological controls, 34 control requirements (a total of 93 requirements) inevitably refer to numerous requirements for software development.

SOFTWARE AND STANDARDS FOR SOFTWARE DEVELOPMENT

According to the ISO/IEC 2382 standard, the software is "the whole or part of the programs, procedures, rules and related documentation of an information processing system". State authorities rarely use open–source operating systems and more often vendor development. Application software consists of program/code units made for a specific purpose, according to user needs. This type of software is not directly related to computer hardware, but relies on system software, especially the operating system, to perform its functionality. The need to develop application software most often arises when a state body wants to solve a problem or get a new service.

Any problem that is solved by software development can be solved in several ways. The methods differ from each other in terms of efficiency, precision, comprehensibility, usefulness, modifiability and/or other characteristics. The main goal of software development is for the software to be comprehensive, stable, understandable, easy to maintain and efficiently works for what it was created for. The development of certain software is almost never finished, but it is constantly improved according to the requirements of the market, the customer, changes in legislation, perceived deficiencies or other procedural, organizational or technological needs.

All over the world there is a large number of software manufacturers in every area of life, business of government bodies or industry when there is not only one exclusive solution for a certain area.

In order to develop quality software, it is necessary that its development is based on adopted standards (international, national, internal) and that numerous evaluations are carried out during its life cycle. The expansion of software development, in various fields, has been accompanied by the proliferation of standards, procedures, methods and tools for software development and management. Proliferation has created difficulties in managing software, especially software that is integrated into products and services. This led to the need to define a common framework for the software

discipline that would help everyone who deals with software to "speak the same language" in the design, development, management and maintenance of software in their environments.

ISO/IEC IEEE 12207 Systems and software engineering – Software life cycle processes. The standard established a common framework for software life cycle processes, with well–defined terminology that the software industry can refer to. It contains processes, activities, and tasks that are applied during the acquisition, supply, development, operation, maintenance, or disposal of software systems, products, and services. These life cycles are achieved through the involvement of stakeholders, with the ultimate goal of achieving user satisfaction. The standard applies to the acquisition, supply, development, operation, maintenance, and disposal (regardless of whether it is done internally or externally within the framework of a government body) of software systems, products, and services and the software part of any system, Software includes the software part of the firmware.

There are also included aspects of the system definition needed to provide context for software products and services. This standard also provides processes that can be used to define, control and improve software life cycle processes within a government agency, department or project. The processes, activities and tasks of this document can also be applied during the procurement of systems containing software, alone or in combination with ISO/IEC/IEEE 15288, Software and systems engineering – Systems life cycle processes. This international and national standard establishes a common process description framework that describes the life cycle of human–made systems. It defines a set of processes and related terminologies from an engineering point of view. These processes can be applied at any level in the hierarchy of a system's structure. Selected sets of these processes can be applied throughout the entire life cycle to manage and perform the systems phase of the life cycle. This is achieved through the involvement of all interested parties, with the ultimate goal of achieving user satisfaction [6].

The basic premise of the standard is that the application and practice of software engineering is a relatively young discipline comparing to traditional branches of engineering. Therefore, the control that usually accompanies traditional engineering projects is not always achievable when it comes to software. Underlying the philosophy of ISO/IEC 12207 is that aspects such as software development and maintenance must be conducted in a manner that represents engineering. The processes specified in this standard form one comprehensive set. Each organization, depending on its goals, can choose the appropriate subset to achieve the goals. The standard is designed in such a way that can be adapted to the needs of the organization, project or specific application. It can be applied in cases where the software is an independent entity or an integral part of a complex system [6].

The standard describes the architecture of software life cycle processes without specifying the way of execution of the activities and tasks that the processes contain. It does not prescribe a specific software life cycle model or method for developing software. The activities and tasks of the development process are selected and mapped into the selected life cycle model and may overlap or mutually influence each other, and be executed iteratively or recursively. ISO/IEC 12207 provides a framework in which processes, activities, and tasks can be identified, planned, and adequately responded to.

In order to ensure an easier application of the ISO/IEC 12207 standard, ISO/IEC TR 24748–3 System and software engineering – Life cycle management – Part 3: Guidelines for the application of ISO/IEC 12207 (System and software engineering – Software life cycle processes) was published. The standard explains how ISO/IEC 12207 can be used in the development of different types of software and which processes, defined by the standard, are relevant in each case. Fundamental life cycle models are also defined and supported by examples: waterfall, incremental, and evolutionary [6].

The evaluation and standardization of tools used in the process of developing information systems create the possibility that the quality of the process itself as well as the final products will be at the desired and expected level. Viewed from the perspective of complex information systems in the development and implementation of which several state authorities participate, the application of standards not only ensures the appropriate quality of the final software as a product and development process but also creates opportunities for the exchange of projects between individual state authorities,

facilitates user training and creates conditions for common work on projects of representatives of various state bodies.

Analogously to living organisms, the software is considered to arise, grow, mature, and disappear, so this process is called the term "system life cycle". The life cycle of an information system based on information technologies includes several stages: planning, analysis, design, implementation, and maintenance.

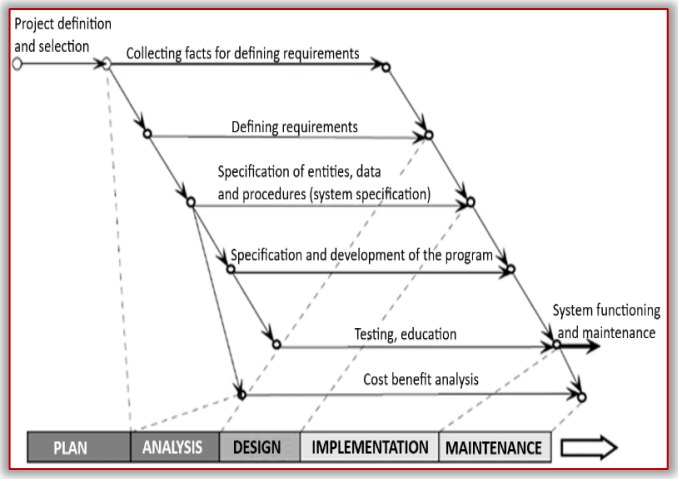

Figure 2. Presentation of software development phases based on ISO 12207 [6]

Planning the development of information systems is one of the most important and difficult functions in modern management. Information system development planning is carried out continuously in order to change things as business circumstances change.

The development planning of an organization's information resources requires the achievement of an architectural framework in which special parts of the system will be harmoniously integrated and which will enable the staged development of the information system and that various special subsystems in the organization can be branched out by various teams of people, successfully planning and rationally using the necessary and available resources. The main purpose of planning and setting up an architectural framework is to achieve information consistency [4].

Information system analysis is the second stage in the life cycle process of information system development. The analysis aims to reveal important information about three key aspects of the analysis:

— analysis and description of the object–system,
— analysis of the existing information system,
— identification of business and user information requirements.

In order to correctly evaluate the existing software of a state body, it is necessary to understand the mission, functions, structure, form, culture, climate, goals, environment and behavior of that state body.

The immediate goals of the analysis of the existing information system are an accurate description and assessment of its properties, and the main purpose is to determine the difference between the properties of the existing software and the desired properties of the newly designed and developed software, which would effectively and efficiently serve in setting and achieving the goals of the state authority for which it is developed.

The final and perhaps the most important segment of the analysis is the identification of user requirements. Users differ according to the nature of the work they perform, the positions they occupy in the structure of the state body, their cognitive and other capabilities, and therefore their functional requirements are also very different.

Investigating the content of those requests, the way and form of their presentation, time and place of delivery, frequency, volume, response time and similar are very difficult, long–term and responsible tasks of the analyst. Much of this information can be successfully found out during the execution of the planning phase however continuity is ensured and more comprehensive and deeper analysis is carried out with changed purpose.

The design of the information system should fully answer the question: how will the system enable the satisfaction of the user needs? In this phase of system development, the logical model of the new system is conceived, the model is developed and the database is designed, the process model is developed, manual and automated procedures are specified, input/output screen forms are designed, reports, printed documents, user dialogue procedures with the system, computer program specifications and program module design, control system design and many other aspects and details of design work.

System design can be defined as drawing, shaping, planning, sketching or arranging many special elements and putting them together into a powerful and unique whole. The analysis system answers the question "What does the system do?" and "What should he do?" to satisfy user requirements, while system design focuses on the key and most complex problem: how to

develop the system and how it should work to satisfy those requirements. System design is a skill and a creative process of finding the best solutions and answering the question "How to do it the best?" Information system designers, by solving all these problems and key design tasks, look for possible alternative "design solutions" that will satisfy the identified information needs of the designer, in the best possible way, during the analysis phase.

The implementation of the information system is very important and in most cases, from the point of view of the end users, the key stage of development. The system can be planned, the analysis carried out, and the design conceived and implemented at an enviable expert level, but its functionality and success will depend on the way of planning and realization of its implementation. Such a plan and its implementation include many important aspects of implementation:

- preparation of implementation,
- implementation and testing of the technology,
- programming,
- testing software products,
- testing of inputs, outputs, databases, and control procedures,
- user education,
- system conversion.

Implementation is the process of complex and responsible transfer of the system from the hands and responsibilities of analysts and designers to the hands of users and operational personnel responsible for the functioning and maintenance of the information system.

Therefore, implementation includes various processes of acquisition, installation, testing, learning, conversion, documentation and its a vital step in ensuring the success of the information system of the state body.

System maintenance is the last stage in the life cycle of the development of the information system of a state body. When the system is fully implemented and put to use by the state authority and its users, the function of its operation and maintenance begins. During the life cycle of the system, numerous changes will occur; many new functional requirements will appear, old functional requirements will be modified or replaced, the real world will change, the environment of the state body, the organization of the state body itself, many technological changes will occur, which will all cause corresponding changes in the model and structure of the information system. Therefore, it is not only a matter of changing existing programs and writing new ones to satisfy new information requirements, but also the development of new versions that require and cause significant changes and modifications in the previous development phases of the system. System maintenance includes the activities of monitoring, evaluation and modification of the system, in order to satisfy desired and necessary continuous improvement.

INFORMATION SECURITY REQUIREMENTS MODEL FOR SOFTWARE

The production of software through standardized phases of the life cycle requires additional efforts in order to establish a software product with the required functionalities. In addition to the initial functionality required for the software by the state authority, which solves some procedural needs in the jurisdiction, it is necessary during all phases to establish and implement measures related to information security. Information security requirements for software are not just a favorable feeling of someone but are defined by the legislation of the state through the Law on Information Security, the Law on Protection of Personal Data, the Law on Critical Infrastructure, the Law on Electronic Services as well as through the acts in the Criminal Code of the Republic of Serbia [7]. Behind the mentioned laws there are by–laws, regulations and other legal procedural acts as well as special state bodies that control the implementation of the stated. In the vast majority of state bodies, persons who perform tasks in the field of information security have been appointed. There is no modern state body that does not use information technologies in its work. All of the above describes the necessary procedural, organizational and technological framework as a prerequisite for a functional information security management system – ISMS.

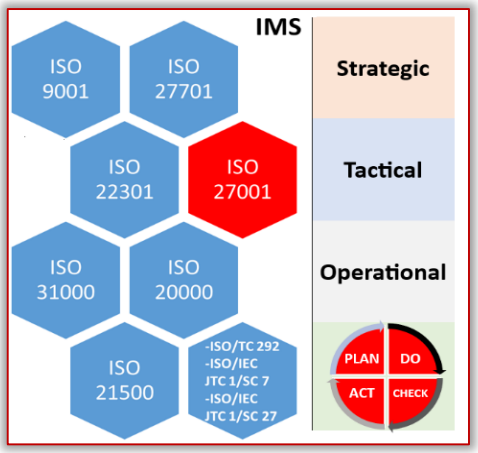

Figure 5. Information security software development matrix

The information security management system must be placed in the strategic, tactical and operational domain, during which it must be coordinated with the actions within its department, but also with other state services. The strategic, tactical, and operational domains must be implemented in the organizational, technological, and procedural framework by fully applying the PDCA – Deming cycle [8].

Table 1. Experienced recommendations for software information security [10]

ISO/TC 292 Security and resilience	ISO/IEC JTC 1/SC 7 Software and systems engineering	ISO/IEC JTC 1/SC 27 Information security, cybersecurity and privacy protection
ISO 22301 Business continuity management systems	ISO/IEC/IEEE 26511 Requirements for managers of information for users of systems, software, and services	ISO/IEC 27001 – Information security management system
ISO 22320 Emergency management	ISO/IEC/IEEE 26531 Content management for product life–cycle, user and service management documentation	ISO/IEC 18033 – Encryption algorithms
ISO 22376 Authenticity, integrity and trust for products and documents	ISO/IEC 26550 Reference model for Product Line Engineering and Management	ISO/IEC 19772 – Authenticated encryption
ISO 28000 Security management system	ISO/IEC 25000 Systems and software Quality Requirements and Evaluation	ISO/IEC 29192 – Lightweight cryptography
ISO 22341 Protective security	ISO/IEC/IEEE 12207 Software life cycle processes	ISO/IEC 15408 – Evaluation criteria for IT security
ISO 22316 Organizational resilience	ISO/IEC 33000 Family Process assessment	ISO/IEC 30111 – Vulnerability handling processes
ISO 22361 Crisis management	ISO/IEC 29155 Benchmarking	ISO/IEC 27035 Information security incident management
…	ISO/IEC 10746 Open Distributed Processing	ISO/IEC 27036 Cybersecurity – Supplier relationships
	ISO/IEC 19770 IT asset management	ISO/IEC 27099 Public key infrastructure
	ISO/IEC/IEEE 29119 Software testing	ISO/IEC 27701 Privacy information management
	ISO/IEC/IEEE 42010 Architecture description	ISO/IEC 29100 – Privacy framework
	…	ISO/IEC 29184 – Online privacy notices and consent
		…

Software is a technological category that has defined requirements in international and national standards of modern countries for many years. In addition to the initial requirements of the ISO 27001 standard – Information security management systems, it is necessary to pay special attention to the fact that the software is not designed to function on a desert island but in interaction with other government bodies. It is necessary to implement the following requirements:

- ISO 27701 – Privacy information management systems,
- ISO 20000 – Information technologies – Service management through the application of the well–known principles of ISO 9001 – Quality management systems with ISO 10001 – Quality management – User satisfaction,
- ISO 31000 – Risk management and ISO 21500 – Project management [8].

The above is only a basis that should be expanded, specifically for the competence of individual state bodies, with the requirements of ISO/TC 292 – Security and resilience, ISO/IEC JTC 1/SC 7 – Software and systems engineering and ISO/IEC JTC 1/SC 27 Information security, cyber security and privacy protection [10].

The above table provides guidelines for the analysis of a clear and complete definition of software in the domains of Security and resilience, Software and systems engineering and Information security, and cyber security and privacy protection, which represent indispensable members of the initial analysis of the phases of planning, analysis, design, implementation, and maintenance of the software life cycle.

CONCLUSION

It is necessary to establish an effective way of dealing with information security risks in software development, which should include a combination of multidisciplinary teams and multiple strategies, taking into account all interested parties, legal requirements, organizational knowledge and technological experience.

These strategies should include the best practices in the field of state administration with the cooperation of all interested parties (especially competent state authorities: prosecution, police, intelligence services) in order to identify and address information security and risk issues, broad education of clients and employees, providing a reliable resource for initial identification and addressing of specific risks related to intranet/internet security in state bodies with a special emphasis on software (all software in use in individual state bodies) as well as innovative technological solutions that help protect against various cyber–attacks.

The given guidelines are focused on providing best practices in government administration to

help stakeholders in the intranet/internet space to understand the role of software and act preventively with the goal of playing an active role in solving information security challenges.

References

[1] Rade Dragovic, Functional recommendations for the establishment of judicial information system, ISDOS – Information system of the state bodies of Serbia, Conference Proceeding 2010
[2] Rade Dragović, Dragan Dragović, Bojan Perović, Đuro Klipa, Strategic management in the judiciary based on decision support systems, YUINFO Conference Proceeding 2013
[3] ISO 22301 – Security and resilience – Business continuity management systems – Requirements, International Organization for Standardization
[4] Zvonimir Ivanović, Rade Dragović, Sergej Uljanov, Strategic regulation model on the high–tech crime vulnerable targets, Western Balkans: from stabilization to integration, International Scientific Conference, Conference Proceeding 2011
[5] ISO/IEC 27001 – Security standard information, cyber security and privacy protection – Information security management systems – Requirements, International Organization for Standardization
[6] ISO 12207 – Systems and software engineering – Software life cycle processes, International Organization for Standardization
[7] Rade Dragovic, Vladimir Kačanovski, Bojan Perovic, Security policy in judicial information system, YUINFO Conference Proceeding 2011
[8] Rade Dragović, Ivan Peljević, Đuro Klipa, Implementation strategy for cryptographic protection in ejudiciary, INFOFEST Conference Proceeding 2012
[9] Rade Dragović, Bojan Perović, Security policy and recommendations for increasing security database in the justice information system, BISEC Conference Proceeding 2012
[10] Internet source: International Organization for Standardization, website: www.iso.org
[11] Rade Dragović, Bojan Perović, Ljubiša Pešić, Enver Nuhović, Đuro Klipa, Recommendations for improving security databases in the judicial information system, YUINFO Conference Proceeding 2012
[12] Rade Dragović, Miodrag Ivković, Bojan Perović, Đuro Klipa, Dataveillance and data mining as a technology support to the process of investigation, TELFOR Conference Proceeding 2011, IEEE conference
[13] Vojkan Nikolić, Rade Dragović, interoperability and security of egovernment of Republic of Serbia, TELFOR Conference Proceeding 2014, IEEE conference

Note: This paper was presented at IIZS 2023 – The XIII International Conference on Industrial Engineering and Environmental Protection, organized by Department of Mechanical Engineering and Department of Environmental Protection of the Technical Faculty "Mihajlo Pupin" Zrenjanin, from the University of Novi Sad, in cooperation with partners – University Politehnica Timisoara, Faculty of Engineering, Hunedoara (ROMANIA), University "St. Kliment Ohridski", Technical Faculty, Bitola (MACEDONIA), "Aurel Vlaicu" University of Arad, Faculty Of Engineering, Arad (ROMANIA), University of East Sarajevo, Faculty of Mechanical Engineering East Sarajevo, Sarajevo (BOSNIA & HERZEGOVINA) and University of Giresun, Faculty of Engineering, Giresun (TURKEY) – in Zrenjanin, SERBIA, in 05–06 October, 2023.

ISSN: 2067-3809

Fascicule 2
[April – June]
tome XVII
[2024]

ACTA Technica CORVINIENSIS
BULLETIN OF ENGINEERING

ISSN: 2067-3809

ACTA TECHNICA CORVINIENSIS – Bulletin of Engineering | e–ISSN: 2067 – 3809
Tome XVII [2024] | Fascicule 2 [April – June]

[1.] Muharrem Hilmi AKSOY, [2.] Ali ÖNER, [1.] Muhammed Osman DUMAN, [1.] Mert TURAN

NUMERICAL ANALYSIS OF GAS–SOLID FLOW IN A REVERSE FLOW CYCLONE SEPARATOR

[1.] Konya Technical University, Faculty of Engineering and Natural Science, Department of Mechanical Engineering, Konya, TÜRKIYE
[2.] İmaş Machinery Inc. R&D Center, Konya, TÜRKIYE

Abstract: Aerocyclone separators are crucial in separating solid particles from gas streams. These cyclones exhibit diverse geometrical configurations in their inlet zones, including tangential, spiral, helical, and axial designs, with variations within the tangential type. Beyond their economic appeal, these devices are characterized by their resilience to high temperatures and pressures, ease of manufacturing, and uncomplicated geometrical structures. Among the factors influencing cyclone performance, the critical parameters of interest encompass dust collection efficiency and pressure loss. The present study employed a Stairmand–type counter–flow cyclone to separate flour particles dispersed within an air medium. A numerical investigation considered cyclone heights of H = 750 mm, H = 1000 mm, and H = 1500 mm. Furthermore, cyclone inlet velocities of 8 m/s, 13 m/s, and 17 m/s were specifically chosen for examination. Particle sizes ranged from 1 to 10 micrometers, ensuring the evaluation extended to conditions achieving 100% collection efficiency. A comprehensive analysis of pressure drop ratios was presented herein, offering insights into the impact of varying inlet speeds and cyclone dimensions.

Keywords: cyclone, collection efficiency, pressure drop, flow analysis

INTRODUCTION

The separation of gases and the solid particles they carry is important in process industries, and it is achieved through various methods. Solid particles can intentionally be present in the gas flow, for example, in pneumatic conveying systems, where it may be necessary for 100% solid recovery at the end of the conveying process to have an economical process [1–2]. The applied centrifugal force forms a vortex inside the cyclone, and the gas swirls toward the conical bottom. Larger particles with a considerable diameter are then pushed towards the wall and separated from the gas. In the conical section, the gas flow reverses direction to move upward over the central part of the cyclone and exits from the top through the gas outlet pipe. Meanwhile, solid particles move downward along the wall and accumulate at the bottom of the conical section [3–4].

Cyclone separators are widely used in industries to separate and collect particles from gases or similar gas mixtures containing solid particles such as dust, chips, or grains. They are used in industrial dust collection systems to capture particles as small as 50 microns. Commercial cyclones can operate at flow rates ranging from 50 to 5000 m3/h. In cases where they do not provide the required efficiency, they can be used in conjunction with high–efficiency collection devices. Cyclone separators are categorized into two groups: axial inlet cyclones and tangential inlet cyclones [5–6]

Shepperd & Lapple, Avant, Parnell & Sorenson cyclone models are commonly used in the agricultural industry. Simpson & Parnell, to address the cotton processing sector's lint problem, used a low–pressure cyclone model. The Stairmand Cyclone was selected in this study due to its high dust collection efficiency [7].

Several parameters influence cyclone performance. These parameters include the type of cyclone, cyclone dimensional ratios, outlet pipe height (stack), cyclone inlet velocity, outlet pipe diameter, temperature, and variations in particle concentration. Altering these parameters can affect cyclone performance criteria, such as pressure drop and efficiency [8].

The literature review comprehensively examines research endeavors focused on comprehending and optimizing cyclone separator performance. Scholars have rigorously investigated the impact of diverse factors such as geometry, flow rates, and particle concentration on cyclone efficiency and pressure drops. Pioneering work by Leith and Licht [9] introduced a theory for calculating particle collection efficiency in cyclone separators, incorporating the drag coefficient to enhance particle collection efficiency. Their efforts also yielded an efficiency model capable of accounting for pressure losses. Subsequent studies, like those by Griffiths and Boysan [10], employed numerical simulations to analyze particle capture efficiency and pressure drops in different cyclones, aligning their findings with existing literature. Barth's [11] model was found accurate for small cyclones, whereas lozia

and Leith's [12] model proved precise for larger counterparts. The integration of CFD analyses further enriched the field, providing reliable predictions for pressure drops and particle capture efficiency. Bohnet [13] delved into experimental studies, examining cyclone performance at high temperatures, revealing significant pressure drops and efficiency curves for specific temperature values. Linden and Gudmundsson [14] explored parameters affecting cyclone collection efficiency, highlighting the critical influence of the ratio of cyclone body diameter to vortex tube inner diameter and its independence from the Reynolds number.

Avcı and Erel [15] introduced an approach to determine optimal cyclone length, finding no efficiency increase beyond a certain length, suggesting potential adjustments at high and low velocities. Avcı and Karagöz [16] explored the effects of flow and geometric parameters, unveiling the significant roles of surface friction, vortex length, and flow regime. Faulkner et al. [17] identified an inverse relationship between cyclone diameter and efficiency. Advanced computational techniques, as evidenced by Kaya and Karagöz [18], emphasized the accuracy of the Reynolds turbulence model in predicting cyclone behavior. Novel designs, like Tan F.'s [19] modified cyclone, showcased the potential for reimagining cyclone structures. Erol et al. [20] employed numerical and experimental methods, refining our understanding of exit pipe diameter influence. Recent studies, including those by Chu et al. [21], Pandey and Brar [22], and El–Emam et al. [23], harnessed advanced computational and experimental techniques, pushing the boundaries of cyclone optimization.

In this study, a Stairmand–type counter–flow cyclone was used to separate flour particles in an air medium. Numerical simulations were conducted with cyclone heights of 750 mm, 1000 mm, and 1500 mm, along with inlet velocities of 8 m/s, 13 m/s, and 17 m/s. Particle sizes ranged from 1 to 10 micrometers, allowing for a thorough evaluation of conditions and achieving 100% collection efficiency. The analysis included a detailed examination of pressure drop ratios, providing valuable insights into the effects of different speeds and cyclone dimensions.

MATERIAL AND METHODS

In the study, the particle bulk density was assumed to be 550 kg/m³, and a flow rate of 1000 m³/h of air contained 18 kg of these particles. Two distinct groups of parameters are employed in the design of aerosol cyclones. This study focuses on parameters based on design, which vary according to the selected cyclone type. The selection and manipulation of these parameters play a pivotal role in the design and performance optimization of aerosol cyclones. Different cyclone types require adjustments in these parameters to achieve desired efficiency and particle separation outcomes. Figure 1 presents the design parameters specific to the Stairmand–type cyclone. These parameters are integral to the intricate process of cyclone design. In Stairmand–type cyclones, the parameters are dimensioned relative to the body diameter "D" [24].

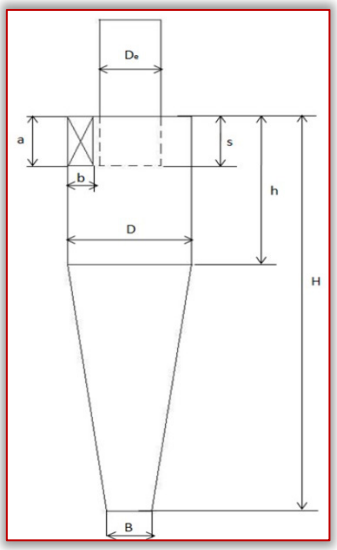

Figure 1. The design parameters of the Stairmand type cyclone

Table 1. The dimensions of the Stairmand cyclone

Parameter	Dimension*D
Cyclone diameter, D	1.0 D
Air outlet pipe diameter, De	0.5 D
Height of air inlet section, a	0.5 D
Width of air inlet section, b	0.2 D
Dip depth of the outlet pipe, s	0.5 D
Cyclone height, H	4.0 D
Body height, h	1.5 D
Dust outlet diameter, B	0.375 D

When multiplied by the body diameter "D", these standardized dimensions provide precise measurements for each component, ensuring consistency and accuracy in the design and evaluation of Stairmand–type cyclones.

In the computational fluid dynamics (CFD) analysis, parameters were meticulously chosen to simulate the complex dynamics within the cyclone separator. Particle density was fixed at 0.80 kg/m3 for flour material. The simulation's choice of spherical particle shape was made to capture real–world scenarios accurately. The gas flowing into the system was at a stable

temperature of 27 °C, with an outlet pressure maintained at 101625 Pa. Furthermore, the air density was chosen as air set at 1.1 kg/m^3, while the viscosity was calculated at 1.7810^{-5} kg/(ms). The ambient temperature was also held constant at 27°C, reflecting standard environmental conditions. The inlet velocities, a critical variable influencing the cyclone's efficiency, were tested at three different values: 8 m/s, 13 m/s, and 17 m/s. This range allowed for a comprehensive analysis of the cyclone's performance under various flow rates, providing valuable insights into its operational flexibility. Moreover, the surface roughness of the cyclone material was specified at 0.39, a factor contributing significantly to the friction between particles and the cyclone walls as taken as a metal sheet. These chosen parameters served as the foundation for the computational analysis, enabling a detailed exploration of the cyclone separator's behavior under different operating conditions.

The K–Epsilon Model has been a foundational tool for simulating turbulent flows in CFD. A modification called the RNG Option was introduced to enhance accuracy in swirling flows. Specifically tailored for swirl–dominated scenarios, this adjustment ensures precise simulations by employing standard wall functions for near–wall treatment. For the CFD analysis, specific boundary conditions are set:

Inlet and Wall: Particles rebound off these boundaries, with their momentum changing as determined by the coefficient of restitution. Outlet (Top): When particles encounter this boundary, their trajectories end, signifying that they have 'escaped.' Outlet (Bottom/Dustbin): Particle trajectories are terminated, and the outcome is recorded as 'trapped.' For evaporating droplets, their entire mass instantly transitions into the adjacent cell's vapor phase. In the case of a combusting particle, the remaining volatile mass enters the vapor phase.

In the realm of CFD analysis, the concept of separation efficiency in cyclone separators is crucial. It quantifies the fraction of particles of a specific size captured within the cyclone concerning those particles of the same size entering the cyclone. Empirical observations have demonstrated that the efficiency of cyclone separators rises with increasing particle mean diameter and density, heightened gas tangential velocity, diminished cyclone diameter, elongated cyclone length, and the removal of gas alongside solids through the cyclone legs. In this context, the Separation Efficiency is precisely defined based on particle history data. It represents the proportion of concentration removed from the incoming feed stream compared to the initial concentration. This efficiency measure is calculated by determining the ratio of trapped particles to the total number of particles tracked in the system, as given in Eq 1.

$$\text{Efficieny} = \frac{\text{N. of particles trapped}}{\text{N. of particles tracked}} \quad (1)$$

In practical engineering applications, derivatives of the k–ε model exhibit comparable structures, featuring transport equations for turbulent kinetic energy (k) and dissipation rate (ε). The Renormalization Group (RNG) k–ε model is grounded in the instantaneous Navier–Stokes equations. It sets the RNG k–ε model apart from the Standard k–ε model is analytical derivation, involving incorporating model constants and supplementary terms within the transport equations [25].

$$\frac{\partial}{\partial t}(\rho k) + \frac{\partial}{\partial x_i}(\rho k u_i) = \frac{\partial}{\partial x_i}\left[\mu_{eff}\alpha_k \frac{\partial k}{\partial x_j}\right] + G_k - \rho\varepsilon + S_k \quad (2)$$

$$\frac{\partial}{\partial t}(\rho\varepsilon) + \frac{\partial}{\partial x_i}(\rho\varepsilon u_i) = \frac{\partial}{\partial x_i}\left[\mu_{eff}\alpha_k \frac{\partial \varepsilon}{\partial x_j}\right] + C_{1\varepsilon}G_k\frac{\varepsilon}{k} - C_{2\varepsilon}\rho\frac{\varepsilon^2}{k} - R_\varepsilon + S_\varepsilon \quad (3)$$

The fundamental disparity between the RNG (Renormalization Group) and the standard k–ε turbulence models lies in the presence of an additional term within the dissipation rate (ε) equation, depicted as follows:

$$R_\varepsilon = \frac{C_\mu \rho \eta^3 (1 - \eta/\eta_0)}{1 + \beta\eta^3}\frac{\varepsilon^2}{k} \quad (4)$$

In this equation, the constant Cμ is set to 0.0845, η≡Sk/ε, η_0 equals 4.38, and β equals 0.012. Notably, the RNG model exhibits heightened sensitivity to strain and streamline curvature impacts when contrasted with the Standard k–ε model, where the constants C1ε and C2ε are 1.44 and 1.92, respectively.

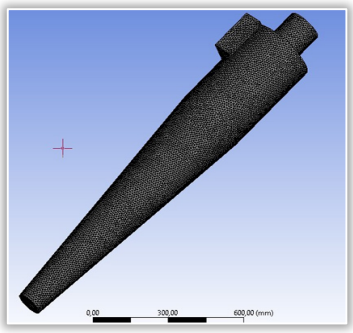

Figure 2. Mesh structure of the cyclone

A mesh independency study indicates that 4x10^5, 9,5x10^5, and 20x10^5 elements are deemed

adequate for 750 mm, 1000 mm, and 1500 mm for the analyses, respectively. A mesh structure used in this study is given in Fig.2.

RESULTS AND DISCUSSION

In the following section, we delve into the results and discussions derived from CFD analysis of cyclone separators. Through the computational simulations, we have explored various parameters that significantly influence cyclone performance, including geometry modifications and flow rates. Tangential and axial velocities are important factors for the particle collection in the cyclones. The total pressure contours in Figures 3, 4, and 5 are presented at inlet velocities of 8, 13, and 17 m/s, respectively. These figures illustrate pressure variations in three dimensions, corresponding to different H heights, denoted as options a, b, and c. Geometric measurements have been adjusted to represent diverse pressure changes in these three–dimensional contexts. Due to swirling velocity within the cyclone, a distinct negative pressure zone manifests in its central region. Remarkably, the pressure reaches its nadir close to the cyclone's center, contrasting sharply with the positive and maximal pressure values observed near the cyclone periphery. This signifies a radial decline in pressure, where the pressure diminishes from the wall towards the core. Notably, as the diameter of the vortex finder decreases, there is a discernible augmentation in pressure. This phenomenon underscores the significant correlation between pressure and velocity. Consequently, an escalation in tangential velocity is anticipated to correspond with an elevation in pressure. Furthermore, the study observes a substantial pressure gradient along the radial direction, emphasizing its pronounced nature in this dimension, while it remains comparatively restricted in the axial orientation. This intricate interplay between velocity, pressure, and geometry underscores the complex dynamics at play within cyclonic systems.

In cyclone design, paramount objectives are maximizing separation efficiency while minimizing pressure drop. A superior separation efficiency and a minimal pressure drop constitute the optimal outcome for cyclone designs. This intricate balance necessitates understanding various physical and geometrical variables that influence cyclone behavior. These variables encompass particle density, gas viscosity, cyclone dimensions, particle cut–off diameter, inlet velocity, and numerous other factors.

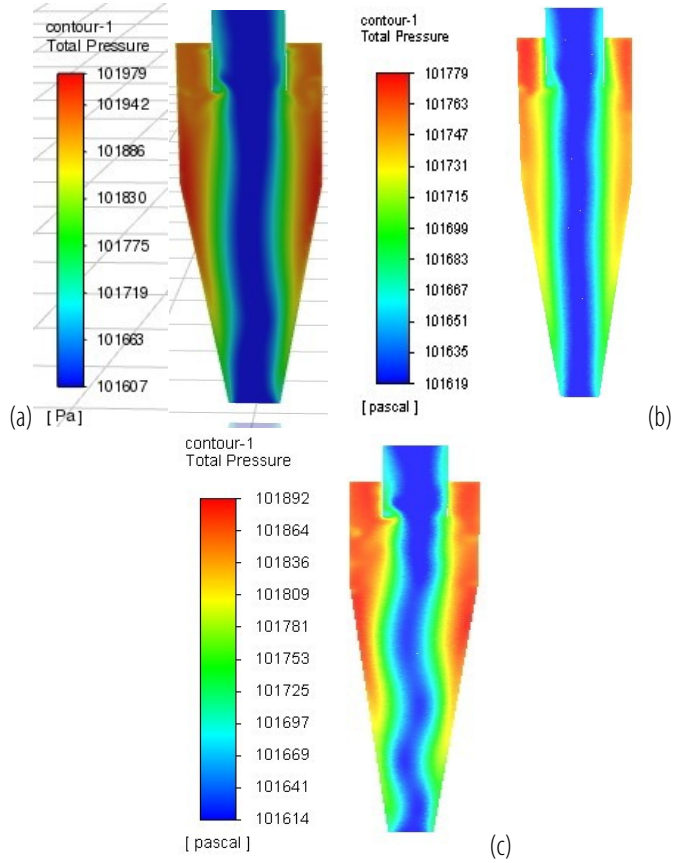

Figure 3. Pressure Contours in Cyclones with (a) H = 750 mm, (b) H = 1000 mm, and (c) H = 1500 mm at a Velocity of 8 m/s.

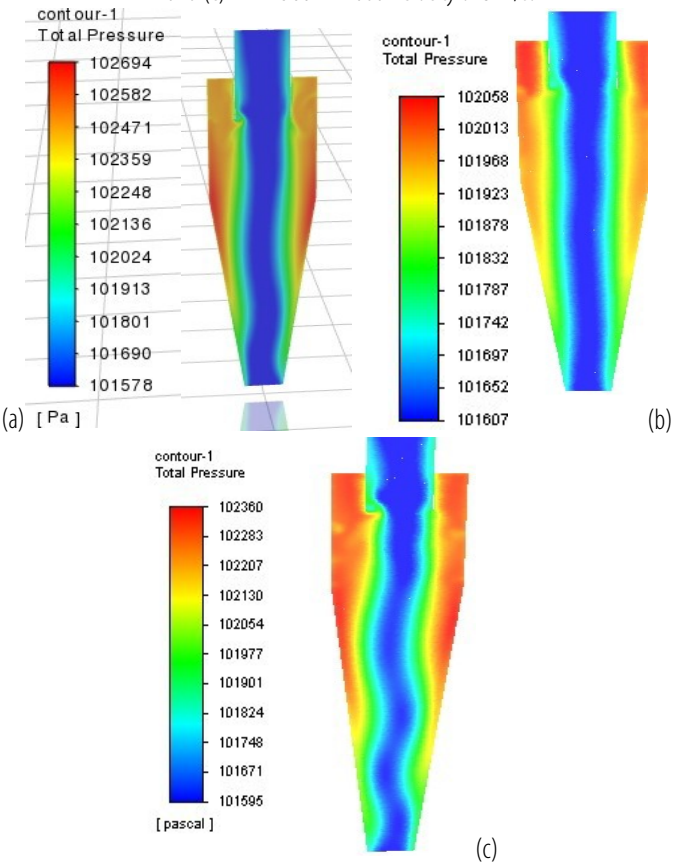

Figure 4. Pressure Contours in Cyclones with (a) H = 750 mm, (b) H = 1000 mm, and (c) H = 1500 mm at a Velocity of 13 m/s.

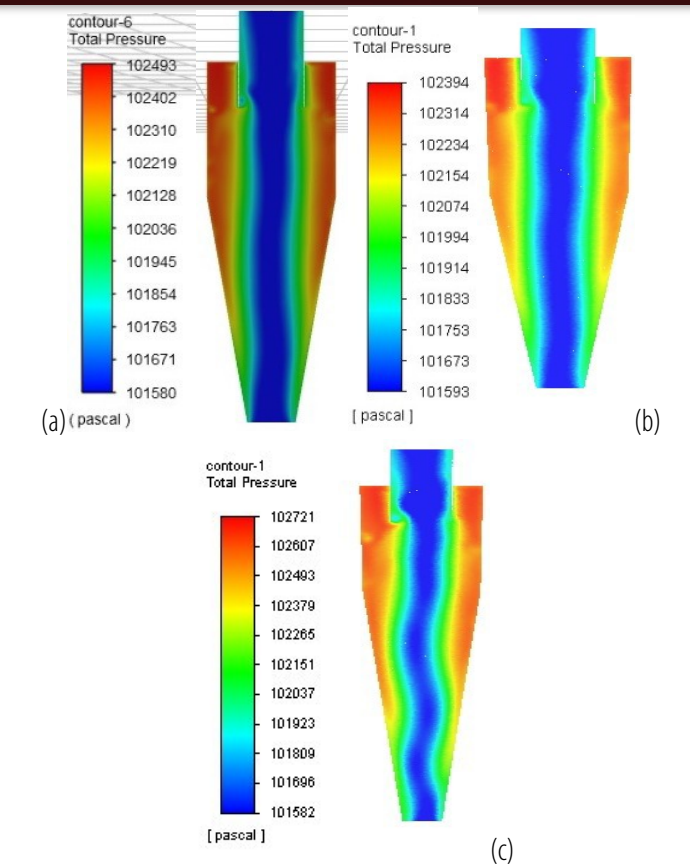

Figure 5. Pressure Contours in Cyclones with (a) H = 750 mm, (b) H = 1000 mm, and (c) H = 1500 mm at a Velocity of 17 m/s.

The manipulation and comprehension of these variables are pivotal in crafting cyclone designs that align with the desired efficiency and pressure drop criteria, reflecting the intricate interplay of diverse parameters in cyclone performance optimization. The impact of inlet velocity on fractional separation efficiency is a critical aspect of cyclone separator performance analysis. Understanding how varying inlet velocities influence particle separation efficiency is essential for optimizing cyclone designs. This parameter significantly affects the cyclone's ability to capture particles of different sizes and densities, directly influencing the separation process's overall efficiency.

In the discrete phase model, particles are introduced at the cyclone's inlet and meticulously tracked to assess fractional separation efficiency, a crucial parameter in cyclone performance evaluation. The separation efficiency represents the ratio of captured particles to those injected, considering incomplete particles. Particles ranging from 1 to 10 μm diameter were released at the inlet to simulate the cyclone's separation efficiency. Figure 6 illustrates the separation efficiency concerning particle diameter at three distinct inlet velocities for a cyclone with different diameters. The graph depicts a direct correlation between efficiency, particle size, and inlet velocity, indicating that higher efficiencies are achieved with larger particles and increased inlet velocities. This relationship is rooted in the proportional nature of centrifugal force to flow velocity, highlighting the direct influence of centrifugal force on collection efficiency. As it is seen, as the H height increases, 100% efficiency is achieved at higher particle size.

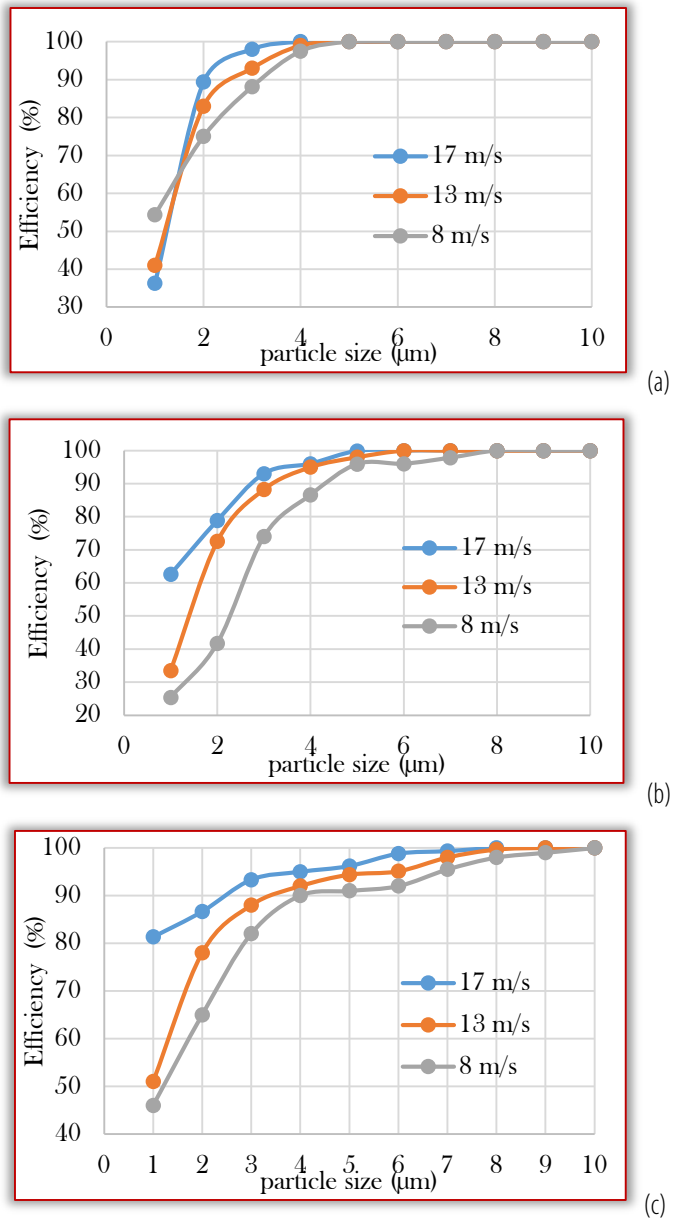

Figure 6. The effect of the inlet velocity on separation efficiency of cyclones (a) H = 750 mm, (b) H = 1000 mm, and (c) H = 1500 mm

CONCLUSION

In this comprehensive study, the intricate dynamics of cyclone separators were meticulously explored through CFD simulations. The focus was on a Stairmand–type counter–flow cyclone utilized for separating flour particles within an air medium. The research delved into an array of crucial parameters, including cyclone heights (H = 750 mm, H = 1000 mm, and

H = 1500 mm) and inlet velocities (8 m/s, 13 m/s, and 17 m/s). This systematic analysis provided deep insights into the cyclone's behavior under diverse operational conditions.

One of the key findings highlighted the significant influence of geometry and flow rates on cyclone performance. The analysis of pressure contours revealed intricate patterns within the cyclone structure. A notable negative pressure zone was observed in the central region due to swirling velocity, with pressure reaching its minimum at the cyclone's center. This was sharply contrasted by positive and maximal pressure values near the cyclone periphery, illustrating a radial decline in pressure from the wall toward the core. Moreover, the reduction in the vortex finder diameter increased pressure, emphasizing the direct correlation between pressure and velocity.

In examining the impact of inlet velocity on fractional separation efficiency, a critical aspect of cyclone performance, the study revealed a direct relationship between efficiency, particle size, and inlet velocity. Larger particles and increased inlet velocities resulted in higher efficiencies, underlining the pivotal role of centrifugal force proportional to flow velocity in the collection process.

Future research directions could delve deeper into integrating advanced materials on surfaces, optimized geometries, and experimental techniques to enhance cyclone separator efficiency further and contribute to sustainable industrial practices in milling and other industries.

References

[1] Jüttner, K., U. Galla, and H. Schmieder. "Electrochemical approaches to environmental problems in the process industry." Electrochimica Acta 45.15–16 (2000): 2575–2594.
[2] Utikar, Ranjeet, et al. "Hydrodynamic simulation of cyclone separators." Computational fluid dynamics. InTech, 2010. 241–266.
[3] Wang, B., Xu, D. L., Chu, K. W., & Yu, A. B. (2006). Numerical study of gas–solid flow in a cyclone separator. Applied Mathematical Modelling, 30(11), 1326–1342.
[4] Liu, Z., Zheng, Y., Jia, L., Jiao, J., & Zhang, Q. (2006). Stereoscopic PIV studies on the swirling flow structure in a gas cyclone. Chemical Engineering Science, 61(13), 4252–4261.
[5] Obernberger, I., Brunner, T., & Bärnthaler, G. (2006). Chemical properties of solid biofuels—significance and impact. Biomass and bioenergy, 30(11), 973–982.
[6] Schummer, P., Noe, P., & Baker, M. (1992). LDV measurements in the vortex flow created by a rotating wall dewatering cyclone. In Hydrocyclones: Analysis and Applications (pp. 359–376). Dordrecht: Springer Netherlands.
[7] Sharma, G., & Majdalani, J. (2022). Effects of various inlet parameters on the computed flow development in a bidirectional vortex chamber. Physics of Fluids, 34(4).
[8] Bhasker, C. (2010). Flow simulation in industrial cyclone separator. Advances in Engineering software, 41(2), 220–228.
[9] Leith , D. , and Licht , W. (1972). AIChE Sym. Ser. 68 : 196
[10] Griffiths, W. D., & Boysan, F. (1996). Computational fluid dynamics (CFD) and empirical modelling of the performance of a number of cyclone samplers. Journal of Aerosol Science, 27(2), 281–304.
[11] Barth, W. (1956). Berechnung und auslegung von zyklonabscheidern auf grund neuer untersuchungen. Brennst.–Warme–Kraft, 8, 1–9.
[12] Iozia, D. L., & Leith, D. (1989). Effect of cyclone dimensions on gas flow pattern and collection efficiency. Aerosol Science and Technology, 10(3), 491–500.
[13] Bohnet, M., Gottschalk, O., & Morweiser, M. (1997). Modern design of aerocyclones. Advanced Powder Technology, 8(2), 137–161.
[14] Lidén, G., & Gudmundsson, A. (1997). Semi–empirical modelling to generalise the dependence of cyclone collection efficiency on operating conditions and cyclone design. Journal of aerosol science, 28(5), 853–874.
[15] Avcı, A., & Erel, G. K. (2003). Siklon separatörlerde uzunluğun verime etkisi ve optimizasyonu. Uludağ Üniversitesi Mühendislik–Mimarlık Fakültesi Dergisi, 8(1), 101–109.
[16] Karagoz, I., & Avci, A. (2005). Modelling of the pressure drop in tangential inlet cyclone separators. Aerosol Science and Technology, 39(9), 857–865.
[17] Faulkner, W. B., Buser, M. D., Whitelock, D. P., & Shaw, B. W. (2008). Effects of cyclone diameter on performance of 1D3D cyclones: cutpoint and slope. Transactions of the ASABE, 51(1), 287–292.
[18] Kaya, F., & Karagoz, I. J. C. E. (2008). Performance analysis of numerical schemes in highly swirling turbulent flows in cyclones. Current science, 1273–1278.
[19] Tan, F., Karagoz, I., & Avci, A. (2016). Effects of geometrical parameters on the pressure drop for a modified cyclone separator. Chemical Engineering & Technology, 39(3), 576–581.
[20] Erol, H. I., Turgut, O., & Unal, R. (2019). Experimental and numerical study of Stairmand cyclone separators: a comparison of the results of small–scale and large–scale cyclones. Heat and Mass Transfer, 55, 2341–2354.
[21] Chu, K., Chen, Y., Ji, L., Zhou, Z., Yu, A., & Chen, J. (2022). Coarse–grained CFD–DEM study of Gas–solid flow in gas cyclone. Chemical Engineering Science, 260, 117906.
[22] Pandey, S., & Brar, L. S. (2022). On the performance of cyclone separators with different shapes of the conical section using CFD. Powder Technology, 407, 117629.
[23] El–Emam, M. A., Zhou, L., & Omara, A. I. (2023). Predicting the performance of aero–type cyclone separators with different spiral inlets under macroscopic bio–granular flow using CFD–DEM modelling. Biosystems Engineering, 233, 125–150.
[24] Brar, L. S., Sharma, R. P., & Elsayed, K. (2015). The effect of the cyclone length on the performance of Stairmand high–efficiency cyclone. Powder Technology, 286, 668–677.
[25] Shaheed, R., Mohammadian, A., & Kheirkhah Gildeh, H. (2019). A comparison of standard k–ε and realizable k–ε turbulence models in curved and confluent channels. Environmental Fluid Mechanics, 19, 543–568.

Note: This paper was presented at IIZS 2023 – The XIII International Conference on Industrial Engineering and Environmental Protection, organized by Department of Mechanical Engineering and Department of Environmental Protection of the Technical Faculty "Mihajlo Pupin" Zrenjanin, from the University of Novi Sad, in cooperation with partners – University Politehnica Timisoara, Faculty of Engineering, Hunedoara (ROMANIA), University "St. Kliment Ohridski", Technical Faculty, Bitola (MACEDONIA), "Aurel Vlaicu" University of Arad, Faculty Of Engineering, Arad (ROMANIA), University of East Sarajevo, Faculty of Mechanical Engineering East Sarajevo, Sarajevo (BOSNIA & HERZEGOVINA) and University of Giresun, Faculty of Engineering, Giresun (TURKEY) – in Zrenjanin, SERBIA, in 05–06 October, 2023.

ISSN: 2067–3809

ACTA TECHNICA CORVINIENSIS – Bulletin of Engineering | e–ISSN: 2067 – 3809
Tome XVII [2024] | Fascicule 2 [April – June]

[1.]Aleksandra ŠUĆUROVIĆ, [1.]Jelena KIURSKI MILOŠEVIĆ, [1.]Eleonora TEREČIK

INVESTIGATING THE IMPLEMENTATION OF INTEGRATED MANAGEMENT SYSTEM (IMS)

[1.] Technical College of Applied Sciences in Zrenjanin, SERBIA

Abstract: In order to sustain their business, companies must balance the fulfilment of requirements of all the parties involved. Their attempts to achieve sustainability rely on numerous international standards, but also on integrated management system which integrates all the elements of a business system (through better quality, improvements in environmental protection, data protection, etc.) into a unique and complete production management system in an organization so that the requirements of all the interested parties could be fulfilled and the business objectives achieved. The results of a survey conducted with the aim of investigating the importance of implementation of IMS in the companies which perform various kinds of sectors and industries are presented in this paper. The obtained results indicate a high level of implementation of different standards, obtained benefits, as well as a high level of the employees' awareness of the need to apply them.

Keywords: integrated management system (IMS), ISO standards, survey

INTRODUCTION

The effort put in advancing the competitiveness of a company in the local and international market has never been a simple task because it involves extreme commitment and responsibility [1]. Competitiveness involves the implementation of different development programs, an integrated management system (IMS) based on ISO standards, innovations in new products and services always with same the aim [2]: to offer quality products, to provide continuing growth, to improve operations, as well as to ensure permanent adjustment of business strategy to market demands. ISO standards constantly have affected the increase of competitiveness of products and companies since the first standard was introduced in the 1990s of the 20th century (series ISO 9000), with all the reviews made so far (ISO 9001, 9004, 14001, OHSAS 18000, ISO 27000) along with the development of the new ones (OHSAS 18001, ISO 22000, ISO 27001, ISO 26000, ISO 45001, ISO 50001) [3]. On the other hand, ISO standards create scientific and technological basis for making legislative, health, safety and environmental frameworks at the state level [4,5,6]. Due to ISO standards and the use of practical models, we have a possibility to solve many everyday problems we face, from global management of water resources to improvement of food safety. It is a notorious fact that the application of ISO 9001 standard is voluntary, but companies are well aware of the importance of having a certificate of successful implementation of this standard. Unfortunately, examples of possessing this certificate just as a formality can always be found because the standard has not been properly implemented, hence, there are no appropriate effects resulting thereof. Therefore, it is necessary for all the employees, particularly the top management, to comprehend the significance of all principles, instructions and requirements of quality management system [5]. Application of the basic ISO 9001 standard is only the beginning. It is desirable for a company to implement other international standards as well, particularly those aiming at environmental protection [4,7]. The implementation of IMS ensures a more efficient realization of set goals and business activities for employers and employees, especially those related to quality (quality management system (QMS)), environmental protection (environmental management system (EMS)), safety and health at work (Occupational Health & Safety OHSAS), risk analysis, critical points control, etc. (HCCP– Hazard analysis and Critical Control Point) [1]. Integrated management system implies permanent quality advancement in business in order to achieve business excellence of a modern organization.

RESEARCH METHODOLOGY

Problem and subject of research

It is a well–known fact that some companies do not possess the ISO certificate; on the other hand, some companies possess it, but just as a formality because the standard has not been properly implemented, and therefore there are no appropriate effects resulting from it. Also, the level of employees' awareness of the importance of implementing various standards is not enviable. In order to verify the veracity of these claims, a survey was conducted, and the subject of the survey were companies from various production activities (glass processing, automotive industry, household chemicals, cosmetics, etc.), as well as from an agency in

the field of providing certification and consulting services.

Research objective

The goal of the investigation was to determine the importance of the implementation of IMS. The obtained results of the investigation indicated the level of awareness of the employees regarding the following: the importance of application of various standards, fulfilment of requirements of different regulations, importance of establishment of quality policy which ensures further definition of quality objectives, re–examination and the method which may be used to improve the quality and environmental policy which should comply with the mission and vision of the company. This investigation shows the real mindset of the employees regarding fulfilment of the requirements of the implemented standards as well as their desire and awareness of possible improvements in effectiveness of the integrated management system.

Research instrument

The employees were asked to fill out the survey containing the questions formulated in such a way so that no confidential information is disclosed while at the same time respondents give responses to the questions within given topics.

Research questions

Questions are formulated to obtain information about the number and type of implemented standards, benefits and improvements observed in the production processes upon their implementation, about advancement in environmental protection, realization of internal and external audits/controls, as well as about the awareness of employees of certain implemented standards in companies which perform various kinds of activities.

Research sample

The survey was conducted in several companies in different industries. The target group were the employees whose positions include an active or passive participation in implementation of various standards. In case the positions of respondents were not directly related to management of standards, the condition was that they were familiarized with the details of the manner in which IMS is implemented in the company they work for.

RESULTS AND DISCUSSION

The survey comprised the total of 30 respondents from 12 different sectors. Most of respondents were from glass production and glass processing – 10 of them from different division so that a wide range of answers could be given from multiple point of view with a valid outcome in compliance with the intention of the survey investigator. There were 4 respondents from automotive industry, 3 respondents from each certification services and consulting services and 3 respondents from both household chemicals and cosmetic product manufacturers. Fewer respondents were from technical examination and analysis as well as from food industry, while the fewest were the respondents from agricultural production, distillation equipment production, road reconstruction, non–metal production, utility services and machine metal processing.

Most of respondents were from quality assurance departments, seven of them, followed by six respondents employed in human resources departments among whom were employees responsible for safety at work and environmental protection. There were 5 respondents from maintenance departments and 3 process engineers, while 3 chemical and cosmetic technologists also took part in the survey. The same number of employees responsible for the certification of ISO standards as technologists took part in the survey and also one respondent from each information technology and logistics and one project manager.

To the question as to which of ISO standards were implemented in their company, most respondents answered ISO 9001, which is shown in Figure 1.

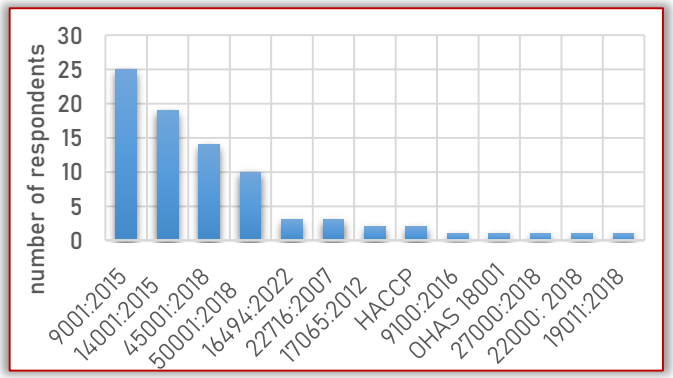

Figure 1. ISO standards share in analysed companies

The work tasks of the respondents from quality assurance departments are mainly related to ISO standard 9001:2015 and they are the most numerous; human resources departments mostly deal with standards focused on environmental issues (ISO 14001:2015 and ISO 45001:2018), while the respondents working in maintenance departments or engineers mostly deal with 50001:2018 standard related to energy

management. The work tasks and duties of the respondents within ISO standards are mostly related to implementation of standards and quality or system advancement which involve monitoring as well. Fewer respondents are in charge of documents presentation to auditors, while seven respondents perform the duties of internal controller once or twice a year (Fig.2).

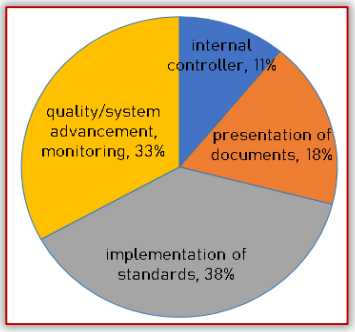

Figure 2. Type of work at the position related to ISO standard

When responding to the question as to whether they thought that the implementation of certain ISO standards could provide benefits to the company, the respondents were asked to give at least two benefits if their answer was positive. Most respondents cited advancement in the business system, which mainly comprised quality, organization of work, comprehensive view of documentation and efficiency (67%). As shown in Figure 3, 18% or 11 respondents agreed that implementation of ISO standards affected the company reputation. Less than 10% of respondents believed that the implementation could result in other benefits such as: consumer confidentiality, expenses reduction, increased product value and rise in employees' awareness, which were all legitimate and accurate answers.

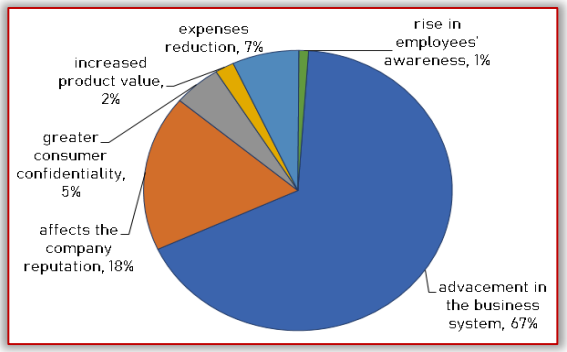

Figure 3. Possible positive benefits of ISO standards implementation

The next question was about the perceived improvements in the production process due to the implementation of ISO standards related to product quality. The respondents mentioned several improvements in the quality of the products which they believed were made due to the implementation of ISO standards; however, they underlined that the greatest effect could be perceived in advancement of the product traceability, from the point where the material entered the manufacturing, until the point where the finished product left the company. One respondent from each group answered that the implementation of standards could also affect the increase in production capacity as well as more qualitative services offered to customers.

The respondents from the companies which had applied ISO 14001 standard noticed a lot of benefits (Figure 4). However, a lot of respondents, 10 of them, admitted that ISO 14001 standard had not been applied in their companies, which makes up 33.33% of the total number of respondents.

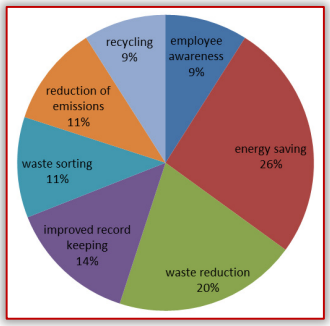

Figure 4. Perceived benefits of application of ISO 14001 standard

Accordingly, the percentages were calculated and presented based on the answers of the remaining 20 respondents who mentioned at least two benefits which they considered derived from the implementation of this standard. Most respondents said that the implementation of the standards focused on environmental issues could contribute to energy saving and reduction of waste. To the question as to which sectors should apply ISO 14001 standard, about 70% of respondents named a large number of companies which, owing to the fact that they are manufacturing companies, generated waste and were considered big or small polluters. Nevertheless, other respondents were resolute regarding industry or sector which should implement this standard. As one reason for the implementation of ISO standards they cited environmental protection and safety of all those found in the work or life environment. Although 10 respondents did not have ISO 14001 standard implemented in their companies, all of them answered this question, which undoubtedly shows that there is awareness of the need to apply this standard. However, two respondents answered that no sector should implement this standard without stating any reason for their opinion.

As much as 97% of respondents said that internal and external audits/controls of ISO standards were performed in the companies they worked for, while only 3% of them answered negatively to this question. In most cases audits were performed once a year as per answers of two thirds of respondents (Figure 5).

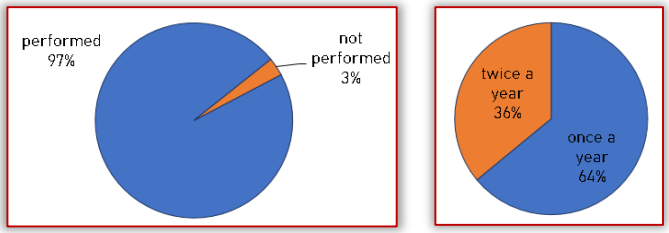

Figure 5. Are controls/audits conducted and how many times per year?

Is it important for all employees in the company to be informed that the company has ISO standards implemented or only those employees whose tasks are related to ISO standards? – this was the question which followed. The majority of respondents, 90% of them said that all employees should be informed, while the rest of them thought that only those employees whose tasks were related to ISO standards should be informed. One part of respondents said that not more than 30% of their co–workers were informed about the implementation of the standards in their company; the other part of respondents thought that this number was somewhere between 51% and 70% of their colleagues, while the largest number of respondents believed that 71–100% of their colleagues were informed about the standards. Although a larger number of respondents was of that opinion, a part of them also said that their colleagues were ill–informed about the manner in which the standard was implemented. Two respondents could not give their opinion about this question.

Finally, the last question in the survey was hypothetical: if they were the owners of the company they worked for, whether they would initiate implementation of ISO standards. There were 97% of positive answers although a part of respondents was not entirely familiarized with those standards which were not implemented in their company or the standards were not related to their assigned tasks. Only one respondent was not interested in application of standards in "his company" if he was to assume the role of a manager or owner.

CONCLUSION

After a detailed consideration of the respondents' answers and the analysis of IMS functioning in different companies, it can be concluded that it is necessary for every production to implement at least one ISO standard so it could be competitive in the market. Although the majority of respondents hold positions related to ISO standard 9001 in the quality assurance departments, 90% of them do not consider ISO 14001 standard less important and believe that it should be implemented in all sectors considered bigger or smaller polluters. The majority of respondents agree that the implementation of the standards may considerably contribute to the company's reputation and advancement of the business system, while the employer has a duty to recognize and realize this need. The answers offer the conclusion that the respondents are well aware of the need to implement ISO standards, although entrepreneurs must be continuously informed about the quality, IMS, business excellence and the similar.

References

[1] Đorđević, D., Bogetić, S., Primena integrisanih menadžment sistema u malim i srednjim preduzećima, Industrija 4, pp. 95–107, 2007.
[2] Rajković, D., Integrisani sistemi menadžmenta u malim i srednjim preduzećima, doktorska disertacija, Univerzitet u Kragujevcu, Mašinski fakultet u Kragujevcu, Kragujevac, 2010.
[3] Internet source: ISO website: https://iso.org.rs/iso–medunardna–organizacija–za–standardizaciju/
[4] Živković, N., Integrisani sistemi menadžmenta, Fakultet organizacionih nauka univerziteta u Beograd, 2012.
[5] Babić, J., Značaj primene međunarodnih ISO standarda za upravljanje preduzećem i obezbeđivanje satisfakcije potrošača, Marketing, pp. 180–188, 2011.
[6] Milutinović, D., Upravljanje totalnim kvalitetom kao osnova modela poslovne izvrsnosti savremene organizacije – isustva apotekarskih organizacija u republici Srbiji, doktorska disertacija, Univerzitet Edukons, Fakultet poslovne ekonomije, Sremska Kamenica 2016.
[7] Oruc, M., Muhamedagić, S., Borić, J., Agić, D., Značaj i promene standard ISO 14001, 10. Naučno–stručni skup sa međunarodnim učešćem "QUALITY 2017", Neum, 2017.

Note: This paper was presented at IIZS 2023 – The XIII International Conference on Industrial Engineering and Environmental Protection, organized by Department of Mechanical Engineering and Department of Environmental Protection of the Technical Faculty "Mihajlo Pupin" Zrenjanin, from the University of Novi Sad, in cooperation with partners – University Politehnica Timisoara, Faculty of Engineering, Hunedoara (ROMANIA), University "St. Kliment Ohridski", Technical Faculty, Bitola (MACEDONIA), "Aurel Vlaicu" University of Arad, Faculty Of Engineering, Arad (ROMANIA), University of East Sarajevo, Faculty of Mechanical Engineering East Sarajevo, Sarajevo (BOSNIA & HERZEGOVINA) and University of Giresun, Faculty of Engineering, Giresun (TURKEY) – in Zrenjanin, SERBIA, in 05–06 October, 2023.

ISSN: 2067–3809

ACTA TECHNICA CORVINIENSIS – Bulletin of Engineering | e–ISSN: 2067 – 3809
Tome XVII [2024] | Fascicule 2 [April – June]

[1.]Solomon Idowu ADEDOKUN, [2.]Johnson Rotimi OLUREMI, [3.] Adetunji Abiodun ADEROJU

EFFECTS OF SYNTHETIC HAIR FIBRE ON THE STRENGTH AND MICROSTRUCTURAL PROPERTIES OF CONCRETE

[1.]Department of Civil Engineering & Environmental Engineering, University of Lagos, Lagos, NIGERIA
[2,3.]Department of Civil Engineering, Ladoke Akintola University of Technology, Ogbomoso, NIGERIA

Abstract: As the use of synthetic hair fibre (SHF) is increasing globally, the rate of hair fibre waste generated is also quite high thereby resulting into environmental pollution. In this study, the effect of SHF waste on the strength and microstructural properties of concrete was investigated. SHF concrete containing the mixture of different percentages of SHF (1, 2, 3 and 4% by weight of cement) were cast using 1:2:4 concrete mix ratio and cured for maximum of 28days to determine the compressive, split tensile and flexural strengths. Scanning Electron Microscopic test was used to examine the micro structural features of SHF concrete. Findings from the study showed that compressive, split tensile and flexural strengths of the concrete reached the optimum value at 2% SHF addition. The SEM test result for the micro structural features of SHF concrete shows reduction in cracks as 2% SHF content. The study therefore revealed that SHF addition to concrete improved the strength and microstructural properties of the concrete. Two (2%) inclusion of the synthetic hair fibre by weight of cement is hereby recommended for the enhancement of the concrete properties.
Keywords: synthetic hair fibre waste; compressive strength; flexural strength; split tensile; microstructural feature

INTRODUCTION

Hairs are considered as waste materials in many parts of the world and it is found in municipal waste streams causing serious environmental problems. They are alternate non–degradable matter that are available in abundance at a little or no cost, and can be used as fibre materials in concrete as a result of its high strength in tension which is equal to that of a copper wire with similar diameter (Ganiron, 2014; Adedokun *et al*., 2016).

Due to non–biodegradable nature of the hair, they can only be disposed of in an economical way by consigning them to landfill and as such they are relatively environmentally unfriendly (Li, 1998; Ganiron, 2014). There is need to effectively utilize these hair fibres in an economical and environmentally friendly ways, and one of such ways is to incorporate them into the concrete as admixtures. In addition, it is very obvious that concrete is weak in tension and hence some measures must be adopted to overcome this deficiency. A way of overcoming this is by introducing hair fibre, which is strong in tension and readily available in large quantity, into the concrete. They are mainly utilized as fibre reinforcing materials in concrete to examine its impacts on the strength properties and cracking control; in order to reduce concrete production cost and to minimize ecological issues created by hair decomposition (Popescu and Hocker, 2007; Jain and Kothari, 2012; Pawar *et al*, 2015). Gupta (2009) through his study on human hair waste concluded that the hair has a large number of uses in many areas ranging from agriculture to medicine to engineering industries. The exceptional properties of human hair such as its unique chemical composition, slow degradation rate, high tensile strength, thermal insulation, elastic recovery, scaly surface, and unique interactions with water and oils, has led to many diverse uses. Utilization of wastes in the concrete production is an environmentally friendly mean of disposing large amounts of materials that would have constituted pollution to land, water and air (Raheem *et al*., 2017a & b; Raheem et al., 2018; Adedokun *et al*., 2021).

Also, there is increase in environmental pollution as a result of the deposition of hair fibre wastes on lands thereby making them unavailable for good purposes. Hence, this made it imperative to use them for other purposes as in construction work. Hair fiber, a fibre deposit/waste with little or no cost, deposited in its millions of tonnes annually around the world is therefore worthy of study. According to Ganiron (2014), hair fibres are very strong in tension and can be used as fibre reinforcing materials in concrete.

Reinforcing concrete with fibres has been said to be a suitable, pragmatic and economic means of overcoming micro-cracks and other concrete deficiencies (Pawar *et al*, 2015; Nila *et al*, 2015). Existing studies (Shakeel *et al*, 2009; Ahmed *et al*, 2011; Ganiron, 2014) are limited to human hair and their impact on CS but this study extended the work of Adedokun *et al*, 2016, which

investigated the influence of SHF addition on the concrete strength by examining the strength and microstructural properties of SHF-concrete. Since the usage rate of synthetic hair fibre in Nigeria is increasing, the amount of waste produced due to its usage is quite high resulting to environmental pollution. As salon and manicure centres are springing up in almost every shopping complex in Nigeria, huge waste materials generated from these centres are mostly synthetic hairs.

Hence, this research investigated the impact of these synthetic hair fibres on the workability, strength and microstructural properties of concrete, as a means of reducing waste and improving the strength and microstructural properties of the concrete. This study therefore focused on the reuse of these synthetic hair fibres in concrete production.

MATERIALS AND METHOD

Materials

The materials used for this study are synthetic hair fibre, ordinary Portland cement (OPC), fine and coarse aggregates and water.

- **Synthetic hair fibre** – synthetic hair fibre (SHF) was collected from Awotan dumpsite (Figure 1a). Awotan dump site is one of Government approved refuse waste dump site at Ido Local Government Area in Ibadan, Oyo State, Nigeria. Figure 1b shows the section of SHF deposit at Awotan dumpsite.

(a) Section of SHF at the dumpsite; (b) Dumpsite approach view
Figure 1. Used synthetic hair fibre at Awotan dumpsite, Ibadan, Nigeria

- **Aggregates** – Sharp sand and granite chippings (of 12 mm size), which are fine aggregate and coarse aggregate respectively, was used for the casting of the concrete. The aggregates are in compliance with the requirements of BS 882 (1982), they are clean, free from salt and impurities (including organic matters).
- **Cement** – The cement to be used for this experiment is the Ordinary Portland Cement (OPC) of grade 32.5 N/mm^2. The cement satisfies such properties as fineness, and soundness, which means that the cement meets the specification of the ordinary Portland cement (BS 12, 1996) on the above properties. This cement is readily available and it is the most commonly used in the construction industry.
- **Water** – The water used was obtained from the public water supply at Laboratory of the Ministry of Works, Oyo State Secretariat, Ibadan. The water was relatively clean and free from acids, oils, alkalis, suspended solids, organic matters and soil. The water is potable and therefore suitable for use in casting as required by BS 3148 (1980).

Testing methods

The various tests conducted in this study are the mechanical test on various brands of SHF, tests on fresh (slump and compacting factor) and hardened (compressive, split tensile and flexural strengths) concrete produced by incorporating different combinations of SHF. The used synthetic hair fibres were incorporated into the concrete 1, 2, 3 and 4% by weight of cement.

- **Mechanical test on SHF**

Mechanical tests were carried out on different brands of SHF (Laminar weaveon, Ultra Braid, Besta Braid and the sample from dump site) using Universal testing Machine – Testometric to evaluate elongation at yield, elongation at limit of proportionality, force at yield, force at limit of proportionality, stress at different force application and Young's modulus. The sample length used for the test is 100mm.

- **Tests on fresh concrete**

The slump and compacting factor tests was performed on the fresh concrete mixes containing different percentages of the synthetic hair fibre wastes (1, 2, 3 and 4% by weight of cement). These tests were conducted on different concrete mixes in order to examine the influence of SHF contents on the workability of the fresh concrete in accordance to BS 1881: part 103 (1983).

— **Tests on hardened concrete**

Tests were conducted on various hardened concrete (cube, cylindrical and prism) samples at different percentages of SHF to determine the compressive strength, split tensile strength, flexural strength and microstructural properties of the samples.

— **Compressive strength test** – The compressive strength test was carried out on specimens cubical in shape of size 150 x 150 x 150 mm^3. Fresh concrete mixes were cast and placed into the cubical cast iron mould, and were compacted with the tamping bar on layers. After 24 hours the concrete specimens were removed from the moulds and immediately submerged in clean fresh water. After days (7, 14, 21 and 28 days) of curing the specimens were tested under the load in a compression testing machine.

— **Split tensile strength** – The ASTM test method was used for the determination of the split tensile strength of cylindrical concrete specimens. This method consists of applying a compressive force along the length of a cylindrical specimen. This loading induces tensile stresses on the plane containing the applied load. Tensile failure occurs rather than compressive failure. Plywood strips were used so that the load could be applied uniformly along the length of the cylinder. The maximum load (*P*) at failure was divided by appropriate geometrical factors to obtain the splitting tensile strength (f_{st}) as shown in equation 1.

$$f_{st} = \frac{2P}{\pi lD} \quad (1)$$

where l = height of cylindrical specimen (300 mm) and D = diameter of cylindrical specimen (150 mm)

— **Flexural strength** – Third–point loading method was used in finding out the loading system of flexural tension. Fresh concrete mixes were cast and placed into the cylindrical cast iron mould, and were compacted with the tamping bar on layers. After 24 hours the specimens were removed from the moulds and immediately submerged in clean fresh water. After days (7, 14, 21 and 28 days) of curing the specimens were tested under the load in a compression testing machine. Then the load (*p*) was applied at a constant rate of 400 kg/min. The flexural strength (*F*) was determined as shown in equation 2.

$$\text{Flexural strength, } F = \frac{pl_e}{bd^2} \quad (2)$$

where l_e = effective span of the beam, b = breadth of the beam and d = beam depth

— **Microstructural analysis** – The microstructural properties of the hardened concrete samples containing various percentages of synthetic hair fibre, SHF (1, 2, 3 and 4% by weight of cement) were determined using Scanning Electron Microscopy (SEM). Images of the concrete samples were produced by scanning the surface of sample with a focused beam of electrons. Samples of SHF–Concrete of 0% SHF, 2% SHF and 4% SHF Concrete were investigated using SEM.

— **Statistical analysis** – The experimental results (CS, STS and FS) of the hardened concrete samples containing various percentages of SHF (1, 2, 3 and 4% by weight of cement) were subjected to statistical analysis using 2–way ANOVA without replication. These analyses were conducted to evaluate the statistical significance of SHF and curing days on the strength properties of the SHF–concrete

RESULTS AND DISCUSSION

Mechanical properties of synthetic hair fibre

The results of the mechanical tests conducted on different brands of synthetic hair fibre together with the blend of all the brands (those obtained from the dump site) are presented in Table 1.

Table 1. Mechanical properties of synthetic hair fibre

Synthetic Fibre Type	Elongation (mm)	Stress (N/mm^2)	Young Modulus (N/mm^2)	Strain
Larimar weavon (Black)	19.848	2.971	15.01	0.198
Ultra Braid (Brown)	6.053	1.324	21.70	0.061
Besta Braid (Purple)	31.890	2.937	9.21	0.319
Blend	14.629	4.040	27.67	0.146

From this table, it was observed from the mechanical properties of synthetic hair fibre of different brands and mixture (sample from the dump site) that under the application of force, Ultra braid (brown) gave the lowest elongation and strain values while Besta braid (purple) undergo the highest elongation and strain indicating that Ultra Braid was the toughest and strongest.

Although, Besta braid is quite elastic, it can be stretched beyond 300% of its original length without breaking while Ultra Braid cannot extend beyond 70% of its original length. This implies that Besta braid is highly ductile, while Ultra Braid has low ductivity. Moreover, it was found that the Young Modulus of the Blend (that is, the mixture from dump site) was the highest.

Hence, the usage of the SHF from the dump site is worthwhile as it will combine all the characteristics of the Synthetic Hair Fibre brands,

and its application will reduce its rate of dumping and accumulation at the dump site, thereby minimizing the environmental pollution and ecological issues associated SHF usage in the surrounding.

Workability of fresh concrete

Workability of the fresh synthetic hair fibre concrete was investigated using slump and compacting factor tests as shown in Table 2. For slump tests, the results showed that the slump value increased from 19 to 38 mm as the percentage of the hair fibre content increased from 1 to 4%, respectively. However, the slump value for the control sample (0% synthetic hair fibre) was 18 mm. This shows that addition of SHF increased the slump of the concrete.

The concrete became more workable as the percentage of SHF increased. That is, the higher the slump, the higher the workability. This could be attributed to presence of the oil in the used synthetic hair fibre. Similarly, the results of the compacting factor increased from 0.846 for 0% SHF concrete mix to 0.968 for 4% SHF mix. This also showed that compacting factor increased with increasing SHF content, indicating an increase in workability of the concrete with the addition of Synthetic hair fibre.

Table 2: Effects of the used synthetic hair fibre on workability (slump and compacting factor) of the concrete

Tests	Percentage of SHF (%)				
	0	1	2	3	4
Slump	18.0	19.0	20.0	25.0	26.0
Compacting factor	0.846	0.852	0.880	0.862	0.899

Compressive strength

Figure 2 presents the influence of synthetic hair fibre (SHF) and curing age on the compressive strength of concrete. The compressive strength for concrete samples containing 1% SHF showed higher values at 7 and 14 curing days than the control concrete samples (0% SHF) but were lower than the control at 21 and 28 curing days. For 2% SHF addition, compressive strengths were significantly higher than those of the control and 1% SHF samples at each of the curing periods. However, the values of the compressive strength for concrete samples containing 3% and 4% SHF were lower than those of the control and 2% SHF samples. This is an indication that the optimum value of the compressive strength is reached at 2% SHF addition.

This finding is also in agreement with the conclusion of the previous studies by Adedokun *et al*. (2016), while Jain and Kothain (2012) and Sreevani and Ajitha (2017) reported the optimum compressive strength at 1.5% addition of human hair, even though these studies did not test the impact of human hair on concrete beyond 1.5% (by weight of cement). In addition, the compressive strength of 29.28N/mm^2 obtained for sample with 2% SHF content (by weight of cement) satisfied the minimum compressive strength of 26 N/mm^2 at 28 days recommended by NIS 439 (2000).

For different curing ages, the results showed that the compressive strength increased as the curing period increased. These results clearly showed that 2% addition of synthetic hair fibre to concrete would not only lead to enhancement in compressive strength but also can lead to a very significant reduction in the environmental pollution and ecological issues resulting from the accumulation of synthetic hair fibre in the surrounding.

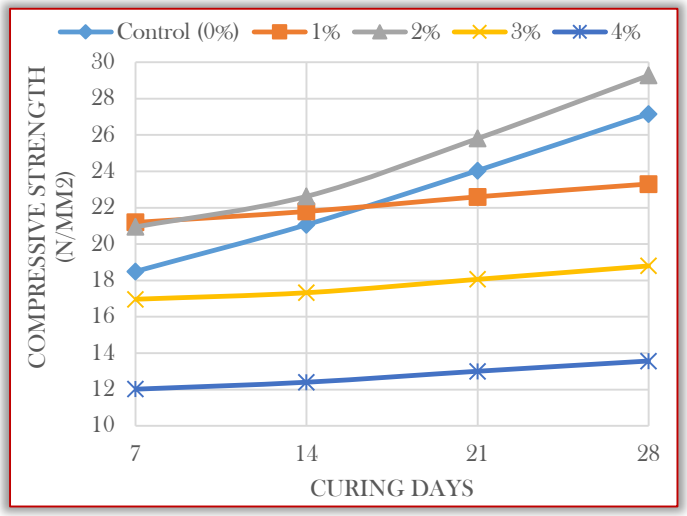

Figure 2. Influence of synthetic hair fibre and curing days on compressive strength of concrete

Table 3 presents the results of the statistical test carried out on the impact of SHF and curing days on the CS of the SHF–concrete using ANOVA at 5% level of significance. From the Table, the p–values are 1.19e–6 and 0.005282 for the SHF and curing day, respectively.

Table 3: Impact of SHF and curing days on CS of concrete

Source of variation	Sum of squares	Degree of freedom	Mean square	*Fcal*	*P–value*	*Fcrit*	Remark
SHF	382.9229	4	95.730	36.84	1.19E–06	3.259	Significant
Curing day	55.5005	3	18.500	7.119	0.005282	3.490	Significant
Error	31.181	12	2.598				
Total	469.6049	19					

The p–value for the SHF is much lower than the adopted 0.05 level of significance. Whereas, for curing day, the value is approximately equal to the adopted level of significance.

In addition, the variance ratio after treatment, Fcal, is 36.84132 (greater than the stipulated ratio of variance, Fcrit of 3.259167) and 7.119663 (>Fcrit of 3.490295).

These two conditions clearly showed that both the SHF and curing day have a statistically significant impact on the CS of concrete, however, the influence of the SHF is much more significant than that of the curing day.

Split tensile strength

The impact of the synthetic hair fibre and curing age on the split tensile strength of the concrete is presented in Figure 3. The split tensile strength for concrete samples containing 1% SHF were higher at 7 and 14 curing days as compared to those of the control concrete samples but were lower than the control at 21 and 28 curing days.

For 2% SHF addition, the tensile strengths were much higher than those of the control and 1% SHF samples at each of the curing periods. However, the values of the tensile strength for concrete samples containing 3% and 4% SHF were lower than those of the control and 2% SHF samples, and this showed the optimum value of the split tensile strength at 2% SHF addition. For different curing ages, the results showed that the split tensile strength increased as the curing period increased.

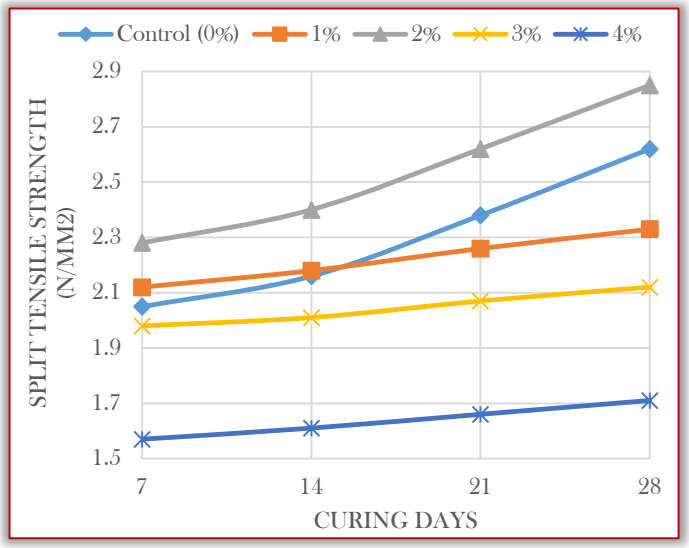

Figure 3. Influence of synthetic hair fibre and curing days on split tensile strength of concrete

Table 4: Impact of SHF and curing days on STS of concrete

Source of variation	Sum of squares	Degree of freedom	Mean square	Fcal	P–value	Fcrit	Remark
SHF	1.809	4	0.4523	45.499	3.71E–07	3.259	Significant
Curing day	0.309	3	0.1031	10.370	0.00119	3.490	Significant
Error	0.119	12	0.0099				
Total	2.237	19					

Table 4 shows the results of the statistical test conducted on the STS of the SHF–concrete to evaluate the impact of SHF and curing day on the STS of SHF–concrete using ANOVA at a 5% level of significance.

The findings from the statistical analysis revealed that the SHF (p–value = 3.71E–07 < 0.05) and curing day (p–value = 0.00119 < 0.05) have statistically significant effects on the STS of the SHF–concrete. However, the lower p–value (3.71E–07) of the SHF than that of curing day (0.00119) is an indication of the greater impact of SHF on STS compared to that curing age.

Flexural strength

Figure 4 shows the influence of the synthetic hair fibre and days of curing on the flexural strength of the SHF concrete. Results from the figure showed higher values of the flexural strength for 1% and 2% SHF concrete samples than those of the control sample (conventional concrete) at all the curing ages, meanwhile the flexural strength for 3% SHF concrete were quite similar to those of the conventional concrete. However, the flexural strength obtained for 4% SHF concrete samples were lower than those of the control samples. Similar to the results of compressive and split tensile strengths, the optimum value of the flexural strength is observed at 2% SHF addition. This finding is also in line with those of Adedokun *et al*. (2016). For different curing ages, the results showed that the compressive strength increased as the curing period increased.

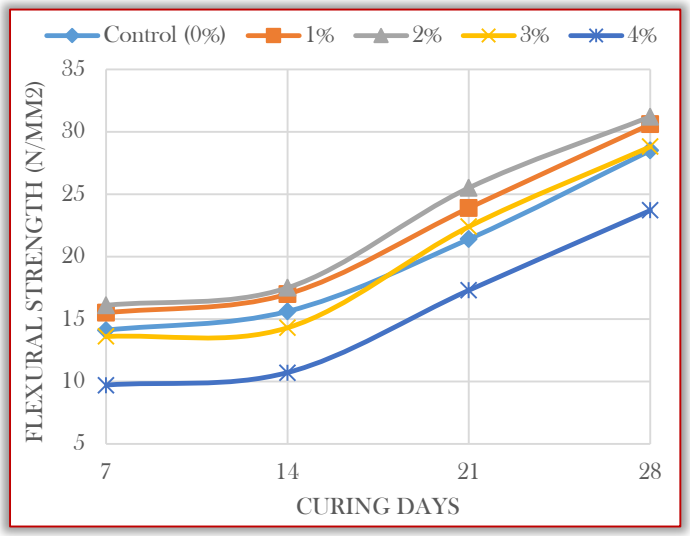

Figure 4. Influence of synthetic hair fibre and curing days on flexural strength of concrete

Table 5 displays the results of the statistical test carried out on the impact of SHF and curing days on the FS of the SHF–concrete using ANOVA at 5% level of significance. The results from the Table that the p–values for SHF and curing day are 7.12E–10 and 1.07E–14, respectively. The p–values

are significantly lower than the adopted 0.05 level of significance. However, unlike the trends observed in CS and STS, the p–value for curing age in FS is lower than that of the SHF, indicating much more influence of curing age on FS than the SHF.

In addition, the Fcal = 135.4133 (>Fcrit = 3.259167) for SHF and Fcal = 1015.913 (> Fcrit = 3.490295) for curing day also confirm that both the SHF and curing day have a significant impact on the FS but the influence of curing day is more significant compared to SHF. Generally, these results clearly showed that both SHF and curing day have a statistically significant impact on the strength properties of the concrete.

Table 5: Impact of SHF and curing days on FS of concrete

Source of variation	Sum of squares	Degree of freedom	Mean square	Fcal	P–value	Fcrit	Remark
SHF	1.251	4	0.312	135.413	7.12E–10	3.259	Significant
Curing day	7.042	3	2.347	1015.913	1.07E–14	3.490	Significant
Error	0.02773	12	0.0023				
Total	8.32222	19					

Microstructural properties

Based on the trend of the results, scanning electron microscopies were conducted for the control sample (without SHF), samples with 2% SHF (optimum result) and 4% SHF (lowest result). From the scanning electron micrograph of concrete without or with hair fibre, the yellow dimension line at the top indicates current ruler size depending on the magnification factor. While the red dimension value represent the field of view which is the magnification.

Figure 5 shows the scanning electron micrograph of concrete with 0% addition Synthetic Hair (control sample). From Figure 5 it was observed from the micro graph that micro cracks were present within the concrete composition. This implied that series of infiltration through the cracks can cause weakness in between the concrete elements with time.

Furthermore, figure 6 presents the result of the scanning electron micrograph of concrete containing 2% Synthetic hair fibre addition.

The micrographs shown in Figure 6 revealed the concrete with 2% synthetic hair fibre where the fibre content was more than 1% by weight of cement. In the figure, the SHF added was found to anchor more concrete components (i.e the fine and coarse aggregates) and this could enhance more strength/bond within the concrete components unlike the sample with no SHF and therefore bridging the micro cracks, delaying crack formation and propagation. In other words, the presence of more synthetic hair fibre enhanced the bonding effect of the concrete elements, and therefore making the infinitesimal or micro cracks to be more strongly bonded.

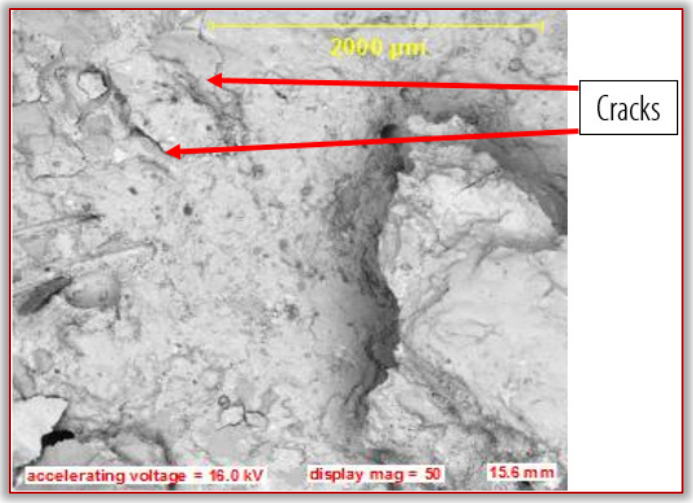

Figure 5: SEM micrograph of concrete with 0% addition of SHF

Figure 6: SEM micrograph of concrete with 2% addition of SHF

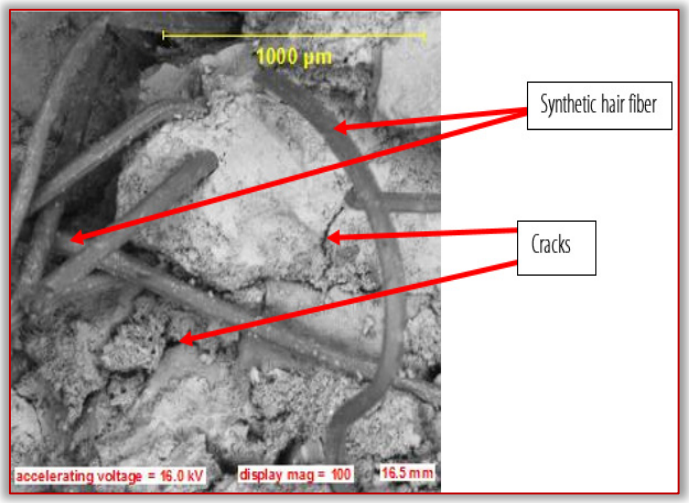

Figure 7: SEM micrograph of concrete with 4% addition of SHF

The image in Figure 7 shows the scanning electron micrograph of concrete containing 4% Synthetic hair fibre addition.

The micrographs indicate concrete containing large volume of the synthetic hair fibres which are not homogenously mixed with the concrete elements. In other words, the components were observed to be too rowdy and larger proportions of the SHF were separated from the other concrete components. This could therefore lead to the formation of a very weak bonding within the concrete components, resulting into decreased concrete properties.

CONCLUSIONS

Based on the results of the study which investigated the impacts of synthetic hair fibre (SHF) on the strength and microstructural properties of concrete, the followings conclusions were drawn.

- The results of the investigation showed that synthetic hair fibre had significant effects on workability, strength and microstructural properties of concrete.
- The slump value of the concrete increased from 19 to 38 mm while the compacting factor value increased from 0.846 to 0.968 as the synthetic hair fibre increased from 0 to 4%, respectively. The two tests indicated that the concrete became more workable as the quantity of synthetic hair fibre in the concrete increased.
- The investigation further revealed that the addition of SHF caused increment in the strength properties of the concrete. The compressive strength, tensile strength and the flexural strength increased with increased synthetic hair fibre (SHF) content from 0 to 2% but decreased beyond this value. This implied that the optimum compressive, split tensile and flexural strength in concrete were achieved with 2% addition of SHF.
- The Scanning Electron microscope test revealed that the addition of the SHF contents in the concrete will reduce the permeability of concrete and thus reduce bleeding of water. It will also control cracking due to both plastic shrinkage and drying shrinkage and moreover, the fineness of the fibres allows them to reinforce the mortar fraction/elements of the concrete thereby controlling crack formation and propagation.
- A 2% addition of synthetic hair fibre (SHF) by weight of cement is therefore recommended generally for improving the workability, compressive strength, tensile strength and flexural strength of concrete. The concrete produced with this fibre can be utilized as light weight concrete with improved strength and durability. Moreover, the usage of SHF with concrete will consequently, reduce the environmental pollution of its deposition effects globally since the blend and other brands investigated behaved generally the same.

References

[1] Adedokun S. I., Ajamu, S. O. & Aderinto, H. T. Effect of Synthetic Hair Fibre Additions on the Strength Characteristics of Concrete, USEP: Journal of Research Information in Civil Engineering, 13 (2): 928–939, 2016.

[2] Adedokun, S.I., Anifowose, M.A., Odeyemi, S.O. & Oluremi, J.R.. Significant Levels of Steel Slag Concrete Produced with Varying Water Cement Ratios, Journal of Engineering Studies and Research, 27 (1): 13–20, 2021.

[3] Ahmed, S., Ghani, F. & Hasan, M. Use of Waste Human Hair as Fibre Reinforcement in Concrete, IEL Journal, 91: 43–51, 2011.

[4] BS 12. Portland cement (ordinary and rapid hardening). British Standard Institution, London, 1996.

[5] BS 882. Specification for Aggregates from Natural Sources for Concrete. British Standards Institution, London, 1992.

[6] BS 1881. Method for determination of Slump, British Standard Institution, London, 1983.

[7] BS 3148. Methods of Test for Water for Making Concrete. British Standard Institution, London, 1980.

[8] Ganiron, T. U. Effects of Human Hair Additives in Compressive Strength of Asphalt Cement Mixture, International Journal of Advanced Science and Technology, 67: 11– 22, 2014.

[9] Gupta A. Human Hair "Waste" and Its Utilization: Gaps and Possibilities, International Journal of Refractory Metals & Hard Materials, 27: 892–899, 2009.

[10] Jain, D. & Kothari, A. Hair Fibre Reinforced Concrete, Research Journal of Recent Sciences, 1: 128–133, 2012

[11] Li, G. Experimental Study of Cement – Asphat Mortar Emulsion Composite, Cement and Concrete Research, 28 (5): 635–640, 1998.

[12] Nila, V. M., Raijan, K. J., Susmitha, A., Riya, B. M. & Neena, R. D. Hair Fibre Reinforced Concrete, International Journal of Advent Technology, Special Issue, pg. 60–67, 2015.

[13] NIS 439. Standard for cement, Standards Organization of Nigeria, 2000.

[14] Pawar, L. B., Bhirud, Y. L. & Yeole, P. M. Effect of Natural and Artificial Fiber on Concrete, International Journal of Modern Trends in Engineering and Research, 2 (7): 594 – 597, 2015

[15] Popescu C. & Hocker H. Hair the most sophisticated biological composite material, Chemical Society Reviews, 37 (8): 1282–1291, 2007.

[16] Raheem, A.A., Adedokun, S.I., Adeyinka, E.A. & Adewole, B.V. Application of Corn Stalk Ash as Partial Replacement for Cement in the Production of Interlocking Paving Stones, International Journal of Engineering Research in Africa, 30: 85–93, 2017a.

[17] Raheem, A.A., Adedokun, S.I., Ajayi, B.R., Adedoyin, O.A & Adegboyega, B.O. Application of Saw Dust Ash as Partial Replacement for Cement in the

Production of Interlocking Paving Stones, International Journal of Sustainable Construction Engineering and Technology, 8(1): 1–11, 2017b.

[18] Raheem, A.A., Adedokun, S.I., Ajayi, B.R., Adedoyin, O.A & Adegboyega, B.O. Application of Corn Hust Ash as Partial Replacement for Cement in the Production of Interlocking Paving Stones, LAUTECH Journal of Civil and Environmental Studies, LAUTECH, Ogbomoso, 1(1): 14–20, 2018.

[19] Sreevani, G. & Ajitha, S.B. Human hair as fibre reinforcement in concrete, International Journal of Engineering Science and Computing, 7 (5): 11358–11364, 2017.

[20] Shakeel, A. Farrukh, G. J., Akhthar, N. & Hasan, M. Use of Waste Human Hair as Fibre Reinforcement in Concrete, International Symposium on innovation and sustainability of structures in Civil Engineering, Guangzhou, China, 2009.

ISSN: 2067–3809

ACTA TECHNICA CORVINIENSIS – Bulletin of Engineering | e–ISSN: 2067 – 3809
Tome XVII [2024] | Fascicule 2 [April – June]

[1.]Mohamed ABDELAZIZ, [2.]Hesham ELKHATIB, [2.]Abdelfatah ABDELMAKSOUD, [2.]Loula A. SHOUMAN

A NEW PROPOSAL FOR THE DESIGN AND MODELING OF PASSIVE SPENT FUEL AUXILIARY POOL COOLING SYSTEM

[1.]Department of Nuclear Safety Research and Radiological Emergencies, Egyptian Atomic Energy Authority, Cairo, EGYPT
[2.]Reactors Department, Nuclear research center, EGYPTIAN Atomic Energy Authority–Cairo, EGYPT

Abstract: Spent nuclear fuel at the spent fuel storage in the research reactors must be in the safe temperature conditions. Utilizing heat–pipe as stand–by cooling system is a suitable method to remove heat generated from the fuel at the storage in the reactors, which considered the second grade of the passive systems from four grads scale. Heat–pipes are considered as passive heat transfer appliances which, when well designed and fabricated, have very long live spans when operating with in temperature limits. In This article, a theoretical that new design and completely passive cooling system using gravity assisted closed two–phase heat–pipe for dissipation the heat from the nuclear reactor spent fuel pool by running as alternative cooling system to be in safe mode. The model considers natural convection by air for the condenser section of the heat–pipe to confine the residual heat. Focus on heat–pipe configuration effect, evaporator and condenser lengths ranges (75, 100, 125 and 150m) and outer diameter ranges was (15, 20 and 25 cm) with 3mm thickness at heat load 150 kW and full filing ratio at evaporator section and ambient air temperature at 30°C, a numerical simulation using a new design of gravity assisted heat–pipe loops was used to investigate the heat–pipe thermal characteristics and performance will analysed. The heat–pipe material is stainless steel and demineralized water was used as the running working fluid. The observation from the results showed that the best performance and thermal characteristics were obtained at a higher heat–pipe length and diameter that the heat pipe could remove 150kW with safe conditions. The computer simulation can then be used to predict the concepts of heat transfer with different inputs

Keywords: safe temperature conditions, passive systems, heat–pipe as stand–by cooling system

INTRODUCTION

Multi–purposes reactors (MPR) after shutdown have residual heat. Accordingly, in case of emergency and after nuclear reactor shut down, heat should be removed to keep fuel temperature within safe limit. Also, MPR have an auxiliary spent fuel tank that should be cooled also to remove the heat generated. In this direction, heat–pipes are suggested to be inactive heat energy transport systems. With appropriate design and made–up, they are considered to be expatriate sealed tubes which have very long lives.

A completely passive cooling system implementing loop heat pipe for cooling and dissipating the nuclear reactor's residual heat is suggest in the current study. The most important parameters that determine if the public will accept nuclear reactors plant are safety features. The only thing which public can imagine is destruction or radioactive hazards on human health whenever they heard about the word nuclear [1].

Safety regulations have been developed, matured, and implemented in the last decades in a very restricted way. Consequently, the accidents risk in nuclear power facilities is declining [2]. There are three serious accidents only at nuclear power plants over 16,210 cumulative reactor of commercial runs in 33 countries: No adverse health or environmental consequences occurred in the Three Mile Island (USA 1979) in which the reactor was completely destroyed.

Significant environmental and healthiness consequences happened in Chernobyl (Ukraine 1986), where the vapor bang and bonfire destruction of the reactor. Since then, the deaths have increased to 56 after 31 people are killed. Fukushima (Japan 2011) where three reactors from a fourth were suffering from the effects of cooling losses because of a huge tsunami. Only the emission due to accidents in Chernobyl and Fukushima leaded to larger hazardous for the community than those face from contact to other sources [3].

The design of nuclear power stations are directed to be in safe hands in functioning situations and secure in case of any fail or scourge. Possible accidents guide to progressive safety enhancements. Mainly current power reactors use a mixture of intrinsic safety characters and engineered safety systems that can be active or passive [4].

Because of the unbalancing between passive and active safety systems, the three previous mentioned nuclear reactors accidents were occurred [5]. Using passive component system and/or the lack of human action step down power failure. Safety will increase in direct proportion with increasing passive safety systems. Thus, passive systems will improve the overall

factor of safety for the Nuclear power plant [6]. The term Passive Safety is not equivalent with the deep–rooted safety because it remains subject to other faults such as structure, mechanical failure and/or human interference. Regardless of that, we will concentrate on the passive safety, since our work is mainly about the usage of heat–pipe for nuclear safety which is a Passive system from grade B [7]. Passive systems must obey some conditions to be accepted: Reliability and availability in short terms, long terms, and under retrograde conditions [8].The accident at the Daiichi nuclear plant proposed reducing credence on active systems to reduce human error factor.

Passive systems types are classified to different categories: Grade A, B, C and D Grade B: no signal input, external power source, no moving mechanical parts but moving working fluids.[9] and [10]. Gravity assisted two–phase, closed heat pipe loops are sealed inactive two–phase heat transfer devices that make use of the highly efficient evaporator and condensation thermal transfer procedure to attain upper limit thermal conductivity among a heat source and a heat sink. The quantity of heat that these devices can carry is several orders higher of magnitude than pure conduction through solid metal. It is more than 200–500 that of copper [11].

The two–phase closed heat–pipe loop may be inclined with small angle or vertically oriented, with a liquid sink at the bottom. At operation, heat–pipe loop transfer heat through the evaporator from an external source to the liquid think. Consequently, a part of the fluid evaporator. Towards the condenser section, the vapor driven by pressure difference force between the condenser and evaporator flows through the adiabatic length. In connection with the condenser part, the steam is condensed into fluid leaving its latent heat of evaporator to the heat pool in the condenser segment. The liquid returns from the condenser to the evaporator internally due to force of gravity. Thus, the hydraulic cycle of the working fluid completed by equilibrated heat transfer [12].

A suggested new design of heat–pipe loop with evaporator and condenser helical configuration with 3 mm thickness as a passive cooling system for a nuclear research reactor main pool and nuclear spent fuel storage pool is proposed to be used to remove this decay heat figure 1.

The design is focused on removing heat from the spent fuel tank of research reactor to be in safely operated. The model considers convection by air naturally for the condensing section of the heat–pipe loop to compensate the residual heat. A numerical model using unique design of heat–pipe loops were investigated the heat transfer [13].

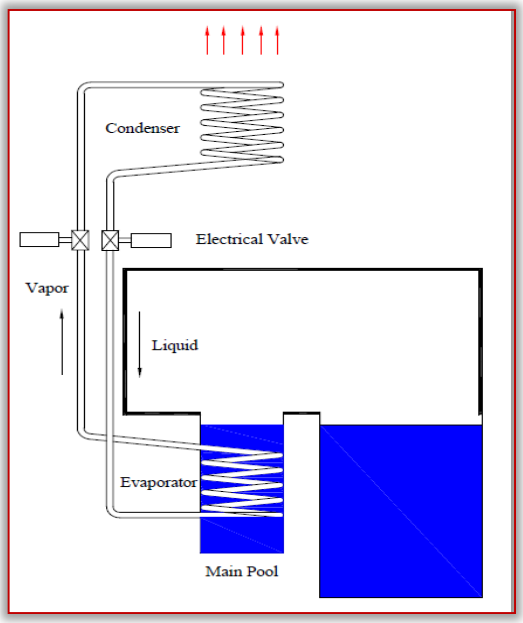

Figure 1. Schematic of Proposed Passive heat–pipe Loops Cooling System

The effects of heat–pipe configuration (evaporator and condenser) were analyzed. Demineralized water was used as the working fluid. The atmospheric air temperature equals (30°C) and circulated around the condensing section as a cooling procedure. Heat input of (Q ≤ 150kW) and working fluid filling ratio (100%) was taken in account. Thermal performance and characteristics was investigated at different heat–pipe lengths (75, 100, 125 and 150m) and diameters (15, 20 and 25cm).

Transient experiments were performed using a water heat pipe having a uniformly heated boiling part and a convectively cooled condenser section [14].

Transient response of the heat pipe to sudden changes of the input electric power to the evaporator heater, at different cooling rates, was investigated [15]. The heat pipe has dimensions according to the followings, 39.3 cm long boiling part, 3.7 cm long adiabatic part, and 17 cm long condensing part. The time constants for the temperature of vapor and the effective throughput power during the start heat–up and shut down cooling transients were estimated depending on the electric power input and the cooling water mass flow rate.

Anhar R. Antariksawan [16] studied heat pipe performance in the reactor cavity cooling system RCCS design. As part of the study, the performance of U–shaped heat pipe is assessed

both through an experiment and numerical simulation methodology. A small U–shaped heat pipe with fins in the condensing section is modeled using the RELAP5/SCDAP code.

The result predicted from model illustrates that the heat pipe could remove the received heat in the boiling section to the environment through the condensing part of that heat pipe using the phenomena of boiling and condensation. However, the steady state condition could not be fulfilled until the end of the calculation. The predicted thermal resistance of the heat pipe is approximately 0.012580°C/W. It is concluded that the model could model reasonably the performance of the heat pipe.

MODEL ASSUMPTIONS

- A one–dimensional flow models.
- The heat–pipe loop is in the vertical orientation.
- The vapor superheat is very small; the vapor is taken at the saturated conditions.
- Constant wall material (Stainless–AISI316) properties, such as (density, specific heat and thermal conductivity).
- The kinetic and potential energy components are neglected in the energy balance equations when compared with heat transfer rate.
- The density, thermal conductivity, enthalpy and other properties of saturated liquid are temperature depended.
- The local wall, working fluid and heat transfer coefficient of the evaporator and the condenser are calculated at mean value for both.
- The heat–pipe starts up from initial condition when the power is suddenly on.

EQUATIONS OF THE MODEL

A model describing both thermal and phase flows of the heat–pipe loop has been performed by M. Abdelaziz, et al [14]. This simpler model has been improved on the one hand in order to provide numerical expressions of the different system variables, and, on the other side, to give the expression of the heat–pipe loop response time as function of the various parameters. Such a model can also give a guide to the design of heat pipe loop.

The primary body investigates the evaporator wall. It is worth to mention that the primary body can be classified as a thermally thin body investigated by a temperature (T_w).

The second body was connected to the whole working fluid which contacts with mutually evaporator wall and working fluid. The working fluid was classified as saturated temperature (T_f). This model investigates a theoretical study of heat–pipe loop behaviour in transient rule.

In this model, the transient thermal behaviour of the heat–pipe loop has been utilized so as to obtain a mathematical expression of the system response. A program depend on the simulation technique was developed to calculate temperature of the heat–pipe loop in addition to the time required to reach ideal condition. This program can be known as a simple tool for modelling and designing heat–pipe loop in transient rule. The heat balance calculations for each body (wall and fluid) give:

$$C_w \frac{dT_w}{dt} = Q_s - h_e . S_e . (T_w - T_f) \quad (1)$$

$$C_f \frac{dT_f}{dt} = h_e - h_e . S_e . (T_w - T_f) - h_c . S_c (T_f - T_{wat}) \quad (2)$$

From equation (1) and by using the finite difference method in certain time step Δt, we obtain T_w.

$$T_w^{n+1}(C_w + h_e . S_e . \Delta t) - . T_f^{n+1}(h_e . S_e . \Delta t) = C_w . T_w^n + \Delta t . Q_s \quad (3)$$

The average fluid temperature from equation (2) and by using the finite difference method we obtain T_f

$$T_f^{n+1}(C_f + \Delta t . h_e . S_e + \Delta t . h_c . S_c) - \Delta t . h_e . S_e . T_w^n = C_f . T_f^n + \Delta t . h_c . S_c . T_{wat} \quad (4)$$

where:

T_w: is the average evaporator wall temperature.

T_f: is the average fluid temperature.

S_e: is the surface area of the evaporator = π*D*L_e

S_c: is the surface area of the condenser = π*D*L_c

Radial heat flux, q_r in evaporator is given as:

$$q_r = Q_{net}/A_r = Q_{net}/(\pi * di * Le) \quad (5)$$

Axial heat flux q_{ax} of heat–pipe is given as:

$$q_{ax} = Q_{net}/A_{cs} = Q_{net} / (\pi * di^2/4) \quad (6)$$

Time constant

From observations of various operating variables of the heat–pipe, show that many nonlinear physical phenomena occur inside it (phase change, counter current flows . . . etc.), values of variables can be well fitted by a simple ''one exponential law'':

$$x(t) = x_{ss}\left(1 - e^{\frac{-(t-t_0)}{\tau_h}}\right) \quad (7)$$

(τ_h) is the time constant corresponding to the variation of the variable X in the heat–up phase.

Where: X_{ss}: variable Value at steady state.

Average evaporator heat transfer coefficient

The process of the heat transfer in the liquid pool of the evaporator section is generally assumed to be common nucleate boiling whose heat transfer coefficient may be calculated from Forester–Zuber equation [17]:

$$h_e = \frac{0.00122 * \Delta T_{sat}^{0.24} * \Delta P_{sat}^{0.75} * cp^{0.45} * \rho_l^{0.49} * k_l^{0.79}}{\sigma^{0.5} * h_{fg}^{0.24} * \mu_l^{0.29} * \rho_v^{0.24}} \quad (8)$$

Average condenser heat transfer coefficient

Natural convection heat transfer on a external surface depends on the geometry in addition to its location. Moreover it depends on the disparity of temperature on the external surface and the properties of the thermo–physical of the fluid involved [18]. The correlations for the average Nusselt number Nu in natural convection are of the form:

$$Gr_L = \frac{g * \beta * (T_s - T_\infty) L_{cr}^3}{\nu^2} \quad (9)$$

where β is Coefficient of volume expansion and equal (1/T) and T is temperature in Kelvin.

The Characteristic length of the pipe is its diameter D.

$$Nu = \frac{h.L_{cr}}{\nu^2} = C(Gr_L * Pr)^n = C * Ra_L^n \quad (10)$$

The values of the constants C and n depend on the geometry of the surface and the flow rule, which is characterized by the variety of the Rayleigh number.

The value of n is (1/4) for laminar flow and (1/3) for turbulent flow. The value of the constant C is normally less than 1.

Where Ra_D is the Rayleigh number, which is the product of the Grashof and Prandtl numbers:

$$Ra_D = Gr_L * Pr = \frac{g.\beta.(T_s - T_\infty)}{\nu^2} \quad (11)$$

The Empirical correlation for the average Nusselt number for natural convection over horizontal cylinder is expressed as:

$$Nu = \left[0.6 + \frac{0.387 * Ra_D^{1/6}}{\left(1 + (0.559/Pr)^{9/16}\right)^{8/27}} \right]^2 \quad (12)$$

When the average convection coefficient and Nusselt number are known, the heat transfer rate Q_{conv} by natural convection from a solid surface at a uniform temperature T_s to the surrounding fluid is known by Newton's law of cooling.

A_s is the heat transfer surface area and h is the average heat transfer coefficient on the surface [19].

$$Q_{conv} = h.A_s(T_s - T_\infty) \quad (13)$$

where A is condenser surface area and expressed as:

$A_s = \pi.D.L$

$$U = \left(\frac{1}{h_i} + \frac{t}{k} + \frac{1}{h_o} \right)^{-1} \quad (14)$$

PROGRAM DESCRIPTION

According to ranges program illustrated in table 1. A mathematical program is designed to solve the presented model. A computer simulation program based on the method of finite difference (Euler) is developed to estimate temperature of heat–pipe loop as well as the time needed to reach steady state condition, also thermal performance and thermal characteristics. The equations are solved by Engineering Equation Solver program (EES) [20].

Table 1. Ranges program of the tests

Heat–pipe material	Stainless–AISI316	Studied parameters	Heat–pipe configuration
Evaporator filing ratio [%]	100	Condenser and evaporator lengths [m]	75, 100, 125 and 150
Ambient temperature [°C]	30	Heat–pipe diameter. [mm]	150, 200 and 250
Heat load [Kw]	150	Material thick. [mm]	3

The developed program comprises three main sections. The first section contains the initial conditions such as the ambient temperature, the basic heat–pipe loop dimensions, material and configuration, cooling flow rate as an input data these parameters are combined to calculate the physical properties of the working fluid and heat–pipe for each section.

The second section of program is activated the program at the saturation temperature of the fluid. This means the transient calculation of the two–phase is started. In this section the mean wall, fluid, evaporator and condenser heat transfer coefficient and cooling flow rate temperature for start–up and steady process are calculated. In the third section, replacement of the initial conditions is achieved by the new calculated data. The program progresses until a steady–state is reached

TRENDS AND RESULTS

Transient start–up operation

Transient test operation is performed at start–up operation and steady–state for loop for nuclear fuel storage tank. These results involve the change of wall and fluid temperatures during the start–up transient operation. Prior to start–up the loop is initially (t = 0 s), then the power input to the evaporator is sudden started. The program is running for each interval of time Δt defined by 4 second till the loop temperature reach the steady state values.

Figure 2 and figure 3 show the average heat–pipe evaporator wall and working fluid temperatures at different evaporator and condenser lengths ranging (75, 100, 125, and 150m) and at different heat–pipe diameters ranging (15, 20 and 25 cm). It was noticed that the best conditions are at evaporator and

condenser lengths at 150 m and at 25cm heat–pipe outer diameter.

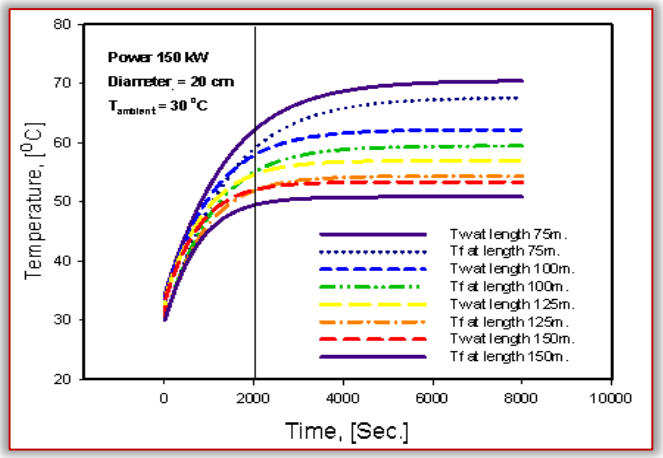

Figure 2. Average wall and fluid temperature at different evaporator lengths.

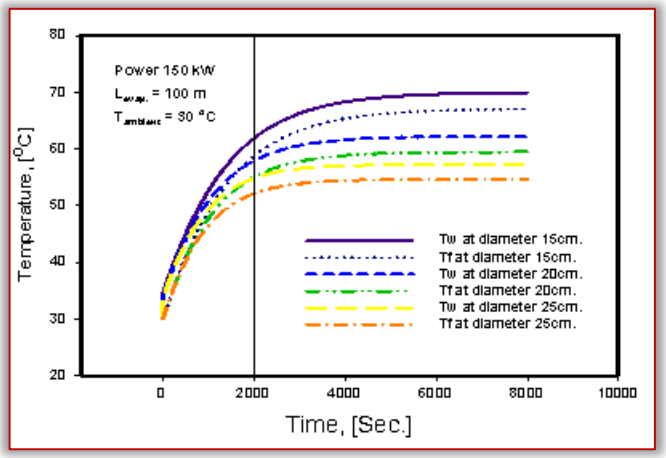

Figure 3. Average wall and fluid temperature at different heat–pipe diameter.

In the current theoretical tests, shown in the above figures, for the loop the time required to reach the steady state operation is about 2000 seconds. The figures indicate the increment of average wall and fluid temperatures with time. The phenomenon is divided into two regions. In the first region, the vapour density is too low to support continuum flow.

Heat gained by the heat–pipe evaporator is absorbed solely as sensible heating, resulting in temperature rise. As a result, the temperature gradient of evaporator section is considered relatively high in the first interval of heating (t = 0–2000 sec.). While the rest of the heat energy forms some vapour which flows from the evaporator and condenses on the beginning section of the condenser section causing its surface temperature to rise. In this period of time the response of condenser section is lower than the evaporator section.

At the time range (t >2000 sec.) the majority heat energy is absorbed as latent heat in working fluid thus, increasing the generated vapour. The vapour temperature is enough to sustain continuum flow. Finally, as the steady state is approached, the rate of temperature increase slows down. This is due to the reduction in temperature difference between vapour and working fluid.

Heat–pipe performance and thermal characteristics

At certain value 150kW of thermal load, Figure 4 and figure 5 illustrates the theoretical average evaporator heat transfer confidents. The estimation is carried out in the case of different heat–pipe lengths ranged from 75 to 150m and diameters ranged from 15 to 25cm. It was shown that the evaporator and condenser heat transfer confidents are reverse proportional with heat–pipe lengths and diameters.

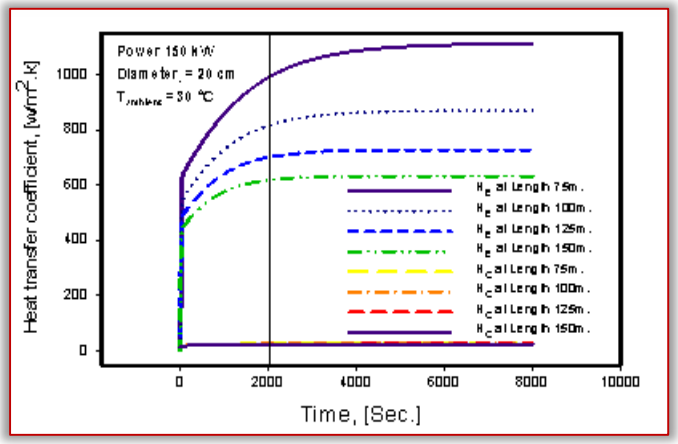

Figure 4.Average evaporator and condenser heat–transfer coefficients at different heat–pipe lengths.

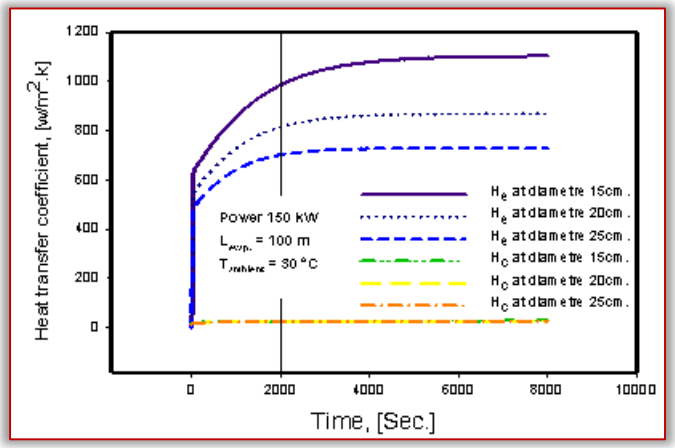

Figure 5. Average evaporator and condenser heat transfer Coefficients at different heat–pipe diameters

In the condenser section, a global heat transfer coefficient (hc) has been considered which combines conduction through the wall and convection (external side of the wall–air) (the cooling section) Figure 6 and figure 7 estimated by the mathematical model Equation (14), show that there little change at the condenser heat transfer coefficient during all processes of the operation for the two processes, heat–up

transient and steady–state on the other hand evaporator heat transfer coefficient is highly changed with the heat–pipe configuration change .

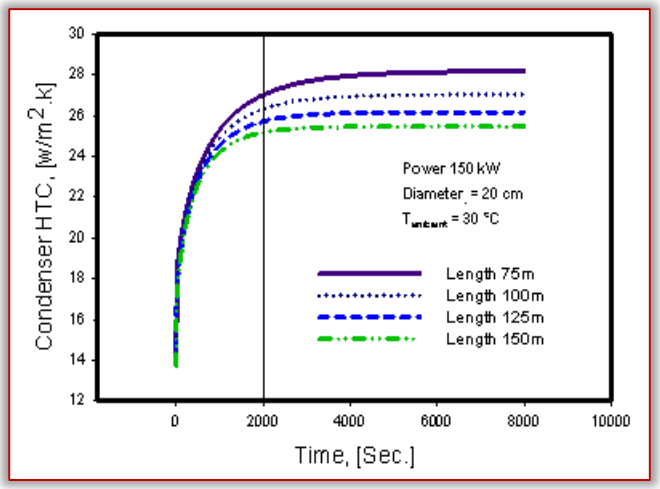

Figure 6. Average condenser heat transfer coefficient at different heat–pipe lengths

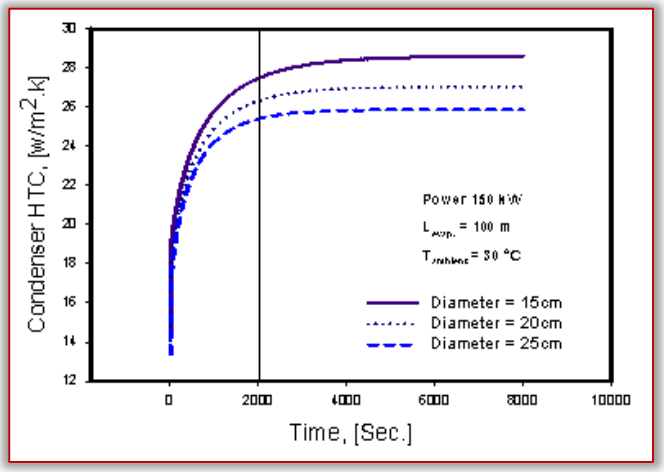

Figure 7. Average condenser heat transfer coefficient at different heat–pipe diameters

Also, the power output from condenser section respectively versus time is observed. The loop is initially at room temperature, and then the power input to the evaporator is increased suddenly from zero to the full power. It was shown from Figure 8 and figure 9 that, the temperatures of each section and the output power increase rapidly at the beginning of operation due to the increase of heat flow from object to another, with time.

But as a result of reduction of the temperature driving forces, the rate of change temperature with time decreases until steady state condition is reached. At steady–state, the power–output remain constant.

From the previous figures it was shown that the time constant needed to reach steady–state is directional proportional with heat–pipe lengths and diameters due to increasing in thermal inertia.

From the results the heat–pipe loop as passive cooling system could remove heat load 150 kW with approximately safe condition especially at heat–pipe configuration at evaporator and condenser length 150m and heat–pipe diameter at 25cm.

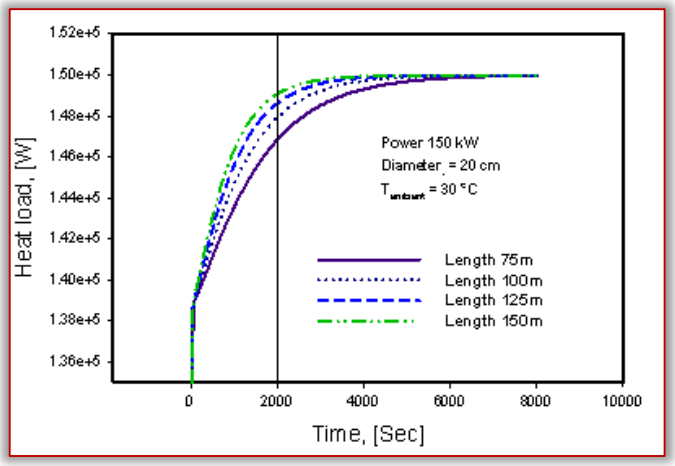

Figure 8. output load from condense section at different heat–pipe lengths

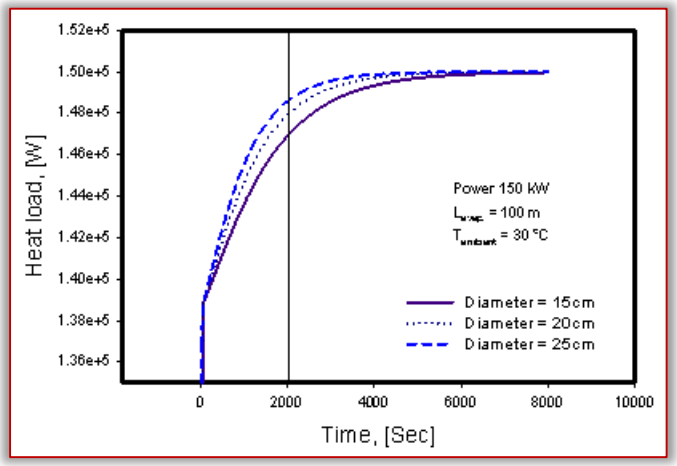

Figure 9. output load from condense section at different heat–pipe diameters

CONCLUSION

A theoretical network model has been proposed to predict the transient response of a heat–pipe loop. A numerical simulation using special design of Stainless–AISI316 heat–pipe loops of passive spent nuclear fuel cooling system used to investigate the thermal performance and characteristics at constant heat–load 150 kW and 30°C ambient temperatures.

Demineralized water was used as the working fluid. The atmospheric air was circulated around the condenser as a cooling system. The effects of heat–pipe configuration (length and diameter) were analysed. The results show that the best thermal characteristic was obtained at higher heat–pipe length and diameter.

The numerical simulation refers to a pattern, and a trend line can be used to predict the

phenomena of heat transfer with different inputs. It was observed that heat pipe's transient response was found to be depending primarily upon heat–pipe configuration. Decreasing at the heat–pipe length and diameter causes a reduction in time constants.

Also it was found that the evaporator heat transfer coefficient was increased with heat–pipe configuration decreased, while the condenser heat transfer coefficients were found slightly changed. From the previous figures the heat–pipe able to remove heat load at 150 kW.

NOMENCLATURE

Ac	[m^2]	Cross section area
cp	[J/kg. K]	Specific heat
D	[m]	Diameter
g	[m/s^2]	Acceleration gravity
h	[W/m^2 .K]	Heat transfer coefficient
h_{fg}	J/kg	Latent heat of vaporization
k	[W/mK]	Thermal conductivity
p	[N/m^2]	Pressure
S	[m^2]	Surface area
T	[K]	Temperature
t	[s]	Time
Gr		Grashof number
Nu		Nusselt number
Pr		Prandtl number
Re		Reynolds number
Ra		rayleigh number
X		Any variable

Special characters

β	[–]	Coefficient of volume expansion
μ	[$N.s/m^2$]	Dynamic viscosity
ρ	[Kg/m^3]	Density
τ	[sec]	Time constant
v	[m^2/s]	Kinematic viscosity

Subscripts

c	Condenser
cr	Characteristic length
cs	Condenser cross sectional area
e	Evaporator
eq	Equivalent
f	Filling ratio
ss	Steady state
L	Liquid
M	Mean
0	Initial
sat	Saturation
v	Vapour
wat	Water
s	Surface
∞	ambient

References

[1] Basic safety principles for nuclear power plants 75–INSAG–3 rev.1, INSAG–12 a report by the International Nuclear Safety Advisory Group.
[2] C. Ye, M.G. Zheng, M.L. Wang, R.H. Zhang, Z.Q. Xiong, The design and simulation of a new spent fuel pool passive cooling system, Ann. Nucl. Energy 58 (2013) 124 to 131.
[3] Fukushima Nuclear Accident Analysis Report. June 20, 2012 Tokyo Electric Power Company, Inc.
[4] IAEA Safety Standards for protecting people and the environment Specific Safety Guide INTERNATIONAL ATOMIC ENERGY AGENCYVIENNAISBN 978–92 –0–109314–1ISSN 1020–525XNo. SSG–34Design of Electrical Power Systems for Nuclear Power Plants
[5] B.S. Jackel, Status of the spent fuel in the reactor buildings of Fukushima Daiichi, Nucl. Eng. Des. 283 (2015) 2 to 7.
[6] V. Ognerubov, A. Kaliatka, V. Vileiniskis, Features of modeling of processes in spent fuel pools using various system codes, Ann. Nucl. Energy 72 (2014) 497 to 506.
[7] X. Wu, W. Li, Y. Zhang, W. Tian, G. Su, S. Qiu, Analysis of the loss of pool cooling accident in a PWR spent fuel pool with MAAP5, Ann. Nucl. Energy 72 (2014) 198 to 213.
[8] V.L. Sailor, K.R. Perkins, J.R. Weeks, H.R. Connell, Severe accidents in spent fuel pools in support of generic safety, Issue 82, Brookhaven National Lab., Upton, NY (USA), Nuclear Regulatory Commission, Washington, DC (USA). Division of Reactor and Plant Systems, 1987.
[9] E.D. Throm, Beyond design basis accidents in spent–fuel pools dgeneric Issue 82, Nucl. Eng. Des. 126 (1991) 333 to 359.
[10] Technical feasibility and reliability of passive safety systems for nuclear power plants. Proceedings of an Advisory Group meeting held in Julich, Germany, 21–24 November 1994.
[11] S. H. Noie, "Heat transfer characteristics of a two–phase closed thermosyphon'' Applied Thermal Engineering, Vol. 25, 2005, pp. 495–506.
[12] D. Reay, R. Mc Glen, P. Kew, Heat Pipes: Theory, Design and Applications, Butterworth–Heinemann, Oxford, UK, 2013.
[13] A. Alizadehdakhel, M. Rahimi, A.A. Alsairafi, CFD modeling of flow and heat transfer in a thermosyphon, Int. Commun. Heat Mass Transf. 37 (2010) 312 to 318.
[14] Loula A. Shouman, M. Abd El–Aziz, Adel Alyan "Theoretical Steady–state Forced Flow Boiling Evaporator for Double–tube Thermosyphon (FFDTT)" International Journal of Scientific & Engineering Research Volume 4, Issue 6, June 2013 ISSN 2229–5518. Atomic Energy Authority, Reactors Department, 13759 Cairo, Egypt
[15] Mohamed S. El–genk and Lianmin Huang"An experimental investigation of the transientresponse of a water heat pipe'', Int. J. Heat Mass Transfer Vol.36,No. 15, pp 3823–3830,1993.
[16] Anhar R. Antariksawan, et al" Assessment of RELAP5 code model to simulate U–shaped heat pipe performance for heat sink" Journal of Physics: Conf. Series 1198 (2019) 022063
[17] P.B Whalley, Boiling Condensation and Gas–Liquid Flow, Department of Engineering Science, University of Oxford, 1989. Heat transfer by Yunus A. Cengel, 2nd eddition, NewYork: McGraw–Hill 2002.
[18] Heat Transfer: A Practical Approach by Yunus A. Cengel (2002–11–01) Hardcover – January 1, 1893
[19] P.G. Anjakar, D.R.B. Yarasu, Experimental analysis of condenser length effect on the performance of thermosyphon, Int. J. Emerg. Technol. Adv. Eng. 2 (2012) 494 to 499.
[20] S.A. Klein and F.L. Alvardo; EES–Engineering Equation Solver; user's Manual for Microsoft Windows Operating Systems, Version 6.160, F–Chart Software, Madison, WI, 2001.

ISSN: 2067-3809

Fascicule 2
[April – June]
tome XVII
[2024]

ACTA Technica CORVINIENSIS
BULLETIN OF ENGINEERING

ISSN: 2067-3809

ACTA TECHNICA CORVINIENSIS – Bulletin of Engineering | e–ISSN: 2067 – 3809
Tome XVII [2024] | Fascicule 2 [April – June]

[1.]Iulian VOICEA, [1.]Nicoleta VANGHELE, [1.]Florin NENCIU, [1.]Cătălin PERSU, [1.]Dan CUJBESCU, [1.]Remus OPRESCU,
[2.]Viorel FATU, [2.]Roxana ZAHARIA, [3.]Elena SIRBU, [4.]Vlad Nicolae ARSENOAIA, [5.]Diana STEGARUS (POPESCU)

THE CONCEPT OF AQUAPONIC AGRICULTURE

[1.]National Institute of Research – Development for Machines and Installations Designed to Agriculture and Food Industry – INMA Bucharest, ROMANIA;
[2.] Research Development Institute for Plant Protection Bucharest, ROMANIA;
[3.] ICEDEAPA Galati, ROMANIA;
[4.] Faculty of Agriculture, Ion Ionescu de la Brad University of Agricultural Sciences and Veterinary Medicine Iasi, ROMANIA;
[5.] ICSI Ramnicu Valcea, ROMANIA

Abstract: The trends, challenges and global guidelines facing agriculture and the agri–food system are multiple, a process of reflection by decision–makers, researches and businessmen being timely and necessary. The expansion of the agricultural and agri–food sector may be significantly limited by the already existing pressure on agricultural land and water resources. Innovative production models are needed to increase productivity while maintaining biodiversity and the quality of natural resources. Aquaponics can be considered a sustainable agricultural production system because it combines plant and animal production, integrates the flow of nutrients through natural biological cycles of nitrification, is carried out without exhausting available resources and without destroying the environment, so without compromising the possibilities of satisfaction of the needs of future generations.

Keywords: aquaculture, sustainability, common fisheries policies, environmental policies

INTRODUCTION

In the context of population growth around the globe and the negative consequences in following climate change, the need for food is increasing. At the same time, habitable surfaces are expanding more and more, especially in the urban environment, so that the land on which it is cultivated is shrinking. Under these conditions, the specialists in the field agricultural is looking for the best solutions to increase production and make resources more efficient.

Farmers around the world make decisions every year about the various tools and technologies they will use to produce the best possible crops. But changing the production system, or even adapting the techniques is a challenge for farmers. And investments are not the real bottleneck. In reality, we lack the agronomic and economic skills to ensure that the transformation of "conventional" farming in the new system will not compromise profitability economy of the farm.

We have to admit that, – and not only in Romania, – many farmers continue to practice conventional agriculture "out of convenience". For to solve problems that can reduce productivity and therefore income agricultural, it is enough to use chemical substances (sometimes of natural origin and ecological and sometimes of artificial origin) and more efficient equipment. But, of many times, we only treat the symptoms this way.

Rapid climate change is one of the most important aspects of the environment we face today, but which will be in our attention constantly and in the near future. These climate changes affect all life from around the globe, but we should be most concerned about the ways in which we will be able to let's continue to farm and produce food in the future.

Crops on today's farmland are probably going to be harder to grow managed tomorrow; the temperature, the precipitation and the transitions of the seasons are increasing unpredictable and difficult crop success. Socially responsible agriculture refers to sustainable production methods and new types of applied technologies and may even be the key to the creation of ecosystems urban nature.

At the same time, socially responsible agriculture can also refer to the product itself, to the simplicity of its production, but also to the multitude of benefits for people and for the environment. In this case, we can discuss one of the foods the future, about which, from the perspective of minimum needs, it can be said that it is produced only socially responsible.

Knowing the key global trends that can influence agriculture, the agri–food system, the management of natural resources and the rural economy, in general, in the next decade, is

extremely necessary, given the importance that food has within every society. Awareness of the impact that these aspects can have contributes to drawing up an agenda that strengthens the resilience and sustainability of agricultural systems (*Gutierrez–Wing, M. and Malone R., 2006)*.

Although the efficiency of agriculture has increased in recent decades, the pressure on agricultural land has intensified, mainly due to demographic factors, changes in consumption patterns, and the urbanization process. If we also add the competition between food and non–food use of agricultural crops (fuel production), land ranges through erosion, desertification, salinization, sea level rise, etc. them.

A vicious circle is created by overexploitation of existing resources, their degradation, increasing pressure on the remaining resources and their further degradation (*FAO, 2017a, Adler P.R. et al, 1996*).

The agricultural area used per person is continuously decreasing from 1.30 to 0.7 ha, in the period 1967–2013 *(FAOSTAT, 2013, Bao, T. et. al, 2023*). There are regional differences in this phenomenon: production growth in Asia in recent decades has been achieved almost exclusively through increased productivity, without an increase in cultivated area, while in Africa, average cereal yields have remained constant, but more land became arable (*OECD, 2016, Basumatary Bwsrang et. al., 2023*).

The expansion of agricultural land takes place at the expense of forests, savanna and natural grasslands, a phenomenon accompanied by the increase in greenhouse gas emissions and the acceleration of the loss of biodiversity. Agriculture is also, and is projected to remain, the largest consumer of global freshwater resources.

Strong competition from the processing industry, power generation and domestic consumers will drive a 55% increase in global fresh water demand by 2050 (*Basumatary Bwsrang et. al., 2023*). Most of this demand is generated in emerging countries, in contrast to the decreasing trend in high–income countries due to the continuous improvement in the efficiency of its use in agriculture and investments in wastewater treatment (*OECD, 2016, Baptista P. 2014*).

Climate change will have a definite adverse impact, especially in countries in the southern regions, and the effects are on both supply and quality and access to food. Changes in the normal values of temperature and precipitation may contribute to the increase of food prices worldwide until 2050 (*Baptista P., 2014*), and this could reduce access to food for vulnerable categories of people (*FAO, 2017a, Bettina König et. al, 2018*). Opinions are nuanced about the impact on agricultural production in the Nordic countries, involving both positive and negative effects (*Brandon Yep et al, 2019*).

The impact for agriculture and the agri–food system is to reduce food loss and waste at all levels of the food chain. This is indeed a systemic change in the current methods of production and consumption, the relationship between producer and consumer and that of "consumers with products and materials" (*Patrick Kangas, 2004*).

Huge economic opportunities would be created, but a political decision, stimulating instruments are needed to promote the circular economy, the transition to this paradigm involving significant costs for the realization of the necessary infrastructure. On the other hand, the fact that this type of economic model operates rather at the regional, national level and does not depend on import markets to meet demand, makes it a serious alternative if reducing the trade deficit becomes a political objective (*OECD, 2016, Bettina König et. al, 2018*).

Aquaponics, or "aquaponics" in English, is the word made up of the first four letters of the word "aquaculture" (growing aquatic plants and animals for the purpose of their commercialization) and the last five letters of the word "hydroponics" (growing vegetables or flowers in nutrient solutions or on a substrate of gravel or sand through which water with chemical fertilizers circulates permanently) in order to name in one word the innovative technology that unites the two culture technologies in one, (*Bittsánszky, András et al, 2016*). Like many other scientific creations of the modern era, aquaponics has its origins in human practices from very distant times.

The Aztecs built floating islands, chinampas (30 x 2.5 m) on the lakes in the Xochimilco and Chalco areas, separated from each other by canals on which they travelled with canoes. On these islands they planted corn, beans, pumpkin, amaranth, tomatoes, chili peppers, flowers, etc. In China, Thailand, Indonesia, people have been growing fish in rice paddies since ancient times, but without knowing that they practice aquaponics. Scientific interest in combining

aquaculture and hydroponics began in the mid–1970s. Sneed, Allen, and Ellis, (1975) are among the first to experiment with soilless plant culture systems as a means of treating fishpond water and removing of nitrogen compounds in recirculating aquaculture systems (RAS).

Reducing the concentration of nitrogen compounds, toxic to fish, becomes a major challenge for recirculating aquaculture and the beginning of the aquaponic era, (*Bohl M., 1977, Collins M, Gratzek J, Shotts Jr E, Dawe D, Campbell L, et al., 1975*).

MATERIAL AND METHOD

The foundations of contemporary aquaponics were laid by researchers at The New Alchemy Institute in the US between the 1970s and 1980s. They first used hydroponic plant culture as a way to improve water conditions for fish, not as an innovative technology for food production. The water quality in fish ponds deteriorates rapidly and requires regular replacement. Starting from the finding that aquatic plants clean water in natural sites, they first added aquatic plants and later terrestrial plants to clean water in fishponds. Dr. John Todd and Nancy Jack Todd conducted research at The New Alchemy Institute that led to a natural wastewater treatment system called the "living machine."

Research by Ronald Zweig (1986) further promoted the idea of integrating plants into an aquaculture system. At the Agricultural Experiment Station of the University of the Virgin Islands (UVI), St. Croix, the first experiments were carried out by Barnaby Watten and Robert Busch, 1984. The most notable results, however, were obtained under the leadership of Dr. James Rakocy, who is called the "father of aquaponics".

The era of modern aquaponics began: Tom and Paula Speraneo, owners of S & S Aqua Farm near West Plains, Missouri, USA, created the first aquaponic system in which the hydroponic culture is on gravel support (Steve Diver, 2000; Rebecca Nelson and John Pade started the quarterly "Aquaponics Journal" in 1997, Pekka Nygard and Stefan Goes, based on the Speraneo model, create an aquaponic system in Harnosand, Sweden (*Bettina König et. al, 2018*).

Intensive recirculating aquaculture systems have important environmental problems because they maintain water quality in the system, in part, by discharging an amount of effluent of 5% to 10% of the recirculated water volume per day and replacing it with fresh water (*Timmons M.B., 2002*). Organic matter, inorganic concentration, and P concentrations in wastewater usually require in–system or post–discharge treatment of effluents (*Gutierrez–Wing M. and R.F. Malone, 2006*). This operation incurs investment and operating costs that negatively influence the selling price of the fish.

Nutrient uptake by plants is one of the most common biological processes involved in contaminant removal in artificial wastewater treatment wetlands (*Debusk, W.F., 1999, Mitsch, W.J. and Gosselink J. 2000*). Adler et al 1996, found that differences in nutrient removal rates of NO3–N and P were dependent on plant number and effluent flow. If plant numbers are high enough, the concentration of nutrients may drop to levels that may be too low to support plant growth.

Rakocy et al, 1997, were able to establish a balanced system by maintaining a large plant growth area relative to the fish production area in a commercial capacity aquaponic system. Rakocy showed that when the ratio between the amount of food given to fish and the area of cultivation for plants is kept within correctly established limits, the amount of nitrogen is sufficient for plant growth. Integrating nutrient flows between aquaculture and hydroponic systems turns a waste stream, toxic to fish, into a gain, given the resulting plant production.

In soil crops, nutrients move to the root surface by diffusion, (*Taiz, L. and E. Zeiger, 2016*). As the plant takes up nutrients from the soil, concentration gradients are formed in the vicinity of the root, and the concentration of nutrients at its surface is reduced compared to the surrounding area. This can lead to a zone of nutrient depletion near the root surface. The ability of continuous root growth, however, extends this region of nutrient uptake beyond the depletion zone. Thus, the optimal uptake of nutrients by plants depends both on the ability of the root system to absorb nutrients and on its ability to extend into the soil.

Unlike soil crops, in the case of hydroponic crops, which use soilless media, when there is a drop in nutrient concentration in the root zone, it is immediately corrected in the next irrigation stage.

Olson established that in hydroponic systems, plants take up nutrients at a constant rate regardless of concentration, as long as the overall ratio and concentration of nutrients in the solution remained nearly the same and the nutrient solution was well mixed and in constant

contact with the roots. (*Olson, C. 1950*). Mass balance nutrient management in closed hydroponic systems shows that once young plants have taken up a sufficient amount of nutrients, concentrations in solution can be reduced because the amount of nutrients required for plant growth is found either in the plant or in solution.

Concentrations of nutrients supplied by fish in the aquaponic system are significantly lower for most nutrients compared to hydroponic systems. However, plants grow very well in these solutions that have lower nutrient levels than "standard" hydroponic solutions, because the plant uptake of organic substances is higher than synthetic substances in hydroponic system solutions, (*Bittsánszky A. et al., 2016*). Rakocy et al, 1997, managed to obtain, for two and a half years, in the pilot aquaponic station at UVI, lettuce productions with nitrogen concentrations 3.5 times lower than in the solutions used in traditional hydroponic systems.

RESULTS

In soil production water is lost through evapotranspiration, percolation into the subsoil, runoff and weed growth. In hydroponic and aquaponic growing systems, water is recirculated. The water that is not taken up by the plants is recirculated. There are no weeds. Nutrients are constantly added by fish in aquaponic systems or humans in the form of nutrients in hydroponic systems and the water returns to the plants. Every drop of water is reused which cannot be achieved in traditional soil farming, (*Perry Baptista, 2014*).

In hydroponics and aquaponics, water loss occurs in two main ways: evapotranspiration and runoff. There is no way to eliminate evapotranspiration but in greenhouses or solariums it can be kept within reasonable limits by controlling the indoor temperature. Leaks sometimes form at the connections between pipes and technological objects that make up the aquaponic system, broken or cracked pipes. Careful and frequent monitoring of the system is the best way to identify and stop water losses. Since maintaining water quality in aquaponic systems is done by hydroponic culture, it is no longer necessary to discharge a quantity of water from the system into the environment and replace it with fresh water as in the case of aquaculture. This reduces the consumption of water, which is a strategic resource of mankind, and protects the environment by eliminating the discharge of effluents.

Aquaponics is a sustainable agricultural production system. Most plant nutrients come from the fish feed following the process of digestion/excretion and nitrification in the biofilter, thus integrating the nutrient flow.

Plants act as biofilters and take effluent from the system that would otherwise have been discharged into the environment and replaced with fresh water. Even though there are thousands of aquaponic systems of various capacities operating worldwide, there are only a few researchers who have reported information on productivity systems. Dr. Rakocy, obtained in the pilot aquaponic system from the University of the Virgin Islands (UVI) in St. Croix, U.S. Virgin Islands, occupying a total area of 500 m2, of which the hydroponic cultivation area is 214 m2, basil productions of 23.4 kg/m2 and 25.00 kg/m2. The production of basil planted in the field, in the same period, was 7.8 kg/m2. In the case of okra production, yields of 2.54 – 2.89 kg/m2 were obtained in the aquaponic system, and in the field, on the control lot, 0.15 kg.m2, (*Rakocy, J., et al., 2014*). In Canada, Dr. Nick Savidov, 2014, obtained 3.7 tons of fish and 3.5 tons of basil annually with a 73 m^3 aquaponic system that has 84 m^2 of hydroponics.

The treatment of solid waste from aquaculture, as a result of undigested feed and unmetabolized feed, is today an operational problem well known to aquaculturists. Solids build–up in aquaculture facilities reduces the quality of the rearing environment and can represent a major ecological footprint. In salmonid culture, the waste situation is better in the last decade, as a result of stricter regulations, a better quality of animal feed and the emergence of efficient technologies for the disposal and processing of waste. At a feed conversion ratio of 1.0 (kg feed/kg rear), the solid dry matter to be removed by mechanical filtration from the rearing water is approximately 100 g per kg feed used or fish produced. Current salmon farms are extremely large and produce many millions of fish each year. The biomass produced annually in most of these farms is between 100–1,000 tons. In addition, the production from farms in terrestrial recirculating system (RAS) and from floating cages, represents biomass 5–10 times higher, i.e. up to 10,000 tons per year per exploitation. These systems are suitable for solids removal.

Raising rainbow trout to optimum commercial size in freshwater farms also produces, in some countries, a substantial amount of biomass and

sludge. Such farms discharge sludge into freshwater streams, lakes and rivers.

The waste discharge from these farms should be properly treated, before re–entering the watercourses. In fresh waters, the removal of phosphorus is vital in terms of eutrophication, hence the obligation to have well–designed and managed effluent treatment systems to effectively retain and neutralize phosphorus. Especially since most of the phosphorus lost from fish farms is usually incorporated into particles that could be filtered with simple, mechanical filters. Trout farmers in Denmark, for example, are subject to strict regulations by environmental authorities to protect freshwater bodies. The storage of solid or semi–solid waste takes place in artificial lagoons, isolated with impermeable membranes, for the removal of nutrients by plants.

Dewatered waste from trout farms contains high levels of nitrogen and phosphorus, the main nutrients for plant production, but is extremely low in potassium. Sludge from aquaculture farms, if stabilized with added lime, is considered a veritable fertilizer for any arable land.

Analysis of heavy metals such as chromium and lead indicates extremely low levels that are actually harmless to the environment. But in most cases, delivering sludge to agriculture means additional operating costs for fish producers.

CONCLUSIONS

In conclusion, the global trends and challenges facing agriculture and the agri–food system are multiple, a reflection process by decision–makers, researches, and business people being timely and necessary. Agricultural and food production is expected to increase due to population and income growth.

The expansion of the agricultural and agri–food sector may be significantly limited by the already existing pressure on agricultural land and water resources. Innovative production models are needed to increase productivity while maintaining biodiversity and the quality of natural resources.

Sustainable production practices are also required by increasing consumer awareness of sustainable and healthy consumption patterns. Success in setting up strong, resilient agri–food systems depends on smart strategies that will manage to integrate

Food security can be said to exist when people in that area have, at all times, physical and economic access to sufficient, safe and nutritious food that meets their dietary needs and food preferences for an active and healthy life. There are four pillars of food security that define, defend and measure the state of food security at local, national and international levels. These are: food availability, food access, food utilization and food stability.

Aquaponics is an opportunity for food security because it produces fish and vegetables simultaneously, can be implemented in any geographical area regardless of soil fertility, and if located in a greenhouse, independent of climate.

Unfortunately, today only a small part, about 1.5% of the total sludge produced in salmon and trout farms in Europe, is removed and processed. What is really serious is the fact that the predominant production of aquaculture products takes place in "cage" systems, floating cages, unsuitable for the collection and handling of waste, coastal areas being "scorched" by the destructive effects of waste from fish feed. This area, of the use of waste from aquaculture systems, remains the grand prize, being a double reward: on the one hand capitalizing on a new salable product line from aquaculture farms, and on the other hand protecting the environment.

An ideal farm or aquaculture system capitalizes on every element of its composition and has a zero nitrogen and carbon footprint. In this field, European and even global research proves to be still at the beginning of the road and the only way in which things can move in the right direction is a much more restrictive legislation on protecting the environment, combined with research programs on intelligent use of aquaculture waste.

Acknowledgement

This paper was financed by MINISTRY OF AGRICULTURE AND RURAL DEVELOPMENT – ROMANIA – MADR – Sectorial Project ADER 25.2.2 Contract no.: ADER 25.2.2 / 18.07.2023 Vertical Aquaponic Farm Adapted To Current Climate Changes and Ministry of Research, Innovation and Digitalization through Program 1 – Development of the national research–development system, Subprogram 1.2 – Institutional performance – Projects for financing excellence in RDI, Contract no. 1PFE/30.12.2021.

References

[1] Adler P.R. et al, (1996). Utilizing byproducts to enhance aquaculture sustainability. World Aquaculture 27:24–26.

[2] Bao, T. et al, (2023). Effects of Vegetable–Fish Co–Culture on CH_4 and N_2O Emissions from an Aquaculture Pond, Agronomy, Vol. 13, Issue 5, Article number 1230

[3] Basumatary Bwsrang et al., (2023). Global research trends on aquaponics: a systematic review based on computational mapping, Aquaculture International, Volume 31, Issue 2, 1115 – 1141

[4] Baptista P. (2014), Water Use Efficiency in Hydroponics and Aquaponics, ZipGrow Inc., http://blog.zipgrow.com/water–use–efficiency–hydroponics–aquaponics/.
[5] Bettina König et al, (2018). Analysis of aquaponics as an emerging technological innovation system, Journal of Cleaner Production, Vol. 180, 232–243
[6] Bittsánszky, András et al, (2016). Nutrient supply of plants in aquaponic systems. Ecocycles. 2. 17–20
[7] Brandon Yep et al, (2019). Aquaponic trends and challenges – A review, Journal of Cleaner Production, Vol. 228, 1586–1599
[8] Bohl M., (1977). Some initial aquaculture experiments in recirculating water systems. Aquaculture 11: 323–328.
[9] Collins M, Gratzek J, Shotts Jr E, Dawe D, Campbell L, et al. (1975). Nitrification in an Aquatic Recirculating System. Journal of the Fisheries Research Board of Canada 32: 2025–2031.
[10] Debusk, W.F. (2019). Wastewater treatment wetlands: Contaminant removal processes. Univ. Florida, Soil Water Sci. Fact Sheet SL 155.
[11] Gutierrez–Wing, M. and Malone R., (2006), Biological filters in aquaculture: Trends and research directions for freshwater and marine applications. Aquacult. Eng. 34:163–171.
[12] Kritika Thakur et al. (2023). An alternative approach towards nitrification and bioremediation of wastewater from aquaponics using biofilm–based bioreactors: A review, Chemosphere, Volume 316, 137849,
[13] Mitsch, W.J. and J.G. Gosselink. (2000). Wetlands, 3rd ed. Wiley, New York.
[14] Olson, C. (1950). The significance of concentration on the rate of ion absorption by higher plants in water culture. Physiol. Plant. 3:152–164.
[15] Patrick K., (2004). Ecological Engineering: Principles and Practice. CRC Press, p.63–65.
[16] Rakocy, J.E. (1997). Integrating tilapia culture with vegetable hydroponics in recirculating systems. World Aquaculture Soc., Baton Rouge, LA.
[17] Rakocy, J.E., (1997). Evaluation of a commercial–scale aquaponic unit for the production of tilapia and lettuce. 4th Intl. Symp. on Tilapia in Aquacult. 1:357–372.
[18] Rakocy, J., și colab, (2014). Aquaponic production of tilapia and basil: comparing a batch and staggered cropping system. Acta Hortic. 648, 63–69
[19] Savidov, N. (2014) Evolution of Aquaponics Design: from UVI to Zero–Waste Commercial Operation, http://www.aquaponicsiberia.com/wp–content/uploads/2016/10/nicksavidov–evolutionofaquaponics.
[20] Sneed K, Allen K, Ellis J (1975). Fish farming and hydroponics. Aquaculture and the Fish Farmer 2: 18–20.
[21] Steve D., (2000), Aquaponics–Integrating Hydroponics with Aquaculture, http://www. attra.org/attra–pub/aquaponic.html.
[22] Taiz, L. and E. Zeiger. (2016). Plant physiology. 4th ed. Sinauer, Sunderland, MA.
[23] Timmons, M.B., et al, (2002). Recirculating aquaculture systems.2nd ed. Northeastern Reg. Aquaculture Ctr. Pub. No. 01–002.
[24] Todd, N.J., (1977). The Book of the New Alchemists. E.P.Dutton, New York City, 174 pp.

Note: This paper was presented at ISB–INMA TEH' 2023 – International Symposium on Technologies and Technical Systems in Agriculture, Food Industry and Environment, organized by University "POLITEHNICA" of Bucuresti, Faculty of Biotechnical Systems Engineering, National Institute for Research–Development of Machines and Installations designed for Agriculture and Food Industry (INMA Bucuresti), National Research & Development Institute for Food Bioresources (IBA Bucuresti), University of Agronomic Sciences and Veterinary Medicine of Bucuresti (UASVMB), Research–Development Institute for Plant Protection – (ICDPP Bucuresti), Research and Development Institute for Processing and Marketing of the Horticultural Products (HORTING), Hydraulics and Pneumatics Research Institute (INOE 2000 IHP) and Romanian Agricultural Mechanical Engineers Society (SIMAR), in Bucuresti, ROMANIA, in 5–6 October, 2023.

ISSN: 2067–3809

ACTA TECHNICA CORVINIENSIS – Bulletin of Engineering | e–ISSN: 2067 – 3809
Tome XVII [2024] | Fascicule 2 [April – June]

[1.]Nicoleta UNGUREANU, [2.]Nicolae–Valentin VLĂDUȚ, [1.]Sorin–Ștefan BIRIȘ,
[1.]Oana Elena MILEA, [1.]Sorin Dan IORDACHE

CONSIDERATIONS ON THE RISK OF CHEMICAL CONTAMINATION WHEN IRRIGATTING WITH WASTEWATER

[1.]National University of Science and Technology Politehnica Bucharest, ROMANIA;
[2.]National Institute of Research – Development for Machines and Installations Designed for Agriculture and Food Industry – INMA Bucharest, ROMANIA

Abstract: The main reason for heavy metals pollution in agriculture is the use of untreated industrial and municipal wastewater for irrigation, followed by the presence of these inorganic contaminants in products such as fertilizers and pesticides. Heavy metals from irrigation wastewater are easily transferred to the soil–crop–crop consumer system, posing severe threats to environmental sustainability, soil and human health. Heavy metals accumulated in the soil are toxic to microorganisms and disrupt the soil ecosystem. Leafy vegetables tend to accumulate higher concentrations of heavy metals than other parts of the crop. After consumption, heavy metals accumulate in certain human organs and cause serious diseases. Emerging pollutants from the category of pharmaceutical products and pesticides are also found in the waste water, which are very difficult to eliminate through the classic purification procedures, and which are easily transferred and cause disturbances, especially in the aquatic ecosystems. In this paper, aspects related to the route of these contaminants from agriculture and their effects on the environment and health are reviewed.
Keywords: wastewater, heavy metals, emerging contaminants, pharmaceutical products, pesticides

INTRODUCTION

Soil ecosystems are critical to human and environmental sustainability. Many pollutants are currently present in the soil, including heavy metals, organic pesticides, radioactive elements (cesium and strontium compounds), selenium, arsenic, fluorine compounds, and so on. These pollutants enter or remain in the soil for a long time, and once they exceed the soil's self–purification capability, they will directly cause contamination of agricultural soils, potentially resulting in the loss of the production capacity of the soil and to soil being removed from the agricultural circuit.

In any agricultural system, irrigation is essential for obtaining satisfactory and sufficient productions. Irrigation is important for economically successful agriculture in arid and semi–arid regions; also, irrigation is frequently required as an additional measure in semi–wet and wet regions. Wastewater irrigation is simultaneously an effective disposal method and a path of water recovery. Irrigation with wastewater reduces the pressure on fresh water sources and the volumes of effluents discharged into the environment.

Chemical contaminants in wastewater, including heavy metals, pharmaceutical compounds and pesticides, are a cause for concern especially in countries at the beginning of industrial development, where industrial wastewaters enter domestic wastewater streams and natural water streams in larger quantities or even in an uncontrolled manner. When crops irrigated with wastewater are intended for human or animal consumption, the risk translates into the possible introduction of unwanted substances into the food chain; the health effects of heavy metals and pharmaceutical compounds (even more if these categories of contaminants are combined), are not yet fully known (*de Santiago–Martin et al., 2020*).

The World Health Organization has established guideline values for a selection of chemicals that may be harmful in the context of agricultural wastewater use (*WHO, 2006*). In addition, starting with 26 June 2023, the new regulation on minimum requirements for water reuse for agricultural irrigation, established by the European Commission, is applied in the European Union (*EC Regulation EU 2020/741*).

HEAVY METALS

Heavy metals are metals and metalloids with densities greater than 5 g/cm^3. The most common heavy metals are arsenic (As), cadmium (Cd), chromium (Cr), copper (Cu), lead (Pb) and mercury (Hg) (*Herawati et al., 2000*). Cadmium, lead, zinc, and copper are the most prevalent heavy metal contaminants in many countries today (*Yan et al., 2022*). Large amounts of heavy metals are produced and emitted in all industries as a result of rapid urbanization, industrialization and intensification of agriculture. Over the last half–century, the worldwide environment has gained a considerable amount of heavy metals (i.e., over 0.03 million tons of chromium and 0.8 million tons

of lead), primarily in the soil (*Yang et al., 2018*). In the European Union, around 3.5 million sites are contaminated with heavy metals, with 0.5 million sites being highly contaminated and in need of remediation (*Mahar et al., 2016*).

The main source of contamination with heavy metals in agriculture is irrigation with untreated industrial or municipal wastewater (or their mixtures), and in some areas even the uncontrolled discharge of these wastewaters that seep into agricultural soils and the groundwater. Untreated wastewater used in irrigation contains high levels of trace elements and heavy metals, being likely to be toxic to plants and obviously posing risks to the environment and human health (*Ungureanu et al., 2020*). In addition, the use of heavy metals in products intended for agriculture (fertilizers, pesticides and other agriculture–based chemicals) is increasingly viewed as a secondary source of pollution in agriculture (*Tchounwou et al., 2012*).

In comparison to potassium and nitrogen fertilizers, phosphate fertilizers contain a significant amount of harmful heavy metals (particularly cadmium and lead) (*Bitew and Alemayehu, 2017*). Heavy metal contamination of soil and crops always occurs in tandem, and it is expected to have consequences on human health. Heavy metals can easily enter the atmosphere, groundwater, soil, and crops, and then the human body by inhalation, ingestion, and skin absorption. Even if these contaminants are present in small amounts (traces), their harmful impacts could disrupt the soil environment. The persistence of heavy metals in the environment is dangerous in the long term, given their long half–life (eg 1460 days for lead and 200 days for cadmium).

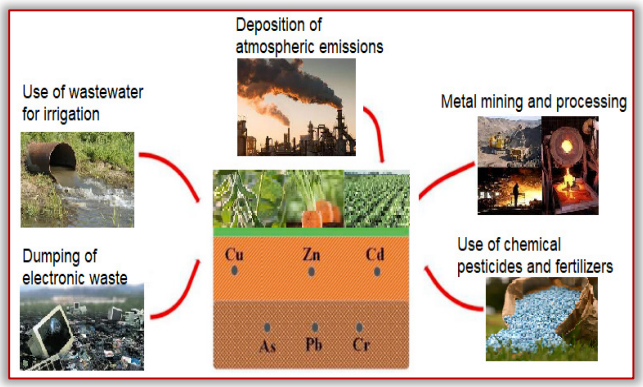

Figure 1 – Anthropogenic sources of heavy metal pollution of agricultural soils

The problem of trace elements and heavy metals in wastewater is mostly attributable to the mixing of municipal, agricultural, livestock, and industrial wastewater streams in the same sewer system in most developing nations. This issue is exacerbated by the flow of untreated industrial wastewaters into natural water bodies, which is permitted under lax pollution control procedures. Mercury, lead, arsenic, copper, cadmium, and manganese are only some examples of potentially dangerous trace metals. It is important to know if traces of heavy metals are: in solution or adsorbed on solids; in organo–metallic or hydroxide forms; in the crystalline structure of suspended materials. Without very accurate distribution data, the development of elimination techniques and guidelines for these harmful elements cannot be effectively designed.

Typically, most treated or partially treated wastewaters have low levels of trace heavy metals, which are within acceptable limits for irrigation water quality. According to *Elgallal et al. (2016)*, treated or partially treated wastewater can be used safely for up to a century without adverse effects on soil, crops, groundwater or the food chain. However, several studies have mentioned that after 50–100 years of irrigation with wastewater, the level of toxic heavy metals in the soil exceeded the maximum permissible limits.

Different properties of the soil (pH, texture, type of oxyhydroxides and amount of organic matter), but also the type of plant crops, generally determine the transport of trace metals and essential components (carbonates, phosphates and clay) from the soil to the plants.

Regular use of wastewater for soil irrigation increases heavy metal concentrations in agricultural crops and these metals are subsequently transferred through the food chain to humans and animals, causing potential long–term health risks. Health risks due to heavy metals contamination can be viewed as occupational hazards because chemical pollutants in wastewater can affect the health of farmers who come into direct contact with the contaminated water during crop irrigation. Some heavy metals are carcinogenic, mutagenic, teratogenic, and endocrine disruptors; they have the potential to cause substantial damage even at very low concentrations, while more dangerous ones can cause neurological and behavioral changes, particularly in children (*Mahar et al., 2016*).

- **Cadmium (Cd)** is not considered an essential element for plants, but is efficiently absorbed by both root and leaf systems. Cadmium has high toxicity and high levels of persistence in

food and the environment, being the most dangerous heavy metal in the environment (*Perez–Lopez et al., 2008*). Studies conducted in China, Japan and Taiwan by *Carr et al. (2004)* showed that rice grown in soils contaminated by irrigation water containing substantial industrial discharges accumulated high concentrations of cadmium (and other heavy metals). Cadmium exposure can produce a wide variety of acute and chronic effects in humans, such as kidney failure, lung failure, bone damage, and hypertension (*Sun and Li, 2011*). Since one way of human exposure to cadmium is through food consumption, assessing and controlling the amount of contaminated food sources, identifying sources of contaminants as well as modifying or eliminating them play a significant role in human health and longevity.

- **Chrome (Cr)** is considered as an environmental pollutant released into the atmosphere mainly due to its intensive use in heavy industries. Chromium is a well–known human carcinogen, and numerous respected institutions worldwide have proven lung cancer as a result of the exposure to this contaminant (*Tirger et al., 2008*).
- **Copper (Cu)** plays an important role in photosynthesis, respiration, carbohydrate distribution, nitrogen reduction and fixation, protein metabolism and cell wall metabolism. Copper regulates the creation of DNA and RNA, and a lack of it severely limits plant reproduction. It is difficult to define and specify the amount of copper in the soil that has harmful effects on plants. In general, before phytotoxic symptoms appear, the degree of copper buildup in plants poses a risk to human health.
- **Iron (Fe)** uptake generally depends on soil pH, calcium and phosphorus concentrations, and ratios of several heavy metals. High soil iron concentrations can cause phytotoxic effects in acid, low phosphorus, acid sulfate, and flooded soils.
- **Lead (Pb).** Airborne lead is readily taken up by plants through leaves, from where it is absorbed into plant tissues. Soil lead is not easily translocated into the edible parts of plants. Soil contamination from agricultural operations has been shown to have a minimal effect on plant lead concentrations. Vegetables cultivated in high lead concentration areas, such as urban and industrial areas, may represent a health risk to those who consume them, because lead absorbed by the human body can harm organs like the heart, bones, and nervous system (*Bruce et al., 2012*).

The different chemical and biochemical transformations that heavy metals can undergo in the aquatic environment deserve special attention. Chemical transformations can affect the bioavailability or toxicity of heavy metals, which can be either enhanced or reduced. Knowledge of the mechanisms underlying the physical, chemical, or microbial transformations of heavy metals is often essential to understanding the health effects of these contaminants.

Farrag et al. (2016) studied the translocation of some heavy metals from soils irrigated with wastewater in some crops such as cabbage, onion, garlic and wheat. Their results showed that Cd, Cr, Cu, Ni, Pb and Zn accumulated in the edible parts of the crops and the concentrations of these heavy metals varied greatly depending on the type of agricultural crop.

The accumulation of even small amounts of metals in soil, plants and food products is a challenge in long–term wastewater irrigation areas due to chronic exposure of consumers to food products from crops irrigated with wastewater containing of heavy metals. Several studies have shown that plants irrigated with wastewater can absorb and accumulate potentially toxic elements in concentrations higher than the maximum permissible limits, with serious implications for public health. Long–term consumption of vegetables potentially contaminated with toxic elements can lead to the continuous accumulation of toxic metals in the kidneys and liver in humans, causing disruptions in the physico–biochemical processes (*Mahmood and Malik, 2014*).

Wastewater used for irrigation has been identified as the potential source of heavy metals such as Cd, Cu, Ni, Cr, Pb, and Zn in the soil, plants, and food products (Table 1). Certain food crops pose greater risks of transferring the heavy metals with which they are contaminated, into the human body. In the case of irrigation with industrial effluents, the risk of contamination with heavy metals and trace elements increases.

Information about different uptake levels of heavy metals by different agricultural crop types is useful to determine which vegetables should be grown in areas known to be contaminated

with specific pollutants. However, when recommending a particular crop, several context–specific factors must be considered, and not all factors are based on consumer health, but also on market value and growing conditions.

Table 1. Concentration of heavy metals in wastewater, soil and vegetables, in relation to transfer and bioaccumulation factors (*Khalid et al., 2018)*

Heavy metal	Vegetable crop	Concentration in wastewater (mg/L)	Concentration in soil (mg/kg)	Concentration in plant (mg/kg)	Transfer factor from wastewater to the soil	Transfer factor from soil to the vegetable
Cd	*Cupressus sempervirens*	0.06	0.03	0.06	0.5	2
Cd	*Raphanus sativus*	-	0.84	0.93	-	1.29
Cd	*Vicia faba*	-	0.11	0.1	-	0.9
Cd	*Oryza sativa*	0.01	3	1.1	300	0.4
Cd	*Spinacia oleracea*	10	5.8	15	0.6	2.6
Cd	*Lactuca sativa*	0.05	1	0.2	20	0.2
Pb	*Triticum*	-	41.56	2.77	-	0.1
Pb	*Raphanus sativus*	0.18	49.4	2.6	274.4	0.04
Pb	*Triticum*	0.585	411.7	26.23	703.8	0.064
Pb	*Convolvulus arvensis*	-	24.7	1.433	-	0.058
Pb	*Triticum*	0.1	33.4	2.3	334.0	0.069
Pb	*Oryza sativa*	-	5.1	0.37	-	0.073
Pb	*Cupressus sempervirens*	9.2	7.1	3.2	0.8	0.5
Zn	*Raphanus sativus*	-	157	57	-	0.41
Zn	*Daucus carota*	0.27	12.4	2.5	45.9	0.202
Zn	*Vicia faba*	0.36	0.42	0.07	1.2	0.2
Zn	*Amaranthus*	1	167	67	167.0	0.4
Zn	*Beta vulgaris*	0.24	1.7	25	7.1	14.7
Zn	*Hordeum vulgare*	0.19	1.4	32.2	7.4	23.0
Zn	*Citrus x sinensis*	0.02	134.22	4.15	6711.0	0.031
Ni	*Cupressus sepervirens*	7.1	11.3	4.7	1.6	0.4
Ni	*Oryza sativa*	1.03	35	1.8	34.0	0.051
Ni	*Raphanus sativus*	-	24.9	11	-	0.42
Ni	*Zea mays*	-	28.13	2.65	-	0.09
Ni	*Abelmoschus esculentus*	1.6	0.3	1.4	0.2	4.67
Ni	*Vicia faba*	0.04	0.55	0.09	13.8	0.2
Ni	*Triticum*	0.22	276.6	27.19	1257.3	0.098
Cu	*Cupressus sempervirens*	4.7	5.4	9.4	1.1	1.7
Cu	*Raphanus sativus*	0.2	5.4	1.2	27.0	0.222
Cu	*Raphanus sativus*	-	32.8	9	-	0.32
Cu	*Lactuca sativa*	-	7.4	8.05	-	1.088
Cu	*Xanthium strumarium*	0.616	0.768	0.791	1.2	1.0
Cu	*Vicia faba*	0.181	0.49	0.04	2.7	0.1
Cu	*Citrus x sinensis*	0.03	94.38	4.352	3146.0	0.046

Since trace elements and heavy metals in wastewater can be toxic to plants at levels below those that pose a significant risk to human health, a certain level of natural protection could also result, because no crop will thrive when irrigated with highly toxic water, and farmers will abandon crops that do not grow satisfactorily before exposing themselves to significant health risks through consumption of those crops (*Kilelu C.W., 2004*).

The uptake of heavy metals varies by plant species and different plant parts (growing above or below ground). In other words, chemical pollutants can be retained on the surface of crops and vegetables that grow above ground, in addition to being absorbed through the roots. In general, the risk of contamination with potentially toxic elements is higher for vegetables that have consumable plant parts below ground than those above ground (*Khalid et al., 2018*). Concentrations of heavy metals accumulated in roots are usually higher than in leaves. Leafy vegetables tend to accumulate more easily the heavy metals, but monocots such as rice accumulate a higher concentration of heavy metals in their roots *(Nabulo G., 2002)*. Increased metal deposition in roots and shoots can be useful or poisonous depending on the type of edible component of the vegetable. For leafy plants, heavy metal deposition in roots is beneficial, whereas for tuber vegetables, significant translocation to shoots is desired. Heavy metal concentrations in plant tissues increase with metal concentrations in irrigation water, and this problem can only be solved by proper wastewater treatment.

Pandey et al. (2012) found that while root vegetables showed higher uptake of heavy metals compared to leafy vegetables and fruits irrigated with wastewater, when atmospheric deposition inputs were considered along with wastewater irrigation, leafy vegetables showed higher levels of contamination.

Several studies have reported high accumulation (above the toxic limit) of potential toxic elements in various edible parts of crops/vegetables worldwide. A study by *Chopra and Pathak (2015)* reported the accumulation of Pb, Cu, Zn, Ni, Cd and Cr in *Beta vulgaris*, *Phaseolus vulgaris*, *Spinacea oleracea* and *Brassica oleracea*. *Mason et al. (2011)* observed the accumulation of Zn, Cu, Mn, Cd, Pb, Ni, Fe and Cr in *Zea mays* (maize) culture irrigated with wastewater and fertilized with sewage sludge. *Jamali et al. (2007)* reported the accumulation of Cd, Cu, Cr, Ni, Pb and Zn in vegetables irrigated with mixtures of wastewater and sewage sludge. *Kiziloglu et al. (2008)* found increases in Cu, Fe, Mn, Zn, Pb, Cd and Ni concentrations in red cabbage and cauliflower crops irrigated with wastewater.

În mod similar, *Balkhair and Ashraf (2016)* found that the level of Cr, Pb, Ni and Cd in the edible parts of okra was higher than the safe limit with levels of 63%, 28%, 90% and 83% respectively in the samples, leading to the conclusion that irrigating the okra crop with wastewater containing potentially toxic elements is not safe for human health. *Khan et al. (2008)* found that leafy vegetables have a higher transfer of Cd, Cu and Ni from soil to plants. *Singh et al. (2010)* compared a range of vegetables contaminated with heavy metals and found the highest concentrations in cabbage, eggplant and leafy vegetables such as lettuce and spinach, compared to other vegetables such as some varieties of squash. A study conducted by *Dickin et al. (2016)* found that compared to other crops, the accumulation of heavy metals even at low concentrations in rice and wheat crops poses a greater risk to humans because these crops are consumed in larger quantities in many diets.

Currently, worldwide, different methods of remediation of soils contaminated with heavy

metals have reached the stage of technological maturity and are successfully implemented, while other methods are in the research–development stage.

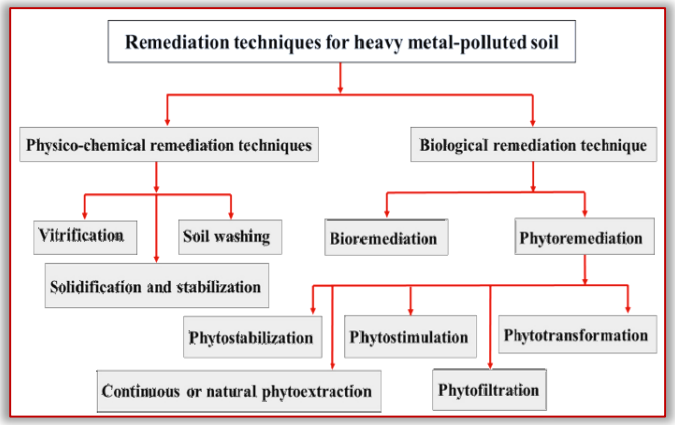

Figure 2 – Anthropogenic sources of heavy metal pollution of agricultural soils (Ashraf et al., 2019)

CONTAMINANTS OF EMERGING CONCERN

Contaminants are considered "emerging" when they have a new source, a different route to people, or novel treatment options (*Gogoi et al., 2018*). Emerging contaminants (ECs) are chemicals, either synthetic or naturally occurring, or microorganisms that are not widely monitored in the environment but have the potential to enter it and have known or suspected detrimental ecological or human health impacts. Emerging contaminants include many micropollutants found in municipal, industrial and agricultural wastewater, such as pharmaceutical products (antibiotics, steroid hormones, x–ray media etc), personal care products, pesticides, insecticides, surfactants, detergents, dyes, polymers, plastics, phthalates, flame retardants, industrial additives.

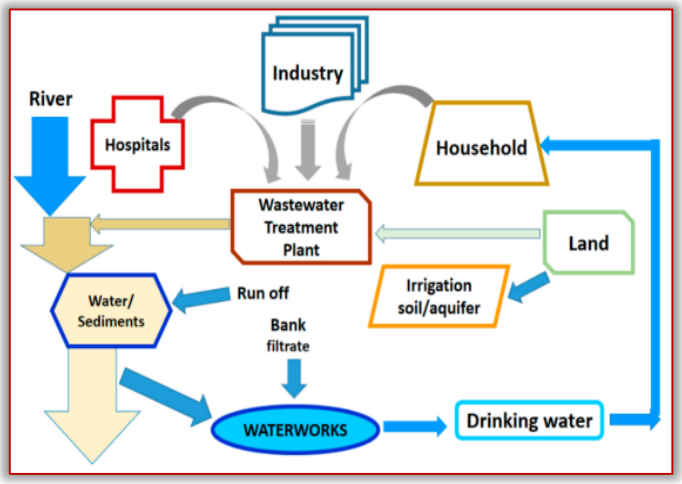

Figure 3 – Sources of emerging pollutants and their routes in the environment *(Vasilachi et al., 2021)*

Exposure to emerging contaminants has a negative impact mainly on the aquatic environment and animals in direct contact with polluted water (mainly surface water) (*Ungureanu et al., 2019*). Released into the environment, emerging contaminants have ecotoxicological effects on aquatic and terrestrial organisms (feminization of aquatic organisms, bacterial resistance, endocrine disruption). In addition, all these emerging chemicals reaching have many negative effects on human health.

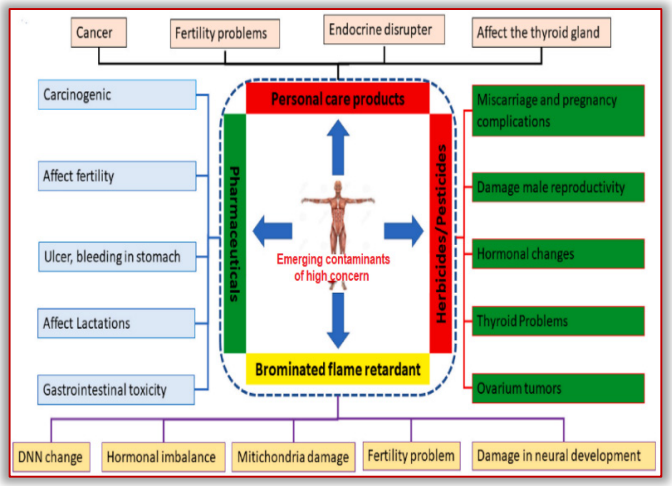

Figure 4 – Negative consequences on human health due to emerging contaminants (*Kumar et al., 2022*)

Although the risks associated with emerging contaminants in treated wastewater used for irrigation are still controversial, some studies have argued that these contaminants are unlikely to pose a serious threat to groundwater, soil, or human health as a result of their application in agriculture. However, there is still a significant lack of studies on the prevalence and fate of emerging contaminants as a result of agricultural wastewater reuse, in terms of their potentially negative effects on the terrestrial ecosystem, uptake by crops and potential impact on human health. through the food chain (*Elgallal et al., 2016*).

Pharmaceutical compounds for human and veterinary use

Pharmaceutical compounds (antibiotics, steroids, contraceptives, analgesics, endocrine–disrupting chemicals, anti–cancer agents, beta–blockers, lipid regulator agents, anti–inflammatory drugs, anticonvulsants, contrast agents etc) are being used in human and veterinary medicine on a daily basis.

Veterinary antibiotics are widely employed in the prevention and treatment of animal infections, but they are also widely utilized to increase productivity, typically in feed and water, which greatly outweighs their usage as animal therapies at the moment. Antibiotics cannot be fully metabolized, so their residues are found in

household wastewater, medical wastewater, livestock and poultry farming wastewater, and, in some cases, in antibiotic production wastewater. The use of veterinary antibiotics as animal growth boosters is prohibited in the European Union due to the numerous environmental concerns (*Ungureanu et al., 2019*).

Steroids are estrogens, androgens, glucocorticoids and progestagens. Natural and synthetic steroids are used in human daily life for contraception and therapy, as well as in livestock production to prevent and treat diseases, boost growth and productivity, and manage animal reproduction. The European Union restricted the administration of steroid hormones for farmed animal fattening due to the negative human health impacts of hormone residues in animal foods (*Ungureanu et al., 2019*). After being assimilated in the human or animal body, these substances are eliminated through metabolic processes in the environment.

In recent years, different concentrations of pharmaceutical compounds, which have negative effects on the environment (especially on the aquatic environment, but also on soil and sediments) have been detected in numerous wastewater flows and natural water bodies. Once in the environment, pharmaceutical products can undergo natural processes such as biodegradation, sorption or dilution, by which their concentrations in water or soil are reduced, or they can be taken up by aquatic organisms and plants. In the case of pharmaceuticals, the transformation products resulting from these processes are most often more soluble and polar than the parent compound and therefore more mobile. The European Medicines Agency specifies that any traces of transformation products exceeding 10% of the concentration of the original compound must be investigated to determine the possible effects on ecosystems.

It was found that there is a slow accumulation of veterinary pharmaceuticals transferred from treated wastewater into plant tissues. The concentration of veterinary pharmaceuticals contained in plants depends on the type of chemical agent, when the wastewater is applied as irrigation water, the type of wastewater and the season (*Christou et al., 2017*). Greater adsorption of chemicals in soil was observed during winter. Although veterinary pharmaceuticals carried into soils irrigated with treated wastewater do not pose a high risk to terrestrial organisms, the concentration of these products must be constantly monitored to trace their movement into the soil layers (*Biel–Maeso et al., 2018*).

It is highly likely that emerging pollutants pose many threats to soil and human health, but long–term studies are still needed to test this hypothesis. Pharmaceutical chemicals in untreated wastewater used for irrigation might pose a threat to agricultural land because their buildup in the soil can impact microorganisms and soil worms for many years, promoting the development of antibiotic–resistant microbes.

Pharmaceuticals can then be carried from the soil to plants and reach the food chain, potentially endangering the human health. There is still a chance that these chemical compounds will be discharged from the soil into groundwater or surface water, creating a risk to aquatic life biocenosis. Detection of low concentrations of pharmaceuticals is challenging and expensive, requiring the use of specialized analytical techniques such as solvent extraction and ultrasound in conjunction with liquid chromatography (*Montemurro et al., 2019*).

The most effective processes in the removal of pharmaceutical compounds from wastewater proved to be the advanced oxidation processes (particularly Fenton oxidation). However, even if advanced wastewater treatment processes are used, often traces of pharmaceutical products are still found in the effluents, which will end up being eliminated in the environment (transferred to surface water bodies, they pose significant risks to aquatic organisms and humans).

Pesticides

Pesticides, a well known group of toxic organic chemicals with widespread use in agriculture and livestock production, have the primary function to boost food output while decreasing weeds and pests. Considering that pesticides have been used for decades and often applied in excess, they are increasingly being detected in wastewater and natural water bodies.

It has been reported that around 95% of pesticides used up to this point did not reach the target insect but were instead deposited in their surrounding habitats (*Nawaz et al., 2021*).

Conventional wastewater treatment processes are not effective in eliminating pesticides, so they are often found in wastewater treatment plant effluents (*Farias et al., 2023*). As partially treated and untreated wastewaters are frequently discharged into agricultural canals,

these chemicals must be considered when developing wastewater reuse guidelines.

To some extent, pesticides can be destroyed in the natural environment by microorganisms' metabolic activity or by chemical degradation, but many recalcitrant pesticides and their metabolites are stable over time in the environment. The potential impacts of pesticides are a cause of obvious concern for farmers and consumers, since the reuse in irrigation of waters containing pesticide residues can negatively affect sensitive species, and human health. Pesticides in aqueous systems are extremely dangerous to aquatic organisms and the ecosystem since they are classed as possible endocrine disrupting agents (*Goh et al., 2023*). In terms of human health, long–term exposure to the active components of certain pesticides and their metabolites has been linked to chronic consequences such as birth abnormalities, organ damage, cancer, nervous system diseases and neurotoxicity (*Meftaul et al., 2020*). Moreover, it is well established that pesticides have the potential to contaminate groundwater due to runoff and leaching processes. Pesticides in drinking water sources are viewed as a possible source of health issues, even at low levels of contamination, due to their functions as endocrine disruptors (*Suwannarin et al., 2021*).

CONCLUSIONS

Heavy metals that contaminate agricultural soils are toxic; they have long biological half–life and are difficult to biodegrade. Cadmium, lead, zinc, and copper are the most prevalent heavy metal contaminants in many countries today.

Heavy metal pollution has serious negative effects for human health and the environment. Some heavy metals are toxic even in trace concentrations, and can cause a variety of diseases, the most affected segment of the population being children. Agricultural workers are frequently exposed to contamination with heavy metals, because they come into direct contact with contaminated soil, with wastewater used for irrigation and with harvested vegetables.

The reuse of wastewater as a substitute for freshwater in agriculture can be helpful to the environment and agriculture, but only if correct treatment, planning and management operations are employed,so as to minimize the risks to the environment and human health.

Acknowledgement

This research was supported by the Romanian Ministry of Research Innovation and Digitalization, through Program 1 – Development of the national research–development system, Subprogram 1.2 – Institutional performance – Projects for financing excellence in RDI, Contract no. 1PFE/30.12.2021.

References

[1] Ashraf, S., Ali, Q., Zahir, Z.A., Ashraf, S., Asghar, H.N. (2019). Phytoremediation: environmentally sustainable way for reclamation of heavy metal polluted soils. Ecotoxicology and Environmental Safety, 174, 714–727.

[2] Balkhair, K.S., Ashraf, M.A. (2016). Field accumulation risks of heavy metals in soil and vegetable crop irrigated with sewage water in western region of Saudi Arabia. Saudi Journal of Biological Sciences**,** 23, S32–S44.

[3] Biel–Maeso, M., Corada–Fernandez, C., Lara–Martín, P.A. (2018). Monitoring the occurrence of pharmaceuticals in soils irrigated with reclaimed wastewater. Environmental Pollution, 235, 312–321.

[4] Bitew, Y., Alemayehu, M. (2017). Impact of crop production inputs on soil health: a review. Asian Journal of Plant Science, 16, 109–131.

[5] Bruce, S.G., Zarema, A., Igor, M.G. (2012). Analysis of Lead toxicity in human cells. BMC Genomics, 13, 344.

[6] Carr, R.M., Blumenthal, U.J., Mara, D.D. (2004). Health guidelines for the use of wastewater in agriculture developing realistic guidelines. In: Wastewater use in irrigated agriculture coordinating the livelihood and environmental realities. Scott, C.A., Faruqui, N.I., Raschid–Sally, L. (Eds.). CABI Publishing.

[7] Chopra, A., Pathak, C. (2015). Accumulation of heavy metals in the vegetables grown in wastewater irrigated areas of Dehradun, India with reference to human health risk. Environmental Monitoring and Assessment, 187, 445.

[8] Christou, A., Karaolia, P., Hapeshi, E., Michael, C., Fatta–Kassinos, D. (2017). Long–term wastewater irrigation of vegetables in real agricultural systems: concentration of pharmaceuticals in soil, uptake and bioaccumulation in tomato fruits and human health risk assessment. Water Research, 109, 24–34.

[9] De Santiago–Martin, A., Meffe, R., Teijon, G., Martinez–Hernandez, V., López–Heras, I., Alonso–Alonso, C., Arenas, M., De Bustamante, I. (2020). Pharmaceuticals and trace metals in the surface water used for crop irrigation: risk to health or natural attenuation? Science of The Total Environment, 705, 135825.

[10] Dickin, S.K., Schuster–Wallace, C.J., Qadir, M., Pizzacalla, K. (2016). A review of health risks and pathways for exposure to wastewater use in agriculture. Environmental Health Perspectives, 124(7), 900–909.

[11] Elgallal, M., Fletcher, L., Evans, B. (2016). Assessment of potential risks associated with chemicals in wastewater used for irrigation in arid and semiarid zones: a review. Agricultural Water Management, 177, 419–431.

[12] Farias, K.C.S., Guimarães, R.C.A., Oliveira, K.R.W., Nazário, C.E.D., Ferencz, J.A.P., Wender, H. (2023). Banana peel powder biosorbent for removal of hazardous organic pollutants from wastewater. Toxics, 11(8), 664.

[13] Farrag, K., Elbastamy, E., Ramadan, A. (2016). Health risk assessment of heavy metals in irrigated agricultural crops, El-Saff wastewater canal, Egypt. Clean Soil, Air, Water, 44(9), 1174–1183.

[14] Gogoi, A., Mazumder, P., Tyagi, V.K., Tushara Chaminda, G.G., An, A.K., Kumar, M. (2018). Occurrence and fate of emerging contaminants in water environment: a review. Groundwater for Sustainable Development, 6, 169–180.

[15] Goh, P.S., Lau, W.J., Ismail, A.F., Samawati, Z., Liang, Y.Y., Kanakaraju, D. (2023). Microalgae–enabled wastewater treatment: a sustainable strategy for bioremediation of pesticides. Water, 15(1), 70.

[16] Herawati, N., Suzuki, S., Hayashi, K., Rivai, I.F., Koyoma, H. (2000). Cadmium, copper and zinc levels in rice and soil of Japan, Indonesia and China by soil type. Bulletin of Environmental Contamination and Toxicology, 64, 33–39.

[17] Jamali, M., Kazi, T., Arain, M., Afridi, H., Jalbani, N., Memon, A. (2007). Heavy metal contents of vegetables grown in soil, irrigated with mixtures of wastewater and sewage sludge in Pakistan, using ultrasonic–assisted pseudo–digestion. Journal of Agronomy and Crop Science, 193, 218–228.

[18] Khalid, S., Shahid, M., Irshad Bibi, N., Sarwar, T., Shah, A.H., Niazi, N.K. (2018). A review of environmental contamination and health risk assessment of wastewater use for crop irrigation with a focus on low and high–income countries. International Journal of Environmental Research and Public Health, 15, 895–921.

[19] Khan, S., Cao, Q., Zheng, Y.M., Huang, Y.Z., Zhu, Y.G. (2008). Health risks of heavy metals in contaminated soils and food crops irrigated with wastewater in Beijing, China. Environmental Pollution, 152, 686–692.
[20] Kilelu, C.W. (2004). Wastewater irrigation, farmers' perceptions of health risks and institutional perspectives: a case study in Maili Saba, Nairobi. Cities Feeding People Series, Report 38.
[21] Kiziloglu, F., Turan, M., Sahin, U., Kuslu, Y., Dursun, A. (2008). Effects of untreated and treated wastewater irrigation on some chemical properties of cauliflower (Brassica olerecea L. var. botrytis) and red cabbage (Brassica olerecea L. var. rubra) grown on calcareous soil in Turkey. Agricultural Water Management, 95, 716–724.
[22] Kumar, R., Qureshi, M., Vishwakarma, D.K., Al–Ansari, N., Kuriqi, A., Elbeltagi, A., Saraswat, A. (2022). A review on emerging water contaminants and the application of sustainable removal technologies. Case Studies in Chemical and Environmental Engineering, 6, 100219.
[23] Mahar, A., Wang, P., Ali, A., et al. (2016). Challenges and opportunities in the phytoremediation of heavy metals contaminated soils: a review. Ecotoxicology and Environmental Safety, 126, 111–121.
[24] Mahmood, A., Malik, R.N. (2014). Human health risk assessment of heavy metals via consumption of contaminated vegetables collected from different irrigation sources in Lahore, Pakistan. Arabian Journal of Chemistry, 7, 91–99.
[25] Mason, C., Mapfaire, L., Mapurazi, S., Makanda, R. (2011). Assessment of heavy metal accumulation in wastewater irrigated soil and uptake by maize plants (Zea mays L.) at Firle Farm in Harare. Journal of Sustainable Development, 4, 132.
[26] Meftaul, I.M., Venkateswarlu, K., Dharmarajan, R., Annamalai, P., Megharaj, M. (2020). Pesticides in the urban environment: a potential threat that knocks at the door. Science of The Total Environment, 711, 134612.
[27] Montemurro, N., Postigo, C., Chiron, S., Barcelo, D., Perez, S. (2019). Analysis and fate of 14 relevant wastewater–derived organic pollutants in long–term exposed soil. Analytical and Bioanalytical Chemistry, 411, 2687–2696.
[28] Nabulo, G. (2002). Assessment of heavy metal uptake by selected food crops and vegetables around Kampala city area, Uganda. Agropolis Technical report. IDRC.
[29] Nawaz, K., Hussain, K., Choudary, N., Majeed, A., Ilyas, U., Ghani, A., Lin, F., Ali, K., Afghan, S., Raza, G., et al. (2011). Eco–friendly role of biodegradation against agricultural pesticides hazards. African Journal of Microbiology Research, 5, 177–183.
[30] Pandey, R., Shubhashish, K., Pandey, J. (2012). Dietary intake of pollutant aerosols via vegetables influenced by atmospheric deposition and wastewater irrigation. Ecotoxicology and Environmental Safety, 76, 200–208.
[31] Perez–Lopez, M., Hermoso de Mendoza, M., Lopez Beceiro, A., Soler Rodriguez, F. (2008). Heavy metal (Cd, Pb, Zn) and metalloid (As) content in raptor species from Galicia (NW Spain). Ecotoxicology and Environmental Safety, 70, 154–162.
[32] Singh, A., Sharma, R.K., Agrawal, M., Marhsal, F.M. (2010). Health assessment of heavy metals via dietary intake of foodstuffs from the wastewater irrigated site of a dry tropical area of India. Food and Chemical Toxicology, 48, 611–619.
[33] Sun, H., Li, L. (2011). Investigation of distribution for trace Lead and Cadmium in chinese herbal medicines and their decoctions by graphite furnace Atomic Absorption Spectrometry. American Journal of Analytical Chemistry, 2, 217–222.
[34] Suwannarin, N., Prapamontol, T., Isobe, T., Nishihama, Y., Hashimoto, Y., Mangklabruks, A., Pantasri, T., Chantara, S., Naksen, W., Nakayama, S. (2021). Exposure to organophosphate and neonicotinoid insecticides and its association with steroid hormones among male reproductive–age farmworkers in Northern Thailand. International Journal of Environmental Research and Public Health, 18, 5599.
[35] Tchounwou, P.B., Yedjou, C.G., Patlolla, A.K., Sutton, D.J. (2012). Heavy metal toxicity and the environment. In EXS 101, 133–164.
[36] Tirger, A., Golbabaei, F., Shah Taheri, S.J.A., Nori, K.A., Hamedi, J., Ganjali, M.R. (2008). A comparative study of affecting factors on concentration of hexavalent chromium as an occupational carcinogens. Scientific Journal of Hamadan University of Medical Sciences Health Services, 2, 52–59.
[37] Ungureanu N., Vlăduț V., Biriș S.Șt. (2019). Emerging contaminants in wastewater. ISB–INMA TEH' International Symposium, 566–576. Bucharest, Romania.
[38] Ungureanu, N., Vlăduț, V., Voicu, Gh. (2020). Water scarcity and wastewater reuse in crop irrigation. Sustainability, 12(21), 9055.
[39] Vasilachi, I.C., Asiminicesei, D.M., Fertu, D.I., Gavrilescu, M. Occurrence and fate of emerging pollutants in water environment and options for their removal. Water, 13(2), 181.
[40] Yan, K., Wang, H., Lan, Z., Zhou, J., Fu, H., Wu, L., et al. (2022). Heavy metal pollution in the soil of contaminated sites in China: research status and pollution assessment over the past two decades. Journal of Cleaner Production, 373, 133780.
[41] Yang, Q., Li, Z., Lu, X., Duan, Q., Huang, L., Bi, J. (2018). A review of soil heavy metal pollution from industrial and agricultural regions in China: pollution and risk assessment. Science of The Total Environment, 642, 690–700.
[42] ***European Commission (2020). Regulation EU 2020/741 of the European Parliament and of the Council, on minimum requirements for water reuse. Brussels, Belgium. https://eur–lex.europa.eu/legal–content/EN/TXT/PDF/?uri=CELEX:32020R0741&from=EN.
[43] ***World Health Organization. (2006). Guidelines for the safe use of wastewater, excreta and greywater. Wastewater Use in Agriculture. Geneva, Switzerland.

Note: This paper was presented at ISB–INMA TEH' 2023 – International Symposium on Technologies and Technical Systems in Agriculture, Food Industry and Environment, organized by University "POLITEHNICA" of Bucuresti, Faculty of Biotechnical Systems Engineering, National Institute for Research–Development of Machines and Installations designed for Agriculture and Food Industry (INMA Bucuresti), National Research & Development Institute for Food Bioresources (IBA Bucuresti), University of Agronomic Sciences and Veterinary Medicine of Bucuresti (UASVMB), Research–Development Institute for Plant Protection – (ICDPP Bucuresti), Research and Development Institute for Processing and Marketing of the Horticultural Products (HORTING), Hydraulics and Pneumatics Research Institute (INOE 2000 IHP) and Romanian Agricultural Mechanical Engineers Society (SIMAR), in Bucuresti, ROMANIA, in 5–6 October, 2023.

ISSN: 2067-3809

ACTA TECHNICA CORVINIENSIS – Bulletin of Engineering | e–ISSN: 2067 – 3809
Tome XVII [2024] | Fascicule 2 [April – June]

[1.] **Chioma Temitope Gloria AWODIJI,** [1.]**Samuel SULE**

PROBABILISTIC ASSESSMENT OF A DOUBLY SYMMETRIC I–STEEL BEAM

[1.]Department of Civil and Environmental Engineering, Faculty of Engineering, University of Port–Harcourt, P.M.B 5323, Choba, Rivers State, NIGERIA

Abstract: This paper presents the findings of a probabilistic evaluation of a doubly symmetric I–steel beam's bending, shear, and deflection limit states. The design adhered to BS 5950, Part 1, 2000. Failure equations for flexure, shear, and deflection were derived, while random variable probabilistic models were sourced from the literature. Optimization using the First–Order Reliability Method (FORM) yielded design points, reliability indices, and sensitivity analyses. The results revealed that the reliability index decreased as beam span increased, with negative indices observed at a load ratio of 1.0 and beam span of 8.5m. Moreover, increasing the beam span to an overall depth ratio above 42 compromised reliability. The design achieved material savings in the plastic section modulus for a target reliability index of 3.0 but increased the modulus for a target index of 3.80 over a 50–year period. The design proved critical in bending, safe in deflection, and satisfactory in shear.

Keywords: Failure analysis, sensitivity analysis, reliability level

INTRODUCTION

In recent times, the Nigerian populace has been witness to an unprecedented and alarming rise in the collapse of building structures, resulting in the destruction of properties worth billions of naira. This distressing trend necessitates the implementation of reliability analysis for structures or their components at every stage of their service lives, rather than adopting a passive approach and observing their eventual collapse [1]. According to the esteemed scholars Mosley and Bungey [2], engineered structures must fulfill the requirements of both the ultimate and serviceability limit states. The strength of any engineered structure inevitably undergoes degradation over time, making condition assessment of utmost importance [3–4].

It is imperative to acknowledge that the design of structures or structural members based solely on codes cannot guarantee absolute safety, as the design may prove inadequate due to poor estimation of loading and may even be uneconomical due to an overestimation of loads. The root cause of poor loading estimation lies in the inherent variability of the design parameters employed in the design equations. The presence of variability in these design parameters renders it exceedingly challenging to accurately predict the safety of engineered structures and cost implications during the design phase [5]. Given the catastrophic consequences that result from structural failure, it is essential for structural engineers to intervene promptly at every stage of a structure's service life, in order to avert the devastating effects that failure and subsequent collapse can inflict.

The implementation of a probabilistic framework has proven immensely beneficial in the condition assessment of various civil engineering facilities, as it effectively addresses the uncertainties associated with design parameters [6]. In light of this, the present study aims to conduct a probabilistic assessment of a doubly symmetric I–steel beam, focusing on the limit state of bending, shear, and deflection, respectively. To achieve this objective, the First–Order reliability method was employed and a bespoke MATLAB code was developed, utilizing the derived failure functions. This code enables estimation of the reliability indices for different values of the random variables, thereby facilitating an investigation into the impact of these variables on the beam's reliability levels.

LITERATURE REVIEW

Esmaeil, et al. [7] conducted an extensive investigation into the reliability index, with a specific focus on optimizing self–centering structures to attain the minimum weight possible by utilizing metaheuristic algorithms. This study encompassed not only linear but also nonlinear reliability problems, thereby providing a comprehensive analysis. The findings of their research unveiled significant results, indicating a noteworthy decrease in weight of 36%, 30%, and 32% for buildings with 10, 15, and 20 storeys, respectively, when uncertainties were not accounted for. However, when uncertainties were factored in, a remarkable weight reduction of 23% was achieved for the same buildings. This implies that the consideration of uncertainties can lead to an increase in failure probability of up to 23%. In addition, the authors made an

interesting observation regarding the performance of the charged system search and colliding bodies optimization algorithms, noting their effectiveness in the context of this study. Consequently, it can be concluded that the incorporation of a reliability index, while leading to the construction of heavier structures, ultimately enhances the overall safety of these structures.

Junho [8] extensively examined the concept of "Reliability–Based Design Optimization (RBDO) of Structures Using Complex–Step Approximation with Sensitivity Analysis". In the study, he conducted a thorough examination of the application of reliability analysis in the field of structural design. Through the meticulous experimentation and examination of various structural optimization problems, encompassing a wide spectrum of statistical variations, he successfully showcased the potential of this method in achieving optimal performance while adhering to highly precise probabilistic constraints. By employing complex–step approximation, the accuracy of RBDO was significantly enhanced, leading to a notable improvement in the overall performance benefits associated with structural optimization.

Jerez et al. [9] in their studies conducted a comprehensive survey to explore the most recent advancements in reliability–based design optimization of structures subjected to stochastic excitation. In their study, they examined various approaches, including the search–based technique, sequential optimization approach, and scheme–based approach. An intriguing observation made by the authors was the significant influence of computational aspects in successfully addressing optimization problems. Furthermore, their comprehensive overview suggests that the methods employed for achieving optimal design in stochastic structural dynamics are no longer confined to academic scenarios but can also serve as valuable tools in solving a wide range of engineering design problems.

The investigation conducted by [10] focused on the examination of reliability analysis and design optimization for nonlinear structures. In order to accomplish this, they employed the Kriging based method and the First–order reliability method (FORM). The Kriging based method, showed greater levels of efficiency and accuracy when compared to the FORM based method and the Monte Carlo Simulation (MCS) method. Interestingly, the Kriging based method did not require the determination of the response sensitivity, thereby enhancing its adaptability for various scenarios.

An examination of the reliability analysis of steel rack frames using the Direct Design Method was carried out by [11]. Furthermore, they developed curves that illustrate the relationship between the system reliability index (β) and the system resistance factors (φs) for these steel rack frames and compared their findings to those of a traditional design approach based on elastic analysis. To carry out their assessment, the researchers employed a combination of the DDM, a formulation of the limit state function, and probabilistic modelling through Monte Carlo simulation. This allowed them to thoroughly investigate the reliability of steel rack frames and derive the system reliability indices.

The results they obtained indicated that the utilisation of the DDM offers more advantages than the traditional design approach based on elastic analysis. Specifically, when the system reliability indices fell within the range of ≤3, they found that similar structural reliability was achieved for both unweighted and weighted unit pallet loading. This observation demonstrated the consistency between the load combination factors and their corresponding coefficients of variation. Overall, the researchers concluded that incorporating sectional imperfections in the analysis model did not yield any discernible benefits in terms of the adopted system resistance factor.

DEVELOPMENT OF LIMIT STATE FUNCTIONS

A limit state function is a representation of a specific failure mode and it establishes a connection between various parameters. Its development is a fundamental aspect of structural engineering and plays a vital role in the design and construction of safe and efficient structures. In this study, the failure functions were developed according to the provisions of [12] for the design of steel structures.

Bending limit state

The limit state of bending happens when the bending moments or tensile stresses are more than what is necessary for the structure to be safe and functional before failing. Equation 1 illustrates its function as follows:

$$G(X) = P_y S_x - 0.125 * 1.6 * q_k * (0.875\alpha + 1) * L^2 \quad (1)$$

Shear limit state

Shear forces that are too great for the structure's safety and serviceability standards before failure cause the shear limit condition. The shear

resistance of the I–section according to [12] is given in equation 2 as:

$$P_v = 0.60 P_y A_v \quad (2)$$

where

$$A_v = Dt \quad (3)$$

The maximum shear force is given by:

$$Fmax = \frac{5wL}{8} = 0.625 * 1.6qk(0.875\alpha + 1) * L \quad (4)$$

The failure function in shear is generated by subtracting equation 4 from equation 2. This is given as shown in equation 5 and equation 6:

$$G(X) = 0.60 P_y Dt - 0.625 * 1.6 * q_k * (0.875\alpha + 1) * L \quad (5)$$

$$G(X) = 0.60 P_y t - 0.625 * 1.6 * q_k * (0.875\alpha + 1) * \frac{L}{D} \quad (6)$$

Let, $\frac{L}{D} = \lambda$

Equation 6 now becomes:

$$G(X) = 0.60 P_y t - 0.625 * 1.6 * q_k * (0.875\alpha + 1) * \lambda \quad (7)$$

where g_k = Characteristic dead load; q_k = Characteristic live load; P_y = Bending strength of steel

Equation 7 is the failure function in shear of the doubly symmetrical I–steel beam.

Deflection limit state

The deflection limit state is a conception that focuses on the gravity of keeping the deflection of a structural member below a certain boundary to ensure the structure's performance and safety, alleviating the risk of failure, and maintaining stability, functionality, and durability. The allowable deflection is shown in equation 8 as:

$$\delta_{all} = \frac{L}{360} \quad (8)$$

Eqution 9 presents the maximum value of deflection for a uniformly loaded beam as:

$$\delta\, max = \frac{0.0052 wL^4}{EI} \quad (9)$$

The limit state function in deflection is developed by subtracting Eq. (9) from Eq. (8) and is given in Eq. (10) as:

$$G(X) = \frac{L}{360} - \frac{0.0052 wL^4}{EI} \quad (10)$$

Substituting the value of w from equation 4 into the equation 10 gives:

$$G(X) = \frac{L}{360} - \frac{0.0052 * 1.6 * q_k * (0.875\alpha + 1) * L^4}{EI} \quad (11)$$

Eq. (11) is the failure function in deflection of the doubly symmetrical I–steel beam.

Probabilistic design of steel beam in bending

The limit state function in bending is given by:

$$G(X) = P_y S_x - M_D - M_L \quad (12)$$

where M_D and M_L are induced moment due to dead and live loads respectively.

Induced moment due to dead and live loads are given by equation 13 and equation 14 respectively.

$$M_D = \frac{g_k L^2}{8} \quad (13)$$

$$M_L = \frac{q_k L^2}{8} \quad (14)$$

Let:

$$P_y = X_1; g_k = X_2; q_k = X_3$$

Equuation 12 now becomes:

$$G(X) = X_1 * S_x - \frac{X_2 L^2}{8} - \frac{X_3 L^2}{8} \quad (15)$$

Or

$$G(X) = \frac{8 S_x X_1}{L^2} - X_2 - X_3 \quad (16)$$

Let the coefficient of X_1 be b. Therefore,

$$\frac{8 S_x}{L^2} = b \quad (17)$$

Eq. (16) now becomes:

$$G(X) = bX_1 - X_2 - X_3 \quad (18)$$

The statistics of the design parameters in equation 18 are used as input variables in the MATLAB code and the value of b corresponding to the target reliability index of 3.0 recommended for beams in flexure is obtained by optimization.

Reliability analysis

The design process for a doubly symmetric I–steel beam, subject to uncertain dead and live loads of 20KN/m and 10KN/m respectively, was conducted in accordance with the design specifications outlined in [12] A UB section with dimensions of 406*140*46Kg/m was determined to meet the necessary criteria for bending, shear, and deflection.

Table 1: Probabilistic models of the basic random variables

N/S	Variable	Unit	Type of Probability distribution	Mean	Standard Deviation	Coefficient of Variation
1	P_y	N/mm^2	Normal	275	27.5	0.10
2	q_k	kN/m	Normal	20	5	0.25
3	I_x	mm^4	Normal	475400000	23770000	0.05
4	E	N/mm^2	Normal	205000	10250	0.05
5	L	mm	Normal	8000	400	0.05
6	D	mm	Normal	528.3	26.415	0.05
7	S_x	cm^3	Normal	2059000	102950	0.05
8	α	_	Fixed	Varying		
9	t	mm	Normal	9.6	0.48	0.05
10	D/L	_	Fixed	Varying	–	–
11	g_k	kN/m	Normal	Varying	–	0.10

The characteristic live load value is kept constant at 20KN/m while the varying load ratio values considered are 0.5, 0.75, 1.0, 1.25, 1.50, 1.75, 2.0 and 2.25 respectively. The values of the characteristic dead load corresponding to the above load ratios are 10KN/m, 15KN/m, 20KN/m, 25KN/m, 30KN/m, 35KN/m, 40KN/m and 45KN/m respectively. The deterministic design for the plastic section modulus of the I–beam

corresponding to the characteristic dead and live loads was carried out and the results obtained are compared with the results of the probabilistic design at target reliability indices of 3.0 and 3.80 respectively. The probabilistic models for the basic random variables are presented in Table 1.

First Order Reliability Analysis

The limit state function $G(X)$ is a function of the basic random variables. $G(X)$ is the limit state function such that $G(X) < 0$ represents unsafe state of a structure, $G(X) > 0$ represents the safe state of a structure and $G(X) = 0$ represents the demarcation between the safe and unsafe state of the structure respectively.

Let the limit state function in the space of n–dimensional input variables $X_1, X_2, \ldots, X_n$ be given by:

$$G = g(X_1, X_2, \ldots, X_n) = 0 \quad (19)$$

Also,

Let the vector of the be random variables with second moment statistics $E(X)$ and $Cov(X, X')$ be $X = [X_1, X_2, \ldots, X_n]'$

The normalized random variables $y_1, y_2, \ldots, y_n$ are introduced by a suitable one to one linear mapping $X = L(y)$ such that $y = L^{-1}(X)$. The corresponding space of y is then defined by the transformation:

$$X = L(y), y = L^{-1}(X) \quad (20)$$

Applying equation 20 maps equation 19 into:

$$h(y_1, y_2, \ldots, y_n) = 0 \quad (21)$$

Where the function h is defined by:

$$h(y) = g[L(y)] \quad (22)$$

Equation (22) represents the failure function in normalized coordinate. The mean value of y is the origin and the projection of y on the arbitrary straight line through the origin is the random variable with the standard deviation of unity.

The reliability index β is the distance between the origin and the failure surface in the normalized coordinate. It is given by:

$$\beta = \min\left(\sqrt{\Sigma(y_1^2 + y_2^2 + \ldots + y_n^2)} \,|\, h(y_1, y_2, \ldots, y_n)\right) = 0 \quad (23)$$

Equation (23) is minimized subject to the constraint that $h(y_1, y_2, ..., y_n) = 0$. The design points on the failure surface are obtained by optimization.

In First–Order reliability method, all non–normal random variables must first be transformed to their equivalent normal random variables before they can be used. This requires that the distribution function of the basic variable and the equivalent normal variable are equated at the design point as:

$$\Phi\left(\frac{x_i^* - \mu_{xi}^N}{\sigma_{xi}^N}\right) = Fx_i(x_i^*) \quad (24)$$

where $\Phi(\cdot)$ = cumulative distribution function of the standard normal variable at the design point; μ_{xi}^N, σ_{xi}^N = mean and standard deviation of the equivalent normal variable at the design point respectively; $Fx_i(x_i^*)$ = cumulative distribution function of the original non–normal variables.

The mean of the equivalent normal variable at the design point is given by:

$$\mu_{xi}^N = x_i^* - \Phi^{-1}[Fx_i(x_i^*)]\sigma_{xi}^N \quad (25)$$

The distribution function of the basic variable and the equivalent normal variable are equal at the design point:

$$\frac{\varphi}{\sigma_{xi}^N}\left(\frac{x_i^* - \mu_{xi}^N}{\sigma_{xi}^N}\right) = fx_i(x_i^*) \quad (26)$$

where $\varphi(\cdot)$and $fx_i(x_i^*)$ = probability distribution function of the equivalent standard normal and the original non–normal random variable respectively.

Applying equation 25;

$$\Phi^{-1}[Fx_i(x_i^*)]\sigma_{xi}^N = x_i^* - \mu_{xi}^N \quad (27)$$

Applying Equation (26), the standard deviation of the equivalent normal variables are given as:

$$\sigma_{xi}^N = \varphi\frac{(\Phi^{-1}[F_{xi}(x_i^*)])}{fx_i(x_i^*)} \quad (28)$$

RESULTS AND DISCUSSION

The results of the MATLAB program automated reliability analysis of a doubly symmetric I–section steel beam are presented in Figure 1 to Figure 6 respectively and Table 2.

Table 2: Values of plastic section modulus (m^3) for varying load ratios obtained from code–based design and reliability–based design at target reliability indices of 3.0 and 3.80

Load Ratio	0.5	0.75	1.0	1.25	1.5	1.75	2.0	2.25
BS 5950: Part 1 (1985)	1472	1696	1919. 9	2143.9	2368	2591.6	2816	3040
RBD (Beta = 3.0)	1520	1720	1920	2120	2288	2560	2768	2928
RBD (Beta = 3.8)	1744	1960	2192	2424	2640	2880	3136	3360

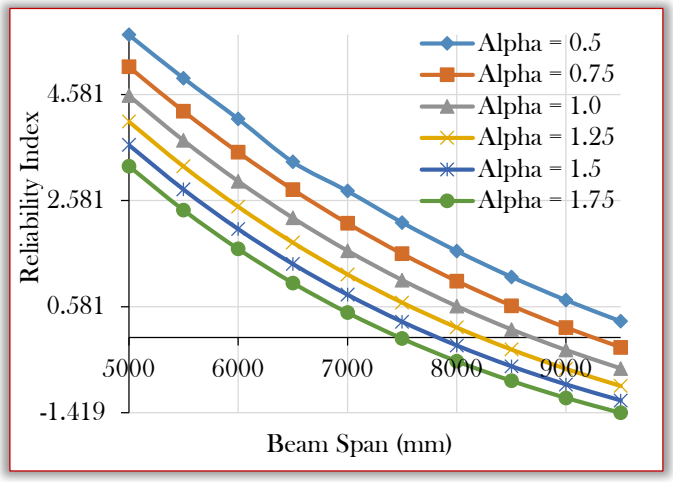

Figure. 1: Relationship between reliability index and beam span for varying load ratio (Bending limit state)

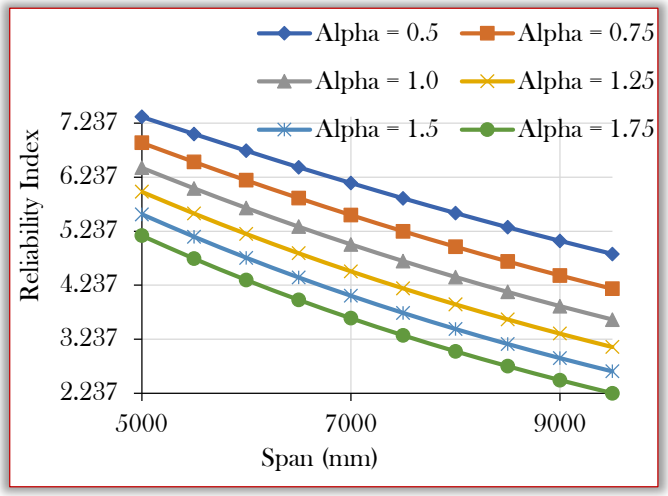

Figure 2: Relationship between reliability index and beam span for varying load ratio (Shear limit state)

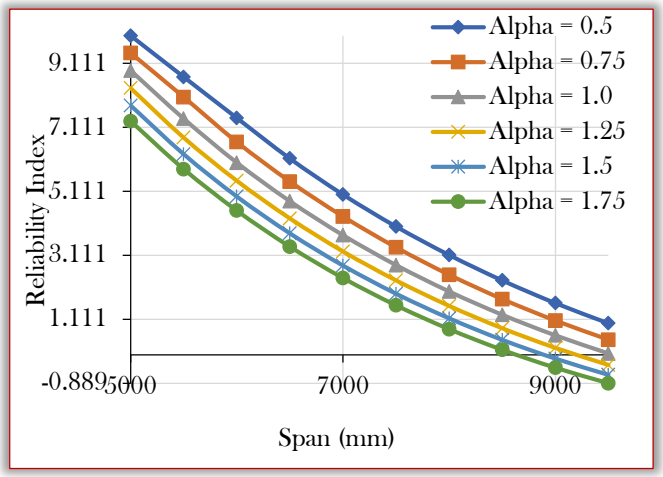

Figure 3: Relationship between reliability index and beam span for varying load ratio (Deflection limit state)

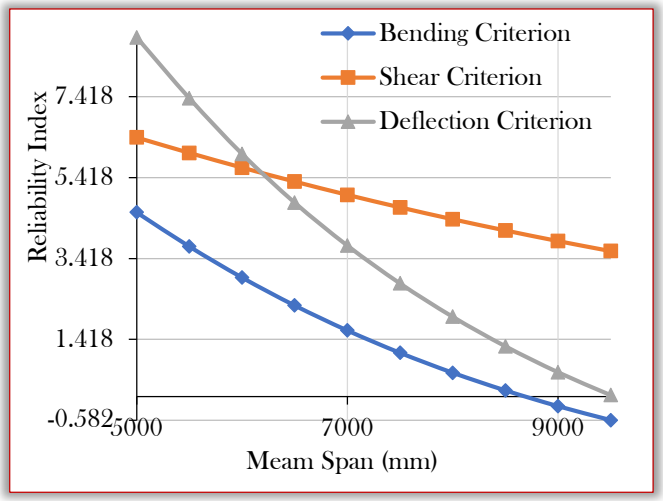

Figure 4: Relationship between reliability index and beam span for varying load ratio (Bending, shear and deflection limit state)

The MATLAB code employed in this study yielded the reliability indices for the bending, shear, and deflection limit states. These indices were determined through the utilization of the first–order reliability method. The obtained results are showcased in Figure 1 to Figure 3 which demonstrate the relationship between the reliability indices and varying load ratios for each limit state. It is evident from the figures that an increase in beam span and load ratio led to a decrease in the reliability indices for the bending, shear, and deflection failure modes. This observation aligns with the conclusions drawn by [13] who found that safety levels decline with an increase in beam span and load ratio.

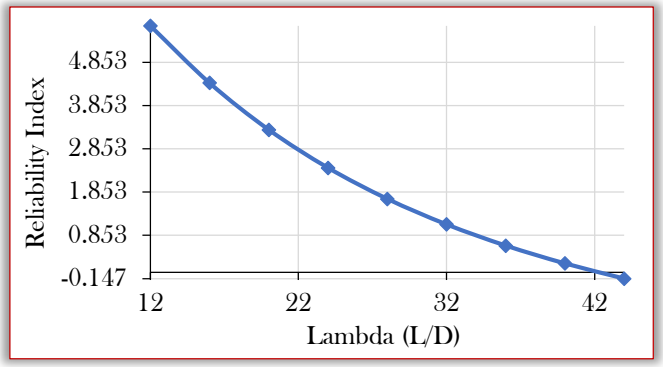

Figure. 5: Relationship between reliability index and lambda at alpha = 1.0 (Shear Limit State)

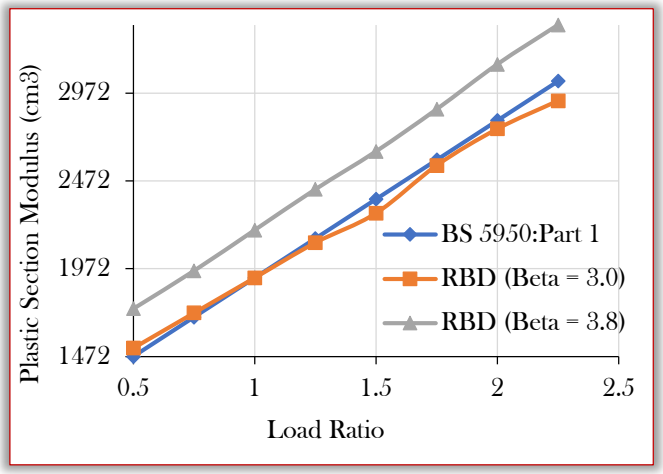

Figure 6: Relationship between load ratio and plastic section modulus values for deterministic and reliability based design

Based on the data presented in Figure 1, it can be seen that the safety indices ranged from –1.419 to 5.708, with an average value of 3.145. Similarly, Figure. 2 showcases the implied safety indices from 2.237 to 7.357, with an average value of 4.798. Furthermore, Figure 3 demonstrates that the implied safety indices vary from –0.889 to 9.98, with an average value of 4.546. Notably, Figure 1 to Figure 3 shows that the average values of the implied safety indices for shear and deflection limit states exceed the recommended range of the target safety index, which is 3.3 to 3.7, for structures with minor to large consequences of failure [14]. In addition, for beam spans beyond 8.5m and load ratios surpassing 1.0, the safety of the beam cannot be ensured as indicated by the negative values of the safety indices [13, 15].

Figure 4 illustrates the range of implied safety indices for the bending limit state, which extends from –0.582 to 4.561, with an average value of 1.990. Similarly, for the shear limit state, the implied safety indices vary from 3.601 to 6.412, with an average value of 5.007. Additionally, the values of the implied safety indices for the deflection limit state range from 0.0399 to 8.87, with an average value of 4.455, as portrayed in Figure 4. Figure 5 depicts the correlation between the safety indices and the beam span–overall depth ratio (Lamda) at a constant load ratio of 1.0. The data from Figure 5 reveals a clear decrease in the reliability index as the beam span–overall depth ratio increases. It is crucial to emphasize that exceeding a beam span–overall depth ratio of 42 would compromise the safety of the beam, as indicated by the negative value of the reliability index. These findings align with the conclusions drawn by [16] which underscore the threat posed to the beam's safety by the negative values of the reliability indices. Hence, when the load ratio is 1.0 and the beam span measures 8.5m, it can be deduced that the design is crucial in terms of bending, secure in deflection, and satisfactory in shear. Additionally, the probabilistic design of the doubly symmetric beam was executed under the bending limit state, considering predefined reliability indices of 3.0 and 3.8, correspondingly. The deterministic values of the plastic section modulus were compared with the design values based on reliability, yielding the outcomes displayed in Table 2.

It can be clearly seen from the Table, that the beam's deterministic and probabilistic design was carried out to establish the plastic section modulus at various load ratios, namely 0.5, 0.75, 1.0, 1.25, 1.5, 1.75, 2.0, and 2.5. It is apparent that for load ratios of 0.50 and 0.75, with a target reliability index of 3.0, the plastic section modulus experiences an increase of 3.3% and 1.42% correspondingly.

At load ratio of 1.0, the values of the plastic section modulus are almost identical. However, at load ratios of 1.25, 1.5, 1.75, 2.0 and 2.25, the readings of the plastic section modulus reduce by 1.13%, 3.49%, 1.23%, 1.73% and 3.83% respectively. This results to savings in the quantity of materials of I–steel beam. As the beam was designed for a target reliability index of 3.80 to reflect the consequences of failure for 50 years design period, the values of the plastic section modulus of the beam increases by 18.5% for 0.5 load ratio, 15.6% for 0.75 load ratio, 14.2% for 1.0 load ratio, 13.1% for 1.25 load ratio, 11.5% for 1.5 load ratio, 11.1% for 1.75 load ratio, 11.4% for 2.0 load ratio and 10.5% for 2.25 load ratio respectively.

CONCLUSIONS

The findings of the probabilistic evaluation of a doubly symmetric I–steel beam in relation to the limit state of bending, shear, and deflection, as per the design requirements outlined in [12] have been presented. The reliability estimates were obtained using a MATLAB automated program developed based on the First–Order Reliability Method. It was observed that the reliability indices decreased as the load ratio and beam span increased for the bending, shear, and deflection failure modes under consideration. It is not advisable to exceed a beam span of 8.5m and a load ratio of 1.0, as these values yielded negative safety indices.

When the load ratio was kept constant at 1.0, the reliability index decreased as the beam span–overall depth ratio increased. A beam span–overall depth ratio exceeding 42 would compromise the safety of the beam. The analysis showed that the design is critical in terms of bending, safe in terms of deflection, and satisfactory in terms of shear. The probabilistic design results for the plastic section modulus of the beam in bending, targeting a reliability index of 3.0 and a constant load ratio of 1.0, indicated material savings for the I–steel beam by considering different beam section choices based on the plastic section modulus values. However, when the beam was designed for a target reliability index of 3.80 to account for failure consequences over a 50–year design period, the values of the plastic section modulus of the beam increased.

Acknowledgement

We would like to thank the Department of Civil and Environmental Engineering for creating the environment that enabled the study to be carried out.

References

[1] Sule, S., Okere, C., Awodiji, C.T.G. (2022). Reliability assessment of a fully laterally restrained steel floor beam to Eurocode 3. World Journal of Engineering and Technology, 10, 626–638, 2022

[2] Mosley, W.H. and Bungey, J. H. Reinforced concrete design. 5th edition, Macmillan Limited, London.

[3] Melchers, R. Structural reliability analysis and prediction. Second Edition, John Wiley and Sons.

[4] Benu, M. J., Sule, S. (2019). Reliability analysis of a solid timber column subjected to axial and lateral loading. Journal of Engineering and Technology, 4(2), 1–5,

[5] Cheng, K., Weng, G., Cheng, Z. (2023). Influence of load partial factors adjustment on reliability design of RC frame structures in China". Scientific Reports. 13, 7260,

[6] Xiaojun, W., Qinghe, S., Fan, W., Ruixing, W., Lei, W. (2019). Comparison of the reliability–based and safety factor methods for structural design. Applied Mathematical Modelling, 72, 68–84
[7] Esmaeil, M. D., Pouria, S., Vahid, B., Amir, H., G. (2023). Reliability–based design optimization of post–tensioned self–centering rocking steel frame structures, Journal of Building Engineering, 75, 106955–106955
[8] Junho, C. (2021). Reliability–based design optimization of structures using complex–step approximation with sensitivity analysis. Applied Sciences, 11(10):4708
[9] Jerez, D. J., Jensen, H. A., Michael, B. "Reliability–based design optimization of structural systems under stochastic excitation: An overview". Mechanical Systems and Signal Processing, 166:108397, 2022
[10] Pinghe, N., Jun, L., Hong, H., Weimin, Y., Xiuli, D., Hongyuan, Z. "Reliability analysis and design optimization of nonlinear structures". Reliability Engineering and System Safety, 198:106860, 2020
[11] Cardoso, F. S., Zhang, H., Rasmussen, K. J. R. (2019). System reliability–based criteria for the design of steel storage rack frames by advanced analysis: Part II – Reliability analysis and design applications". Thin–walled Structures, 141, 725–739
[12] BS 5950–1. "Structural use of steelwork in building". British Standard Institution, 1985.
[13] Abubakar, I., Peter, H.P. (2012). Failure investigation of reinforced concrete cantilever retaining walls". Nigerian Journal of Technology, 31(3), 248–260.
[14] JCSS. "Probabilistic model code". Publication of Joint Committee on Structural Safety, 12th draft, 2001.
[15] NKB. "Recommendations for loading and safety regulations for structural design". Nordic Committee on Building, Report, No. 36, 1978, Press Limited, London.
[16] Abejide, O.S. (2014). Reliability of bending, shear and deflection criteria of reinforced concrete slabs". Nigerian Journal of Technology, 33(3), 394–400,

ISSN: 2067-3809

Fascicule 2
[April – June]
tome XVII
[2024]

ACTA Technica CORVINIENSIS
BULLETIN OF ENGINEERING

ISSN: 2067-3809

ACTA TECHNICA CORVINIENSIS – Bulletin of Engineering | e–ISSN: 2067 – 3809
Tome XVII [2024] | Fascicule 2 [April – June]

[1.] **Vishnu Kumar SINGH**

ASSEMBLY AND PACKAGING IN CORRUGATED BOXES TO ENHANCE PRODUCTIVITY

[1.] Department of Mechanical Engineering (Maintenance), IIMT College of Polytechnic, Pradesh, INDIA

Abstract: This project investigates productivity linked assembly in the paper industry, with a focus on the production of corrugated cardboard boxes. The research encompasses the entire production process, from the sourcing of raw materials to the manufacturing and quality testing of the final product. The primary raw material for this industry is wood, which is currently facing a shortage due to environmental concerns. The study aims to understand how industries are managing the shortage of high–quality, cost–effective products. It delves into packaging issues, discussing them with manufacturers, and subsequently develops constraint models to address these issues. In the production process, boxes of varying sizes are made to accommodate different packaging needs. These boxes undergo rigorous testing for tear strength and compression resistance to ensure their durability. Modifications are made during the manufacturing process, such as altering flute sizes and layering panels both vertically and horizontally, to enhance the box's strength. Once produced, the boxes are tested for their suitability within the industry. The study concludes by proposing measures to alleviate constraints faced by entrepreneurs and the food industry, such as the implementation of digitalization and the establishment of supplier agreements.
Keywords: paper packaging, sourcing, constraints, testing, cost

INTRODUCTION

In the current scenario, paper is required due to its easy use in the manufacturing process and helps in paper packaging of various products and solves the problem of unemployment. The leading role of paper in mass communication and education is positive. On the one hand, it is the basic raw material of the paper packaging industry; On the other hand, the printed press needs it for advertising purposes and the industry invests heavily in advertising to attract the attention of customers and also increase product sales easily. Greater awareness is needed from consumers and the industry to fully appreciate this type of revolution. There is another segment in this paper industry.

One of them is raw material manufacturers like paper mills that use pure bamboo which is mainly available in South India and some industries like Orient Paper Mills, Sandeep Paper Mill, Andhra Paper Mills and Star Paper Mills. In the production of the boxes, raw materials such as silicates, adhesives to attach the paper and threads to sew the boxes are used. These industries are more of a small sector covering 60–70% of the demand in the MSME sector and agencies are conducting research in this area as new packages are introduced for adaptation. Due to the advanced techniques available in the manufacturing sector for mass production, the high demand is mainly in the food processing industry to save money and extend the shelf life of canned products.

PROBLEM STATEMENT

When packing materials in boxes, the tear strength of the paper is not tested and papers of different weights are used, for example from 80 to 140 grams. The use of heavier paper weights affects the cost of corrugated boxes because the boxes can support this weight. No advanced techniques are used during the manufacturing process to increase strength, which can be achieved by using narrow flutes in vertical and horizontal gluing in smaller layers such as 3–layer, 5–layer and 7–layer. During the corrugation process, flutes of different sizes need to be made, saving paper costs.

By procuring the raw material in the right quantity, in the right quality, at the right price and at the right time, sales and marketing strategies can be planned through the use of production, packaging and transportation capacities, which is not done correctly. A case study of fruit packaging is carried out to reduce not only the product cost but also the cost of paper raw materials. If a corrugated box is of inferior quality, it may be damaged and the entire product stored in the box may not meet company standards.

ADDITIONAL CHALLENGES IN PAPER INDUSTRY

- Increase in raw material costs. In the area of flexible packaging, the prices for these raw materials have recently risen significantly. Due to tight supplies, prices for polypropylene, used in resins, bottles and packaging films, are also rising.

- Perishability of the contents. Flexible packaging companies are not only under pressure to innovate their offerings, but at the same time must ensure that their products are designed to protect the contents of the packaging from the external environment.
- The industry's problems are mainly due to the shortage of raw materials in the country. With the increase in population, the use of all types of wood is constantly increasing.
- Most industrial facilities are located in remote locations that rarely attract the attention of the younger generation. This leads to a labor shortage, which further impacts the industry's production.
- The Indian paper industry is facing one of the most difficult phases in history due to the novel coronavirus (Covid–19) pandemic that has impacted supplies, hampered by unavailability of shipping containers and import of huge quantities of handicrafts is exacerbated by China importing paper from India.

OBJECTIVE OF THESIS

Given the size of the paper packaging industry in India, constraints on inputs, processing and marketing need to be removed for rapid development.

Considering the above perspective, the objectives of the study were set as follows:

- A study on the limitations of the Indian paper packaging industry in terms of input, processing and marketing.
- Propose measures to eliminate constraints and promote industrial development.
- Develop models for a potential packaging entrepreneur considering factory size, demand forecasts, cost structure, investments, product range and supplier relationships/contracts.

Generally, flutes A and B are used (Figure 1). The performance of the plate depends on the type and direction of the flute, which depends on the type and weight of the item packaged.

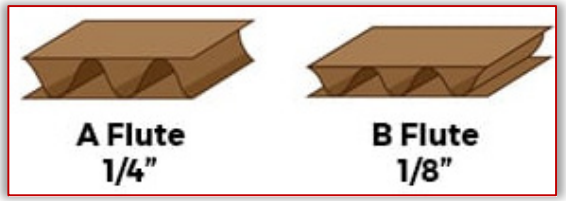

Figure 1: Flutes A and B

Generally, the flutes (Figure 2) in the box are vertically oriented to ensure maximum resistance to insertion. A–flute is used when top–down compressive strength is important, such as for non–load–bearing products stacked high in a warehouse. Fragile items are also packed in Type A corrugated boxes. High–density products are best packaged in B–fluted boxes. The C–flute design is a compromise between A and B–flutes with pretty good stacking resistance and notable rigidity for the E–flute is used for special purposes and is not as common as A and C flutes. Double–layer and multi–layer corrugated cardboard (Figure 3) can combine two or more groove types to achieve better properties and performance.

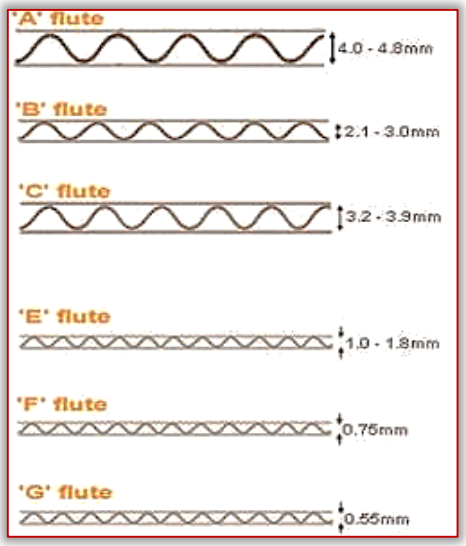

Figure 2: Types of Flute

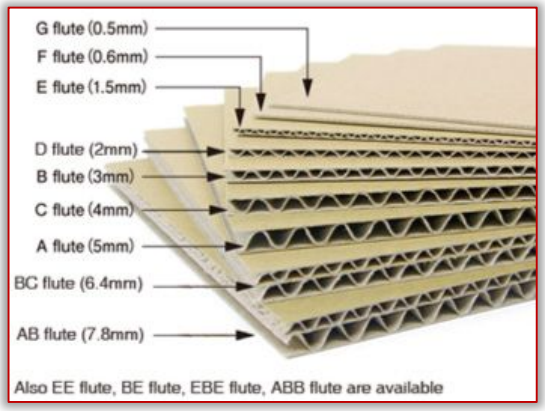

Figure 3: Flutes in corrugated cardboard

METHODOLOGY

In this method, paper is used as a raw material along with glue in a machine to make corrugated boxes (Figure 4). In the previous cases, the box produced was designed to have only horizontal flutes. Therefore, the resistance of the box was not technically increased by using the flutes vertically and horizontally, increasing the resistance by 5 or 7 layers and using different sizes and types for this purpose. (Figure 5).

Applying the flute in the manufacture of the box not only saves cost, but also conserves the food product stored in the box, as the search includes

the guava fruit in the search and finds it in different patterns (Figure 6) with different weights, resulting in a cost–effectiveness ratio. Also, height of flutes and number of flutes per linear meter was noted (Figure 7). Various testing machines were used, such as burst strength testers, vibration machines and other machines.

Figure 4: Corrugated cardboard roll

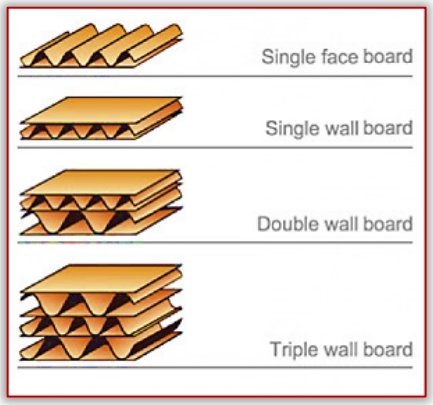

Figure 5: Types of corrugated board

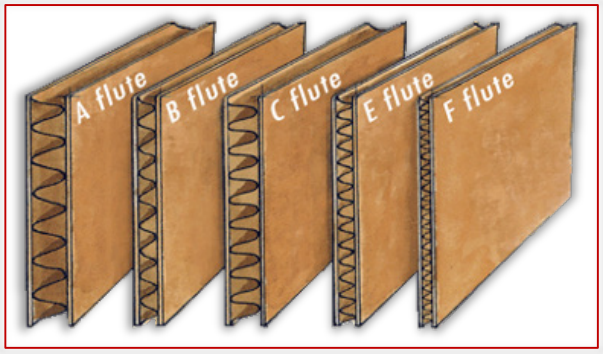

Figure 6: Different patterns of corrugated box

Flute Type	Height of Flute In mm	Number of Flutes per linear meter
A-flute	0.187	36+3
B-flute	0.098	51+3
C-flute	0.130	42+3
E-flute	0.036	96+3

Figure 7: Flute Type details

RESULT ANALYSIS

The researcher visited 30 industries, including 10 large industries, which were asked to complete the questionnaire. Responses were received from only three sectors. The data collected from the completed survey is presented in the table. It is observed that capacity utilization is different across the three sectors due to delay in procurement of raw materials and unavailability of quality packages on time. The boxes were damaged during distribution/physical transportation and adequate testing was not performed. The corners of the boxes were damaged and the boxes were open due to the poor quality of the sewing thread used. This shows that technical issues are not taken into account. Appropriate testing machines should be used.

RESEARCH FINDINGS & LIMITATIONS

This study prioritized the main issues related to the objective, taking into account all factors affecting cost, distribution, quality and technical measures. Test results show that for guava packaging, a vertical flute height of 0.273 resulted in a 98% improvement in breakage rate. This shows that packaging quality can help reduce guava packaging losses during transportation. The study suggests quality and improvement.

The packaging industry in India is far behind that of developed countries. There is a great need for rapid development of the packaging industry in India. The need for industrial development in India can be fully understood if one considers that almost 20–25% of fresh fruits and vegetables, 30% of animal products including dairy and meat products, 10–11% of cereals and 7% of the food produced, 10% of cement, chemical and industrial products are lost due to inadequate packaging.

Our economy is still largely based on agriculture. Recognition of the need to modernize the agricultural industry and give further impetus to the agricultural sector. It is estimated that a strong food processing sector would help accelerate agricultural activities as well as diversification and marketing of agricultural products, channeling them towards increasing exports on the one hand and creating more opportunities to improve nutrition, employment and income generation in rural areas.

A diverse agricultural sector with different soils and climates provides an increasingly broad raw material base suitable for the production of a rapidly expanding range of processed foods.

Rapid urbanization, increasing numbers of working women and increasing per capita income have contributed to rapid growth and changing demand patterns. India offers huge investment and growth opportunities in the processed food sector.

CONCLUSION & RECOMMENDATION

After passing the tests, you need to pay special attention to the technical aspects and use the right raw material, such as: when sewing, if the thread is not of required quality, it will destroy the item packed in the box. During packaging and testing, it was found that the corners of the packed boxes were damaged by non–technical activities. It is therefore recommended to carry out proper planning before starting production. It has been observed that the entire process is carried out on mechanically operated machines. Therefore, efficiency is interrelated during the production process in the paper industry.

Further analysis of paper availability is needed as it impacts costs and destroying more trees creates problems for the paper industry. The availability of raw materials is currently at risk. Therefore, it is necessary to protect the environment in order to increase the production of food and reduce the cost of the production process. Therefore, more research is needed to save the country revenue. Because currently this sector plays an important role in creating jobs for people and, according to literature analysis, can generate good incomes.

References

[1] Annual Report (1999–2000), Indian Council of Agricultural Research, New Delhi.
[2] Annual Report (1998–99), I.C.A.R New Delhi.
[3] Agro Climatic Regional Planning, Planning Commission, ARPU Working Paper No 10, August 1998.
[4] Althen P.C, The Aluminum can Fd.Technol, 1965,102,794.
[5] Anon (1960) Outlook Bright for thin Tinplate in clash with Aluminum cans, Steel, 147, No 24 , 109–11.
[6] Anon (1967) Modern Packaging (40),(9),95.
[7] Anon PET, its time has come ,Food Engineering International, March 1985,40
[8] Anon,(1984) Retortable plastic cans ,Food Engineering,56(4).58
[9] Anandaraman S, Reinecium GA (1980) Microencapsulation of flavors.– Food flavouring, ingredients, packaging and processing 1(9)14.
[10] Anon (1981) sealed in flavors Food–Flavoring, in ingredients, processing and packaging 3(12)23.
[11] https://www.thehindubusinessline.com/markets/commodities/how–the–paper–industry–has–been–affected–by–the–3–c–factors/
[12] https://www.flexpackmag.com/articles/90214–four–challenges–facing–flexible–packaging
[13] http://www.amkur.co.in/my–blog/the–challenges–faced–corrugation–industry–in–india
[14] https://www.printweek.in/features/corrugated–box–industry–grappling%C2%A0with–price–hikes
[15] Briston.J.H and Katan (1974).L.Lplastics in contact with Food Trade Press Ltd. London.
[16] Briston J.H& GOSSELIN C.C (1968) Introduction to Plastics, Newness–Butterworth, London.
[17] Cellulose Films in Packaging, Indian Institute of Packaging, Bombay.
[18] Balasubramnyam, N Indiramma. A.R and Anandaswamy, B., Evaluation of the shelf life of packed salty biscuits Indian Food Packer, 1981, 35, No,6, 14–19.
[19] *** Effect of Packaging on Quality of Sohan Halwa During Storage Journal of Food Science and Technology, 1984, 21, No.3,167.
[20] *** Facts Figures, National Horticultural Board, Ministry of Agriculture, Govt. of India, Gurgaon.
[21] *** Guide to Tinplate, International Tin Research Institute, Publication no.622, England, P.11.
[22] *** Glass Containers in Packaging Indian Institute of Packaging, Bombay.
[23] Hanlon, J.F,(1971) Handbook of Packaging Engineering Mc Grow Hill Book company New York
[24] Hoare, W.E, Hedges, E.Sand, Barry .B.T.K, The Technology often plate

ISSN: 2067–3809

ACTA TECHNICA CORVINIENSIS – Bulletin of Engineering | e–ISSN: 2067 – 3809
Tome XVII [2024] | Fascicule 2 [April – June]

[1.] Alexandru Constantin NECHIFOR, [2.] Raul–Bogdan MIRCEA, [3.]Dan Ovidiu GLĂVAN, [4.]Theoharis BABANATSAS

ANALYSIS OF THE IMPACT OF QUALITY COSTS IN THE MANUFACTURING PROCESSES OF ROMANIAN COMPANIES

[1–4.]"Aurel Vlaicu" University of Arad, ROMANIA

Abstract: The main purpose of the research is to provide a deep understanding of the costs of quality and to propose practical solutions for improving the performance and efficiency of the manufacturing processes of Romanian companies. This aims to increase market competitiveness and improve financial results through effective quality management. Starting from a specific condition in SMEs from Romania, the pattern presents an operational structure specialized in quality monitoring, traceability and statistical control, based on integrated module in general software. Data is collected and monitored in real time and the system ensures quality compliance at all stages of production. Through its modern functionalities blockages are eliminated, waste of time is avoided, materials and money are saved, and, finally, it strengthens the business partnerships and the company's position in the market. Results regarding particular implementation are preserved. Using data is collected and monitored in real time and the system ensures quality compliance at all stages of production.

Keywords: Quality Monitoring, Integrated software, SME, quality continuous improvements, PCB Production

INTRODUCTION

The paper focuses on evaluating and understanding how the costs associated with quality influence the performance and efficiency of production processes in Romanian companies. This involves a detailed analysis of quality costs, which include prevention costs, evaluation costs, internal defect costs, and external defect costs. The objectives are represented by:

- identifying the types of quality costs,
- assessing the impact of quality costs, respectively
- determining the relationship between quality costs and organizational performance.

The main purpose of the research is to provide a deep understanding of the costs of quality and to propose practical solutions for improving the performance and efficiency of the manufacturing processes of Romanian companies. This aims to increase market competitiveness and improve financial results through effective quality management.

At the present time, research on the impact of quality costs in the manufacturing processes of Romanian companies is in a variable stage of development in Academic Studies. There are various academic studies and doctoral theses that explore the topic of quality costs in the context of Romanian industry, most of them focusing on theoretical aspects and case studies.

MATHERIALS AND METHODS

The structure of the quality cell depends on the size and nature of the enterprise. In small companies, this is often reduced to one person, while in companies with more than 200 employees, quality management is done by a team whose staff is on average 1% of the total employees. In companies with thousands of employees, we often find a central department and quality departments with the following structure: product design; supply chain; production; after sale; administration.[1]

Improving quality means, among other things, making less faulty products with same amount of effort or cost, which usually gives a lower unit cost.[2]

According to standards ISO 9000 – 20000, the quality costs represent the costs that are made in order to achieve the targeted quality, ensuring the customer's trust and assuming the losses when the targeted level of quality is not reached

Quality tools are essential for ensuring and continually improving quality within any organization. These tools help identify problems, analyze causes, and implement solutions. Here is an overview of the most common and essential quality tools:

- Ishikawa Diagrams (Cause–and–Effect Diagrams or Fishbone Diagrams): These diagrams are used to identify and visualize possible causes of a specific effect or problem. They help organize and systematize ideas, making it easier to identify root causes.

— Flowcharts: Flowcharts are used to graphically represent a process. They help in understanding the steps of a process and identifying potential points for improvement.
— Pareto Chart: A Pareto chart is a graphical representation that shows the most significant factors in a data set. It is based on the Pareto Principle (80/20 rule), which states that 80% of problems are often due to 20% of causes. This helps prioritize issues to address the most impactful ones first.
— Control Charts: Control charts are used to monitor processes over time and identify any variations from the standard. They help in distinguishing between common cause variations and special cause variations, facilitating process control and improvement.

RESULTS AND DISCUSSION

In terms of the number of employees, in 2024 it remained approximately the same as in 2023 in almost two thirds of companies (67.84%), the share of companies that recorded slight increases in the number of employees compared to the previous year was of 17.42%, and the share of companies that registered a slight decrease was 6.74%

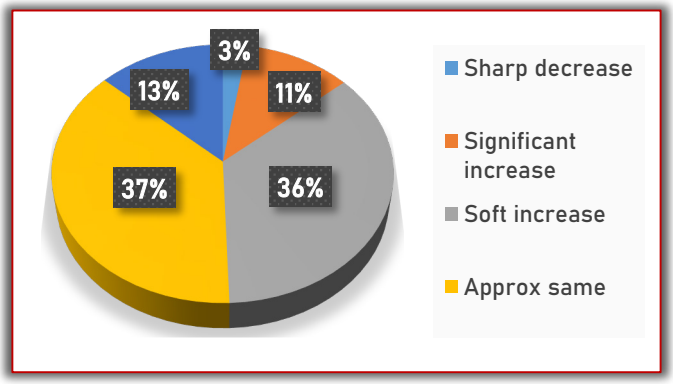

Figure 1. Physical volume of sales

Physical volume of sales represents the actual amount of products sold in a specific period, measured in physical units (eg kilograms, liters, pieces, etc.), in contrast to the value of sales, which is measured in units monetary.

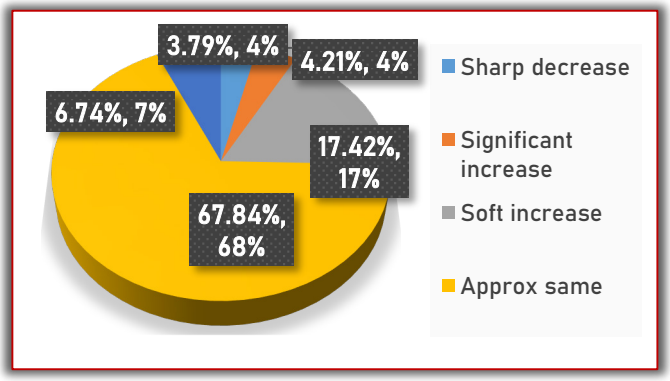

Figure 2. No. of employees

The export analysis shows that 62.5% of the companies registered exports approximately equal to those of the previous period, and only 20.54% of them had slight increases.

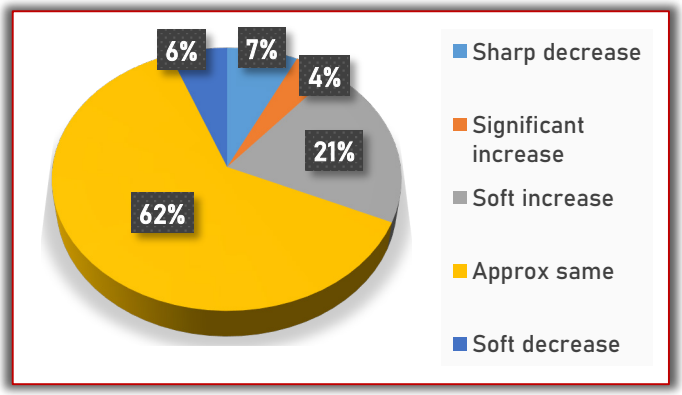

Figure 3. Export analysis

The evolution of the profit size shows that 39.66% of the companies registered stagnation regarding this indicator, and 34.88% of the companies had a slight tendency to increase the size of the profit.[3]

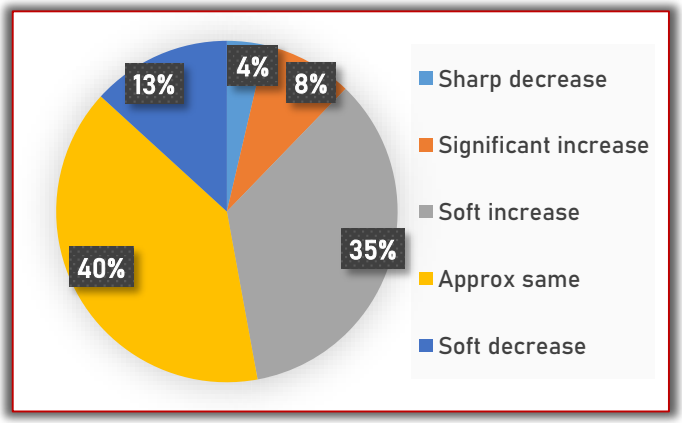

Figure 4. Profit size

A key element that has significantly contributed to economic growth in recent years is the ability of Romanian companies to adopt and use a management capable of responding quickly to complex environmental challenges, in terms of flexibility and adaptability. In 2023, the capacity of the company's management to cope with the environment and the complex economic situation in Romania was appreciated as being of average level within SMEs. Thus, a directly proportional link can be seen between the size of the enterprise and its ability to adapt to current economic challenges. Thus, only 11.87% of respondents consider this capacity as high, 45.29% consider this capacity as medium or low (22.24%).[4]

Since 1987, when the ISO 9000–9004 series appeared, the concept of quality policy has been classified along with the evolutions they have had in managerial theory. The policy of a company, including the quality policy, is in

connection with the strategic management of the organization, an aspect emphasized by Igor Ansoff since 1976.[5]

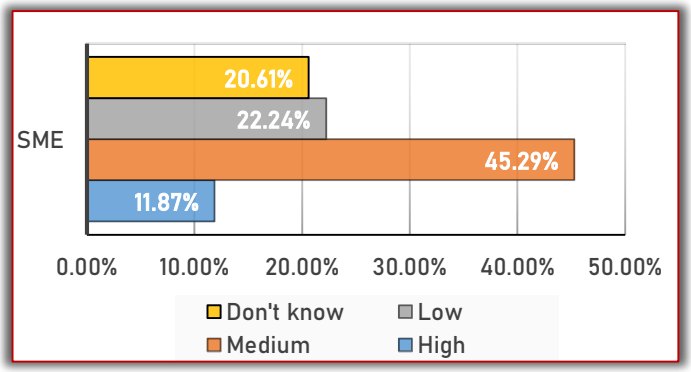

Figure 5. Management`s ability to respond to challenges in 2023

Strategic management is defined as a systematic approach that aims to substantiate and achieve the company's objectives. The rationale for strategic leadership answers the questions WHERE you want to go, WHAT is the reason for being, WHAT it aims to be, HOW it will be achieved. The structuring of the managerial philosophy (including quality) is done according to the answers it must give in vision, mission, policy and strategy.[6]

The solution proposed: The main software used is SAP, in which we included our modulated program, represented by a database.

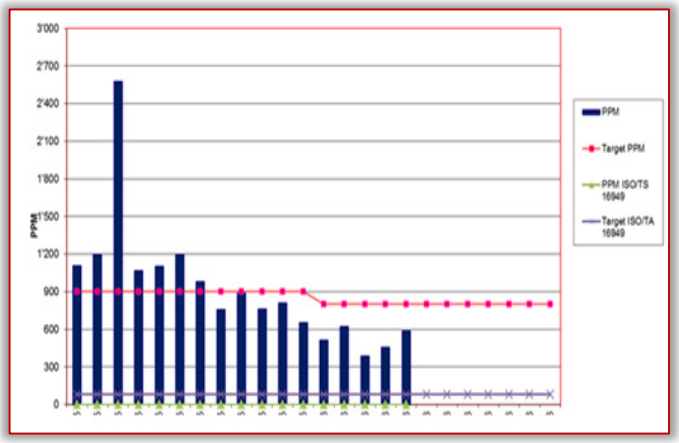

Figure 6. Evolution chart of PPM customers

In order to gain the competitive advantage, the most important component of the strategy, companies must pay attention to the strategic objectives and options that must be based on diagnosis, market research and the subordination of national strategies.

The development of a managerial strategy, including the philosophy of quality, requires outlining a vision of the future state of the system. To run a business, you need both an overview and a vision of quality

Although all these programs are powerful, we considered it a challenge to create a program module focused exclusively on quality and that integrates perfectly with the main software.

CONCLUSIONS

After implementing this software, we noted the first improvements: Research shows that effective quality cost management has a significant impact on the operational and financial performance of firms. Quality costs, if well managed, can significantly reduce losses and improve firms' competitiveness in the global market.

As proposals we highlight:

- Continuous Research: Promoting continuous research in the field of quality costs to develop new and more effective management methods. This research should include case studies from various industries to provide a complete picture.
- Government Policies: Authorities should support quality management initiatives through incentive and funding policies, encouraging companies to invest in quality.
- Knowledge Sharing Platforms: Creating national platforms for sharing knowledge and experiences in the field of quality, where firms can learn from each other and implement best practices.

Studies show that an appropriate balance between the costs of prevention, evaluation and defects is essential. Investing in prevention and assessment is more effective in the long term than managing defects, both internal and external

Companies that invest in quality and improve manufacturing processes not only reduce the cost of defects, but also benefit from a better reputation and increased customer loyalty.

References

[1] Xenakis, DM Dunn, DS "Quality improvement via quality costs".(2023) – ASQC's 51st annual quality congress proceedings.
[2] Adrian, D. (2001). Managementul Proiectelor. Brasov: Disz Tipo.
[3] Dale E. Hall, Y. K. (1993). Proceedings of the Simposium on Quality Management.
[4] De Barrie, G. D. (2017). "Quality Costing", page 138. Taylor&Frances Group.
[5] Gogue, J. (1997). "Management de la Qualité". Paris : Ed. Economica.
[6] Harrington, H. J. (1987). Poor–Quality Cost,. American Society for Quality, OCLC 14965331.
[7] Hoyle, D. (2017). "Quality Management Essentials", page 25–26. Elsevier .
[8] Hoyle, D. (2017). "Quality Management Essentials", page 49, 145. Elsevier .
[9] Ionescu, C. (1997). Ëxcelenta industriala, practica si teoria calitatii. Bucuresti: Ed. Economica.
[10] Jens J. Dahlgaard, G. K. (n.d.). Fundamentals of Total Quality Management.
[11] Kevin Tatroe, P. M. (2013). "Programming PHP: Creating Dynamic Web Pages",Chapter 1. O'Reilly Media Inc.
[12] Mike Bourne, P. B. (2011). "Handbook of Corporate Management", page 167. John Wiley and Sons Ltd.

[13] Mike Bourne, P. B. (2011). "Handbook of Corporate Performance Management",page 81. Johnh Willey and Sons Ltd.
[14] Misiurek, B. (Taylor & Francis Group). "Standardized Work with Training Within Industry: Eliminating Human Errors in Production and Service Processes", page 4 . 2016.
[15] Montgomery, D. C. (2020). "Introduction to Statistical Quality Control", page 8. Wiley.
[16] O. Nicolescu, I. C. (2020). Starea de sanatate a managementului din Romania in 2019, Ed. A XI–A. Bucuresti: Ed. Prouniversitaria.
[17] Odeh, R. (n.d.). "Parts per Million Values for Estimating Quality Values", page v. CRC Press.
[18] Practices, T. K. (2021, December 22). https://solutionsreview.com/data–management/the–best–data–quality–tools–and–software/, .
[19] R. Chevalier, E. D. (1996.). "Le management de la qualite. Grenoble: Presses Universitaires de Grenoble.
[20] Tucu, D. (2016). Optimizarea Costurilor Calitatii in Sistemele Industriale. Timisoara: Eurostampa
[21] Zhu, L., Johnsson, C., Varisco, M., & Schiraldi, M. M. (n.d.). Key performance indicators for manufacturing operations management – gap analysis between process industrial needs and ISO 22400 standard. Proceedings of the 8th Swedish Production Symposium (SPS 2018).

ISSN: 2067-3809

ACTA TECHNICA CORVINIENSIS – Bulletin of Engineering | e–ISSN: 2067 – 3809
Tome XVII [2024] | Fascicule 2 [April – June]

[1.] **Michael C. EZEGBIRIKA,** [1.] **Samuel SULE**

COST OPTIMIZATION OF A DOUBLY REINFORCED CONCRETE BEAM

[1.] Department of Civil and Environmental Engineering, University of Port Harcourt, P.M.B 5323, Port Harcourt, Rivers State, NIGERIA

Abstract: In this research, the cost optimization of a simply supported doubly reinforced concrete beam with uniformly distributed load was performed under constraints from Eurocode 2. This research presents a relationship between the components of the reinforced concrete beam, its resultant manufacturing costs and the optimization model developed to minimize such costs. This relationship was constrained geometrically by real life estimates and behaviourally by conventions defined in Eurocode 2. Whilst the cost optimization procedure was carried out using Microsoft Excel, results from further analysis showed a direct relationship between the span, optimized costs and original costs. The relationship observed for the concrete class however, showed that an increase in the grade of concrete led to a decrease in the optimized and original costs.
Keywords: cost optimization, doubly reinforced concrete beam, Eurocode 2, optimization, real life estimates

INTRODUCTION

Reinforced concrete (RC), is one of the most commonly used materials for the construction of the built environment, and with that, reinforced concrete beams are one of the most ubiquitous structural element present in everyday life as every structure experiences flexure due to a combination of permanent (dead) and variable (live) loads. However, despite their common presence, very few of them are designed with the cost of their construction being put among top considerations.

The conventional design process of reinforced concrete members does not take into account the cost of the structural element. Usually a trial and error process is applied given that structural design is an iterative process. The first step in the design process is usually the making of the initial design, after which the designer makes an overall guess about the possible optimum solution consistent with his or her experience, knowledge, constraints, and requirements. The analysis of the structure is then carried out using initial design. Based on the results of the analysis, a re–design of the structure is carried out if any of the constraints is not satisfied. The efficiency of the design process depends heavily on the quality of the initial guess, which, if good, will reduce the number of analysis–design cycles. In the real–life design of the structures, it is inevitable to take into account the cost of the beams at some point when the structure is to be constructed. There is an absence of cost consideration when designing the structural element.

Related concepts to the focus of this research have been explored in previous literature. As seen in Ildiko, *et al*., (2010), which used the nonlinear programming approach (NLP) to optimize RC beams of rectangular cross–section. The objective function of the beam's construction costs was derived, including material and labor cost items. However, the paper did not provide a comprehensive account of how the optimization was carried out on the objective function with respect to the derived constraints.

Khaled, *et al*., (2004), which used STAAD III to design safe cross sections and Microsoft Excel to calculate steel and concrete quantities. A sensitivity analysis was also performed on the model.

Bhalchandra and Adsul (2012) conducted a cost optimized design of doubly reinforced beams with uniformly distributed and concentrated load. The results showed that the Genetic Algorithm technique generated a cost less than the GRG and Interior Point optimization techniques.

Galeb (2018) focused on achieving optimization objectives through simulated annealing, which mimics the thermal annealing of heating solids critically. When the temperature is reduced, the atoms tend to be ordered and form crystals with the minimum possible internal energy. This implies that the optimum cost of the beam always takes the minimum bounds of the specified constraints.

Antunes (2017) focused on optimizing shell structures using Building Information Modelling software. The heuristic used evaluates the possible solutions and selects the most suitable solutions. BIM allows for full integration between design and fabrication processes, as well as the

ability to store and manipulate multiple layers of object–oriented information.

The research by Salim, *et al.*, (2018) demonstrates the cost minimization of both singly and doubly reinforced concrete rectangular beam sections through the use of the Artificial Neural Networks Application. The derivation of cost coefficients for concrete and steel was not discussed.

With the background of the research and its literature explored, the scope of the research work is limited to the design of the beam with Eurocode 2 and optimizing it with an algorithm applied via an Excel spreadsheet and the thorough testing of the model.

The design of a doubly reinforced concrete beam with Eurocode 2 at ultimate limit state, with constraints placed by the code was the chosen approach. There was a mathematical modelling of the structure as a cost optimization problem. Microsoft Excel was used to run the numerical process to optimize the modelled cost.

The cost model was developed with a consideration of materials alone regardless of labour involved. An evaluation of the cost optimization procedure of the structure was limited with respect to an increasing span and various concrete classes.

As described earlier, cost considerations are often lacking when designing structural elements such as in this case, a doubly reinforced beam. In addition, most optimization methods tend to be only applied in concrete design and mixture proportions, with most of these methods not considering the costs of plain concrete, reinforcement and formwork costs as functions. These actions often have consequences later on in the life cycle of the project, as unforeseen changes can wield considerable influence over the cost of constructing the structural element. However, a great influence on cost can be achieved at the initial phases of the life cycle of the project.

In this paper, the cost optimization of a doubly reinforced concrete beam is carried out using the moment constraint of Eurocode 2 (2004).

MATERIALS AND METHODS

Materials

Eurocode 2 (2004) was used to develop a mathematical representation of a concrete structure. An Excel spreadsheet was used to set up the model and the optimization process was executed using Excel's Solver Tool.

Methods

— Development of the Objective Function

The total cost of constructing the doubly RC beam, is the sum of material costs required for the fabrication of certain constituents and construction of the entire member (Ildiko, *et al.*, 2010). Figure 1 shows the cross–section of a doubly reinforced concrete beam.

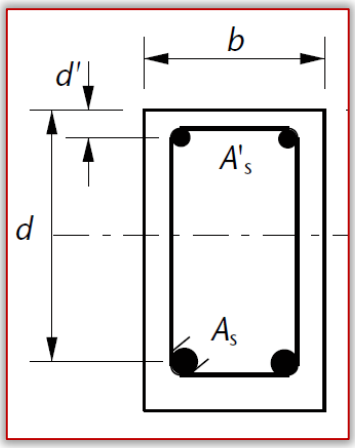

Figure 1: Section of a doubly reinforced concrete beam.

The objective function was derived as follows:

$$\text{Total Cost } (C_T) = c_c\left[\left(bh - (A_{sc} + A_{st})\right) \times L \times u_c\right] + c_s[A_{sc} + A_{st}] + c_f[b + 2h] \quad (1)$$

where:

C_T = Total cost of manufacturing the singly reinforced concrete beam.

c_c = Cost coefficient of concrete in cost per mass (naira per kg).

c_s = Cost coefficient of reinforcement steel, in cost per cross–sectional area (naira per mm²).

c_f = Cost coefficient of formwork, in cost per length (naira per m).

b = Width of the beam (mm).

h = Height of the beam (mm).

d = Effective depth of tension reinforcement bar (mm).

d^l = Effective depth of compression reinforcement bar (mm).

A_{st} = Total area of tension reinforcement steel (mm²).

A_{sc} = Total area of compression reinforcement steel (mm²).

L = Length of the beam (m).

u_c = Unit weight of concrete (kg/m³).

— Design Constraints

The stress–strain diagram for the doubly reinforced concrete section is shown in Figure 2.

The constraints developed included the behavioural constraints and geometric constraints. Given the nature of the structure, flexural constraints were the focus of the design constraints. The geometric constraints were

developed from realistic values of doubly reinforced beams in use.

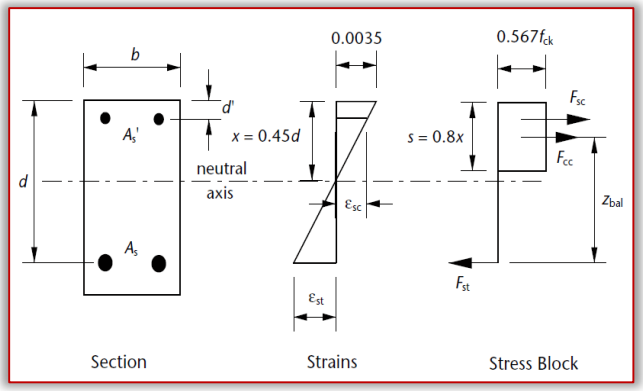

Figure 2: A doubly reinforced concrete section with strain diagram and stress block.

Behavioural constraints:

$$M_{bal} \leq M \leq M_R \quad (2)$$

$$K > 0.167 \quad (3)$$

$$\frac{x}{d} < 0.45 \quad (4)$$

Geometric constraints:

$$\frac{d^I}{d} \leq 0.171 \quad (5)$$

$$150 \leq b \leq 350 \quad (6)$$

$$400 \leq h \leq 700 \quad (7)$$

$$1500 \leq A_{st} \leq 2500 \quad (8)$$

$$300 \leq A_{sc} \leq 800 \quad (9)$$

Optimization Model Formulation

With the objective function, constraints and the required input parameters defined, the model was summarized in the following mathematical format:

$$\text{Minimize: Total Cost, } C_T = c_c[(bh - (A_{sc} + A_{st})) \times L \times u_c] + c_s[A_{sc} + A_{st}] + c_f[b + 2h] \quad (10)$$

Subject to:

$$M_{bal} \leq M \leq M_R \quad (11)$$

$$K > 0.167 \quad (12)$$

$$\frac{x}{d} < 0.45 \quad (13)$$

$$\frac{d^I}{d} \leq 0.171 \quad (14)$$

$$150 \leq b \leq 350 \quad (15)$$

$$400 \leq h \leq 700 \quad (16)$$

$$1500 \leq A_{st} \leq 2500 \quad (17)$$

$$300 \leq A_{sc} \leq 800 \quad (18)$$

To find:

$$X = [X_1 X_2 X_3 X_4]^T$$

where:

$b = X_1$

$h = X_2$

$A_{st} = X_3$

$A_{sc} = X_4$

The optimized values of the aforementioned design variables are obtained by optimization.

Optimization Process

The mathematical expressions described above for the model was replicated in Microsoft Excel using a spreadsheet. This was then optimized with Excel's Solver Tool, after which the required results were recorded.

Development of the Excel Spreadsheet

The objective function, input parameters, design parameters, computed values, constraints and their aforementioned formulas were appropriately placed in the Excel spreadsheet shown in Figure 3, with the corresponding Solver dialogue box in Figure 4.

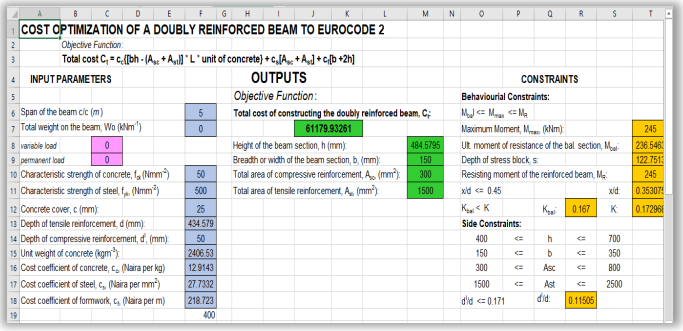

Figure 3: Excel spreadsheet developed to perform cost optimization on a doubly reinforced concrete beam to Eurocode 2.

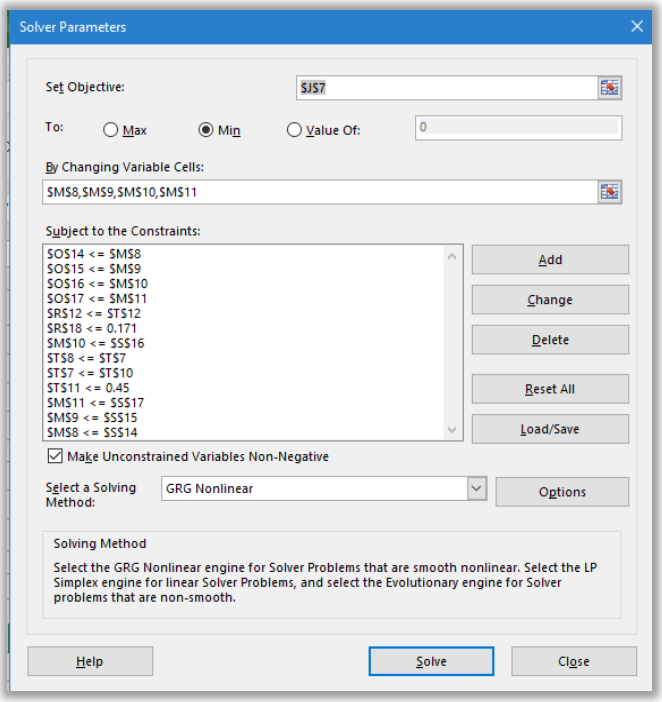

Figure 4: Excel Solver dialogue box with the model's objective function, design variables and constraints in place.

Generation of Results

After using the Solver dialogue box to solve the optimization model, the values in the cells containing the design variables were changed due to the success of the operation. This also led to a corresponding change in the cost of the beam. The previous values of both the objective function and design variables are recorded, as well as the corresponding values after the optimization process has been completed.

RESULTS AND DISCUSSION

Design Example

A selected beam of known dimensions was setup in the model for cost optimization. The relevant input parameters utilized for this are shown in the table below.

Table 1: Input Parameters for the case study used for the design example.

Input Parameters	Values
Span of the beam c/c (*m*)	5
Maximum Moment, M_{max}, (kNm):	443
Characteristic strength of concrete, f_{ck} (Nmm^{-2})	25
Characteristic strength of steel, f_{yk}, (Nmm^{-2})	500
Concrete cover, c (mm):	25
Depth of tensile reinforcement, d (mm):	510
Depth of compressive reinforcement, d', (mm):	50
Unit weight of concrete (kgm^{-3}):	2406.53
Cost coefficient of concrete, c_c, (Naira per kg)	12.914
Cost coefficient of steel, c_s, (Naira per mm^2)	27.733
Cost coefficient of formwork, c_f, (Naira per m)	218.723

Upon the execution of the optimization procedure, the new values for the design variables and cost objective function were observed and recorded as is shown in Table 2.

Table 2: Results from the cost optimization of the design example.

Design Variables	Original Values	Optimal Values	
h	560	673.031	
b	280	264.965	
A_{sc}	694.368	434.844	
A_{st}	2365.773	2075.482	
Objective Function	Original Cost	Optimal Cost	Gain (%)
C_T	109063.915	97292.96	10.793

The original cost is decreased by 10.793 % of its value. This is the cost savings due to the cost optimization of the selected beam under the preassigned parameters. A reduction all the values of the design variables except for the overall beam depth which was increased from 560 mm to 673.031 mm was also observed.

Effect of Span Length on Cost Optimization of the Model

An evaluation of the relationship between the span length and the resulting original cost and optimal costs under cost optimization was performed on the model. Keeping loading conditions constant and increasing the span of the beam, the resulting effects of the cost optimization was observed and recorded.

The span increase was directly proportional to the increase in the original and optimized costs as seen in Figure 5, even though the optimized costs closely matched the direction and slope of the original costs.

The gains from cost optimization with respect to increasing span lengths however were very minute, as seen in the trend line generated in Figure 6. The gains ranged from 0.264% at 1 m span to 0.210% at 10 m, with the highest gains being at 3 m with 0.229% and the lowest at 5 m with 0.176% gain.

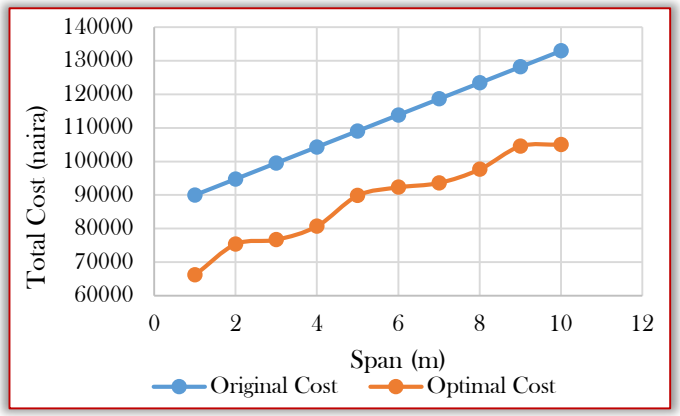

Figure 5: Graph of costs against span under cost optimization.

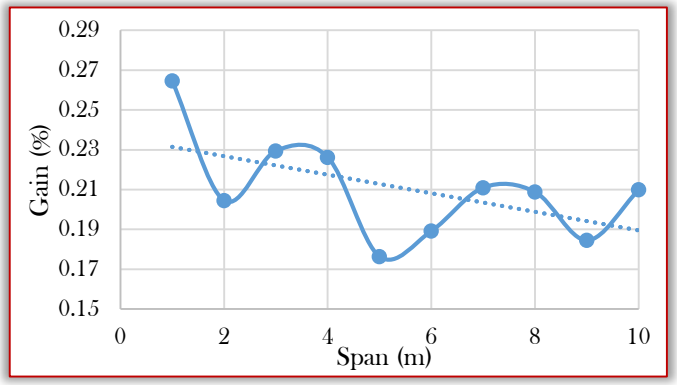

Figure 6: Graph of gain (%) against span under cost optimization.

Effect of Concrete Grade on Cost Optimization of the Model

The identical procedure carried out in the previous section was repeated for various concrete classes. The characteristic strength values of these classes (f_{ck}) is a parameter that influences the costs of the structure and is unique and representative of each class.

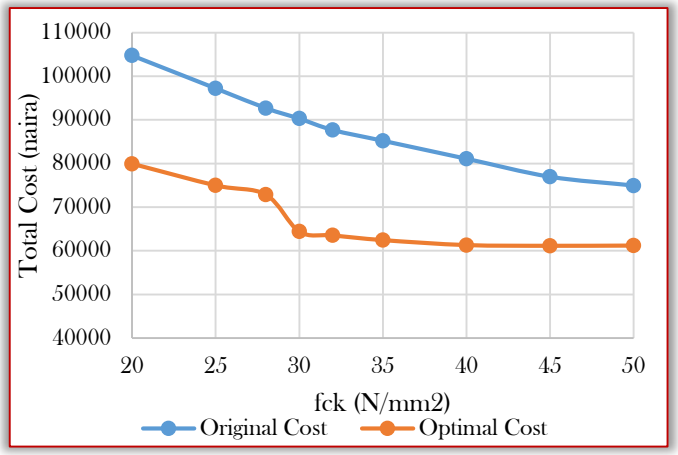

Figure 7: Graph of costs against characteristic concrete strengths under cost optimization

Increase in the characteristic strength of concrete (which implies the use of a different grade or class of concrete for design or

manufacture) led to a steady decline in the both the original cost and optimized cost, as seen in Figure 7. The gain (%) however, shown in Figure 8, due to increase in the characteristic concrete strength of the concrete classes decreased initially before increasing to 28.68%, after which it steadily declined to 18.345% for the concrete class of 50/60.

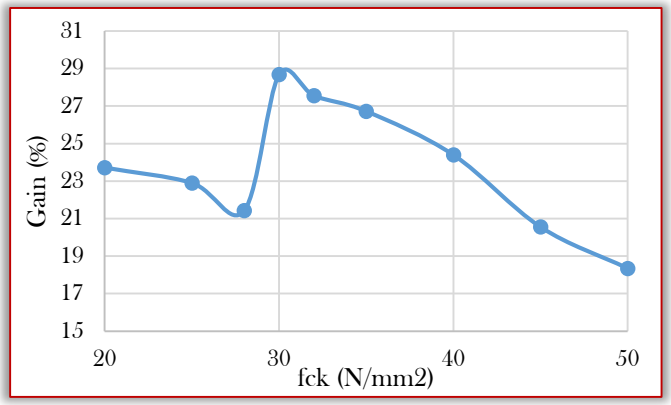

Figure 8: Graph of gain (%) against characteristic concrete strengths under cost optimization.

CONCLUSION

Based on the results obtained from this study, the following conclusions can be drawn:

- The height of the beam was increased in the case study whilst all other design variables were decreased on the execution of the cost optimization process. The height increased from 560 mm to approximately 673.0311 mm.
- Increase in the span of the member led to an increase in the original costs, as well as the optimized costs, even though the latter were smaller than the former.
- The gains from cost optimization with respect to increasing span lengths however were very minute. The gains ranged from 0.264% at 1 m span to 0.210% at 10 m, with the highest gains being at 3 m with 0.229% and the lowest at 5 m with 0.176% gain.
- The minute values of gain indicated that there were no additional gains derived by increasing the span of the beam whilst under cost optimization.
- Increase in the concrete class led to a decrease in the original and optimized costs of the beam. The decline in the values of the optimized costs however was observed to be slower and there could possibly be a scenario where a high enough concrete class would receive no benefit from the developed model's cost optimization.
- The gain (%) due to increase in the characteristic concrete strength of the concrete classes decreased initially before increasing to 28.68%, after which it steadily declined to 18.345% for the concrete class of 50/60.

Acknowledgements

We want to appreciate Engr. Dr. Samuel Sule, for his instructions, guidance and understanding. We also want to thank the entire staff of the department of Civil and Environmental engineering for their support. Finally, we want to say thank you to family and friends for their financial and emotional support.

References

[1] Antunes, A. F. D. R. (2017). BIM–Based Parametric Optimisation of Structural Systems (Masters Dissertation). Tecnico Lisboa, Lisbon, Portugal.

[2] Bhalchandra, S. A., and Adsul, P. K. (2012). Cost Optimization of Doubly Reinforced Rectangular Beam Section. International Journal of Modern Engineering Research (IJMER), Vol. 2, Issue. 5, pages 3939–3942.

[3] EuroCode 2 (2004) "Design of concrete structures – Part 1–1: General rules and rules for buildings."

[4] Galeb, A. C. (2018). Optimum Design of Doubly Reinforced Concrete Beams Using Simulated Annealing. International Journal of Civil Engineering and Technology (IJCIET), Volume 9, Issue 10, pp. 61–70.

[5] Ildiko, M, Kolbitsch, A., and Kravanja, S. (2010). Cost Optimization of Reinforced Concrete Beams. Proceedings of the Third International Conference on Modelling, Simulation and Applied Optimization Sharjah, U.A.E, January 20–22, 2009.

[6] Khaled, A., Ibrahim, M. M., and Ehab, S. (2004). Cost Optimization of Reinforced Concrete Elements. Asian Journal of Civil Engineering (Building and Housing), Vol. 5, No 3–4, pages 161–174.

[7] Salim, T. Y., Ikhlas, S. A., and Saddam, M. A. (2018). Optimum Design of Singly and Doubly Reinforced Concrete Rectangular Beam Sections: Artificial Neural Networks Application. Iraqi Journal of Civil Engineering, Vol. 6, No. 3, pp. 1–19.

ISSN: 2067–3809

Fascicule 2
[April – June]
tome XVII
[2024]

ACTA Technica CORVINIENSIS
BULLETIN OF ENGINEERING

ISSN: 2067-3809

ACTA TECHNICA CORVINIENSIS – Bulletin of Engineering | e–ISSN: 2067 – 3809
Tome XVII [2024] | Fascicule 2 [April – June]

[1.] Adnan RAMAKIĆ, [2.] Zlatko BUNDALO, [3.] Dušanka BUNDALO, [4.] Mirko SAJIĆ

DEEP LEARNING BASED INTELLIGENT SECURITY SYSTEM FOR HOMES

[1.]Technical Faculty, University of Bihać, Bihać, BOSNIA & HERZEGOVINA
[2.]Faculty of Electrical Engineering, University of Banja Luka, Banja Luka, BOSNIA & HERZEGOVINA
[3.]Faculty of Philosophy, University of Banja Luka, Banja Luka, BOSNIA & HERZEGOVINA
[4.]Independent University of Banja Luka, Banja Luka, BOSNIA & HERZEGOVINA

Abstract: In today's world, technology is omnipresent. In many areas of human life, people use some kind of new technology. From smartphones that people use every day to intelligent systems built into the cars. Accordingly, many technologies are also used in homes. Some of these include smart thermostats, appliances, lighting and various voice assistants. In some cases, all of that is implemented as one system. In this paper, some methods that can be used for security purposes in homes and other buildings have been analyzed and studied. The methods mentioned in this case form an intelligent security system based on deep learning. The described example of a security system can be used for both access to the house and access to the outside of the house. In this case, the methods of gait recognition, face recognition and vehicle recognition, i.e., cars recognition, were used and analyzed. Accordingly, three deep learning models were developed and described for the gait, face and vehicle recognition. The analysis, the defined settings and the results obtained in relation to the developed models were also described.
Keywords: Intelligent security system, deep learning, gait recognition, face recognition, vehicle recognition

INTRODUCTION

The use of new technology is inevitable in many areas of human life. Technology is advancing every day, so its use will be even more present in the future. If we take a period of just the last 30 years as a reference, we should notice many advances in technology. One example of this is the smartphone, what people use on a daily basis for many tasks. From basic texting in e–mail correspondence to the use of advanced artificial intelligence tools for translations, image creating and editing, etc. Another interesting example is modern car that is equipped with different types of technologies that support the driver while driving, such as modern advanced driver assistance systems *(ADAS)* or systems for autonomous driving.

Based on the above, even modern houses are not immune to new technology. Modern homes contain various elements such as smart thermostats, heating, ventilation and air conditioning systems (HVAC), appliances, lighting, various voice assistants, etc. In some cases, this is all combined in one system. The security aspect is also crucial for any modern home. Different identification methods can be used to achieve different levels of security in home access. For example, to enter the house, people can enter different combinations of numbers (Personal Identification Number, PIN) or use more advanced methods such as voice or speech recognition, face recognition, etc. The methods mentioned are usually based on certain characteristics, i.e., extracted features, of the human body such as fingerprint, palm, face, voice or speech, eye elements (retina or iris), gait, etc.

This paper is primarily concerned with the aspect of security required for access and entering the house and house yard. In other words, for access and entering the interior and exterior of the property, house or building. Three methods are proposed and used for this purpose. Two of the methods are used for person identification, gait recognition and face recognition. Gait and face recognition are intended for access and entering all parts of the property, both indoors and outdoors, for the persons. The third method is used to recognize vehicles, in this case cars. The mentioned vehicle recognition is intended for access and entering the yard from the street and access and entering the garage. Accordingly, three deep learning models were developed and described in this paper. In connection with the developed models, the analysis, the defined settings and the obtained results were described.

The paper is structured as follows. After the introductory section, the second section describes an example of an intelligent security system for houses and buildings. The architecture of the models, the defined settings and the datasets used are described in the third section. The fourth section describes the results obtained in relation to the models and datasets used. Concluding remarks are made at the end.

EXAMPLE OF AN INTELLIGENT SECURITY SYSTEM FOR HOUSES

An intelligent security system can be realized with different methods and technologies. In this paper, the intelligent security system is based on the deep learning approach. The system is based on two known methods for person identification, face and gait recognition, as well as method for vehicle recognition. The two mentioned methods for people recognition are intended for the identification of persons entering all parts of the property, both indoors and outdoors. In other words, gait and face recognition are used when entering the house, garage or yard from the street. The vehicle recognition is used when a car enters the yard from the street or enters the garage. An example of scheme of a house and adjoining yard with an intelligent security system is shown in Figure 1.

Figure 1 shows an example of a plot of land (property) on which the house (H), garage (G) and yard (Y) are located with associated security elements (cameras). In this example, there are five RGB (Red, Green, Blue) cameras to monitor the entire property. Different cameras with different ranges can be used in this context. RGB–D sensors (Red, Green, Blue – Depth) can also be used. The use of a particular type of camera depends on the methods to be implemented. In other words, if a method requires depth images, for example, it is necessary to install an RGB–D sensor. In this example, methods intended for identification use RGB images, so it is sufficient to install RGB cameras.

The cameras are located at the main entrances to the house, garage and yard. The cameras are labeled *C1*, *C2*, *C3*, *C4* and *C5*. The cameras are used to detect persons and cars and capture images of anyone attempting to enter the house, garage and yard. To gain access to the yard, a person or vehicle must be detected by the camera *C1* located at the main entrance. That means that images should be taken for a person or vehicle. The taken images are used in all used methods, gait, face and vehicle recognition. In this part, all mentioned methods should be implemented. The person should be identified by gait or face recognition methods, while the vehicle should be identified based on vehicle recognition method. If a person or vehicle is positively identified, they can enter the yard from the street.

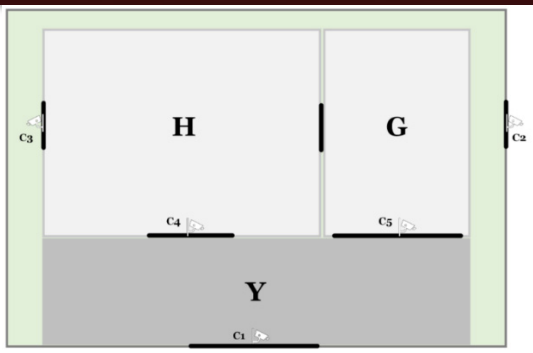

Figure 1. An example of scheme of a house and adjoining yard with an intelligent security system

In addition, persons can enter the property via the side entrance (auxiliary entrance), which is monitored by camera *C2*. This means that persons who want to gain access to the yard from that side must be detected by camera *C2*. In this case, images should also be taken for a person, as in the case of the main entrance and camera *C1*. The only difference in this case is that the side entrance is only intended for people. This means that gait and face recognition should be implemented so that persons can be detected and identified, to enable access and entrance.

To enter the house, persons should use one of two entrants monitored by cameras *C3* and *C4* and must be detected with cameras *C3* and *C4*. In this example, camera *C4* is located at the main entrance of the house, while camera *C3* is located at the side entrance. Gait and face recognition methods should be implemented in this case.

Camera *C5* is used to access and enter the garage. To enter the garage, all methods should be implemented as in the case of access to the main entrance to the property.

If, for example, a certain person wants to enter the house through the main entrance, this person should be detected by the camera *C4*. When the person is detected, the identification process begins. The persons can be identified by their gait or their face. Gait recognition is suitable for identification purposes at a greater distance. If the person approaches the main entrance from a greater distance, it will be identified by their gait, as this method requires more steps to identify the person. In the event of a positive identification, the door at the main entrance is unlocked. If for some reason the person is not identified by the gait, identification is done by the face. Over 90 percent should be the confidence in the identification of a certain person or vehicle to gain access to the house or yard. The default identification method for longer distances is gait recognition, while face

recognition is used for shorter distances. If, for any reason, gait recognition is unable to identify a certain person, face recognition begins.

A *Gait Energy Image (GEI)* [5] was used as a method for gait recognition. GEI is an image containing the silhouettes of a person during a gait cycle, where mentioned silhouettes are normalized, aligned and temporally averaged [5]. Examples of the GEI images from *Casia Dataset B* [22][23][12] are shown in Figure 2.

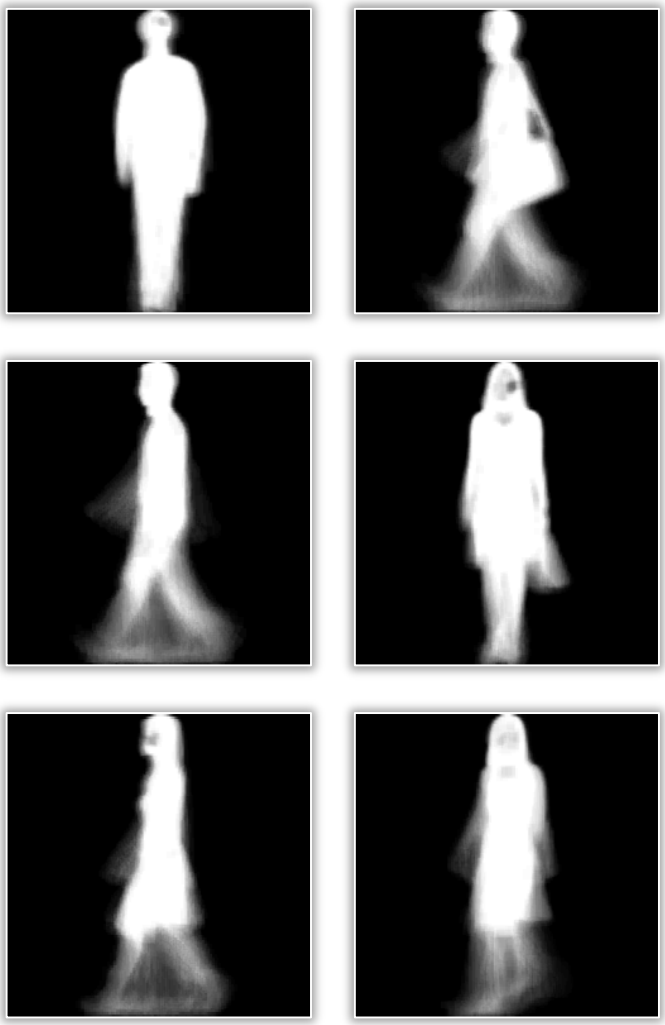

Figure 2. Examples of GEI images (*Casia Dataset B*) [22][23][12]

Approaches to gait recognition [14] can generally be divided into two categories, those based on appearance and those based on models. In appearance–based approaches, silhouettes of the individuals are usually the basis for the methods presented. In model–based approaches, a model serves as the basis for the methods presented. The mentioned model is based on some human body characteristics such as the length of the legs or arms etc. Some interesting works on gait recognition can be found in [1,3,4,6,7,10,13,15–20].

In addition to gait recognition, face recognition is also an interesting method for identifying people. It is a method that is widely used today. This type of method is usually used for smaller distances, but can also be used at a greater distance similar as for gait recognition. This is possible because today there are various cameras with a long range, so that face images can be taken from a greater distance and people can be identified. Compared to gait recognition, face recognition does not require as many steps, making it quicker and easier to implement in this context. Some interesting elements related to face recognition can be found in [2].

In general, an identification system can be roughly divided into two parts. One part is *the identification part* and the other is *the database (dataset) creation part*. In the database creation part, the images for each person and vehicle are captured and stored (image acquisition). The identification part involves capturing a new image of a certain person or vehicle and comparing it with the images stored in the database. In this context, features can be extracted from the images and then the features form the database.

With the rapid development of artificial intelligence and easier access to the tools and platforms for developing machine or deep learning models, the identification process is now usually carried out using machine and deep learning approaches. In this context, a model should be developed to identify individuals and vehicles and a database should be created, i.e., images should be captured for each person and vehicle (image acquisition). The database is used to train and validate the model. To identify a specific person or vehicle, a new image of the person or vehicle must be captured and transferred to the developed model. For the methods used in this paper, this is shown in the Figure 3.

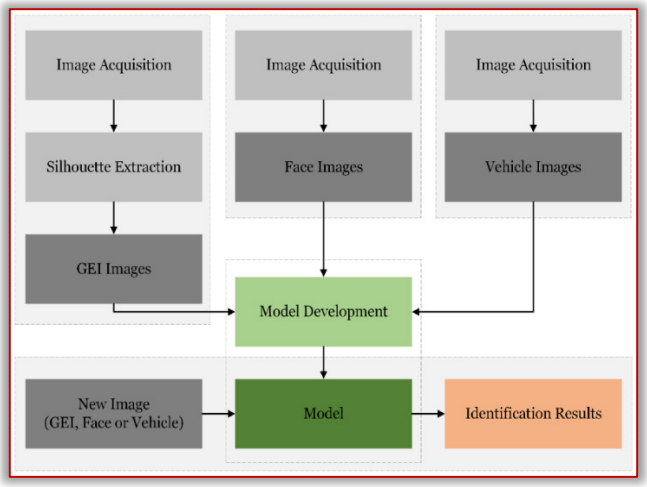

Figure 3. Identification methods based on deep learning

Figure 3 shows how each of the models was developed. In other words, Figure 3 shows the steps required to develop each model. In the case of gait recognition, it is necessary to capture images for each person while walking, i.e. in gait, and then perform image processing. After that, the silhouettes of a person should be extracted from the images, processed, and then GEI images should be created. When GEI images have been created for each person, the database was created. Then, a model for gait recognition should be developed, trained and validated on GEI images. The same process takes place for face and vehicle recognition. The only difference is that in the case of gait recognition, the silhouettes must be extracted from the images and then the GEI images have to be created. In the case of face and vehicle recognition, it is sufficient to capture images of faces and vehicles, respectively. The above text describes the process of database creation and model development for each of the methods. During identification, a new image of a person must be taken and passed to the model so that the person can be identified.

MODEL ARCHITECTURE, SETTINGS AND DATASETS USED

A total of three models were developed, as already mentioned in the text. One model for each of the methods used, i.e., for gait, face and vehicle recognition. The *TensorFlow* [21] platform was used for model development together with *Keras* [8]. From *Keras*, the *Keras Sequential* model was used. All three models consist of a *preprocessing layer*, *convolution layers*, *pooling layers*, *reshaping layer*, *core layers* and *regularization layer* (in models for face and vehicle recognition). Three datasets were used in the development of the models. In the case of gait recognition, the *Casia Dataset B* [22][23][12] was used. *The Facial Images: Faces95* [11] dataset was used for the face recognition model. A separate own dataset with 10 classes, i.e., images for ten different cars, was used for vehicle recognition.

Casia Dataset B, a well–known gait dataset, consists of the images of 124 subjects recorded from 11 views. The subjects in *Casia Dataset B* have a normal gait or have clothing and carrying condition changes. It should be noted that silhouette images and GEI images are also available in *Casia Dataset B*. These images are especially suitable for research and methods based on appearance–based approaches. *The Facial Images: Faces95*, face dataset, contains images of faces of 72 subjects with a resolution of 180 x 200, where the background is a red curtain. Own dataset contains the images of the cars taken from different angles, taking into account all sides of the cars. The images are high–resolution.

From the *Casia Dataset B* and the *Faces95* dataset, 20 subjects (20 classes) were randomly selected and used for the training and validation process of the developed models. On the other hand, all 10 vehicle classes were used from our own dataset for vehicle recognition. All GEI images from the *Casia Dataset B* were used for each subject, taking into account all views and all conditions such as normal gait, clothing and carrying condition changes. A total of 2200 GEI images were used, 110 GEI images for each subject. In the training and validation process, the images were divided so that 80 percent were used for training and 20 percent for validation, for all three models. This means that of this number of GEI images, 1760 images were used for training and 440 images for validation.

In the case of the *Faces95* dataset, 20 face images were used for each subject. A total of 400 images, with 320 images used for training and 80 images for validation. For vehicles, 80 images per class were used, making a total of 800 images. Of this number of images, 640 images were used for training and 160 images for validation. Data augmentation was also performed for the *Faces95* and own vehicle datasets to increase the diversity of the training set. Further training options are 20 *epochs* and the *Adaptive Moment Estimation Optimizer (Adam)* [9] was used.

RESULTS AND DISCUSSION

After analyzing the developed deep learning models for gait, face and vehicle recognition, the following results were obtained. In the case of the model for gait recognition, the validation accuracy for the defined settings and the dataset used, as described in the previous section, was 99,32%. The face recognition model had a validation accuracy of 98,75%. In contrast, the model for vehicle recognition had a validation accuracy of 100%. The results obtained can be seen in Figure 4 and Table 1.

Table 1. Validation Accuracy for Developed Models

Developed Model for Method	Dataset	Validation Accuracy
Gait Recognition	*Casia Dataset B*	99,32%
Face Recognition	*The Facial Images: Faces95*	98,75%
Vehicle Recognition	*Own Dataset*	100%

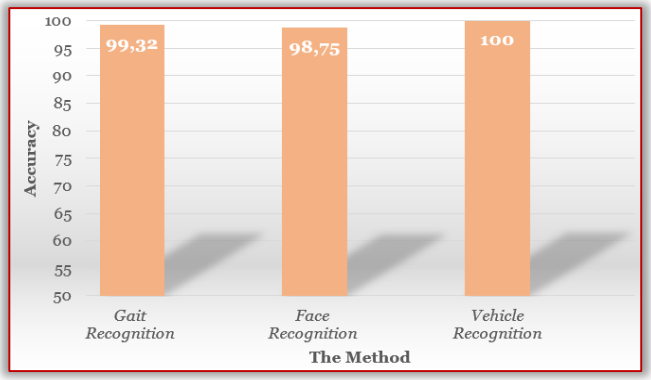

Figure 4. Validation Accuracy for Developed Models

As is shown in Table 1 and Figure 4, all three developed models for gait, face and vehicle recognition achieved high results in terms of accuracy, what is above 98% in all three cases. That means that all three methods are interesting and promising for use in various security systems. Figure 5 shows the training and validation accuracy for all three developed models. The left side of the image represents the training and validation accuracy for the model for gait recognition, the middle part of the image for the model for face recognition and the right side of the image for the model for vehicle recognition.

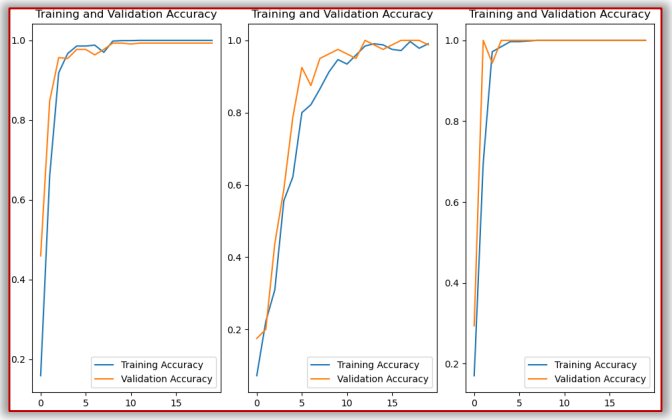

Figure 5. Training and validation accuracy for developed models (left – gait recognition, middle – face recognition, right – vehicle recognition)

As can be seen from the previous text on the models developed and the results presented, all three methods are promising for use in various security systems and applications. The models developed for the methods provided good results in all three cases. Although a relatively small number of classes were used in all three cases (20 for gait recognition, 20 for face recognition and 10 for vehicle recognition), the obtained results are very promising. To support this, the models for gait and face recognition were also trained and validated with a larger number of classes from datasets used, using 50 randomly selected subjects in both cases. The obtained results in terms of accuracy were also high, exceeding 95% in both cases. In the case of gait recognition, different GEI images were also used. This means that the model was trained and validated only with GEI images taken at 0 degrees and with images taken at 90 degrees.

It should also be noted that gait recognition methods such as GEI require more steps to identify a person. This means that RGB images of a person must first be captured during a gait cycle, after which the person's silhouettes must be extracted and then GEI images are created. This is a challenging task that must be performed in real–time, as the person can quickly disappear from the camera's field of view. In the case of face recognition, this is easier as only the face images should be captured. The advantage of gait recognition methods is that a person can be identified over a greater distance and without the person knowing that the identification process is underway. The face recognition is used for smaller distances and is faster. But, a potential problem and disadvantage of face recognition can be changes to a person's face, such as a beard, glasses, wearing a hat, etc. All this should be taken into account when preparing a dataset for the development of a face recognition model.

In the case of vehicle recognition, only the images of the cars are taken into account during model development. This is potentially disadvantageous, as the same car with the same color can enter a house yard. For this reason, the vehicle recognition model should be coupled with a license plate recognition system, i.e. *automatic number plate recognition (ANPR)*, to achieve the highest level of security. In view of the above, it would be interesting to analyze another method of gait recognition instead of the GEI method in future research. It would also be useful to compare the performance of the appearance–based and the model–based method of gait recognition. In particular, it would be useful to obtain results in terms of speed of identification and reliability of identification.

CONCLUSION

An example of an intelligent home security system based on deep learning was analyzed and described in this paper. The intelligent system is based on three methods to identify people or vehicles. These methods are gait, face and vehicle recognition. Gait and face recognition is for identifying people who want to access and enter certain part of the property such as house, garage or yard, i.e., both indoors and outdoors. Vehicle recognition is intended for entering the yard from the street and entering

the garage. A well–known method called Gait Energy Image or GEI was used as the method for gait recognition.

In light of the above, three deep learning models were developed for each of the methods. The *TensorFlow* platform with *Keras* was used to develop the models. The *Keras Sequential* model was used. Three datasets were used in the development of the models for the training and validation process. The well–known *Casia Dataset B* was used as the gait dataset. On the other hand, *The Facial Images: Faces95* was used as the face dataset. A separate own dataset with 10 classes was used for the vehicles. The results obtained in terms of validation accuracy were very promising for all three models developed. The results achieved are above 98% for all three models.

In the future, it would be interesting to analyze another method of gait recognition instead of GEI. It would also be useful to compare the performance of the appearance–based and the model–based method of gait recognition, taking into account the speed of identification and the reliability of identification.

References

[1] Arora, P. and Srivastava, S. (2015). Gait Recognition Using Gait Gaussian Image. In: 2nd International Conference on Signal Processing and Integrated Networks (SPIN), 791–794. IEEE.

[2] Barnouti, N. H., Al–Dabbagh, S. S. M. and Matti, W. E. (2016). Face Recognition: A Literature Review. International Journal of Applied Information Systems, 11(4), 21–31.

[3] Bashir, K., Xiang, T. and Gong, S. (2009). Gait Recognition Using Gait Entropy Image.

[4] Chattopadhyay, P., Roy, A., Sural, S. and Mukhopadhyay, J. (2014). Pose Depth Volume Extraction from RGB–D Streams for Frontal Gait Recognition. Journal of Visual Communication and Image Representation, 25(1), 53–63. Elsevier.

[5] Han, J. and Bhanu, B. (2005). Individual Recognition Using Gait Energy Image. IEEE Transactions on Pattern Analysis and Machine Intelligence, 28(2), 316–322. IEEE.

[6] Hofmann, M., Bachmann, S. and Rigoll, G. (2012). 2.5D Gait Biometrics Using the Depth Gradient Histogram Energy Image. In: 5th International Conference on Biometrics: Theory, Applications and Systems (BTAS), 399–403. IEEE.

[7] Iwashita, Y., Uchino, K. and Kurazume, R. (2013). Gait–based Person Identification Robust to Changes in Appearance. Sensors, 13(6), 7884–7901. MDPI.

[8] Keras. Link: https://keras.io [Accessed 25/03/2024]

[9] Kingma, D. P. and Ba, J. (2014). Adam: A Method for Stochastic Optimization. arXiv preprint arXiv:1412.6980.

[10] Kumar, M. N. and Babu, R. V. (2012). Human Gait Recognition Using Depth Camera: A Covariance Based Approach. In: Proceedings of the 8th Indian Conference on Computer Vision, Graphics and Image Processing, 1–6.

[11] Libor Spacek's Facial Images Databases. Link: https://cmp.felk.cvut.cz/

[12] Official Web Page of the Institute of Automation, Chinese Academy of Sciences. Link: http://www.cbsr.ia.ac.cn/

[13] Preis, J., Kessel, M., Werner, M. and Linnhoff–Popien, C. (2012). Gait Recognition with Kinect. In: 1st International Workshop on Kinect in Pervasive Computing, 1–4. New Castle, UK.

[14] Ramakić, A. and Bundalo, Z. (2022). Gait Recognition as an Approach for People Identification. In: International Symposium on Innovative and Interdisciplinary Applications of Advanced Technologies, 717–726. Springer.

[15] Ramakić, A., Bundalo, D. and Bundalo, Z. (2023). An Approach to Gait Recognition Using Deep Neural Network. Acta Technica Corviniensis–Bulletin of Engineering, 16(2), 1–6.

[16] Ramakić, A., Bundalo, Z. and Bundalo, D. (2020). A Method for Human Gait Recognition from Video Streams Using Silhouette, Height and Step Length. Journal of Circuits, Systems and Computers, 29(7), 2050101. World Scientific.

[17] Ramakić, A., Bundalo, Z. and Bundalo, D. (2023). An Example of Solution for Data Preparation Required for Some Purposes of People Identification or Re–Identification. Journal of Circuits, Systems and Computers, 32(10), 2350164. World Scientific.

[18] Ramakić, A., Bundalo, Z., Bundalo, D. and Vidović, Ž. (2023). Frontal Gait Recognition Based on Deep Learning Approach. Annals of the Faculty of Engineering Hunedoara–International Journal of Engineering, 21(3).

[19] Sivapalan, S., Chen, D., Denman, S., Sridharan, S. and Fookes, C. (2011). Gait Energy Volumes and Frontal Gait Recognition Using Depth Images. In: International Joint Conference on Biometrics (IJCB), 1–6. IEEE.

[20] Sivapalan, S., Chen, D., Denman, S., Sridharan, S. and Fookes, C. (2012). The Backfilled GEI–A Cross–capture Modality Gait Feature for Frontal and Side–view Gait Recognition. In: International Conference on Digital Image Computing Techniques and Applications (DICTA), 1–8. IEEE.

[21] TensorFlow. Link: https://www.tensorflow.org [Accessed 25/03/2024]

[22] Yu, S., Tan, D. and Tan, T. (2006). A Framework for Evaluating the Effect of View Angle, Clothing and Carrying Condition on Gait Recognition. In: 18th International Conference on Pattern Recognition (ICPR), 441–444. IEEE.

[23] Zheng, S., Zhang, J., Huang, K., He, R. and Tan, T. (2011). Robust View Transformation Model for Gait Recognition. In: 18th International Conference on Image Processing, 2073–2076. IEEE.

ISSN: 2067–3809

ACTA TECHNICA CORVINIENSIS – Bulletin of Engineering | e–ISSN: 2067 – 3809
Tome XVII [2024] | Fascicule 2 [April – June]

[1.]Maša BUKUROV, [1.]Nikola OLUŠKI

THE DEVELOPMENT OF MATHEMATICAL MODELS OF VISCOUS FLUID FLOW AND ARISING ISSUES

[1.] University of NoviSad, Faculty of Technical Science, Novi Sad, SERBIA

Abstract: Although the greatest names in science have been grappling with one of the most complex problems for the past three centuries, the problem of turbulent viscous fluid flow has not been represented by a closed system of equations to this day. The attempts of Euler, Navier, Stokes, Bussinesque, Reynolds, Prandtl and others are getting in the last 50 years new support, such as computational fluid dynamics i.e., numerical modeling but also artificial intelligence with its tools such as deep learning and neural networks which are supposed to provide turbulence closure modeling. A historical overview and efforts of modern science and modern techniques are presented in this paper as well as some arising issues.
Keywords: viscous fluids flow, turbulence modeling, deep learning

INTRODUCTION

The development of fluid mechanics can be traced through historical data related to the great names of science, primarily mathematicians and physicists, but also engineers, inventors and lovers of the rich field of fluid studies. The first written document about fluid behavior was left to us 250 years B.C. by Archimedes entitled "On floating bodies". Despite the two–millennium study of fluids, to this day we do not have a closed mathematical model that describes the turbulent flow of a viscous fluid.

In 1755 Leonhard Euler (1707–1783) formed his famous equation for ideal fluid flow. After Euler, it appears that only Navier was motivated to formally tackle this problem and to succeed in solving it in 1822. He expanded Euler`s equation by introducing the viscous forces. Many investigators had put effort into solving the equation of motion for viscous flows as developed by Navier, and like him, Stokes had a very clear intention on the practicality of his efforts by confronting theory with experiments [1] in the 1830s and 1840s. This may be a reason why he and Navier became associated with the equation of motion for viscous flows. However, it would be fair to call the equation Euler–Navier–Stokes if it is necessary to include in the name the contribution of Stokes which was not fundamental, [1].

The Euler equation is given as:

$$\frac{d\vec{v}}{dt} = \vec{f} - \frac{1}{\rho}\text{gradp} \qquad (1)$$

where are:

$\vec{v}$– velocity vector,$\vec{f}$– body forces, p – pressure, ρ – density.

Hence the Navier–Stokes (N–S) equations being an extension of Euler's given in vector form also represents nonlinear partial differential equations:

$$\frac{d\vec{v}}{dt} = \vec{f} - \frac{1}{\rho}\text{gradp} + \nu\Delta\vec{v} + \frac{1}{3}\nu\text{grad div}\vec{v} \qquad (2)$$

where ν is kinematic viscosity. The continuity equation which is coupled with Navier–Stokes equations reads:

$$\frac{\partial\rho}{\partial t} + \text{div}(\rho\vec{v}) = \rho\bar{\varepsilon} \qquad (3)$$

where $\bar{\varepsilon}$ is specific yield of source or sink is also a partial differential equation.

MATERIAL AND METHODS

The aim of this paper is to present the development of a mathematical model that describes the flow of a viscous fluid, future tendencies and arising issues. In doing so, literary data were used that followed the development of fluid mechanics in the last two and a half centuries. The literature data are in abundance. It takes a lot of time to establish a solid path which can be followed through the labyrinth of investigations, research and experiments conducted by many famous and less famous scientists.

In this paper the main question will be if it is possible to solve one of the hardest problems in fluid mechanics, as well as in computational science, the problem of turbulence modeling, or turbulence closure modeling using modern techniques of deep learning or deep neural networks. Also, what does the future bring in this field from the standpoint of an educator.

In order to design certain objects such as aircraft, ships, submarines or turbine blades it is needed to estimate certain quantities with which

the fluid flow field interacts with the objects, such as lift or drag. The starting point in fluid dynamics is the Navier–Stokes equations. They are time and space–dependent conservation of momentum equations. Navier–Stokes equations together with continuity equation represent a set of nonlinear partial differential equations which can be solved analytically only for a certain number of examples for laminar fluid flow in 2D, but solving these equations in 3D is, even nowadays, if not impossible, then extremely difficult, [1]. Previously, engineers made further approximations and simplifications to the equation set until they had a group of equations that they could solve. Contemporarily, high–speed computers have been used to solve approximations to equations using a variety of techniques, e.g., finite difference, finite volume, finite element, and spectral methods, [2].

ANALYTICAL APPROACH

Today N–S equation represents one of the seven most important unsolved problems established by the Clay Institute of Mathematics. A fundamental problem in analysis is to decide whether such smooth, physically reasonable solutions exist for the Navier–Stokes equations. [3]. There are analytical solutions for the laminar fluid flow examples, but the turbulent flow is much more complicated. It is represented with Reynolds equations which are time–averaged Navier–Stokes equations. By doing so, an unknown term – Reynolds stresses is introduced. They represent the impact of the turbulent fluctuations on the mean flow. The Reynolds equations are partial differential *equations of second order and of elliptical type that do not* possess analytical solutions. In order to solve these equations, it is necessary to introduce not only time averaging but also some additional hypothesis which will establish a connection between turbulent stresses and averaged velocities.

Flow over an obstacle produces turbulent separated structures over a wide range of scales with existing patterns. Large–scale structures (eddies, vortices) are mainly responsible for either drag, lift or mixing efficiency. It would be an extremely expensive simulation if it would characterize every single degree of freedom. Instead, a reduced order model would be sufficient to present how the big energy–containing structures work together to change the property of interest (e.g. drag on a boundary layer). Kolmogorov turbulent energy cascade shows length scales of existing eddies or vortices in a turbulent flow, Figure 1.

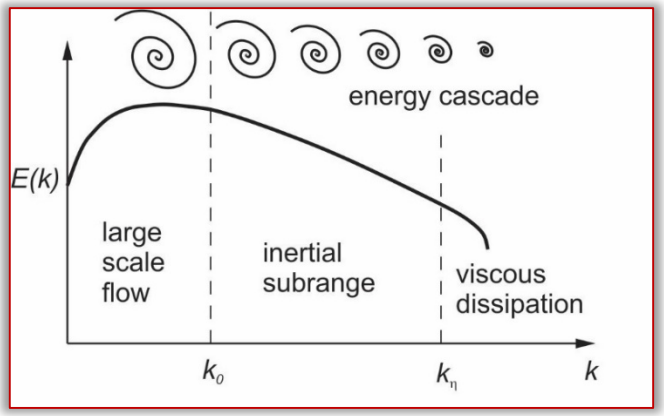

Figure 1. Kolmogorov turbulent energy cascade

The exact solutions of the Euler equation and Navier–Stokes equation are proposed by different authors using different methods. Among the most effective are Lie group theory and Baecklund transformation, symmetry reduction method [4], or transformation into the linear diffusion equations on a different basis [4–6]. Moreover, the N–S equations are solved by introducing some simplifications, e.g. the Cole–Hopf transformation is applicable for an incompressible flow and allows reducing the Navier–Stokes equation to the Einstein – Kolmogorov equation, [7].

Some authors [8] proposed the conversion of Navier–Stokes equations to ~~a~~ one linear diffusion equation based on the proposed linear velocity operator concept where the velocity operator is formulated in terms of a generalized new physical parameter.

The examples of flows for which analytical solutions are possible to find, with certain restraints, are those through ducts, pipes, coaxial gaps, between two parallel plates, etc. [9]. However, analytical solutions to even the simplest turbulent flows do not exist, [10].

Computational Fluid Dynamics (CFD)

In order to calculate how the object interacts with the fluid, and vice versa, it is necessary to simulate fluid flow to estimate quantities of interest. One way to do that is by using Computational Fluid Dynamics (CFD). CFD is a science that, with the help of digital computers, produces quantitative predictions of fluid–flow phenomena based on the conservation laws (conservation of mass, momentum, and energy) governing fluid motion and it complements experimental and theoretical fluid dynamics [11]. CFD enables analyses of complex problems involving fluid–fluid, fluid–solid or fluid–gas interaction, minimizes the planning time and

saves costs of experiments. The results of CFD simulations are numerical solutions of the governing equations of fluid dynamics.

Real flow structures might have many orders of magnitude of scales both in space and time and instead of modeling all of them which is very expensive for computers, it is possible to approximate how small scales affect the big energy–containing scales that are actually of the main interest since they are mostly responsible for a lift and drag. This field is called closure modeling.

The turbulence modeling should enable avoidance simulation of a wide range of turbulent scales and provide closure of turbulence modeling. This field is rapidly progressing with a constant flow of results in literature, and recently the support of artificial intelligence and its tools, machine learning and more advanced deep neural networks, provide a better understanding of turbulence and the possibility of optimizing real fluid flow.

Direct Numerical Simulation (DNS)

Direct Numerical Simulation (DNS) is a research tool of CFD; it does not provide exact solutions to the Navier–Stokes equations for engineering problems. The aim of DNS is to get a detailed, both in spatial and temporal scales, model of a flow field, e.g., flow around an airfoil, or a turbine blade. But typically, it is too expensive, and lasts too long; even with Moore's law of exponentially growing computer power, it will still take too much time to simulate the largest scale turbulent problems at all resolutions in space and time, not to mention optimization process which would take even more time. Because of that it is a must to do the turbulence modeling.

Problem of Turbulence Modeling

One of the most demanding and intriguing problems of fluid mechanics is the problem of turbulence. The wide range of scales of time and space in turbulent flows demands significant resources, both in time and computer configuration to model turbulence.

Turbulent flow is characterized with oscillatory behavior of physical properties; hence they can be represented such as averaged value plus fluctuation, Figure 2.

$$v = \bar{v} + v' \quad (4)$$

In addition to velocity, other turbulent flow properties also show oscillatory characteristics. In order to model a turbulent flow, it is necessary to approximate turbulent stresses, which are too demanding in time and computer power requirements to model.

The engineering computation of turbulent flows therefore relies on simpler descriptions with introduction of the statistical consideration of the flow.

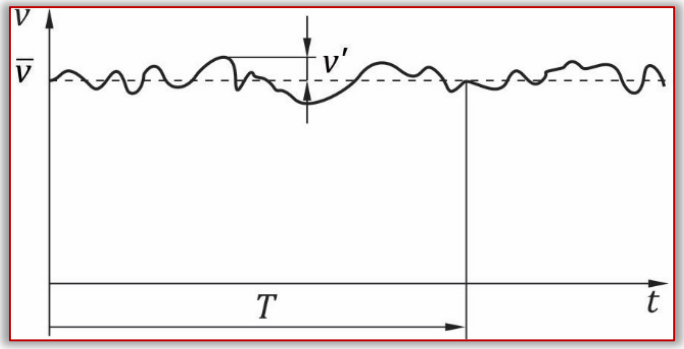

Figure 2. Instantaneous velocity in turbulent flow v, averaged velocity $\bar{v}$ and fluctuation v'

Bussinesque proposed methods for presenting viscous stresses, and Reynolds contributed. The work of Prandtl, Kolmogorov, Taylor and von Karman [12] was aimed to characterize turbulence. With the growth of computer power, possibilities of numerical simulations increased, but simplified engineering approximations continue to remain popular and widespread, [13].

There are many approaches [14,15], but the two most common approaches are RANS (Reynolds Averaged Navier–Stokes) and LES (Large Eddy Simulation). The RANS approach is based on time–averaged Reynolds equations and requires closures to represent the turbulent stresses and scalar fluxes emerging from the averaging process. The discipline of turbulence modeling has evolved using a combination of intuition, asymptotic theories and empiricism, while constrained by practical needs such as numerical stability and computational efficiency, [13].

The large eddy simulation (LES) technique of turbulence modelling reduces the complexity of simulation by focusing on turbulence on larger length scales and larger time scales, while the smaller scale flow behavior can be described using a subgrid model. The LES technique is an exact method which is still computationally tractable, while the RANS is a less precise method which is more computationally efficient than LES.

Machine Learning (ML)

Fluid mechanics, with massive amounts of data increasing daily, either from experiments or simulations, is a field with massive potential for machine learning, rapidly becoming an integral part of everyday life.

Simply put, machine learning is building models from data using optimization. More precisely,

machine learning algorithms are a growing set of data–intensive optimization and regression techniques ideal for these types of high–dimensional, non–linear, non–convex, and constrained optimizations [16].

The essential tasks in fluid dynamics are connected to reduced–order modeling, experimental data processing, shape optimization, turbulence closure modeling, and control [17]. Machine learning can be used for three main objectives:

— to accelerate direct numerical simulations
— to improve modeling basically in the context of LES and RANS and
— to obtain more robust reduced order models, [18].

Machine learning application in fluid dynamics encounters many obstacles, as mentioned in [17]. But this is a very fast–growing field with constant advance which can be seen in papers produced recently in the field of reduced order modeling [19], or for detecting interface between turbulent and non–turbulent flow [20].

One of the most developed segments of ML is image processing. It is also an aspect of ML applicable to improve flow visualization, what is done in [21], where was conducted super–resolution analysis of grossly under–resolved turbulent flow field data.

A group of authors [22] used ML to stabilize fluid flow in the wake of a fluidic pinball, and in [23], to stabilize an open cavity flow experiment. In order to improve Reynolds–averaged Navier Stokes (RANS) turbulence models, ML is applied in the paper [24] using a data–driven approach. In [13] is presented how machine learning and data–driven methods are being used to tackle the closure problem and how machine learning can make a practical impact on everyday industrial flows.

Optimization problems are also solved increasingly well with the aid of machine learning, and instead of using the full Navier–Stokes equations, which are far too demanding in computer power and time, it is possible to build surrogate models with the aid of ML that are accurate and fast enough to use in real–time for feedback control.

Another mighty tool of ML is deep neural networks (DNN), the dominant data mining tool for big data applications [25], using an artificial neural network with multiple layers between the input and output layers.

In case of RANS modeling in [26] is presented how a custom deep neural network with additional tensor input based on prior physical knowledge can be improved compared with a generic neural network architecture that does not embed this invariance property.

RESULTS AND DISCUSSION

In the future, mechanics of fluids will take a central role in many fields of human activities, including energy sector, transportation, utility sector, etc. Most of these activities will be enabled by advanced fluid mechanics models and controls, and these tasks can generally be written as challenging optimization problems. These optimizations are nonlinear, non–convex, multi–scale, very high dimensional, and that is exactly where the machine learning is significantly advancing.

In the 21st Century, computational methods and software tools are put on another level. An increase in computer power has made engineering and scientific computations more available and economically viable.

Modeling has become a mainstream step in engineering analysis and design of products, processes, and systems. However, the required training that engineering and science students often receive is not at the adequate level. Therefore, they may not have all the background training required to use software packages. This has created a challenge for industry to have trained professionals who can create "reliable" models and fully utilize commercially available software packages.

On the other hand, students, engineers, and scientists may not have the luxury of time and training to learn all the necessary technical subjects like physics, mathematical modeling, numerical methods, and programming languages.

Therefore, some arising thoughts and questions are:

— The theory is chasing the praxis, but the experiment remains the primary tool in fluid flow analysis, even though CFD has gone a long way with a lot of data and is constantly advancing. But, we need both experiment and computation [27].
— There is a transition from first principles to data–driven techniques.
— The abundance of data from experimental research and simulations provided asolid base for machine learning. Application of deep learning and neural networks provided additional advancement in closure problems. However, the physical involvement is logical and should be prioritized overthe mathematical approach.

— How should the students be thought?There can be two kinds of schools: one deep and broad, and the other will treat the application of CFD and ML as black box. That would lead to two kinds of engineers: engineers with wide knowledge, capable of thinking broadly and capable of introducing new concepts, and engineers who will specialize in a narrow field, with less ability to provide some general solutions. The first approach requires longer education, more devotion and more abundant resources.

CONCLUSION

Under the umbrella of authority such as Euler, Navier, Stokes, Reynolds, Prandtl, etc., it is difficult to stand out and deviate from the established path. And that is exactly the step that should be taken: to step away from the problem and try to look at it from another angle, by possible expansion of the system boundaries in order to, at least, get nearer to the solution of the turbulence closure problem.

The existing transition from first principles (such as the Navier–Stokes equation) to data–driven techniques is exactly such a step which leads us to the solution using another way: ML. What is important is that machine learning should not become a black box and must be connected to physically interpretable and generalizable models which are clear, trustworthy, and repeatable under different circumstances and can be interacted with. The most important issue is the future education of engineering and science students and to which extent it should be provided to them.

Educational institutions must embrace a dynamic approach to equip the next generation of engineers with the skills and mindset needed to tackle these complex problems. This involves fostering a deep understanding of both traditional principles and cutting–edge techniques like machine learning. Thus, the paramount challenge ahead is to seamlessly integrate machine learning while reshaping the education of future engineers.

References

[1] Bistafa, S. R., On the development of the Navier–Stokes equation by Navier, Revista Brasileira de Ensino de F´ısica, Vol. 40, No. 2, p.2603, 2018

[2] Bell, J.B., Colella, P. and Glaz, H.M., A second–order projection method for the incompressible Navier–Stokes equations. J. Comput. Phys., Vol. 85, pp. 257–283, 1989.

[3] Carlson, J. Jaffe, A. and Wiles, A. Editors: The Millennium Prize Problems, Clay Mathematics Institute American Mathematical Society, 2006.

[4] Liu, M., Li, X., Zhao, Q.: Exact solutions to Euler equation and Navier–Stokes equation. ZeitschriftfuerangewandteMathematik und PhysikZAMP, Z. Angew. Math. Phys., Vol. 70, pp. 43, 2019.

[5] Gunawan Nugroho, Ahmed M.S. Ali, Zainal A. Abdul Karim: A class of exact solutions to the three–dimensional incompressible Navier_Stokes equations. Applied Mathematics Letters., 23, 1388_1396 (2010).

[6] Mohammadein, S. A.1, Gad El–Rab, R.A., and Ali, M.S.: The Simplest Analytical Solution of Navier–Stokes Equations, Inf. Sci. Lett. 10, No. 2, 159–165, 2021

[7] Vladimir V. KULISH* & José L. LAGE: Exact solutions to the Naiver–Stokes equation for an incompressible flow from the interpretation of the Schroedinger wave function. School of Mechanical & Aerospace Engineering, Nanyang Technological University, Singapore 639798, Source arXiv, Jan 2013.

[8] Mohammadein, S. A. New Treatment of Fluid Mechanics with heat and Mass Transfer: Theory of Diffusion. Submitted to Appl. Math & Info Sci Lett.

[9] Bukurov, Ž., Cvijanović, P.: Mehanikafluidazbirkazadataka, Univerzitet u Novom Sadu, Fakultettehničkihnauka, Novi Sad, 1987.

[10] Moin, P.,Mahesh, K.: Direct numerical simulation: A Tool in Turbulence Research, Annu. Rev. Fluid Mech. Vol. 30, pp.539–78, 1998.

[11] [Hu, H.H.: Computational Fluid Dynamics, Fluid Mechanics, Fifth Edition, Elsevier Inc., 2012.

[12] Darrigol, O.: Worlds of flow: A history of hydrodynamics from the Bernoullis to Prandtl, Oxford University Press, 2005.

[13] Duraisamy, K., Iaccarino, G., Xiao, H.: Turbulence Modeling in the Age of Data, Annual Review of Fluid Mechanics, No. 51, pp. 1–23, 2019.

[14] Girimaji, S.S.; Partially–Averaged Navier–Stokes Model for Turbulence: A Reynolds–Averaged Navier–Stokes to Direct Numerical Simulation Bridging Method, Journal of Applied Mechanics, Vol. 73 No.3, pp 413–421, 2006.

[15] Spalart, P. R.: Detached–Eddy Simulation, Annual review of Fluid Mechanics, Vol. 41, pp. 181–202, 2009.

[16] Brunton, S., Kutz, J.N., Manohar, K., Aravkin, A.Y., Morgensen, K., Klemisch, J. Goebel, N., Buttrick, J., Poskin, J., Blom–Schieber, A.W., Hogan, T., McDonald, D.: Data–Driven Aerospace Engineering: Reframing the Industry with Machine Learning, Published Online:20 Jul 2021,

[17] Brunton, S. L., Noack B.R., Koumoutsakos, P.: Machine Learning for Fluid Mechanics, Annual Review of Fluid Mechanics, Vol. 52, pp.477–508, 2020.

[18] Vinuesa, R., Brunton, S.: Enhancing computational fluid dynamics with machine learning, Nature Computational Science, Vol. 2, pp. 358–366, 2022.

[19] Loiseau, J.C., Noack, B.R., Brunton, S.L.: Sparse reduced–order modeling: Sensor–based dynamics to full–state estimation, Journal of Fluid Mechanics, Volume 844 , pp. 459 – 490, 2018.

[20] Li, B., Yang, Y., Zhang, X., He, G., Deng, B., Shen, L.: Using machine learning to detect the turbulent region in flow past a circular cylinder, J. Fluid Mech., Vol. 905, A10, 2020.

[21] Fukami, K., Fukagata, K., Taira, K.: Super–resolution reconstruction of turbulent flows with machine learning, J. Fluid Mech., Vol. 870, pp. 106–120, 2019.

[22] Maceda, G., Li, Y., Lusseyran, F., Morzynski, M., Noack, B.R.: Stabilization of the fluidic pinball with gradient–enriched machine learning control, J. Fluid Mech., Vol. 917, A42, 2021.

[23] Maceda, G., Varon, E., Lusseyran, F., Noack, B.R.: Stabilization of a multi–frequency open cavity flow with gradient–enriched machinelearning control, J. Fluid Mech., Vol. 955, A20, 2023.

[24] Grabe, C., Jäckel, F., Khurana, P.: Data–driven augmentation of a RANS turbulence model for transonic flow prediction, International Journal of Numerical Methods for Heat & Fluid Flow, Vol. 33 No. 4, pp. 1544–1561, 2023.

[25] Kutz, J.N.: Deep learning in fluid dynamics, J. Fluid Mech., Vol. 814, pp. 1–4, 2017.

[26] Ling, J., Kurzawski, A., Templeton, J.: Reynolds averaged turbulence modelling using deep neural networks with embedded invariance, Journal of Fluid Mechanics, Vol. 807, pp. 155–166, 2016
[27] Goldstein, S.: Fluid Mechanics in the First Half of this Century, By Annu. Rev. Fluid Mech. Vol. 1, p.1–29. 1969.

Note: This paper was presented at IIZS 2023 – The XIII International Conference on Industrial Engineering and Environmental Protection, organized by Department of Mechanical Engineering and Department of Environmental Protection of the Technical Faculty "Mihajlo Pupin" Zrenjanin, from the University of Novi Sad, in cooperation with partners – University Politehnica Timisoara, Faculty of Engineering, Hunedoara (ROMANIA), University "St. Kliment Ohridski", Technical Faculty, Bitola (MACEDONIA), "Aurel Vlaicu" University of Arad, Faculty Of Engineering, Arad (ROMANIA), University of East Sarajevo, Faculty of Mechanical Engineering East Sarajevo, Sarajevo (BOSNIA & HERZEGOVINA) and University of Giresun, Faculty of Engineering, Giresun (TURKEY) – in Zrenjanin, SERBIA, in 05–06 October, 2023.

ISSN: 2067-3809

ACTA TECHNICA CORVINIENSIS – Bulletin of Engineering | e–ISSN: 2067 – 3809
Tome XVII [2024] | Fascicule 2 [April – June]

[1,2.]Adeolu A. ADEDIRAN

SYNTHESIS AND CHARACTERIZATION STUDIES OF SI–BASED REFRACTORY COMPOUNDS DERIVED FROM CORN COB

[1.]Department of Mechanical Engineering, Landmark University, Omu–Aran, Kwara State, NIGERIA
[2.]Department of Mechanical Engineering Science, University of Johannesburg, SOUTH AFRICA

Abstract: The synthesis and characterization of Si–based refractory compounds derived from corn cob was reported. Size reduction of the corn cob was achieved using a planetary mills. Carbothermal processing route was used for the production of the Si–based refractory compounds after acidic treatment. The carbothermal processing was done at temperature window of 600–900°C. The reaction products were analyzed using Fourier transmission infrared spectrometer (FTIR), scanning electron microscope (SEM) and X–ray diffractometer (XRD). The results obtained show that, at 600°C, there were different polytypes of silica phases in the refractory compounds. However, as the temperature increase up to 900°C, there were SiC phases in the reaction products. This trend was also corroborated with the results obtained from the XRD and FTIR respectively. The morphological features also agrees with the trend reported in the XRD.
Keywords: refractory compounds, structure, corn cob, silicon carbide

INTRODUCTION

Silicon carbide is among the most active compounds utilized in the design of construction and hybrid ceramic materials for high operating temperatures due to a combination of properties including low density, high decomposition temperature, lack of phase transitions across a wide temperature range, superior mechanical qualities, non–interaction with corrosive environments, and the highest oxidation resistance among the refractory carbides [1–3]. It has the potential to be used as a reinforcement material for nanoscale components, protective coatings, and refractory matrices [3]. Currently, a wide variety of techniques have been described for the synthesis of SiC, however the majority of them were only performed in laboratories. Mechanical milling [4,5], rapid carbothermal synthesis [6–8], SHS procedures [9], microwave synthesis [10], polymer pyrolysis [11], sol–gel processes [12], CVD [13], and laser synthesis [14] are a few of these techniques. Each of the aforementioned procedures has benefits as well as drawbacks over the others, such as cheaper precursors used, lower reaction temperatures, higher product purity, etc [15].

One of the simplest and most cost–effective methods for producing silicon carbide–based refractory compounds out of all of these techniques is carbothermal processing, according to reports [2]. The traditional approach for producing SiC powders is exceedingly expensive and has substantial processing costs, which are quite rare, particularly in the developing Nation. Due of the relatively high cost of producing SiC, researchers have explored an alternative route for this production, hence, the use of agricultural wastes.

Wastes are items that have been rejected, disposed of, or left unmanaged because they can no longer be used and were produced without the aim of being used again [16]. Agricultural wastes were described by [17], as organic byproducts of plant life, including oil palm, corn, rice, and coconut shells, as well as seeds, fruits, leaves, and roots.

Agricultural wastes are defined by [18] as the leftovers from the cultivation and processing of raw agricultural products such fruits, vegetables, meat, poultry, dairy products, and crops. Animal waste, food processing waste, and agricultural waste all fall under the category of agriculture. Techniques for managing waste including waste reduction, reuse, and recycling must be properly taken into account. Because it will be challenging to implement goals to achieve zero waste from agricultural activities, efforts should be strengthened to reduce waste. Using eco–friendly strategies that employ the waste created for alternative activities without any form of treatment is also essential.

The transformation of agricultural waste into useable forms looks to be the most environmentally benign, economically viable, and sustainable approach to waste management.

Several studies have reported the use of different agro wastes materials in the production of Si–based refractory compounds [2,19,20] with potential use as reinforcement in metal matrix composite. Corn cob is reach in silica content among other important refractory compounds, thus making it a potential material for the production of Si–based refractory compounds. The leftover from corn includes a sizable amount of corn cob. According to authors [21], maize cobs make up between 40 and 50 percent of all corn produced. One example of an agricultural waste is corn cobs (a byproduct of sweet corn). Due to inadequate waste management in society, this byproduct leads to environmental pollution, which causes health issues among others. In an effort to reduce production costs due to the availability of raw materials, and less expensive methods; as well as to control waste in society, efforts have been made to transform this agricultural waste into useful materials that will be highly appealing to scientific and technological communities, especially in developing countries. The presence of refractory compounds in corn cob (CC) makes it a candidate material for the synthesis of a Si–based refractory compounds. For the larger–scale development of SiC, corn cob is viewed as a very promising material. The purpose of this work is to analyze the effect of carbothermal treatment temperatures on the production of silicon based refractory compounds from corn cob.

MATERIALS AND METHODS

Experimental materials

The experimental materials utilized were corn cobs which were gotten from the Landmark University Farm, Omu–Aran, in large quantities, distilled water for the washing of the corn cob, leaching agent (Hydrochloric acid) which were used to remove impurities from the cob, a sieve which is used to drain the acid from the corn cob when rinsing it with water and a set of nose masks, gloves to protect from the acid and beakers which were used to dissolve the solute in the solvent.

Preparation of Agro wastes

To remove impurities that might prevent the solid creation of silicon–based refractory compounds from corn cob, experimental specimens were carefully prepared according to recognized techniques adopted by [2, 22, 23]. The corn cobs for sample preparation were thoroughly rinsed in clean water to remove every forms of dirt and volatile materials which has been accumulated during the period of time it has been on the farm and during transportation to the lab. These materials were sun–dried for (as shown in the Figure 1) three (3) days (7 h/day) to remove the moisture or water content present as a result of the initial washing. After, they were subjected to a temperature of 100°C for three (3) hours in an electric oven to eliminate the residual moisture. The corn cobs were later pulverized using a ball milling machine to increase the surface area of the corn cob and to reduce the size of the corn cob to powder form. The reduction in size and increase in surface area is necessary to enhance the reaction process.

Figure 1: Sun drying process of the corn cob

Synthesizing of Corn cob samples

Carbothermal processing was adopted in the production route for the production of Si–based refractory compounds from corn cob. The process sequence used have been earlier reported by authors [2]. An analytical four digit weighing balance, CY224C, 0.1mg was used to weigh a known mass of corn cob.

A 400 ml of hydrochloric (as the leaching agent) was added to the weighed corn cob and a magnetic steering machine was used for stirring operation. After a while, 40 g of the dried samples were collected and placed in the graphite crucible which was then charged at a temperature ranging from 700°C – 900°C in an electrical furnace for an hour as earlier reported by [24].

The furnace was later turned off to cool before samples were removed from the crucibles. Table 1 shows the designation of the samples and heat treatment temperature.

Table 1: Sample designation and heat treatment temperature

Sample designation	Carbothermal temperature (°C)
(A)	700
(A0)	800
A1)	900

The dried samples were gathered, weighed, and examined for structural characterizations such as Fourier–Transform Infrared Spectroscope (FTIR) and X–Ray Diffraction to determine their suitability for the Si–based refractory compounds.

Fourier transform infrared (FTIR) spectroscopy

The functional groups existing in the reaction products were identified using FTIR.

About 100–250 mg of kBr powder was mixed with 8–12 mg of refractory compounds from corn cob (RCC). The mixtures were compacted under 20–40 MPa compaction load. The functional groups in the reaction products were later accessed through this treatment sequence.

X–ray diffractometer (XRD)

The phases present in the reaction products after the carbothermal processing of the RCC were scanned by XRD.

A backloading preparation method was used for the XRD scanning, the analysis was done using PANalytical Empyrean diffractometer with PIXcel detector and fixed slits with Fe filtered Co–Ka radiation in a scan range of 2theta ranging from 10° to 90° at 10° scan step. The phases present were identified using X'Pert Highscore plus software.

Scanning electron microscope (SEM)

The morphological features of the reaction products were accessed using an extreme resolution Analytical Field Emission Scanning Electron Microscope– (JEOL, USA) equipped with energy dispersive spectroscope (EDX) operating with an accelerating voltage of 15 kV.

RESULTS AND DISCUSSION

Mass recovery/ reduction

The representative recovery yield at different treatment temperature are displayed in Figure 2. Initially, a mass of 40g was kept constant for each batch (A0, A, and A1 respectively). It is evident from Figure 2, that there was sufficient time for the transformation of Si–based refractory elements in the corn cob at higher temperature as compared to samples A0 and A.

The reduction in the yield of A1 further corroborate this observation. The implication is that, at higher treatment temperature, the volatile materials are given off during the carbothermal treatment, hence, a reduction in the mass of the Si–based refractory compounds. It can be inferred from Figure 2 that sample A displayed a value of 73.88% by mass recovery, A0 had 76.65% while A1 had 83.05%.

At higher temperature, the reaction sequence favoured the formation of SiC phases, thereby, enhancing the mass recovery rate. This trend is in line with the pattern obtained from the XRD and FTIR spectroscopy.

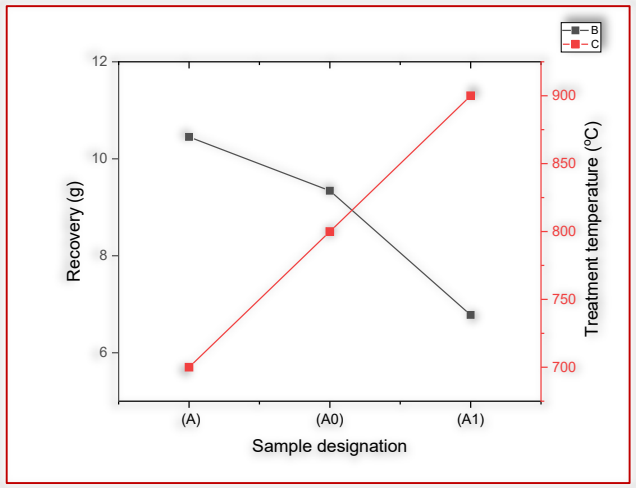

Figure 2. Variation in mass recovery rate with treatment temperature

Fourier–Transform Infrared Spectroscope (FTIR)

Table 2 shows the pronounced peaks in the reaction products for the FTIR spectra of the RCC treated at 700°C, 800°C, and 900°C respectively. Also, previous work were benchmark with the current study, the trend of the results are as presented in Table 2.

Table 2: benchmarking the variations in the wavelength associated vibrations with previous studies and current work

Wavelength (cm^{-1})	Associated vibration	References
3670 – 3000 1093 828	O–H stretching Si–O–Si Si–C	[25]
1091.75 – 3500	O–Si–O stretching and bending	[26]
821.92 1629.66	Si–C bond H–OH bending vibration	[26]
3472 1740 800–679	O–H stretching O–H bending Si–C stretching	Current study

From Figure 3, the legend A, Ao, and A1 are the IR spectra for the corn cob ranging from the carbothermal heat treatment at 700°C, 800°C and 900°C respectively. It is evident from the carbothermal heat treatment at 700°C, the presence of O–H functional group and a stretching band was observed at a broad peak of wavelength 3390 cm^{-1}. Similarly, at a wavelength of 2450 cm^{-1}, N–O stretching at a low peak was observed.

The presence of C=C functional group as a bending band is located at about 930 cm^{-1} wavelength value. A functional group of O–Si–O was observed at a wavelength of 1490 cm^{-1}. It is evident that Si–C presence was noted at about 679 cm^{-1} of wavelength value in the stretching band.

At temperature of 800°C, it was identified that O–H functional group in stretching band was

present at wavelength of 3390 cm^{-1}. The presence of O–H functional group is as a result of dehydration during the process of treatment. At wavelength value of 1530 cm^{-1} shows the presence of N–O functional group in the asymmetric stretching band. At a broad peak of 1100 cm^{-1}, C–C bending stretching band was indicated. Si–C shows its presence in the stretching band at wavelength value of about 610 cm^{-1}.

At a temperature of 900°C, a broad peak in the stretching band which indicates the presence of O–H functional group with a wavelength of 3390 cm^{-1} was noticed in the spectra. It is noted that C=O functional group in the stretching band having a wavelength of 1800 cm^{-1} was observed in the spectra. It is worthy of note that, N–O functional group in the stretching band occurred at a wavelength of 1530 cm^{-1}. A low broad peak of wavelength 1100 cm^{-1} indicated the presence of C–C functional group in the stretching band. However, the presence of Si–C functional group is indicated with a sharp peak in the stretching band at a wavelength value of 850 cm^{-1}, this was within the margin earlier reported by authors [26,27] in the formation of SiC.

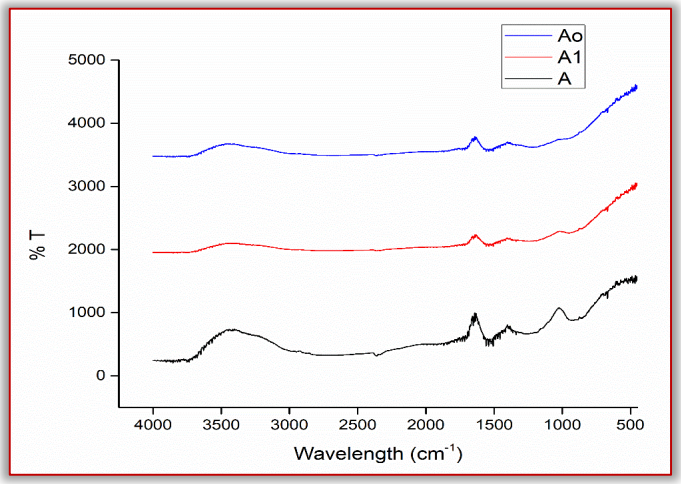

Figure 3. FTIR Spectra for Corn Cob at 900 °C

X–ray Diffraction

The XRD of the RCC are as displayed in Figure 4. Sample A and Ao showed a similar trend in peak values, hence, the legend displayed in Figure 4 was used to capture Ao. It was observed at a temperature of 700°C that at a 2Theta range of 20°–30°, SiO_2 was formed with a peak value of percentage transmittance of 2000 and 4000 respectively.

At a 2Theta range of 30–40°, the presence of SiC phase (showing a low peak) and SiO_2 were observed at a peak value of transmittance of 9000 which is the most pronounced peak in these spectra and 5000 respectively. It was also observed that at 2Theta range of 55–58°, there was a formation of SiC at a lower peak value. The formation of SiC was low in this spectra due to low treatment temperature that the corn cob was subjected to.

However, at a temperature of 900°C which is a higher treatment temperature compare to the former, the formation of SiC was observed to be more in this spectra. Also, SiO_2 was observed at a 2Theta range of 20–30° at a pronounced peak with a value of percentage transmittance of 18000. The temperature was sufficient for the phase transformation reaction of SiO_2 and C to yield SiC.

At 2Theta range of 30–80° the formation of SiC was observed in this spectra at peak values of percentage transmittance of 10000, 4000, 6000, 2500, and 5200 respectively. The formation of more SiC in this spectra is as a result of higher treatment temperature of 900°C required for transformation of SiO_2 and C to SiC. However, at relatively lower treatment temperature of 700°C, it was noted that some unreacted phase of SiO_2 polytypes precipitate in the reaction products.

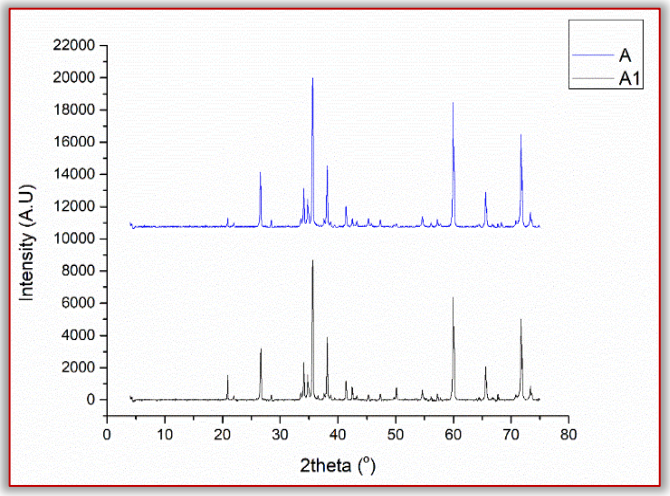

Figure 4. XRD Pattern for Corn Cob at 700 °C and 900 °C

Morphology assessment

The variation in the morphological features of the RCC at varying temperatures are as shown in Figure 5(a) and (b). Evidently, Figure 5a shows the representative scanning electron image (SEM) with EDX of an amorphous phase of the RCC. It is evident from the EDX profile the presence of Silicon (Si), Iron (Fe), Oxygen (O), and Carbon (C) all establishing the presence of SiC (low peak), SiO_2 and Fe_2O_3. It is noted that the presence of Chromium (Cr) and Potassium (K) indicate impurities elements in the RCC. This trend is similar to the findings reported by [28].

The heterogenous nature of the RCC is well captures in the morphological features displayed in Figure 5b. Evidently, the peak in the spectra

show a high value of Silicon (Si), Oxygen (O), and Carbon (C). It is noted that the silica phase reacted with the carbon constituent in the structure thereby yielding SiC phase. This trend was also consistent with the results obtained in the XRD spectra.

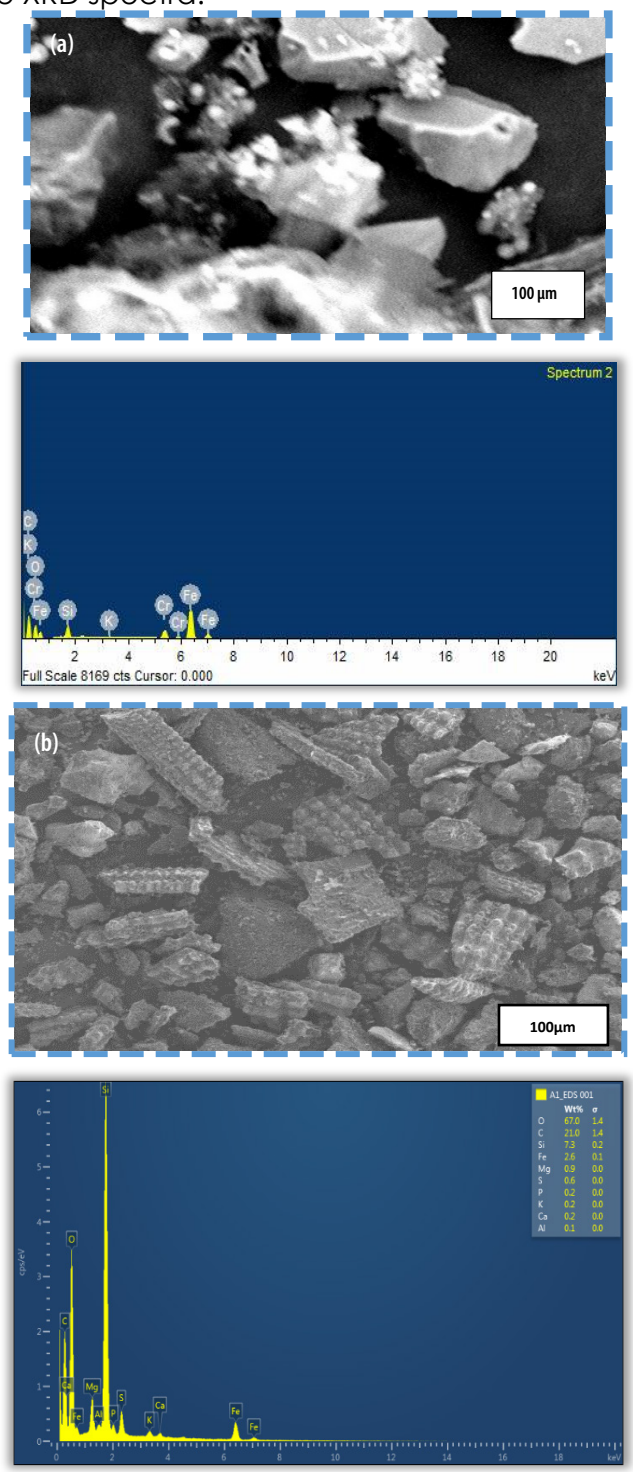

Figure 5: Showing the morphology of RCC (a) at 700 °C (b) 900 °C

CONCLUSIONS

The study reports on the synthesis and characterization studies of Si–Based Refractory Compounds derived from Corn Cob. From the results obtained, higher temperature treatment favours the formation of SiC phase. The heterogenous nature of the RCC was evident in the morphology. The wave number of the FTIR spectra for the formation of Si–C was at par with previous reports in the literature.

Acknowledgment

The author appreciates the valuable contribution from Ani Princewill Chukwuebuka at the preliminary stage of material sourcing and characterization.

References

[1] Patenaude, J., Wyatt, B.C., Nemani, S.K, Anasori, B (2024). A generalized and scalable self–assembly method of 2D carbides to metal powders. MRS Advances

[2] Adediran, A.A, Alaneme, K.K, Oladele, I.O, Akinlabi, E.T (2018). Processing and structural characterization of Si–based carbothermal derivatives of rice husk. Cogent Engineering 5 (1), 1494499

[3] Simonenko, E. P., Simonenko, N. P., Derbenev, A. V., Nikolaev, V. A., Grashchenkov, D. V., Sevastyanov, V. G., Kablov, E. N. & Kuznetsov, N. T. (2013). Synthesis of nanocrystalline silicon carbide using the sol–gel technique. Russian Journal of Inorganic Chemistry. Volume 58, pages 1143–1151.

[4] Chaira D., Mishra B.K., Sangal S., (2007). Synthesis and characterization of silicon carbide by reaction milling in a dual–drive planetary mill, Materials Science and Engineering A, Structural Materials Properties Microstructure Processing 460, 111–120.

[5] Ren R. M., Yang Z. G., Shaw L. L. (2002), Synthesis of nanostructured silicon carbide through an integrated mechanical and thermal activation process, Journal of the American Ceramic Society 85 (4), 819–827.

[6] Real C., Alcala D., Criado J.M., (1997). Synthesis of silicon carbide whiskers from carbothermal reduction of silica gel by means of the constant rate thermal analysis (CRTA) method, Solid State Ionics 95 (1–2), 29–32.

[7] Pan S., Zhang J., Yang Y., Song G., (2008). Effect of process parameters on the production of nanocrystalline silicon carbide from water glass, Ceramics International 34 (2), 391–395.

[8] Narciso–Romero F.J., Rodriguez–Reinoso F., Diez M.A., (1999). Influence of the carbon material on the synthesis of silicon carbide, Carbon 37 (11), 1771–1778.

[9] Yang Y., Lin Z.M., Li J.T., (2009). Synthesis of SiC by silicon and carbon combustion in air, Journal of the European Ceramic Society 29 (1), 175–180.

[10] Ebadzadeh T., Marzban–Rad E., (2009). Microwave hybrid synthesis of silicon carbide nanopowders, Materials Characterization 60 (1), 69–72.

[11] Narisawa M., Shimoda M., Okamura K., Sugimoto M., Seguchi T., (1995). Reaction– mechanism of the pyrolisis of polycarbosilane and polycarbosilazane as ceramic precursors, Bulletin of the Chemical Society of Japan 68 (4), 1098–1104.

[12] Cerovic L., Milonjic S.K., Zec S.P., (1995). A comparison of sol–gel derived silicon–carbide powders from saccharose and activated carbon, Ceramics International 21 (4), 271–276.

[13] Cao L.Z., Jiang H., Song H., Li Z.M., Miao G.Q., (2010). Thermal CVD synthesis and photoluminescence of SiC/SiO2 core–shell structure nanoparticles, Journal of Alloys and Compounds 489 (2), 562–565.

[14] Schaaf P., Kahle M., Carpene E., (2005). Reactive laser synthesis of carbides and nitrides, Applied Surface Science 247 (1–4), 607–615.

[15] Károly Z., Mohai I., Klébert Sz., Keszler A., Sajó I.E., Szépvölgyi J., (2011), Synthesis of SiC powder by RF plasma technique, Powder Technology, 214, (3), 300–305.

[16] Omojola A., Daramy V.V.K., Victor S.A., (2021). Trends in the development and utilization of agricultural wastes as heterogeneous catalyst for biodiesel production, J. Energy Inst., 98, 244–258
[17] Ibrahim H. K., Abdulhamid A. S., Abdulkareem S., Shuaib–Babata Y. L., Popoola O. T., Kareem A. G., Adeyi A. M., Busari O. Y., Ambali I. O., (2019). Development of Abrasive Sandpaper Grains from Agro–Waste Material for Polishing of Wood Surface. Adeleke Univ. J. Eng. Technol., 2, 1, 48–60.
[18] Obi F. O., Ugwuishiwu B. O., Nwakaire J. N., (2016). Agricultural Waste Concept, Generation, Utilization, and Management. Nig. J. Technol., 35, 4, 957 – 964
[19] Adediran, A.A, Alaneme, K.K, Oladele, I.O (2019). Synthesis of Si–based refractory compounds from coconut shell by carbothermal method. International Journal of Engineering Research in Africa 41, 20–25
[20] Adediran, A.A., Alaneme, K.K., Oladele, I.O., Akinlabi, E. T, Bayode, B.L (2021). Effects of milling time on the structural and morphological features of Si–Based refractory compounds derived from selected Agro–Wastes. Materials Today Proceedings: Volume 38, Part 2, 2021, Pages 928–933
[21] Fakhar, Ali I., Muhammad A., Farhan S., Aasma A., Sumaira S., Arooj S., Mahvish Z. S., Sunanda B., and Muhammad A.. (2023). Nutritional, functional and ethno-medical properties of sweet corn cob: a concurrent review. International Journal of Food Science & Technology
[22] Pereira, M.L.G., Figueira, D.S.S., Girolamo, B.R., & Vernilli, F., (2020). Synthesis of silicon carbide from rice husk. Cerâmica, 66(379), 256–261
[23] Guo, X., Zhu, Li, W., and Yang, H., (2013). Preparation of SiC powders by carbothermal reduction with bamboo charcoal as renewable carbon source. J Adv Ceram 2, 128–134
[24] Guo, Y.P., Yang, S.F. Yu, K.F. Zhao, J.Z. Wang, Z.C. Xu, H.D. (2002). The preparation and mechanism studies of rice husk based porous carbon. Mater Chem Phys, 74 (2002), pp. 320–323
[25] Li, C., Zhao, X., Gao, M., Kong, F., Chen, H. (2023). Effectively Controlled Structures of Si–C Composites from Rice Husk for Oxygen Evolution Catalyst. Molecules, 28, 6117
[26] Adediran, A.A., Alaneme, K.K., Oladele, I.O. Akinlabi, E.T (2019). Processing and structural characterization of Si–based carbothermal derivatives of bamboo leaf. Procedia Manufacturing, Volume 35, Pages 389–394
[27] An, Z., Xue, J., Cao, H., Zhu, C., Wang, H. (2019). A facile synthesis of silicon carbide nanoparticles with high specific surface area by using corn cob. Advanced Powder Technology, 30(1), 164–169
[28] Pinto, J., Paiva, A., Varum, H., Costa, A., Cruz, D., Pereira, S., Fernandes, L., Tavares, P., Agarwal. J. (2011). Corn's cob as a potential ecological thermal insulation material. Energy and Buildings 43, 1985–1990

ISSN: 2067–3809

ACTA TECHNICA CORVINIENSIS – Bulletin of Engineering | e–ISSN: 2067 – 3809
Tome XVII [2024] | Fascicule 2 [April – June]

[1.]Vlad Nicolae ARSENOAIA, [2.]Iulian VOICEA, [2.]Florin NENCIU, [2.]Catalin PERSU,
[2.]Dan CUJBESCU, [3.]Viorel FATU, [4.]Corina MOGA

AGRICULTURAL SECTOR PERSPECTIVES AND TRENDS IN THE CURRENT GLOBAL CONTEXT

[1)] Department of Pedotechnics, Faculty of Agriculture, Ion Ionescu de la Brad University of Agricultural 8 Sciences and Veterinary Medicine, 700490, Iasi / ROMANIA;
[2)] National Institute of Research – Development for Machines and Installations Designed to Agriculture and Food Industry – INMA Bucharest / ROMANIA;
[3)] ICDPP Bucharest / ROMANIA;
[4.)] Romanian Academy, National Institute for Economic Research, Center for Study and Research for AgroForestry Biodiversity "Acad. David Davidescu"/ ROMANIA

Abstract: Agriculture is an important branch of any national economy, with functions between the most diverse: biological, main source of economic activity and use of the labor force, ecological factor of environmental protection and combat against desertification in many areas of the Earth, a way of life, a technical tradition and cultural and, last but not least, agriculture is a side of civilization. Smart agriculture takes into account soil evaluation and environmental aspects from all perspectives and applies technological solutions for efficient fertilization, plant protection measures, and nutrient extraction. In recent years, the significant development of Internet of Things (IoT) technologies has made the integration of communication, automation, and control information into farms a very trendy "trend". Agriculture will be the field with the greatest digitization in the coming years; intelligence artificial in agriculture will be massive and unstoppable. The capability of drones is constantly expanding, the devices being equipped with high–definition photo–video cameras, thermal imaging sensors, infrared filming, parcel mapping and zoning systems, and simultaneously the volume of data increases fast. In the long term, "connected farms" will prove extremely valuable to the entire population of the planet considering the need to maximize production agricultural.
Keywords: circular economy, agricultural sector, globalization and liberalization, digital technologies

INTRODUCTION

"If agriculture is to feed the world, it must become an industry", said Geoffrey Carr, and fortunately, this has already begun to happen. The population is expected to grow to ten billion by 2050 – each year it will increase by the population of Germany (80 million) – so we must find a way to feed an additional 'Germany' every year, all while keeping agricultural land areas unchanged. This is not easy, especially considering urban expansion. For this reason, the world will need much more efficient farms to produce enough food: In the most modest scenario of economic growth, agriculture will need to grow by at least 50% compared to the current situation.

While extreme hunger and poverty have been reduced globally since 1990, there are still 800 million people suffering from chronic hunger and 2 billion people suffering from malnutrition. Agricultural growth remains generally three times more effective in reducing poverty than any other sector. In conclusion, if we think strictly in economic terms, there is a growing market for agricultural products, but we need to see if we have the resources to meet this growing demand (*Geoffrey Carr. et al, 2016*).

At an elementary level: food comes from plants, which not only feed humans but also animals. In recent years, plants in agriculture have become an important element in energy production. In fact, plants are experts at converting energy through photosynthesis. They transform solar energy into plant energy in the form of carbohydrates and fats, and then convert mineral nutrients into proteins and vitamins. Ultimately, the resulting biomass generates another form of "energy". All of these processes lead us to the conclusion that mineral fertilizers are crucial. In 2008, researchers at Wageningen University in the Netherlands demonstrated that mineral fertilizers are responsible for feeding over 50% of the global population!

Smart agriculture takes into account soil evaluation and environmental aspects from all perspectives and applies technological solutions for efficient fertilization, plant protection measures, and nutrient extraction. In recent years, the significant development of Internet of Things (IoT) technologies has made the integration of communication, automation, and control information into farms a very trendy "trend".

In the field of smart agriculture, introducing technology elements into farm management, such as tracking and monitoring the entire production process from crop establishment, processing, transportation, to sale, leads to incredible yields and quality in volatile climates with increasingly diverse natural disasters and diseases. In addition to population growth in the coming years, another aspect to consider when

discussing the future of agriculture is climate change and the increasingly advanced field of research.

The advantages of climate change include creating conditions for the cultivation of plants that could not be grown in Romania before. This includes exotic varieties originating from outside our geographic area that have gradually acclimated and can now be cultivated in our country, which was inconceivable just a few years ago.

The main issue for farmers remains access to financing. Despite undeniable progress in agricultural financing over the past 15 years, with diverse sources including funds allocated from the state budget, European funds, and an increase in bank credit and commercial credit, the approach of financial institutions toward agriculture remains cautious. In Romania, agriculture continues to hold a very important status, although it undergoes a process of property and exploitation system transformation. It remains one of the priority branches in the production of material goods, a vital and irreplaceable support for the existence and progress of human society, especially given that the economic and social progress of the contemporary world is closely correlated with the level of achievements in agriculture. It cannot be conceived without the strong development of this branch of production. Romania has approximately 9 million hectares of land, of which half are cultivated with modern technologies, although not yet at a Western level. Nevertheless, Romania achieved record grain production last year (over 10 million tons of wheat and over 15 million tons of corn), surpassing major players like France and Poland. Romania's potential in the field of agriculture is enormous. In a few years, Romania can play an essential role in the Black Sea region and in Europe's agricultural economy.

Precision agriculture is also beginning to take shape in our country. It is, in fact, an extraordinary opportunity for increasing productivity and, consequently, for increasing income. As a country with significant agricultural potential, Romania could become one of the top markets for harnessing IoT technology for the purpose of enhancing and streamlining agricultural production.

Understanding key global trends that can influence agriculture, the agri–food system, natural resource management, and rural economies in the coming decades is essential, given the importance of food in every society. Awareness of the impact these factors can have contributes to creating an agenda that strengthens the resilience and sustainability of agricultural systems.

The OECD defines megatrends as "slow–forming social, economic, political, environmental, or technological changes that, once launched, exert a profound and lasting influence on many, if not most, human activities, processes, and perceptions" (*OECD, 2016*). Presenting the main trends that can contribute to changing the configuration of agriculture and the agri–food system and stimulate innovation capacity in the years to come will follow the classification proposed by the OECD (socio–demographic, economic, environmental, technological, and political changes). When analyzing the influence and impact of current trends, such as population growth, urbanization, population aging, climate change, digitalization of economies, and the advancement of globalization and liberalization processes, their strong interdependence cannot be overlooked.

The absolute increase in the number of consumers, regional population dynamics, its structure by age groups, and by rural versus urban areas are variables without which understanding the evolution of the agri–food system is difficult to conceive. Demographics remain an important factor for the dynamics of all economic sectors. However, it is an essential parameter to explain the evolution of food demand, which depends on the number of consumers seeking to satisfy their vital physiological needs primarily.

According to the medium variant projection of the United Nations, it is expected that the global population will reach 8.5 billion by 2030 and 9.7 billion people by 2050 (*UN, 2015*). Therefore, food systems must ensure food security for an additional 2 billion people in the next 30 years. The largest demographic growth will be in less developed regions, in countries with middle and low incomes, influenced by the rate of economic growth, the level of education, the degree of female workforce participation, and other factors. In developed regions, the population growth rate is much slower or even declining.

MATERIAL AND METHOD

The decrease in the share of working–age people is a process that also characterizes developed countries. The central scenario of the OECD's long–term growth projection assumes

that the migration of young people across national borders could offset the aging decline in most OECD economies. In fact, several countries have already initiated immigration policies to compensate for job shortages in certain sectors (*FAO, 2018b*). These policies target three significant labor market gaps:

- highly skilled workers in high–tech sectors,
- workers to meet the demand for low–paid jobs that have become unattractive to local workers (agriculture and construction), and
- additional workers in the healthcare and other services due to an aging population.

By 2050, due to high economic growth rates and demographic structural imbalances, a major destination for migrants (especially from Africa) may become Southeast Asia and, in particular, China. Consequently, the size and importance of ethnic minority communities will increase, with specific challenges regarding dietary consumption patterns in these areas (*OECD, 2016*). Therefore, in these regions, increasing urbanization and changing working conditions will shape environmental and living conditions, and, as a result, food demand and eating behaviors in the decades to come.

The largest migratory flows are national migrations within state borders, typically from rural to urban areas, often as a consequence of rural poverty, lack of job opportunities, and poor infrastructure. The urban population has steadily increased over the past decades. Over 6 billion people are expected to be part of the urban population by the year 2050 (from 33% in 1960 to 62% in 2050), and nearly all of this growth will occur in cities in developing countries, with 90% of it in Asia and Africa. In absolute terms, this means a net increase of 2.4 billion people in the urban population, which is more than the total population growth during this period (2.2 billion) *(FAO, 2017a)*.

Urbanization brings many benefits to the population, such as access to electricity, improved water supply, better sanitation, educational opportunities, and it acts as a driver of domestic demand. On the other hand, the urban population generates a growing demand for processed and packaged food products. This leads to a shift in the nutritional content of diets, as processed products, often high in energy, sugar, and salt, influence obesity rates (*FAO, 2017b*). Apart from the impact on dietary consumption patterns, there are also issues related to the logistics of the agri–food system. Serving a large population requires high standards for food safety and logistics in the agri–food supply chains (*Satterthwaite et al., 2010*). One of the powerful consequences of this process, in the absence of rigorous regional development planning, is rural depopulation, increased costs of public services, decreased quality of life in rural areas, environmental degradation, and often an inequitable distribution of land *(FIT4FOOD2030)*.

The income level of the population plays a significant role in shaping the future of agriculture and the agri–food sector, as it represents the primary variable that influences the dietary consumption patterns of the population (*Godfray et al., 2010*). Higher rates of income growth per capita are expected in low– and middle–income countries. Economic development will be accompanied by an increase in the quantities and values of agricultural demand, as well as a change in the consumption pattern. The trend is a shift from a cereal–based diet to a diet richer in meat, dairy, and other resource–intensive food items (*Cirera and Masset, 2010; FAO, 2017b*), with implications for the sustainable use of natural resources.

Population growth, income growth, and changes in dietary patterns are among the primary factors that will impact future demand for agricultural products. At an annual growth rate of approximately 1.1% in global demand for agricultural products until 2050 (considerably lower than the 2.2% rate over the past four decades), the global supply of agricultural products by 2050 should be 60% larger than in 2005–2007, as suggested by certain projections (*Alexandratos and Bruinsma, 2012*).

Concerning the increase in agricultural productivity to meet global demand, there are no one–size–fits–all answers. Historically, global agriculture has been able to meet the growing demand for agricultural products over time. These improvements in agricultural productivity have been due to the use of irrigation, fertilizers, and the expansion of arable land. However, the sustainability of global agricultural intensification, given deforestation, land degradation, and water pollution, is a subject of concern.

Although agricultural efficiency has increased in recent decades, the pressure on agricultural land has intensified primarily due to demographic factors, changes in dietary patterns, and urbanization. When we add the competition between food and non–food uses of agricultural crops (such as biofuel production) and the loss of agricultural land due to erosion,

desertification, salinization, rising sea levels, etc., we understand the challenge of sustainable resource management to maintain their quality. A vicious cycle is created through the overexploitation of existing resources, their degradation, increasing pressure on the remaining resources, and further degradation of those resources (*FAO, 2017a*).

The agricultural land area per person has been continuously decreasing from 1.30 ha to 0.7 ha between 1967 and 2013 (*FAOSTAT, 2013*). There are regional variations in this phenomenon: in Asia, over the past few decades, increased production has been achieved almost exclusively through increased productivity, without an expansion of cultivated land, while in Africa, average cereal production has remained constant, but more land has become arable (*OECD, 2016*).

The expansion of agricultural land occurs at the expense of forests, savannahs, and natural grasslands, accompanied by an increase in greenhouse gas emissions and an acceleration of biodiversity loss. Agriculture is also, and is expected to remain, the largest consumer of global freshwater resources. Strong competition from the processing industry, electricity production, and household consumers will result in a 55% increase in global freshwater demand by 2050 *(FIT4FOOD2030)*.

Climate change will have a clear unfavorable impact, especially in countries in the southern regions, and its effects will be felt on both food supply and the quality and access to food. Changes in temperature and precipitation patterns can contribute to an increase in global food prices by 2050 (*Porter et al., 2014*), potentially reducing access to food for vulnerable populations (*FAO, 2017a*). Opinions on the impact on agricultural production in northern countries are nuanced, involving both positive and negative effects (*Porter et al., 2014*).

The increase in life expectancy, income, education levels, the digital economy, urbanized lifestyles, and more have influenced changes in consumer eating habits. The changes in consumption preferences today are significant compared to just one generation ago. Consumers are becoming increasingly concerned about nutrition, health, and sustainability in supply chains, carbon emissions, ethical considerations, and more. In other words, consumers are becoming more responsible regarding the impact of their choices.

The Center for Food Literacy defines food literacy as "understanding the impact of food choices on our health, environment, and economy "The prevalence of diet–related health conditions and allergies has increased awareness of the relationship between food and health. Health has become a major concern for consumers today and is often the primary motivation for food choices. Additionally, greater awareness of the origin of food has led to an increased demand for local or regional products. More transparency is being sought, with consumers wanting more information about ingredients, their origin, production methods, processing, and distribution.

Challenges related to increasing agricultural supply have been addressed so far through the intensification of agricultural land use, irrigation, and the use of chemicals. Global agricultural production tripled between 1961 and 2015. However, there have been negative effects on the natural resource base of agriculture, including land degradation, increased pest and disease resistance, loss of biodiversity, deforestation, greenhouse gas emissions, nitrate pollution, etc.

The growing demand for food, increased quality requirements, environmental considerations, and the need to avoid negative impacts on limited resources all require the development and use of innovative technologies for the future.

RESULTS

The use of digital technologies (such as 3D printing, the Internet of Things, cloud computing, robotics, etc.), along with the utilization of new materials (nano– and biotechnological), synthetic biology, and the large volume of accessible data (Big and Open Data), underlie the fourth industrial revolution (Agriculture 4.0) (FIT4FOOD2030). Digital technologies and new data analysis processes based on artificial intelligence will impact every stage of the agri–food chain: primary production, processing, distribution, and consumption (for example, through product selection and adapting diets based on the daily health parameters of each individual).

A multitude of remote sensing techniques, from field sensors to drones and satellite imagery, now provide real–time information about crop conditions. Robotics is explored in both primary production, from planting to harvesting (identifying weeds and diseases, precise pesticide application, and harvesting), as well as in processing industries.

Blockchain technology, recently used in the agri–food sector to track the trading of agricultural products, has an impact on the speed of transactions, transparency, and the efficiency of the supply chain. By interconnecting stakeholders along the supply chain, it ensures control and analysis of the journey of each product from the farm to the consumer.

A huge volume of data (Big Data) that covers various segments of the agri–food supply chain can be captured and analyzed (using sophisticated algorithms) to increase efficiency through the implementation of Internet of Food platforms (*Kouma, 2011*). This large amount of information and analysis influences current consulting systems. Social media has a significant role in gathering information about consumer behavior (digital shadow). Distribution can use this information to predict changes in demand for specific products and to generate differentiated, and even individual, pricing *(FIT4FOOD2030)*.

Open access to digital information tends to change business models, even for major and established companies in the agricultural product trade. For instance, if Cargill has built its market power over the past hundred years on the basis of limited access by farmers to market information, today, this information is available even to the most remote agricultural producers. This new context forces Cargill to reinvent itself, integrating intelligent applications for farmers into its offerings (such as facial recognition software for cattle farms), using new satellite data technologies for monitoring and assessing crops, and expanding its business to new sources of protein (aquaculture and cultured meat), taking into account the new challenges of the agri–food system (*Parker M., Blas J, 2018*).

Massive investments in Agtech companies in recent years anticipate the emergence of further innovations. The new markets created offer new business opportunities for entrepreneurs. It can also be an opportunity for emerging countries to reduce the technological gap, especially in the context of decreasing equipment costs and expanding open–source practices (*OECD, 2016*).

A massive transformation in the way agricultural businesses operate is expected, beyond what we used to call precision agriculture. However, the adoption of these technological innovations (even the adaptation of sustainable agricultural systems and practices) requires investments in research and development (R&D). Agricultural research intensity (the share of public spending on research and development in agriculture's contribution to GDP) is over 5 times higher in high–income countries compared to low–income countries (*Pardey, Chan–Kang, and Dehmer, 2014*).

The rate of economic growth in emerging countries and the expansion of communication and information technologies will strongly shape the evolution of this phenomenon, possibly even shifting the center of gravity of the global economy more towards the east and the south. This will also influence global governance structures to reflect the new configuration brought about by the multitude of participants in a multipolar economic world (*OECD, 2016*).

Until the early 1980s, the state played a significant role in shaping and marketing agricultural production in most countries. Governments were involved in the agricultural and agri–food market through intervention and control measures to generate fiscal revenues and, in some cases, to gain political control. However, since the 1980s and 1990s, many of these state intervention and control systems have come under pressure to liberalize. Nevertheless, in the last decade, new trade barriers in favor of domestic industries have been applied with greater frequency (*OECD, 2016*).

Globalization and liberalization have led to increased investments in agriculture, the development of the food industry, and the growth of international food trade. The increased global food flow, the development of global distribution networks, and the rise of private standards have significantly favored the concentration of primary production and the consolidation of agricultural lands, promoting the development of large farms (*Reardon et al., 2003*). However, this has also led to a constant erosion of food production systems and local food patterns (*Holden, 2018*).

The impact on agriculture and the agri–food system is the reduction of food losses and waste at all levels of the food chains. This indeed represents a systemic change in current methods of production and consumption, the relationship between producers and consumers, and that of "consumers with products and materials" (*Stahel, 2016*).

However, significant economic opportunities would be created, but political decisions and incentive tools are required to promote a circular economy. The transition to this paradigm involves

substantial costs for building the necessary infrastructure. On the other hand, the fact that this type of economic model operates more at the regional and national levels and is less reliant on import markets to meet demand makes it a viable alternative if reducing the trade deficit becomes a political objective (*OECD, 2016*).

CONCLUSIONS

Concerns about food security and safety have shaped the agricultural system, and these issues have been at the center of a series of food scandals since the 1990s (BSE, dioxin, avian flu, swine flu, etc.). This has led to the implementation of risk management systems and product tracking systems (traceability), and even the emergence of demand for special products (e.g., organic eggs).

Urbanization, the participation of most family members in the labor market, and time constraints have led to an increased demand for convenience foods. While often criticized, especially due to their low nutritional value and packaging waste, this type of food is experiencing significant growth today, driven by fresh–cut and packaged products.

The future of food products is about quality, taste, health, fresh and local products, as well as differentiation and customization. Various pressures on the agri–food sector, such as low consumer prices, raw material availability, increasing food safety regulations, health concerns, high innovation costs, etc., have created the need for economies of scale and led to strong consolidation processes within the sector.

Many mergers and acquisitions have taken place in recent years, resulting in the creation of massive corporations that exercise control over decisions within the agri–food system. New forms of regulation are required to mitigate the risk of unfair business practices, ensure the fair distribution of profits across the agri–food chain, and promote its sustainability.

In conclusion, the global trends and challenges facing agriculture and the agri–food system are manifold, and it is an opportune and necessary process for decision–makers, researchers, and businesspeople to reflect upon.

Agricultural and food production is expected to increase due to population growth and rising incomes. However, the expansion of the agricultural and agri–food sector can be significantly limited by the existing pressure on agricultural land and water resources. Innovative production models are required to enhance productivity while maintaining biodiversity and preserving the quality of natural resources. Sustainable production practices are demanded due to the increasing consumer awareness of sustainable and healthy consumption patterns. Success in shaping robust and resilient agri–food systems depends on intelligent strategies that can integrate digitization, new collaboration methods within the agri–food supply chain, and the circular economy.

Acknowledgement

This paper was financed by Ministry of Agriculture and Rural Development – Romania – MADR – Sectorial Project ADER 21.1.1 and Ministry of Research, Innovation and Digitalization through Program 1 – Development of the national research–development system, Subprogram 1.2 – Institutional performance – Projects for financing excellence in RDI, Contract no. 1PFE/30.12.2021.

References

[1] Alexandratos N, et al, (2012). World Agriculture Towards 2030/2050: The 2012 Revision, Food and Agriculture Organization of the United Nations, ESA Working Paper no. 12–03
[2] EC, 2018. European Commission. Circular Economy – Implementation of the Circular Economy Action Plan; European Commission: Brussels, Belgium, 2018.
[3] FAO, 2018a. The future of food and agriculture – Alternative pathways to 2050. Rome, 2018
[4] FAO, 2018b. The State of Food and Agriculture 2018. Migration, agriculture and rural development. Rome
[5] FAO, 2017a. The future of food and agriculture – Trends and challenges. Rome
[6] FAO, 2017b. The state of food and agriculture – Leveraging food systems for inclusive rural transformation. Rome
[7] FIT4FOOD2030. Report on baseline and description of identified trends, drivers and barriers of EU food system and R&I, Deliverable 2.1, Towards FOOD 2030 – future–proofing the European food systems through Research & Innovation.
[8] Godfray H., Charles J. et al.,(2010). Food Security: The Challenge of Feeding 9 Billion People. Science, 327, 812–818.
[9] Holden N.M., et al., (2018) . Review of the sustainability of food systems and transition using the Internet of Food. Science of Food, 2 (1), 18.
[10] JRC, 2017. Unfair Trading Practices în the Food Supply Chain.
[11] Kouma J.P., Lui L., 2011. Internet of Food. In 2011 IEEE International Conferences on Internet of Things, and Cyber, Physical and Social Computing
[12] Lee Smith, (2018.) The Top Global Trends, Driving the Fourth Agricultural Revolution, September 19, 2018, https://www.planet.com/pulse/top–global–trends–fourth–agricultural–revolution.
[13] OECD, 2016. An OECD horizon scan of megatrends and technology trends în the context of future research policy, OECD's Directorate for Science,
[14] Parker M., Blas J., (2018). America's Largest Private Company Reboots a 153–Year–Old Strategy, Boomberg Businessweek, 7 June 2018. (https://www.bloomberg.com).
[15] Pardey P., et al. (2014). Global food and agricultural R&D spending, 1960–2009. InSTePP Report. Saint Paul, USA, University of Minnesota.
[16] Porter J.R., et al, (2014). Food security and food production systems.

[17] Reardon T., et al. (2003). The rise of supermarkets in Africa, Asia and Latin America. American journal of agricultural economics, 85 (5), 1140–1146.
[18] Satterthwaite D. et al,, (2010). Urbanization and its implications for food and farming, Phil. Trans. R. Soc. B 2010, 365 2767–2767, volume 365, issue 1554, 2010
[19] Stahel, Walter R., (2016). The circular economy, Nature News, Nature Publishing Group, Mar 23. UN, 2015. World Population Prospects: The 2015 Revision, Key Findings and Advance Tables. Working Paper No. ESA/P/WP.241. United Nations, Department of Economic and Social Affairs, Population Division (2015).
[20] Xavier Cirera, (2010). Edoardo Masset, Income distribution trends and future food demand, Phil. Trans. R. Soc. B 2010 365 2767–2767, volume 365, issue 1554, 2010

Note: This paper was presented at ISB–INMA TEH' 2023 – International Symposium on Technologies and Technical Systems in Agriculture, Food Industry and Environment, organized by University "POLITEHNICA" of Bucuresti, Faculty of Biotechnical Systems Engineering, National Institute for Research–Development of Machines and Installations designed for Agriculture and Food Industry (INMA Bucuresti), National Research & Development Institute for Food Bioresources (IBA Bucuresti), University of Agronomic Sciences and Veterinary Medicine of Bucuresti (UASVMB), Research–Development Institute for Plant Protection – (ICDPP Bucuresti), Research and Development Institute for Processing and Marketing of the Horticultural Products (HORTING), Hydraulics and Pneumatics Research Institute (INOE 2000 IHP) and Romanian Agricultural Mechanical Engineers Society (SIMAR), in Bucuresti, ROMANIA, in 5–6 October, 2023.

ISSN: 2067-3809

Fascicule 2
[April – June]
tome XVII
[2024]

ACTA Technica CORVINIENSIS
BULLETIN OF ENGINEERING

ISSN: 2067-3809

MANUSCRIPT PREPARATION – GENERAL GUIDELINES

Manuscripts submitted for consideration to **ACTA TECHNICA CORVINIENSIS – Bulletin of Engineering** must conform to the following requirements that will facilitate preparation of the article for publication. These instructions are written in a form that satisfies all of the formatting requirements for the author manuscript. Please use them as a template in preparing your manuscript. Authors must take special care to follow these instructions concerning margins.

INVITATION

We are looking forward to a fruitful collaboration and we welcome you to publish in our ACTA TECHNICA CORVINIENSIS – Bulletin of Engineering. You are invited to contribute review or research papers as well as opinion in the fields of science and technology including engineering. We accept contributions (full papers) in the fields of applied sciences and technology including all branches of engineering and management.

ACTA TECHNICA CORVINIENSIS – Bulletin of Engineering publishes invited review papers covering the full spectrum of engineering and management. The reviews, both experimental and theoretical, provide general background information as well as a critical assessment on topics in a state of flux. We are primarily interested in those contributions which bring new insights, and papers will be selected on the basis of the importance of the new knowledge they provide.

Submission of a paper implies that the work described has not been published previously (except in the form of an abstract or as part of a published lecture or academic thesis) that it is not under consideration for publication elsewhere. It is not accepted to submit materials which in any way violate copyrights of third persons or law rights. An author is fully responsible ethically and legally for breaking given conditions or misleading the Editor or the Publisher.

ACTA TECHNICA CORVINIENSIS – Bulletin of Engineering is an international and interdisciplinary journal which reports on scientific and technical contributions. Every year, in four online issues (fascicules 1–4), ACTA TECHNICA CORVINIENSIS – Bulletin of Engineering [e-ISSN: 2067-3809] publishes a series of reviews covering the most exciting and developing areas of engineering. Each issue contains papers reviewed by international researchers who are experts in their fields. The result is a journal that gives the scientists and engineers the opportunity to keep informed of all the current developments in their own, and related, areas of research, ensuring the new ideas across an increasingly the interdisciplinary field. Topical reviews in materials science and engineering, each including:

- surveys of work accomplished to date
- current trends in research and applications
- future prospects.

As an open-access journal ACTA TECHNICA CORVINIENSIS – Bulletin of Engineering will serve the whole engineering research community, offering a stimulating combination of the following:

- Research Papers – concise, high impact original research articles,
- Scientific Papers – concise, high impact original theoretical articles,
- Perspectives – commissioned commentaries highlighting the impact and wider implications of research appearing in the journal.

ACTA TECHNICA CORVINIENSIS – Bulletin of Engineering encourages the submission of comments on papers published particularly in our journal. The journal publishes articles focused on topics of current interest within the scope of the journal and coordinated by invited guest editors. Interested authors are invited to contact one of the Editors for further details.

BASIC MANUSCRIPT REQUIREMENTS

The basic instructions and manuscript requirements are simple:

- Manuscript shall be formatted for an A4 size page.
- The all margins of page (top, bottom, left, and right) shall be 20 mm.
- The text shall have both the left and right margins justified.
- Single-spaced text, tables, and references, written with 11 or 12-point Georgia or Times New Roman typeface.
- No Line numbering on any pages and no page numbers.
- Manuscript length must not exceed 15 pages (including text and references).
- Number of the figures and tables combined must not exceed 20.
- Manuscripts that exceed these guidelines will be subject to reductions in length.

The original of the technical paper will be sent through e-mail as attached document (*.doc, Windows 95 or higher). Manuscripts should be submitted to e-mail: redactie@fih.upt.ro, with mention "for ACTA TECHNICA CORVINIENSIS".

STRUCTURE

The manuscript should be organized in the following order: Title of the paper, Authors' names and affiliation, Abstract, Key Words, Introduction, Body of the paper (in sequential headings), Discussion & Results, Conclusion or Concluding Remarks, Acknowledgements (where applicable), References, and Appendices (where applicable).

THE TITLE

The title is centered on the page and is CAPITALIZED AND SET IN BOLDFACE (font size 14 pt). It should adequately describe the content of the paper. An

abbreviated title of less than 60 characters (including spaces) should also be suggested. Maximum length of title: 20 words.

AUTHOR'S NAME AND AFFILIATION

The author's complete name(s) follows the title and is also centered on the page (font size 11 pt). A blank line is required between the title and the author's name(s). Last names should be spelled out in full and succeeded by author's initials. The author's affiliation (in font size 11 pt) is provided below. Phone and fax numbers do not appear.

ABSTRACT

State the paper's purpose, methods or procedures presentation, new results, and conclusions are presented. A nonmathematical abstract, not exceeding 200 words, is required for all papers. It should be an abbreviated, accurate presentation of the contents of the paper. It should contain sufficient information to enable readers to decide whether they should obtain and read the entire paper. Do not cite references in the abstract.

KEY WORDS

The author should provide a list of three to five key words that clearly describe the subject matter of the paper.

TEXT LAYOUT

The manuscript must be typed single spacing. Use extra line spacing between equations, illustrations, figures and tables. The body of the text should be prepared using Georgia or Times New Roman. The font size used for preparation of the manuscript must be 11 or 12 points. The first paragraph following a heading should not be indented. The following paragraphs must be indented 10 mm. Note that there is no line spacing between paragraphs unless a subheading is used. Symbols for physical quantities in the text should be written in italics. Conclude the text with a summary or conclusion section. Spell out all initials, acronyms, or abbreviations (not units of measure) at first use. Put the initials or abbreviation in parentheses after the spelled-out version. The manuscript must be writing in the third person ("the author concludes... ").

FIGURES AND TABLES

Figures (diagrams and photographs) should be numbered consecutively using Arabic numbers. They should be placed in the text soon after the point where they are referenced. Figures should be centered in a column and should have a figure caption placed underneath. Captions should be centered in the column, in the format "Figure 1" and are in upper and lower case letters.

When referring to a figure in the body of the text, the abbreviation "Figure" is used illustrations must be submitted in digital format, with a good resolution. Table captions appear centered above the table in upper and lower case letters.

When referring to a table in the text, "Table" with the proper number is used. Captions should be centered in the column, in the format "Table 1" and are in upper and lower case letters. Tables are numbered consecutively and independently of any figures. All figures and tables must be incorporated into the text.

EQUATIONS & MATHEMATICAL EXPRESSIONS

Place equations on separate lines, centered, and numbered in parentheses at the right margin. Equation numbers should appear in parentheses and be numbered consecutively. All equation numbers must appear on the right-hand side of the equation and should be referred to within the text.

CONCLUSIONS

A conclusion section must be included and should indicate clearly the advantages, limitations and possible applications of the paper. Discuss about future work.

Acknowledgements

An acknowledgement section may be presented after the conclusion, if desired. Individuals or units other than authors who were of direct help in the work could be acknowledged by a brief statement following the text. The acknowledgment should give essential credits, but its length should be kept to a minimum; word count should be <100 words.

References

References should be listed together at the end of the paper in alphabetical order by author's surname. List of references indent 10 mm from the second line of each references. Personal communications and unpublished data are not acceptable references.

- *Journal Papers:* Surname 1, Initials; Surname 2, Initials and Surname 3, Initials: Title, Journal Name, volume (number), pages, year.
- *Books:* Surname 1, Initials and Surname 2, Initials: Title, Edition (if existent), Place of publication, Publisher, year.
- *Proceedings Papers:* Surname 1, Initials; Surname 2, Initials and Surname 3, Initials: Paper title, Proceedings title, pages, year.

ISSN: 2067-3809

INDEXES & DATABASES

We are very pleased to inform that our international scientific journal ACTA TECHNICA CORVINIENSIS – Bulletin of Engineering completed its 16 years of publication successfully [2008–2023, Tome I–XVI].
In a very short period the ACTA TECHNICA CORVINIENSIS – Bulletin of Engineering has acquired global presence and scholars from all over the world have taken it with great enthusiasm.
We are extremely grateful and heartily acknowledge the kind of support and encouragement from all contributors and all collaborators!

ACTA TECHNICA CORVINIENSIS – Bulletin of Engineering is accredited and ranked in the "B+" CATEGORY Journal by CNCSIS – The National University Research Council's Classification of Romanian Journals, position no. 940 (http://cncsis.gov.ro/).
ACTA TECHNICA CORVINIENSIS – Bulletin of Engineering is a part of the ROAD, the Directory of Open Access scholarly Resources (http://road.issn.org/).

ACTA TECHNICA CORVINIENSIS – Bulletin of Engineering is also indexed in the digital libraries of the following world's universities and research centers:

WorldCat – the world's largest library catalog
https://www.worldcat.org/
National Lybrary of Australia
http://trove.nla.gov.au/
University Library of Regensburg – GIGA German Institute of Global and Area Studies
http://opac.giga-hamburg.de/ezb/
Simon Fraser University – Electronic Journals Library
http://cufts2.lib.sfu.ca/
University of Wisconsin – Madison Libraries
http://library.wisc.edu/
University of Toronto Libraries
http://search.library.utoronto.ca/
The University of Queensland
https://www.library.uq.edu.au/
The New York Public Library
http://nypl.bibliocommons.com/
State Library of New South Wales
http://library.sl.nsw.gov.au/
University of Alberta Libraries – University of Alberta
http://www.library.ualberta.ca/
The University of Hong Kong Libraries
http://sunzi.lib.hku.hk/
The University Library – The University of California
http://harvest.lib.ucdavis.edu/

ACTA TECHNICA CORVINIENSIS – Bulletin of Engineering is indexed, abstracted and covered in the world-known bibliographical databases and directories including:

INDEX COPERNICUS – JOURNAL MASTER LIST
http://journals.indexcopernicus.com/
GENAMICSJOURNALSEEK Database
http://journalseek.net/
DOAJ – Directory of Open Access Journals
http://www.doaj.org/
EVISA Database
http://www.speciation.net/
CHEMICAL ABSTRACTS SERVICE (CAS)
http://www.cas.org/
EBSCO Publishing
http://www.ebscohost.com/
GOOGLE SCHOLAR
http://scholar.google.com
SCIRUS – Elsevier
http://www.scirus.com/
ULRICHSweb – Global serials directory
http://ulrichsweb.serialssolutions.com
getCITED
http://www.getcited.org
BASE – Bielefeld Academic Search Engine
http://www.base-search.net
Electronic Journals Library
http://rzblx1.uni-regensburg.de
Open J-Gate
http://www.openj-gate.com
ProQUEST Research Library
http://www.proquest.com
Directory of Research Journals Indexing
http://www.drji.org/
Directory Indexing of International Research Journals
http://www.citefactor.org/

ISSN: 2067-3809